GHENT UNIVERSITY

FACULTY OF PHARMACEUTICAL SCIENCES

Laboratory for General Biochemistry and Physical Pharmacy
nanomedicines & biophotonics

What you see is what you get

The physicochemistry of nanoparticles dictates how they cross ocular delivery barriers and alter autophagy

Karen Peynshaert

Pharmacist

Master of Science in Drug Development

2018

Thesis submitted to obtain the degree of

Doctor in Pharmaceutical Sciences

Proefschrift voorgedragen tot het bekomen van de graad van

Doctor in de Farmaceutische Wetenschappen

Dean

Prof.dr.apr. Jan Van Bocxlaer

Promotors

Prof.dr.apr. Katrien Remaut

Prof.dr.apr. Stefaan De Smedt

Members of the Exam Committee

Prof. dr. **Filip Van Nieuwerburgh** (chairman)	Ghent University, Belgium
Prof. dr. **Bruno De Geest** (secretary)	Ghent University, Belgium
Prof. dr. **Lieve Moons**	Catholic University of Leuven, Belgium
Dr. **Julie De Zaeytijd**	Ghent University Hospital, Belgium
Prof. dr. **Deniz Dalkara**	Sorbonne University, France
Prof. dr. **François Paquet-Durand**	University of Tübingen, Germany

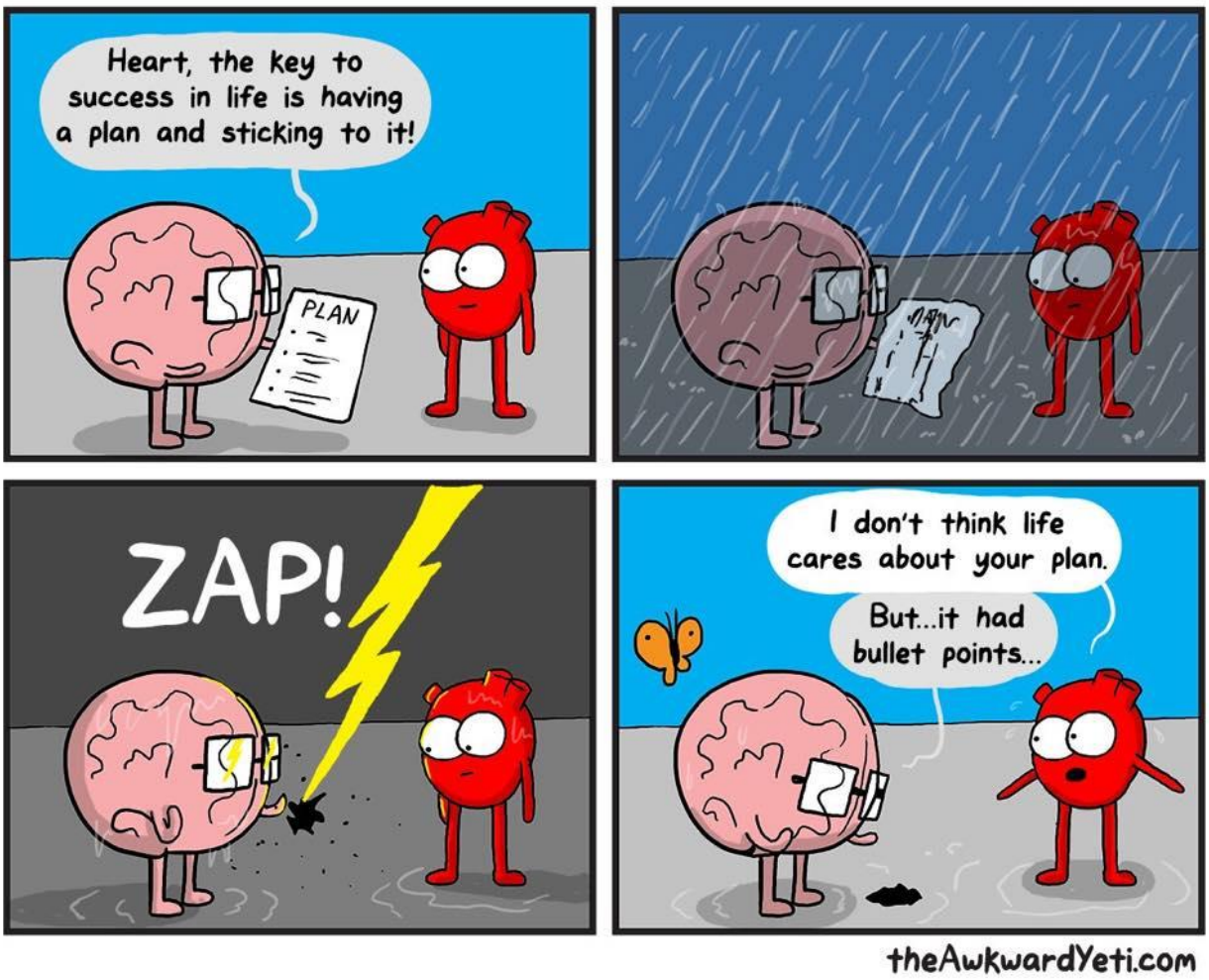
Heart, the key to success in life is having a plan and sticking to it!
PLAN
ZAP!
I don't think life cares about your plan.
But...it had bullet points...
theAwkwardYeti.com

Ghent, January 4th , 2018

The promotors:

Prof.dr.apr. Katrien Remaut

Prof. dr. apr. Stefaan De Smedt

The author:

Apr. Karen Peynshaert

Table of contents

LIST OF ABBREVIATIONS

3-MA	3-methyladenine
AAV	adeno-associated virus
ACD	autophagic cell death
AgNP	silver nanoparticle
AMD	age-related macular degeneration
atg	autophagy gene
ATP	adenosine triphosphate
AuNP	gold nanoparticle
BDNF	brain-derived neurotrophic factor
BRB	blood-retinal barrier
CeO_2	cerium oxide
CLEAR	Coordinated Lysosomal Expression and Regulation
CLQ	chloroquine
CNT	carbon nanotube
CNTF	ciliary neurotrophic factor
COLIV	Collagen IV
CRISPR	Clustered Regularly Interspaced Short Palindromic Repeats
DLS	dynamic light scattering
DNA	deoxyribonucleic acid
DOPE	dioleoylphosphatidylethanolamine
DOTAP	dioleoyltrimethylammonium propane
DQ BSA	derivatively quenched bovine serum albumin
DR	diabetic retinopathy
ER	endoplasmic reticulum
ERG	electroretinogram
FBS	fetal bovine serum
FDA	Food and Drug Administration
FITC	fluorescein isothiocyanate
FRAP	Fluorescence Recovery After Photobleaching
GA	gradient alloyed
GAG	glycosaminoglycan
GCL	ganglion cell layer

GDNF	glial cell-derived neurotrophic factor
GFP	green fluorescent protein
HA	hyaluronic acid
HEPES	4-(2-hydroxyethyl)-1-piperazineethanesulfonic acid
iBRB	inner blood-retinal barrier
ILM	inner limiting membrane
INL	inner nuclear layer
IONP	iron oxide nanoparticle
IOP	intra-ocular pressure
IPL	inner plexiform layer
IVT	intravitreal
LAMP-1	lysosome-associated membrane protein 1
LC3	microtubule-associated protein 1 light chain 3
LCA	Leber congenital amaurosis
LF2000	lipofectamine 2000
LHON	Leber hereditary optic neuropathy
MFI	mean fluorescence intensity
MIO-M1	Moorfields/Institute of Ophthalmology-Müller 1
MPA	3-mercaptopropionic acid
Mred	mitotracker deep red
mTORC1	mammalian target of rapamycin complex 1
NA	nucleic acid
NFL	nerve fiber layer
NIR	near infrared
NP	nanoparticle
oBRB	outer blood-retina barrier
ONL	outer nuclear layer
OPL	outer plexiform layer
PAMAM	polyamidoamine
PBS	phosphate buffered saline
PCR	polymerase chain reaction
pDNA	plasmid DNA
PEG	polyethylene glycol
PI	propidium iodide

PLGA	poly(lactic-co-glycolic acid)
PR	photoreceptor
PS	polystyrene
QD	quantum dot
RGC	retinal ganglion cell
RNA	ribonucleic acid
ROI	region of interest
ROS	reactive oxygen species
RP	retinitis pigmentosa
RPE	retinal pigment epithelium
SCS	suprachoroidal space
SEM	scanning electron microscopy
SLN	solid lipid nanoparticle
SPR	surface plasmon resonance
SPT	single particle tracking
TBHP	tert-butyl hydroxyperoxide
TEM	transmission electron microscopy
TFEB	transcription factor EB
VEGF	vascular endothelial growth factor
VNB	vapor nanobubble
VR	vitreoretinal
WHO	world health organisation
ZnO	zinc oxide

Aim and outline

Vision impairment is estimated to affect 253 million people worldwide. Besides the obvious negative impact of this disability on the daily activities and social interactions of these people, it has been shown that vision impairment enhances the chance of unemployment and risk of suffering from depression and anxiety disorders. In view of these observations, worldwide effort is committed to gaining insight into the underlying causes of blinding pathologies and exploring options for their treatment. Vision impairment can be provoked by a wide variety of retinal diseases which can be inherited or acquired by origin. In both cases, several gene therapy strategies have been conceptualized that could represent viable treatment options. A primary requirement for potent retinal gene therapy is the effective delivery of therapeutic genes to the retina. This delivery could be facilitated by packaging the genes in nanoparticles (NPs) of which there is an endless variety thanks to the recent nanotechnology boom. Nevertheless, while proof-of-concept of many of these gene carriers has been well-established in *in vitro* cell cultures, the delivery of therapeutic genes to the retina *in vivo* remains troublesome due to the many drug delivery barriers present at the back of the eye. Surely, the interaction of NPs with these drug delivery barriers remains poorly characterized which hinders the progression of nanomedicine for retinal gene therapy. In the **first part** of the thesis, the principal aim is therefore to gain insight into the various **drug delivery barriers in the eye** and more importantly, to explore the potential links between **NP physicochemistry** and the NPs' ability to cross these barriers. Since we are convinced that intravitreal (IVT) injection is a safe and straightforward method to deliver therapeutics close to the retina this thesis will mainly focus on the barriers encountered following this injection, i.e. the vitreous and inner limiting membrane (ILM).

Chapter 1 provides a general introduction to the anatomy of the eye and the retina. Considering our interest in IVT injection and the close proximity of Müller cell endfeet to the ILM and vitreous, we will furthermore concentrate on the Müller cell as target cell type and look into its intriguing morphology and many functions. Next, we present an overview of the most well-documented inherited and most prevalent acquired retinal diseases and discuss the various forms of retinal gene therapy and gene carriers that can be applied to treat these diseases.

In **Chapter 2** the administration routes that can be applied to deliver therapeutic genes to the retina are explained together with the drug delivery barriers encountered. We describe in detail the composition of each ocular barrier and review the available literature on their barrier role toward all types of therapeutics, ranging from macromolecules to NPs. At the same time, we look into the influence of the size, charge and lipophilicity (i.e. physicochemistry) of the therapeutic(s) (carrier) on

their ability to overcome each barrier. Finally, the most valuable available *in vitro* and *ex vivo* methods to study the interaction of therapeutics and their carriers with these barriers are summarized.

In **Chapter 3** we aim to personally support researchers in the design of novel effective NPs by presenting a novel *ex vivo* model that allows to investigate the interaction of therapeutic carriers with the vitreoretinal interface, a highly important barrier encountered after IVT injection. We apply basic polystyrene beads as model particles to validate this model and look into the relative barrier role of the vitreous and ILM as drug delivery barriers.

Based on our interest in applying Müller cells for the gene therapy strategy of 'neuroprotection', **Chapter 4** describes a preliminary *in vitro* study where we evaluate the ability of Müller cells to take up a standard liposomal vector and process its pDNA or mRNA cargo into green fluorescent protein (GFP). Moreover, we explore the Müller cell's performance in stressful circumstances by examining the liposome-induced transfection efficiency and cytotoxicity in hypoxic, hyperglycemic and oxidatively stressed cells – conditions linked to diabetic retinopathy and glaucoma.

Besides retinal drug and gene delivery, a lot of organic as well as inorganic NP types are currently investigated for a myriad of biomedical applications. Unfortunately, the clinical translation of most of these NPs is severely hampered by concerns regarding their safety. Many common mechanisms of NP toxicity have indeed been discovered thus far of which autophagy alteration is a more recent discovery. Autophagy is an intracellular degradative process that is vital to preserve cellular homeostasis. In light of its importance within the cell, autophagy disruption has been linked to the pathogenesis of several diseases. While there is a high number of publications examining the interaction between NPs and the autophagy pathway, the diversity of NPs and methods applied prevents us to draw overall conclusions. In the **second part** of the thesis, the aim is therefore to look into the influence of NPs on the **autophagy pathway**, and more specifically, to attempt to decipher the impact of **NP physicochemistry** on their ability to affect autophagy.

Chapter 5 provides a general introduction to nanomedicine, nanotoxicology and the autophagy pathway. More specifically, we summarize the most widely investigated organic and inorganic NPs for biomedical applications, the mechanisms by which NPs can affect the cell's homeostasis as well as the autophagy pathway along with available methods to study it. Finally, we provide an overview of the mechanisms by which NPs can affect the autophagy pathway and discuss the most valuable studies examining NP-autophagy interactions while attempting to link NP physicochemistry to their effect on autophagy.

In **Chapter 6** we present a nanotoxicological study on Quantum Dots (QDs), highly fluorescent NPs researched for imaging applications. We aim to look into the impact of surface chemistry on cellular toxicity by carefully comparing the effects of two QDs that only differ in their surface coating, i.e. 3-mercaptopropionic acid and polyethylene glycol. To this end, we examined the aggregation profile, cellular uptake, cytotoxicity and associated ROS levels of QDs, and studied their effect on lysosomes and autophagosomes - the two most essential organelles of autophagy.

Chapter 7 discusses the recent progress of nanotechnology and debates its future goals in context of toxicology and retinal gene therapy. At the same time, we position the work presented in this thesis within the broad scope of both fields. We highlight the predominant issues that currently limit nano to progress to the clinic along with conceptual guidelines that could help the field to advance (more) efficiently. Finally, having these guidelines in mind, we look into non-viral retinal gene delivery as a case study and attempt to envision how this research area should proceed.

1

A general introduction to the anatomy of the eye, retinal diseases and retinal gene therapy

Karen Peynshaert[a,b], Stefaan De Smedt[a,b], Katrien Remaut[a,b]

[a]Lab of General Biochemistry and Physical Pharmacy, Faculty of Pharmaceutical Sciences, Ghent University, Ottergemsesteenweg 460, 9000 Ghent, Belgium.
[b]Ghent Research Group on Nanomedicines, Ghent University, Ottergemsesteenweg 460, 9000 Ghent, Belgium.

ABSTRACT

Our eyes are wonderful sense organs of unimaginable complexity that grant us vision. They allow us to appreciate the world's beauty, to sense danger and to support our emotional communication through eye contact. Seeing the fundamental role vision plays in our existence, its loss has an immense impact on a person's life. Sadly, at this moment vision impairment affects 253 million people worldwide.[1] In light of this, a vast amount of research in the last decades has been dedicated to deciphering the biology and biochemistry of the retina along with identification of blinding gene mutations, disease pathogenesis and treatment strategies. In this thesis we have investigated several ocular drug delivery barriers with as ultimate goal to assist in the optimization of nanomedicines for treatment of retinal diseases. As an introduction to these studies, this chapter will provide a basic overview of the anatomy and function of the eye, the retina, and our target of interest, i.e. the Müller cell. We will briefly touch upon the most studied inherited and most prevalent acquired retinal diseases to finally discuss the various gene therapy strategies to treat these blinding disorders.

Table of Contents

1. ANATOMY OF THE EYE

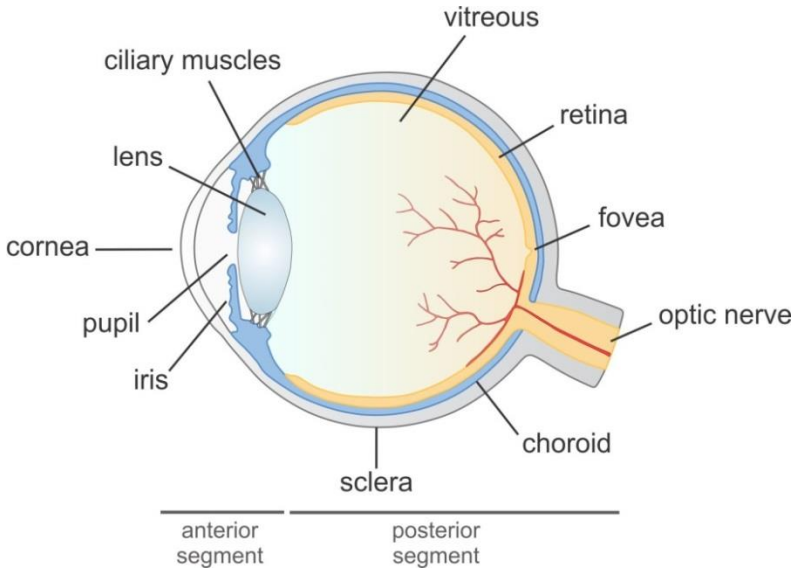

Figure 1.1 | Schematic representation of the anatomy of the eye.

The human eye has a spherical shape with an average diameter of 25 mm. The eye globe can be roughly divided in two segments: the anterior and the posterior segment (**Figure 1.1**).

Anterior segment

The anterior segment refers to the area in front of the lens and is made up of several structures that have as primary goal to guide light to the retina at the back of the eye. The **pupil**, which has a black appearance, represents the aperture that allows light to be projected onto the retina. The colored muscle tissue covering this pupil, i.e. the **iris**, functions as a diaphragm that controls the amount of light entering the eye. The outer surface of the anterior segment is the **cornea**, a transparent layer performing as a lens with great refractive power. The cornea therefore serves as the first essential element of the ocular optical system. The second light-focusing element of the anterior segment is the crystalline **lens** itself. Interestingly, while the focus of the cornea is fixed, the **ciliary muscles** surrounding the lens allow to tune light refraction by altering the lens' curvature. This elegant system enables us to form a sharp image of objects despite varying distances.

Posterior segment

The posterior segment refers to the region behind the lens and includes the vitreous chamber, the retina, the choroid and the sclera. The **vitreous chamber** is the largest fluid-containing chamber in the eye and is filled with the transparent vitreous gel. The retina lies between the vitreous gel and the choroid and contains various cell types as discussed further in this chapter. Between the retina and the sclera lies the **choroid**, a highly vascularized layer supplying the outer retina with oxygen and nutrients. The blood supply of the inner retina is arranged by retinal blood vessels that stem from

one central retinal artery at the optic nerve head. This optic nerve can be found at the very back of the eye and is comprised of a bundle of ganglion cell axons wired toward the brain.[2] Finally, the **sclera**, also referred to as "the white of the eye", creates a supportive outer wall that contributes to the firm shape of the eye. It protects the inner structures against physical damage and against the potential invasion of pathogens. For a detailed description of the structure and function of the different parts of the posterior segment we refer the reader to **Chapter 2**.

2. THE RETINA

While many ocular structures are necessary for obtaining optimal vision, the most indispensable part is unquestionably the retina. Indeed, the retina forms the fundamental link between the eye and the brain which is vital for image processing. This demanding task requires a myriad of interactions between a variety of cell types. To this end, the retina exhibits an elegantly organized multilayer structure where no detail is coincidental yet carefully selected by evolution.

The human retina is approximately 500 µm thick and is located between the vitreous and the choroid. At the anterior side, it is separated from the vitreous by the inner limiting membrane (ILM), an extracellular matrix that forms an important drug delivery barrier as discussed in **Chapter 2** and studied in **Chapter 3**. As depicted in **Figure 1.2.**, the retina is divided into two regions being the inner and outer retina which each comprise multiple cell layers.

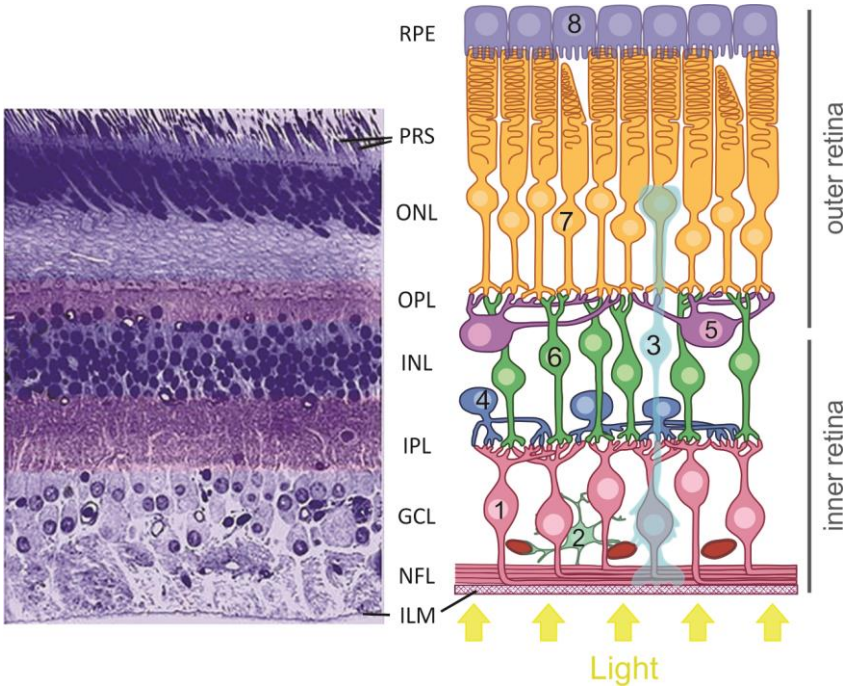

Figure 1.2 | Schematic drawing of the cellular organization of the retina. ILM: inner limiting membrane; NFL: nerve fiber layer; GCL: ganglion cell layer; IPL: inner plexiform layer; INL: inner nuclear layer; OPL: outer plexiform layer; ONL: outer nuclear layer; PRS: photoreceptor segments; RPE: retinal pigment epithelium. 1: ganglion cell; 2: astrocyte; 3: Müller cell; 4: amacrine cell; 5: horizontal cell; 6: bipolar cell; 7: photoreceptor cell; 8: retinal pigment epithelium cell. Figure on the left is taken from [3].

After light has crossed the entire thickness of the retina it activates the **rod** and **cone PR**s by hitting the visual pigment in their disc membranes. The absorption of incoming photons by these pigments (e.g. rhodopsin) next triggers a biochemical cascade which ultimately generates an electrical signal that will be sent to the brain via various neuronal cell types: **horizontal, amacrine, bipolar** and **retinal ganglion cells (RGCs)**. The distribution of rod and cone PRs is not uniform across the retina since several regions can be distinguished (indicated in **Figure 1.3A**). The region of the optic nerve does not display the light-sensing PRs resulting in the famous '**blind spot**'. In contrast, the **macula** or 'yellow spot' in the central region contains a high number of cone receptors responsible for daylight vision. Within this macular region, the **fovea** is characterized by the highest density of cone PRs responsible for detailed high resolution vision (**Figure 1.3B**).[4] Curiously, many vertebrates lack this human-like fovea though they often do exhibit a similar cone-dense region referred to as the visual streak or area centralis.[5] While the central region of the retina primarily harbors cone PRs, the periphery is highly rod-dominated. These rod PRs are activated by dim light and are therefore accountable for night vision.

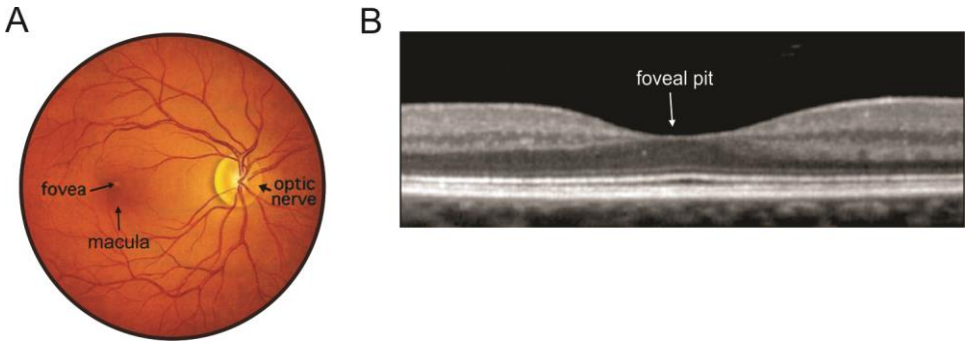

Figure 1.3 | A) The retina as seen through an ophthalmoscope. Image taken from [3]. B) Optical coherence tomography showing the foveal pit. Image taken from [6].

Next to PRs and neurons the retina also accommodates three types of glial cells i.e. microglia, astrocytes and Müller cells. The **microglia**, the immune cells of the retina, sense homeostasis with their many processes and so support in retinal surveillance.[7] When activated, for example in response to injury or pathological stimuli, they undergo morphological changes and migrate to the region of injury.[8] Arrived at the site of interest they phagocytose damaged neurons and secrete neuroprotective factors to help the retina to recover.[7] **Astrocytes** mainly reside in the inner layers of the retina where they closely interact with retinal blood vessels and help to maintain the blood-retinal barrier (BRB). In addition, like all glial cells, they support surrounding neurons by secretion of neuroprotective factors. The morphology and many functions of the **Müller glia** cell is discussed further in this chapter.

The last cell type worth mentioning are the retinal pigment epithelium cells (**RPE**) which form a monolayer situated between the PRs and the choroid. They execute a multitude of functions including phagocytosis of the outer segments of PRs and support of the outer retina homeostasis through the provision of neuroprotective factors. In addition, the RPE represents a fundamental element of the visual cycle since it is responsible for the re-isomerization of all-trans retinal into 11-cis retinal, an essential component of the rod pigment rhodopsin.[9] The RPE furthermore forms the outer BRB by tightly regulating trans-epithelial transport (cfr. **Chapter 2**).

3. THE MÜLLER CELL

The Müller cell is named after its finder Heinrich Müller who in 1851 described these cells as radial fibers offering structural support to neighboring cells (**Figure 1.4 A**).[10] While extensive research in the following century refined our view on Müller glial morphology and behavior, half of the currently known functions of the Müller cell have been discovered in the last 20 years.[11] Müller cells are the principal glial cell type in the retina and are responsible for the support of retinal neurons. Their unique **radial morphology** matches this purpose since the Müller cell connects with each neuronal

cell type by spanning the entire thickness of the retina. Their endfeet are located in the inner retina and abut in the ILM. In the outer nuclear layer (ONL), they ensheath the PR somata and extend their microvilli into the subretinal space. Additionally, they interact with various cell types via their many side branches (**Figure 1.4 B**).

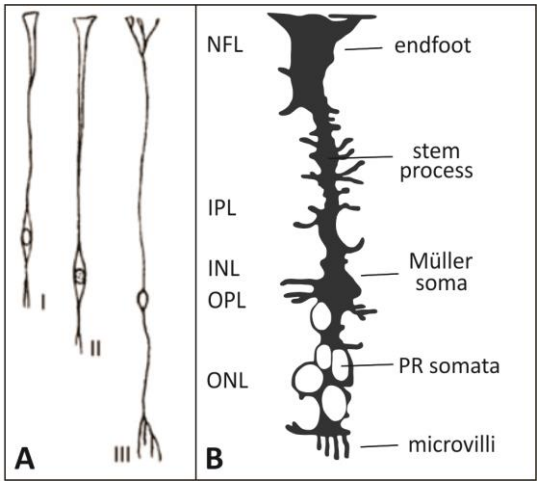

Figure 1.4 | Schematic drawing of Müller cell morphology. A) Heinrich Müller's original drawings of Müller cells isolated from the retina's of fish (I), frog (II) and pigeon (III) [10]. B) Drawing of a Golgi-stained Müller cell, adjusted from [12].

The Müller cell executes a great variety of essential functions which nearly all assist in the functional, metabolic or structural **support of retinal neurons**. Surely, Müller cells assist in the survival and function of PRs and neurons by secretion of neurotrophic factors, growth factors, cytokines and anti-oxidants.[13] They aid in the preservation of retinal homeostasis by controlling the transport of water, ions and waste. They furthermore influence synaptic activity through uptake of neurotransmitters, production of their precursors and release of gliotransmitters. They serve as a soft substrate for neuronal outgrowth and influence the inner blood-retinal barrier (iBRB) by close interaction with its endothelial cells.[11] Müller cells also help to efficiently guide incoming light to the PRs by functioning as so-called 'optical fibers'. Certainly, thanks to their fine-tuned morphology and subtle changes in refractive index along the different retinal layers, scattering of light is reduced and its focus on PRs is enhanced. In 2001, the intriguing discovery was made that Müller cells can exhibit stem cell properties.[14] Upon retinal injury, Müller cells were proven capable to dedifferentiate, proliferate and generate neural stem cells.[11] This finding changed our view on retinal regeneration completely and opened the door for a range of new therapies.[15] In fact, the peculiar characteristics and functions of the Müller cell make this cell type an interesting target for many ocular therapies, as will be further debated in **Chapter 3 and 4**. Astonishingly, the examples of Müller glia functions explained here are merely a selection; Bringmann *et al*. presents a full overview in [11].

In response to pathogenic stimuli such as oxidative stress or injury, Müller cells can be triggered to morph into an active state called **gliosis**. This pro-active transformation involves changes on a morphological, biochemical and physiological level and is initiated in an attempt to protect the retina and/or aid in its recovery.[16] During gliosis Müller cells exhibit at least the following three characteristics: increase in cell size, proliferation and upregulation of intermediate filaments such as glial fibrillary acidic protein.[13] Unfortunately, Müller cell gliosis often works contra-productive and results in exacerbation of the retinal damage. Examples of gliosis adverse effects are glial scar formation, functional uncoupling from neurons and release of pro-inflammatory cytokines.[13] Strikingly, Müller cells respond to virtually all pathogenic stimuli but are also considered as the ultimate survivors of the retina because of their resistance to stress.

4. RETINAL DISEASE

Our vision is dependent on a complex interplay of cells and pathways. A defect in one of these elements, as present in retinal diseases, can therefore have detrimental effects on our vision. Unfortunately, retinal dystrophies are quite common. Their underlying causes are mostly multifactorial yet usually depend on genetic aberrations and/or environmental factors. In this section we will briefly point out the most clinically investigated inherited retinal disorders and the most prevalent acquired ones.

Hereditary diseases

The majority of disease-causing mutations are located in genes expressed in the RPE or the PRs. An example of a well-characterized inherited disease is **retinitis pigmentosa** (RP), which is an umbrella term for a heterogeneous group of retinal disorders each associated with PR loss. With more than 60 causative genes identified and a prevalence of 1 in 3000 to 5000 individuals, it is the most commonly inherited retinal dystrophy.[17,18] Its inheritance mode relies on the causative gene and includes autosomal dominant, autosomal recessive and X-linked.[17] A common form of RP originates from mutations in the RHO gene encoding for the visual pigment rhodopsin.[19] Since these RHO mutations have mainly consequences for rod PRs, patients usually first experience loss of peripheral and night vision. Yet, further progress of the disease is typically also characterized by cone cell death due to the initial loss of rod PRs.[20]

Despite the rareness of **Leber Congenital Amaurosis** (LCA), a third of the clinical trials so far have been focusing on a specific type of LCA caused by loss-off-function mutations in the RPE65 gene.[21] Surely, the autosomal recessive heritance of this gene makes LCA-RPE65 an ideal candidate for gene replacement therapy. This RPE65 gene, expressed in the RPE, is partially responsible for the

isomerization of all-trans retinal to 11-cis retinal. Since the latter component is essential for the function of the pigment rhodopsin, LCA is usually characterized by a very early onset.[22]

Choroideremia is an X-linked recessive degenerative retinal disease with an estimated prevalence of 1 in 50.000. Choroideremia-associated retinal degeneration is linked to mutations in the CHM gene which encodes for Rab-escort protein 1 (REP1), an essential protein for effective intracellular traffic in the retina. The disease usually initiates with loss of night vision to gradually progress towards overall blindness. The small gene size of CHM and loss-of-function nature of its mutations combined with the slow progression of the disease makes choroideremia an ideal target for gene therapy. Indeed, next to LCA, choroideremia is one of the most investigated disease targets in clinical trials.[22a]

Finally, while most blinding mutations affect genes expressed in the outer retina, also the inner retina harbors cells worth targeting with gene therapy. An example of a retinal dystrophy originating in the inner retina is **Leber's Hereditary Optical Neuropathy** (LHON). LHON's pathogenesis derives from mutations in essential elements of the mitochondrial respiratory chain. This mitochondrial defect next results in ganglion cell dysfunction which clinically leads to rapid loss of central vision with a typical onset age between 20 – 30 years.[23] A specific challenge does lie in the fact that the mitochondria should be targeted instead of the nucleus.[24]

Acquired diseases

Next to inherited diseases correlated with specific genetic mutations, many retinal disorders are linked to aging and/or underlying diseases such as diabetes. In fact, these acquired disorders represent the largest fraction of blinding diseases. The cause of these diseases are usually multifactorial where also genetics play a role since family history is often regarded as a risk factor.

Reaching above 30 million of visually impaired individuals worldwide, **age-related macular degeneration** (AMD) is surely regarded as one of the leading causes of vision impairment.[25] AMD is a classic example of a multifactorial disease with as established influencing factors family history, smoking and nutrition.[26] It primarily affects the elderly who suffer from progressive PR damage leading to loss of central vision, a condition that greatly hinders their daily activities and independence. Clinically, two distinct types can be distinguished: 'dry' AMD characterized by geographic atrophy, and 'wet' AMD identified by choroidal neovascularization. While dry AMD has no standardized treatment protocol, wet AMD is usually treated by intravitreal (IVT) injection of antibodies against vascular endothelial growth factor (VEGF).[26]

The World Health Organization (WHO) estimates that **diabetic retinopathy** (DR) is responsible for 15% of blindness in Europe & the USA. This is not surprising since the prevalence of diabetes is on the

rise and more than a third of diabetic patients suffer from DR.[27] The molecular and biochemical mechanisms lying at the root of DR are highly complex and not yet fully understood, although it is hypothesized that the hyperglycemia and high levels of oxidative stress associated with diabetes trigger pathways that next elicit inflammation and upregulation of multiple growth and inflammatory factors which eventually contribute to the typical features of DR being neovascularization and BRB disruption.[28] In its advanced stage DR can induce macular edema or progress into proliferative DR where vascular leakage and angiogenesis are the key concerns, respectively.

Glaucoma is a general term for several neuropathies with as common hallmark the progressive loss of RGCs which leads to a gradual decline in vision. In contrast to AMD and DR, the pathogenesis of glaucoma generally originates in the anterior segment of the eye. A well-established risk factor for glaucoma development is indeed elevated intraocular pressure (IOP). However, is it clear IOP is not the only risk factor that should be monitored since a normal IOP does not guarantee a glaucoma-free life, nor do patients with high IOP necessarily develop glaucoma. In primary open-angle glaucoma, the most prevalent form, elevated IOP is usually caused by decreased drainage of fluid via the trabecular meshwork. Considering the loss of RGCs the retina of glaucomatous patients is characterized by alteration of the optic nerve and nerve fiber layer.[29]

5. RETINAL GENE THERAPY

Gene therapy strategies

Hereditary as well as acquired retinal dystrophies can be treated by gene therapy. Depending on the disease and its progression different gene therapy strategies are valuable. In general, these strategies can be divided into two main categories i.e. gene-specific and non gene-specific approaches.

Gene-specific approaches

The **gene replacement** strategy (also referred to as gene augmentation) is the most widely investigated approach for treatment of retinal diseases and is based on the supplementation of a healthy version of the mutated gene. This strategy is mostly valuable for retinal dystrophies caused by loss-of-function mutations, since in these cases the function of the protein needs to be compensated without the need for abolishing the mutant protein. As mentioned before, the majority of these mutations occur in genes expressed in the outer retina like PRs or RPE cells. Thanks to the extensive research dedicated to this approach, most clinical trials up to now are based on gene replacement. In fact, this strategy reached a milestone only very recently since the first gene therapy treatment for RPE65-dependent LCA has been recommended for approval by the U.S. Food and Drug Administration (FDA).[30]

Dominant diseases that are caused by gain-of-function mutant alleles producing proteins with dominant negative or abnormal functions require a different strategy, i.e. **gene silencing**. In this case, the mutant mRNA is the main target which can be nullified by application of antisense nucleotides, ribozymes or an RNA interference approach based on shRNA or siRNA.[30a] If necessary, even a two-step approach called 'suppression and replacement' could be applied where besides interfering with the mutant mRNA, a healthy copy of the gene is supplemented that is resistant to gene silencing.[30b] The most widely investigated disease targets for this approach are until now autosomal dominant forms of RP.[30c]

Another gene-specific approach is **gene editing** such as the CRISPR/Cas system. In this technology, which is based on an anti-viral defense system of bacteria, a Cas9 nuclease complex is guided to a specific location of the genome by a synthetic 'guide' RNA where it generates double strand breaks. Depending on the treatment aim, these breaks can be repaired by joining the ends in a random fashion (Non-homologues End Joining), or by Homology Directed Repair where the gene is precisely replaced based on a donor template. Since this enables us to remove existing genes and replace them by new ones, this approach is especially relevant for gain-of-function mutations where it is necessary to eliminate the unwanted effects of the mutated protein. The rapid advancement of this technology has caused a revelation in the gene therapy field, also in the ocular context (cfr. **Chapter 7**).

Non gene-specific approaches

Neuroprotection is a therapeutic strategy that focuses on the preservation of healthy neurons and the prevention of neuronal cell death regardless of the underlying genetic anomaly or pathogenic cause. This mutation-independent approach has therefore, in contrast to the gene replacement concept, the potential to treat a great variety of retinal diseases – inherited and acquired.[31] Neuroprotection is currently explored for diseases involving retinal ganglion cell and/or PR death of which the most commonly investigated diseases are glaucoma, RP and DR.[32–39] In view of the short intravitreal half-life of proteins**,** an interesting tactic to ensure a prolonged neurotrophic effect is to deliver genes encoding for neuroprotective factors (e.g. growth factors, anti-apoptotic proteins) to the retina.[32,37] After successful retinal uptake of the therapeutic genes, the transduced cells can then express the neurotrophic factors and secrete them in their surroundings to enhance neuron survival. This strategy will be further discussed in **Chapter 4** where we look into Müller cells as targets for this approach.

In **optogenetics** genes encoding for light-sensitive proteins are introduced into retinal neurons with the aim to let them take over the role of the lost PRs.[40] The most widely investigated optogenetic

proteins are variants of channelrhodopsin, a light-gated ion channel that initiates cell depolarization when triggered. Potential cell types targeted by this strategy nearly all reside in the inner retinal layers and include amongst others ganglion cells and bipolar cells. Interestingly, since the optogenetic approach does not require viable PRs, this strategy could be used to treat patients in advanced stages of retinal degeneration.[31,41]

Another gene therapy approach has been investigated specifically for wet AMD with the goal to find an effective long-term alternative to the frequent IVT injection of anti-VEGF antibodies. This approach, currently evaluated in clinical trials, is the viral delivery of **genes encoding for a soluble VEGF receptor** that could serve as a decoy for the excessive VEGF present in the retina.[21]

Gene carriers

For all gene therapy strategies presented above the smart design of an appropriate gene carrier is essential to guide the therapeutic gene through the many physiological and cellular barriers. Gene carriers can be classified in two types i.e. viral carriers and non-viral carriers.

Viral vectors

In context of retinal gene therapy, most clinical success has undoubtedly been achieved with viral vectors, of which the **adeno-associated vector** (AAV) has proven to be the most effective in transducing retinal cells.[42] AAVs are small non-enveloped viruses (~25 nm) that have an icosahedral capsid which contain single-stranded DNA (**Figure 1.6**). Their cellular tropism and induced expression kinetics depend highly on the AAV's capsid serotype. Indeed, it has been reported that the naturally occurring serotype capsids mainly vary in the looped-out domains presented on the surface, therefore highly influencing their cellular interactions.[43] To gain optimal transduction efficiency a lot of research has therefore been dedicated to the exploration of naturally occurring AAV capsids as well as capsid engineering. As a result of these studies many vectors have been developed that generate high levels of transgene expression after subretinal injection, with clinical trials mostly focusing on AAVs of serotype 2, 5 and 8.[42]

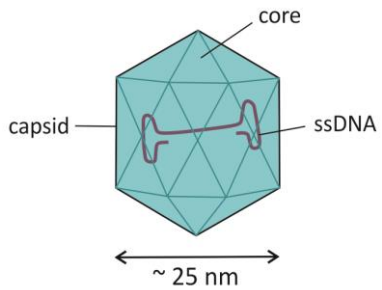

Figure 1.6 | Schematic drawing of an AAV vector.

However, considering the invasiveness of subretinal injection as explained in **Chapter 2**, there remains a lot of interest in an AAV able of efficiently transducing the retina following IVT administration. As a leading example, Dalkara *et al*. developed the AAV2-7m8 vector which successfully transduced mouse and macaque PRs after IVT injection. The vector variant was found by a strategy called *in vivo* directed evolution.[44] Here, libraries of AAV variants are injected intravitreally into mice, after which the variants capable of reaching the outer retina are isolated by harvesting of PRs. After genomic extraction, the respective viral *cap* genes are then amplified by PCR for cloning and repackaging. Repeating this cycle eventually leads to the most powerful vector variant.[45]

Non- viral vectors

Despite the highly promising results generated with viral vectors, a few limitations should be taken into account. A relevant limitation of AAVs is for example their limited cargo capacity of 5 kb which is not sufficient for inherited diseases originating from mutations in larger genes (e.g. Stargardt disease). Furthermore, while the eye is considered as an immunoprivileged organ, AAV administration has been reported to induce innate as well as adaptive immune responses.[46] This immune response was found to be dependent on the administration route since IVT injection led to a more substantial humoral response than subretinal administration in non-human primates.[46] Since these limitations might be circumvented by applying non-viral particles, many research groups, including ours, aim to explore the potential of these carriers for ocular (gene) therapy (cfr. **Chapter 3 and 4**).

Indeed, non-viral vectors might up to now lack the efficiency of their viral counterparts, their high cargo capacity, beneficial safety profile and straightforward surface modification definitely encourage further research. As discussed in **Chapter 5**, nanomedicine has known an immense boost over the last decade resulting in an ever increasing versatility of particle designs and compositions. Nanomedicine has also been gaining more attention in the ocular field, where studies mainly focus on soft NPs based on lipids (cfr. **Chapter 4**),[47,48] proteins[49,50] or polymers[51,52]. A full overview of the variety of particles developed for retinal drug delivery is given by Naash *et al*,[53] though we have selected and discussed the most promising nanoparticle studies in **Chapter 7**.

6. REFERENCES

1. Bourne, R. R. A. *et al.* Magnitude, temporal trends, and projections of the global prevalence of blindness and distance and near vision impairment: a systematic review and meta-analysis. *Lancet Glob. Heal.* **5,** e888–e897 (2017).

2. Ganglion Cell Physiology by Ralph Nelson – Webvision. at <http://webvision.med.utah.edu/book/part-ii-anatomy-and-physiology-of-the-retina/ganglion-cell-physiology/>

3. Simple Anatomy of the Retina by Helga Kolb – Webvision. at <http://webvision.med.utah.edu/book/part-i-foundations/simple-anatomy-of-the-retina/>

4. Curcio, C. A., Sloan, K. R., Kalina, R. E. & Hendrickson, A. E. Human photoreceptor topography. *J. Comp. Neurol.* **292,** 497–523 (1990).

5. Mowat, F. M. *et al.* Topographical characterization of cone photoreceptors and the area centralis of the canine retina. *Mol. Vis.* **14,** 2518–27 (2008).

6. Moshiri, A. What OCT Reveals About the Fovea. (2012). at <https://www.retinalphysician.com/issues/2012/may-2012/what-oct-reveals-about-the-fovea>

7. Li, L., Eter, N. & Heiduschka, P. The microglia in healthy and diseased retina. *Exp. Eye Res.* **136,** 116–130 (2015).

8. Saijo, K. & Glass, C. K. Microglial cell origin and phenotypes in health and disease. *Nat. Rev. Immunol.* **11,** 775–787 (2011).

9. Strauss, O. The Retinal Pigment Epithelium in Visual Function. *Physiol. Rev.* **85,** 845–881 (2005).

10. Müller, H. Zur Histologie der Netzhaut. *Zeitschrift für Wiss Zool* 234–237 (1851).

11. Reichenbach, A. & Bringmann, A. New functions of müller cells. *Glia* **61,** 651–678 (2013).

12. Reichenbach, A. & Bringmann, A. *Müller Cells in the Healthy and Diseased Retina*. (Springer, 2010).

13. Bringmann, A. *et al.* Cellular signaling and factors involved in Müller cell gliosis: neuroprotective and detrimental effects. *Prog. Retin. Eye Res.* **28,** 423–51 (2009).

14. Fischer, A. J. & Reh, T. A. Müller glia are a potential source of neural regeneration in the postnatal chicken retina. *Nat. Neurosci.* **4,** 247–252 (2001).

15. Goldman, D. Müller glial cell reprogramming and retina regeneration. *Nat. Rev. Neurosci.* **15,** 431–42 (2014).

16. Bringmann, A. & Wiedemann, P. Müller glial cells in retinal disease. *Ophthalmologica* **227,** 1–19 (2011).

17. Shintani, K., Shechtman, D. L. & Gurwood, A. S. Review and update: Current treatment trends for patients with retinitis pigmentosa. *Optometry* **80,** 384–401 (2009).

18. RetNet. at <https://sph.uth.edu/retnet/>

19. Sung, C. H., Davenport, C. M. & Nathans, J. Rhodopsin mutations responsible for autosomal dominant retinitis pigmentosa. Clustering of functional classes along the polypeptide chain. *J. Biol. Chem.* **268,** 26645–26649 (1993).

20. Mendes, H. F., Van Der Spuy, J., Chapple, J. P. & Cheetham, M. E. Mechanisms of cell death in rhodopsin retinitis pigmentosa: Implications for therapy. *Trends Mol. Med.* **11,** 177–185 (2005).

21. Bennett, J. Taking Stock of Retinal Gene Therapy: Looking Back and Moving Forward. *Mol. Ther.* **25,** (2017).

22. Redmond, T. M. *et al.* Mutation of key residues of RPE65 abolishes its enzymatic role as isomerohydrolase in the visual cycle. *Proc. Natl. Acad. Sci. U. S. A.* **102,** 13658–13663 (2005).

22a. MacLaren, R. E. *et al.* Retinal gene therapy in patients with choroideremia: Initial findings from a phase 1/2 clinical trial. *Lancet* **383,** 1129–1137 (2014).

23. Majander, A. *et al.* Childhood-onset Leber hereditary optic neuropathy. *Br. J. Ophthalmol.* **0,** 1–5 (2017).

24. Sahel, J.-A. & Roska, B. Gene Therapy for Blindness. *Annu. Rev. Neurosci.* **36,** 467–488 (2013).

25. International AMD Alliance. *The Global Economic Cost of Visual Impairment*. (2010).

26. Fritsche, L. G. *et al.* Age-Related Macular Degeneration: Genetics and Biology Coming Together. *Annu. Rev. Genomics Hum. Genet.* **15,** 151–171 (2014).

27. Stitt, A. W. *et al.* The progress in understanding and treatment of diabetic retinopathy. *Prog. Retin. Eye Res.* **51,** 156–186 (2016).

28. Safi, S. Z., Qvist, R., Kumar, S., Batumalaie, K. & Ismail, I. S. Bin. Molecular mechanisms of diabetic retinopathy, general preventive strategies, and novel therapeutic targets. *Biomed Res. Int.* **2014,** 801269 (2014).

29. Weinreb, R. N., Aung, T. & Medeiros, F. A. The Pathophysiology and Treatment of Glaucoma. *Jama* **311,** 1901 (2014).

30. FDA Advisory Committee Unanimously Recommends Approval of Investigational LUXTURNA™ (voretigene neparvovec) for Patients with Biallelic RPE65-mediated Inherited Retinal Disease. *Spark Therapeutics press release* (2017). at <http://ir.sparktx.com/news-releases/news-release-details/fda-advisory-committee-unanimously-recommends-approval>

30a. Jiang, L. *et al.* Long-term RNA interference gene therapy in a dominant retinitis pigmentosa mouse model. *Proc. Natl. Acad. Sci. U. S. A.* **108,** 18476–81 (2011).

30b. Millington-Ward, S. *et al.* Suppression and replacement gene therapy for autosomal dominant disease in a murine model of dominant retinitis pigmentosa. *Mol. Ther.* **19,** 642–649 (2011).

30c. Farrar, G. J., Millington-Ward, S., Palfi, A., Chadderton, N. & Kenna, P. F. in *Gene- and Cell-Based Treatment Strategies for the Eye* (ed. Rakoczy, E. P.) 43–60 (Springer Berlin Heidelberg, 2015). doi:10.1007/978-3-662-45188-5_4

31. Dalkara, D., Duebel, J. & Sahel, J.-A. Gene therapy for the eye focus on mutation-independent approaches. *Curr. Opin. Neurol.* **28,** 51–60 (2015).

32. Nafissi, N. & Foldvari, M. Neuroprotective therapies in glaucoma: I. Neurotrophic factor delivery. *Wiley Interdiscip. Rev. Nanomedicine Nanobiotechnology* **8,** 240–254 (2016).

33. Matteucci, A. *et al.* Neuroprotection by rat Müller glia against high glucose-induced neurodegeneration through a mechanism involving ERK1/2 activation. *Exp. Eye Res.* **125,** 20–9 (2014).

34. Hernández, C., Dal Monte, M., Simó, R. & Casini, G. Neuroprotection as a therapeutic target for diabetic retinopathy. *Curr. Diab. Rep.* **16,** 29 (2016).

35. Jindal, V. Neurodegeneration as a Primary Change and Role of Neuroprotection in Diabetic Retinopathy. *Mol. Neurobiol.* **51,** 878–884 (2015).

36. Foxton, R. H. *et al.* VEGF-A is necessary and sufficient for retinal neuroprotection in models of experimental glaucoma. *Am. J. Pathol.* **182,** 1379–1390 (2013).

37. Wilson, a M. & Di Polo, a. Gene therapy for retinal ganglion cell neuroprotection in glaucoma. *Gene Ther.* **19,** 127–136 (2012).

38. Hanumunthadu, D., Dehabadi, M. H. & Cordeiro, M. F. Neuroprotection in glaucoma: Current and emerging approaches. *Expert Rev. Ophthalmol.* **9,** 109–123 (2014).

39. Lipinski, D. M. *et al.* CNTF Gene Therapy Confers Lifelong Neuroprotection in a Mouse Model of Human Retinitis Pigmentosa. *Mol. Ther.* **23,** 1308–19 (2015).

40. The Lasker/IRRF Initiative for Innovation in Vision Science. Restoring vision to the blind: Gene therapy for vision loss: the road ahead. *Transl. Vis. Sci. Technol.* **3,** 5 (2014).

41. Busskamp, V., Picaud, S., Sahel, J. a & Roska, B. Optogenetic therapy for retinitis pigmentosa. *Gene Ther.* **19,** 169–175 (2012).

42. Auricchio, A., Smith, A. J. & Ali, R. R. The future looks brighter after 25 years of retinal gene therapy. **28,** 982–987 (2017).

43. Zincarelli, C., Soltys, S., Rengo, G. & Rabinowitz, J. E. Analysis of AAV Serotypes 1–9 Mediated Gene Expression and Tropism in Mice After Systemic Injection. *Mol. Ther.* **16,** 1073–1080 (2008).

44. Ramachandran, P. S. *et al.* Evaluation of Dose and Safety of AAV7m8 and AAV8BP2 in the Non-Human Primate Retina. *Hum. Gene Ther.* **28,** 154–167 (2017).

45. Dalkara, D. *et al.* In vivo-directed evolution of a new adeno-associated virus for therapeutic outer retinal gene delivery from the vitreous. *Sci. Transl. Med.* **5,** 189ra76 (2013).

46. Reichel, F. F. *et al.* AAV8 Can Induce Innate and Adaptive Immune Response in the Primate Eye. *Mol. Ther.* **25,** 2648–2660 (2017).

47. Apaolaza, P. S. *et al.* Structural recovery of the retina in a retinoschisin-deficient mouse after gene replacement therapy by solid lipid nanoparticles. *Biomaterials* **90,** 40–49 (2016).

48. Martens, T. F. *et al.* Effect of hyaluronic acid-binding to lipoplexes on intravitreal drug delivery for retinal gene therapy. *Eur. J. Pharm. Sci.* **103,** 27–35 (2017).

49. Huang, D., Chen, Y. S. & Rupenthal, I. D. Hyaluronic acid coated albumin nanoparticles for targeted peptide delivery to the retina. *Mol. Pharm.* **14,** 533–545 (2017).

50. Kim, H., Robinson, S. B. & Csaky, K. G. Investigating the movement of intravitreal human serum albumin nanoparticles in the vitreous and retina. *Pharm. Res.* **26,** 329–337 (2009).

51. Andrieu-Soler, C. *et al.* Intravitreous injection of PLGA microspheres encapsulating GDNF promotes the survival of photoreceptors in the rd1/rd1 mouse. *Mol Vis* **11,** 1002–1011 (2005).

52. Peters, T. *et al.* Evaluation of polyesteramide (PEA) and polyester (PLGA) microspheres as intravitreal drug delivery systems in albino rats. *Biomaterials* **124,** 157–168 (2017).

53. Adijanto, J. & Naash, M. I. Nanoparticle-based technologies for retinal gene therapy. *Eur. J. Pharm. Biopharm.* **95,** 353–367 (2015).

2

In vitro and ex vivo models to study drug delivery barriers in the posterior segment of the eye

An adapted version of this chapter is in press:

Karen Peynshaert[a,b] , Joke Devoldere[a,b], Stefaan De Smedt[a,b], Katrien Remaut.[a,b] In vitro and ex vivo models to study drug delivery barriers in the posterior segment of the eye. *Advanced Drug Delivery Reviews* (2017)

[a]Lab of General Biochemistry and Physical Pharmacy, Faculty of Pharmaceutical Sciences, Ghent University, Ottergemsesteenweg 460, B9000 Ghent, Belgium.
[b]Ghent Research Group on Nanomedicines, Ghent University, Ottergemsesteenweg 460, B9000 Ghent, Belgium.

ABSTRACT

Many ocular disorders leading to blindness could benefit from efficient delivery of therapeutics to the retina. However, despite extensive research into drug delivery vehicles and administration techniques, efficacy remains limited because of the many static and dynamic barriers present in the eye. Comprehension of the various barriers and especially how to overcome them can improve our ability to estimate the potential of existent drug delivery vectors and support the design of new ones. To this end, this chapter gives an overview of the most important ocular barriers for each administration route to the back of the eye. For each barrier, its biological composition and its role as an obstacle toward macromolecules, nanoparticles and viral vectors will be discussed; special attention will be paid to the influence of size, charge and lipophilicity of drug(s) (carrier) on their ability to overcome each barrier. Finally, the most significant available *in vitro* and *ex vivo* methods and models to test the potential of a therapeutic to cross each barrier are listed.

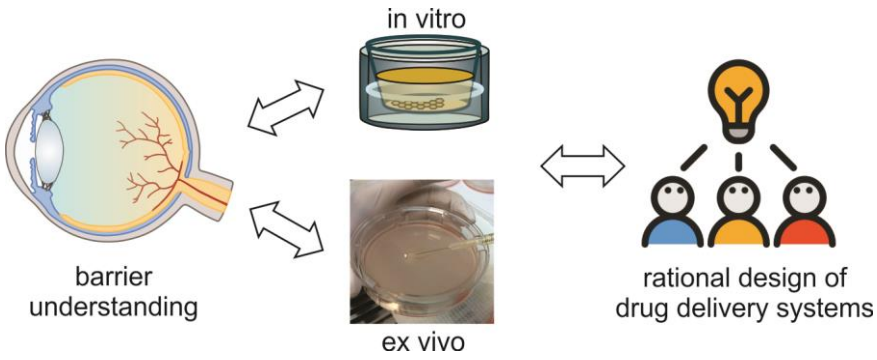

Table of contents

1. INTRODUCTION

In **Chapter 1** we discussed several therapeutic strategies to treat the wide variety of hereditary and acquired retinal diseases. However, the success of all these strategies is highly dependent on the delivery of the drugs and/or their carriers to the target site. To this end a great variety of advanced drug delivery systems are being investigated and developed, such as intravitreal implants and nanoparticles (NPs). However, although the eye is an easily accessible organ, its many physiological and anatomical barriers still considerably restrict effective delivery of therapeutics to the target site.

A detailed characterization of the obstacles drug delivery carriers have to overcome is essential to define the barrier role of a specific ocular tissue. This in its turn allows for smart adjustments to the drug delivery carriers in line with the barriers' properties. *In vivo* experiments are of great value to determine the overall efficiency of a drug delivery system with all barriers in place. *In vitro* and *ex vivo* studies, on the other hand, enable us to examine each barrier in the delivery process on its own, providing preliminary evidence of the ability of a delivery system to overcome this single barrier. Furthermore, *ex vivo* explant cultures allow us to experiment on ocular tissues of larger, more relevant species (e.g. pig, non-human primates or even human eyes) providing valuable information without proceeding to costly and labor-intensive *in vivo* work. The proper use of *in vitro* and *ex vivo* models can thus signify a great step forward in the design and optimization of therapeutics and their vehicles for ocular drug delivery.

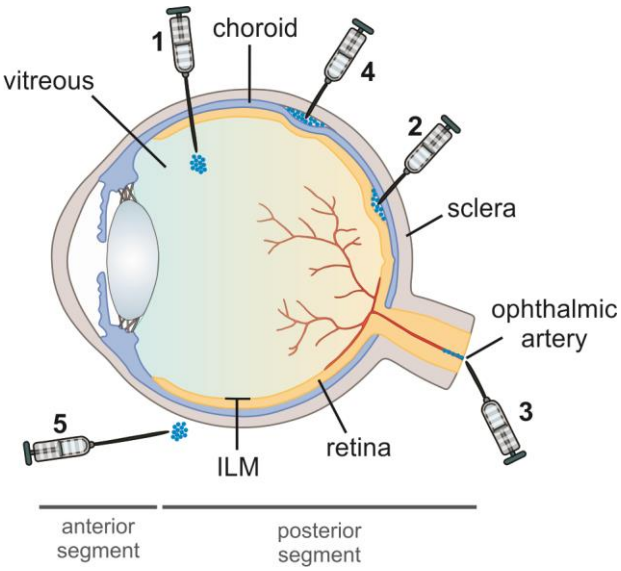

Figure 2.1 | Overview of administration routes to target the posterior segment. 1: intravitreal injection; 2: subretinal injection; 3: systemic injection; 4: suprachoroidal injection; 5: transscleral administration; ILM: inner limiting membrane.

As discussed in **Chapter 1**, many blinding diseases find their origin in the retina which requires drug delivery to the posterior segment. To reach this segment several administration routes are available,

as illustrated in **Figure 2.1**. Even though some administration routes are clinically preferred over others, each route comes with its own advantages and set of obstacles to conquer.[1] In this chapter, we will discuss the biological structure of the barriers and biological obstacles encountered for each of these administration routes while linking drug (carrier) physicochemistry to successful barrier passage. Finally, we will give a summary of the most relevant *in vitro* and *ex vivo* methods that might be useful in research focusing on advanced drug delivery in the posterior segment of the eye.

2. BARRIER COMPOSITION AND ROLE

Barriers encountered after intravitreal injection

During intravitreal (IVT) injection a drug formulation is injected into the vitreous humor of the eye (**Figure 2.1**). In the clinic, IVT injections happen on a daily basis for a plethora of drugs, with currently anti-VEGF (Vascular Edothelial Growth Factor) medication as the most routinely injected therapeutic against AMD. Delivering the therapeutics directly into the vitreous offers several benefits. Firstly, several anterior barriers are bypassed and the drug is delivered close to the target site. Secondly, the procedure is safe and relatively easy to perform.[2,3] Given these advantages IVT injection is a widely investigated administration route for the delivery of an increasing variety of drug delivery systems, ranging from gene vectors to biodegradable implants.[4] For retinal delivery of non-viral vectors to the inner retina, IVT injection is furthermore also our administration route of choice (cfr. **Chapter 3**). Still, established disadvantages of this technique compared to subretinal gene therapy are: a) the considerable dilution of the gene carriers in the vitreous volume, and b) the immune surveillance in the vitreous which can result in the formation of neutralizing antibodies against .e.g. AAV2 vectors.[4a] Overall, the intraocular location of the therapeutics is no guarantee for success, since the therapeutic efficiency is known to be highly dependent on the therapeutics' ability to migrate from the injection site toward the retina.[5] In this regard, there are two main obstacles that hamper successful therapy after IVT injection, namely the vitreous and the inner limiting membrane (ILM).

Vitreous

The vitreous body is a transparent gel-like structure with a volume of about 4 ml that occupies approximately 80% of the human eye. The function of the vitreous body is a recurring subject of discussion, but is mostly considered to regulate eye size during eye development.[6] Due to its extremely high water content (98%-99%), the density of the vitreous body approximates that of water.[5,7] The gel structure is composed of a 3-dimensional network of collagen fibers of collagen types II, IX, and V/XI, with collagen type II being the most abundant (60-75%). These collagen fibers provide the vitreous with flexibility and strength against mechanical tensions.[7] The spaces in between these fibrils are filled with glycosaminoglycans (GAGs) of which hyaluronic acid (HA), a

highly hydrated negatively charged GAG, represents the bulk (**Figure 2.2**). The function of this linear polymer is to stabilize the collagen net and to ensure a swelling effect.[8] The remaining fraction of GAGs is represented by chondroitin sulfate and heparin sulfate.[9] Interestingly, the composition of the vitreous is not uniform throughout the whole vitreous body but different anatomical regions can be identified. Traditionally, the vitreous is regarded as consisting of two fractions.[9a] The largest volume is taken in by the central vitreous, which is characterized by a more liquid state owing to the low density of its collagen network. The cortical vitreous that delineates the retina contains higher concentrations of collagen as well as HA providing it with high mechanical strength.[7] Interestingly, various investigators have indicated the presence of a complex area in front of the human macula which is fluid-like. This area, referred to as the 'bursa premacularis' is furthermore surrounded by multiple cisterns (fluid-filled cavities).[9b] While these structures have been identified in human eyes, it is up to now unclear to which extent the same or similar structures are present in the vitreous gel of other species. A well-described phenomenon that affects the structure of the vitreous humor is liquefaction. During this process, which is mostly induced by age, the vitreous degrades leading to a loss of its gel-like appearance and an increase of its free water content; both factors that can influence the barrier function of the vitreous.[10]

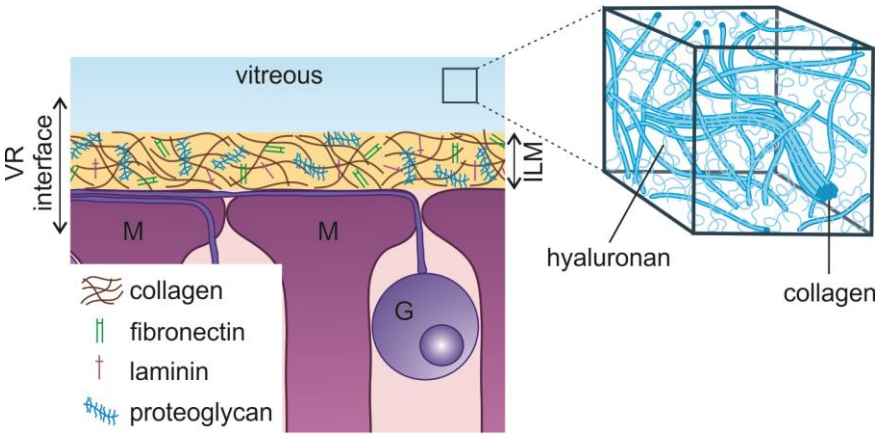

Figure 2.2 | Schematic drawing of the vitreoretinal (VR) interface and vitreous. The vitreoretinal interface is constituted from peripheral vitreous, the inner limiting membrane (ILM) and the endfeet of the Müller cells. The ILM has an extracellular matrix structure which forms the basement membrane of the Müller cells (M). The vitreous gel is formed by a network of collagen fibers of different types, mainly type II. The spaces in between these fibrils are filled with glycosaminoglycans, of which hyaluronic acid is the most abundant. G: ganglion cell. Vitreous figure is adapted from [7].

In general, two types of barriers can be differentiated within the vitreous: the anatomical or static barrier represented by the vitreous structure itself, and the physiological or dynamic barrier represented by the flow processes and clearance pathways taking place in the vitreous. The fact that the vitreous represents an anatomical barrier toward drug diffusion has already been discovered early on, when Sakamoto *et al*. revealed that a vitrectomy significantly enhanced the transduction

efficiency of viral vectors from the vitreous.[11] In the same line, also the penetration of non-viral vectors seems to be hindered by the vitreous gel structure.[5] In this case, it is reported that the particle surface characteristics are of great importance. A general trend can be recognized: positively charged NPs are blocked in their diffusion by interaction with the negatively charged components of the vitreal network,[12–17] while negatively charged particles, based on for example poly lactic-co-glycolic acid (PLGA) or human serum albumin, distribute successfully across the vitreous humor.[17–20] Various surface coatings such as polyethyleneglycol (PEG) and HA have therefore been explored to shield the surfaces of cationic particles in order to improve the migration of the particles through the vitreous.[14,21,22]

While NP charge evidently influences particle diffusion, the impact of particle size is less obvious. Xu *et al*. have estimated the average pore size of bovine vitreous to be ~550 ± 50nm and indeed witnessed that 1 µm sized particles were not able of maneuvering through the meshwork.[16] In contrast, Martens *et al*. observed that negatively charged particles up to 1 µm were mobile in bovine vitreous based on a similar model.[13] This suggested pore size of 550 nm is surely large enough for small molecules and antibodies to diffuse freely through the vitreal meshwork. In addition, since the NP size for ocular (gene) therapy usually varies from 10 to 500 nm, the mesh size should not represent an obstacle for particles as well. However, as will be discussed in the ILM section, it is important to keep in mind when aiming for retinal targets that there is also a size limit for penetration through the ILM that probably lies lower.

Next to the anatomical barrier inherent to the vitreous structure, drug distribution is also influenced by physiological obstacles like clearance pathways and intraocular flow processes. The most important flow processes within the eye are the convective flows. These flows are driven by the pressure difference between the front and back side of the vitreous and are oriented in an anterior-posterior direction.[23,24] While these flows have barely any effect on the distribution of small drugs with high diffusivity, they can have a substantial effect on larger, less diffusible therapeutics, especially in larger species such as humans.[23–25] The physicochemical characteristics of molecules/particles have a huge impact on the way they are cleared and thus influence their half-life in the eye. Smaller more lipophilic entities are usually cleared at the posterior side since these are easily able of crossing the blood-retina barrier, leading to short intravitreal half-lives of a couple of hours. Larger more hydrophilic therapeutics, on the other hand, are eliminated through the anterior route which is dominated by the aqueous humor outflow. These entities, for example antibodies, tend to remain within the vitreous for a longer time with half-lives reaching 100 hours.[26] Next to the intrinsic flow processes taking place within the eye, drug distribution is likely also influenced by the vitreous humor motion associated with eye movement (i.e. saccadic movement). However, the

impact of this motion on intravitreal drug delivery is hard to predict since its influence has until now mainly been studied in vitreous substitutes.[27,28]

Inner Limiting Membrane

The ILM forms the structural boundary between the vitreous and the retina and is mainly composed of collagen type IV, laminin and fibronectin which form an intertwined network.[29] Essentially, this extracellular matrix represents the basement membrane of the Müller cells and thus aligns with their endfeet (**Figure 2.2**).[30] There is strong evidence that the lens and ciliary body are the primary production sites for ILM proteins during embryogenesis.[29,31] The ILM has proven essential for the early development of the eye, seeing its absence is associated with retinal abnormalities including an aberrant ganglion cell layer.[32,33] In the fully developed eye, however, the ILM is likely not essential since ILM peeling is not correlated with severe adverse effects.[34] Also, it was observed that the ILM of macaques is not regenerated even one year after its removal.[35]

In rabbits the pore size of the ILM meshwork is estimated between 10 and 25 nm, yet it is unclear if this can be extrapolated to other species.[36] Similar to the vitreous, the composition of the ILM is not consistent over the entire tissue but varies regionally.[8] Also the thickness of the ILM differs per region, where the thickness of the foveal ILM is substantially thinner compared to parafoveal regions.[37] Another important fact is that the ILM varies greatly between different species: Transmission electron microscopy (TEM) data revealed that the ILM of an adult mouse is merely 100 nm thick while atomic force microscopy measurements proved that the ILM thickness of a human retina can measure up to 4 µm.[37,38] It has furthermore been shown by several research groups that the ILM layer thickens with age.[29,39] Since the thickness of the ILM undeniably influences its barrier function it is assumed that the barrier is more easily surmountable in smaller animals, such as mice, than in larger ones, like non-human primates and humans.

There are many reports on the physical barrier role of the ILM in context of non-viral and viral gene delivery to the retina. IVT injection *in vivo* seldom leads to effective gene expression in larger animals than rodents, often because of the accumulation of the vectors at the ILM.[40–43] In fact, Dalkara *et al*. elegantly demonstrated in rats that inducing mild enzymatic digestion of the ILM by protease treatment exceptionally enhanced the transfection efficiency of several AAV serotypes from the vitreous.[44] Similarly, when the ILM is breached due to retinal disease, viral transduction is greatly improved when compared to ILMs in a healthy state. [45,46] Also Takahashi *et al*. witnessed that surgical ILM peeling substantially enhanced AAV transduction of the inner retina in cynomolgus monkeys.[42] Taken together, these observations convincingly substantiate the barrier role of the ILM for viral drug delivery to retinal targets. Interestingly, interaction of viral vectors with binding sites at the ILM (e.g.

laminin receptor or heparan sulfate) might enhance their accumulation at the vitreoretinal interface, allowing the vectors to further diffuse into the retina and produce gene expression.[44,45,47–49] Be that as it may, too strong affinity of viral vectors to ILM binding sites might prevent the vectors to move beyond the ILM.[49,50]

Several research groups have reported on the barrier role of the ILM toward non-viral particles, where a clear trend regarding particle charge is noticeable. Indeed, in rodent as well as bovine species positively charged NPs are virtually entirely obstructed by the ILM while neutral to negatively charged ones do penetrate into the retina.[15,51] Regarding particle size the trend is less apparent since the majority of studies has been performed on rodents. In this species, particles up to 350 nm penetrated into the retina, though it is not certain this observation can be extrapolated to larger species such as cow or human.[15,20,36,52] Peculiarly, Bourges *et al*. detected that highly negative polylactide particles of ~150 nm and neutral ones of ~350 nm accumulated at the ILM 1 h after IVT injection followed by penetration into the rat retina.[52] This suggests that, similar to viral vectors, presence of binding sites in the ILM might facilitate the diffusion of carriers into the retina.

Also for macromolecules the ILM reduces or even blocks retinal passage depending on the physicochemical properties of the molecule. While negatively charged 20 kDa sized dextrans passed the ILM smoothly, positively charged molecules of the same size were virtually all blocked by the ILM.[51] Since even negatively charged dextrans of 2000 kDa in size penetrated more efficiently into the bovine retina than 20 kDa positively charged molecules, it is obvious that charge surely represents the dominant factor defining passage of macromolecules through the ILM.[51]

Barriers encountered after subretinal injection

A subretinal injection is an injection right below the neural retina, in between the photoreceptor (PR) layer and the retinal pigment epithelium (RPE) layer (**Figure 2.1**).[53,54] A typical volume of around 150 to 500 µl is injected in humans, leading to a transient detachment between these two layers.[55,56] Complications are relatively common and more severe when compared to e.g. IVT injection, as this retinal detachment can result in PR death and loss of vision. The whole procedure is also quite invasive, as subretinal injection is usually preceded by full anesthesia and a vitrectomy.[57] Despite the drawbacks of this administration route, it is very effective to deliver therapeutics right at the target site. Subretinal injections are therefore mostly applied for larger entities such as gene vectors or cells that are therapeutically relatively ineffective using other administration routes.[58] As a matter of fact, subretinal injection is the most clinically investigated delivery route for retinal gene therapy.[59,60] Since the injection site is so close to the retina, practically all barriers in the posterior segment are

circumvented. Gene expression is however often limited to the injection site, suggesting that the primary barrier for efficient therapy following subretinal injection is the retina itself.[61]

Neural retina

The retina is the tissue at the back of the eye that receives light and transmits it to the brain where the signals are further processed into an image. As described in **Chapter 1** it is constituted of a neatly organized multilayered structure that allows interplay between its PRs, neurons and glial cells (**Figure 2.3**). The barrier role of the retina can be attributed to its dense structure, which prevents free diffusion of (therapeutic) macromolecules and carriers. In light of this, Jackson *et al*. have observed that the retinal exclusion limit, i.e. the maximum molecule size able of freely diffusing through the retina, is dominantly defined by the inner and outer plexiform layer.[62] This limit is approximately 76 kDa for a fixed human retina, though since therapeutic antibodies such as bevacizumab (Mw 149 kDa) have been reported to cross the entire thickness of the retina,[63,64] we expect the molecular size limit to be higher in unfixed tissue. More recently, Tao *et al*. concluded from similar experiments that the inner and outer nuclear layers are the predominant diffusional barriers (**Figure 2.3**).[65] While these observations are based on free diffusion it should be noted that active cellular transport of the drug (carrier) by a retinal cell type can ensure the distribution of macromolecules or drug carriers throughout the whole retina.

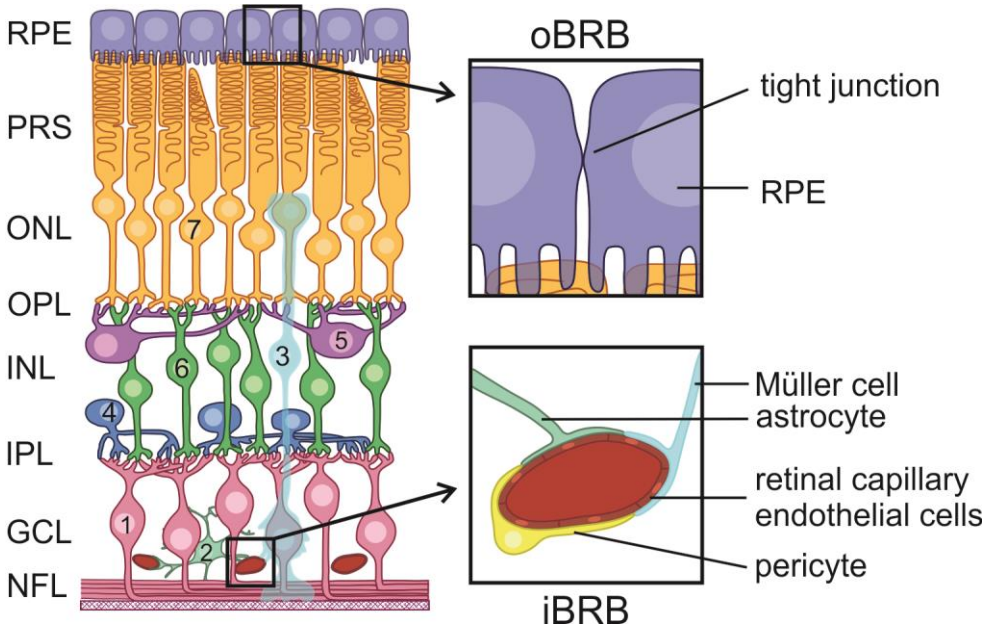

Figure 2.3 | Schematic drawing of the retina and blood-retina barrier (BRB). NFL: nerve fiber layer; GCL: ganglion cell layer; IPL: inner plexiform layer; INL: inner nuclear layer; OPL: outer plexiform layer; ONL: outer nuclear layer; PRS: photoreceptor segments; RPE: retinal pigment epithelium. 1: ganglion cell; 2: astrocyte; 3: Müller cell; 4: amacrine cell; 5: horizontal cell; 6: bipolar cell; 7: photoreceptor cell. The inner BRB (iBRB) is formed by the tight juntions of the endothelial cells of the inner retinal vasculature. The Müller cells and astrocytes influence the endothelial cells through the secretion of growth factors and transfer of nutrients and waste products. The outer BRB (oBRB) is composed of the tight junctions of the RPE cells.

Besides static hindering the diffusion of therapeutics, certain components within the retina might interact with subretinally injected therapeutics.[66,67] Similar to the vitreous and the ILM, GAGs which are present in the interphotoreceptormatrix and on the surface of RPE cells, can bind therapeutic entities and in this way block their diffusion toward the target cells as suggested by Pitkänen *et al*.[51,68] Finally, also the outer limiting membrane (OLM) represents a semipermeable barrier, limiting the diffusion of entities out of the extracellular space that surrounds the PR segments into the ONL. As an example, 150 kDa FITC – dextran had great difficulty in exiting the subretinal space in the rabbit retina while its 10 kDa version easily diffused up to the vitreous.[68a] In any case, the diffusional barrier can easily explain why gene expression after subretinal injection is more than often limited to the outer retina and RPE layer.[69] Clinical trials administering gene vectors by subretinal injection therefore mainly focus on diseases that have an initial causative mutation in the PRs or RPE cells.

Barriers encountered after intravenous administration

Intravenous administration, or injection in the blood stream, is a widely applied administration route in the clinic (**Figure 2.1**), including in ophthalmology. A few examples of intravenously administered therapeutics for ocular diseases are anti-inflammatory drugs for uveitis,[70] antibiotics for endophthalmitis[70] and verteporfin for choroidal neovascularization.[71] While intravenous administration leaves the eye untouched and is therefore less invasive, the bioavailability of drugs in the retina after this type of administration is very low (< 5%).[72] This is partly attributed to the marginal fraction of blood flow in the eye compared to the blood flow of other organs like the liver.[73] Intravenous injection therefore also requires higher volumes of the therapeutic to be administered to achieve therapeutic levels in the eye which inevitably raises the chance of unwanted off-target effects. Furthermore, it is well-established that the binding of serum proteins followed by recognition by the immune system can lead to rapid clearance of the therapeutics.[74] Nevertheless, researchers agree that there might be a future for ocular therapy via intravenous administration if efficient ocular targeting can be achieved. However, the efficient delivery in the eye of the therapeutic entity via the bloodstream is no guarantee for success. On the contrary, the presence of the blood-retinal barrier (BRB) within the eye signifies a major restriction for the permeation of compounds from the ocular blood flow into the retina.[75]

Blood-Retinal Barrier

The BRB contributes to the control of retinal homeostasis by tightly regulating the exchange of fluid and molecules between the blood and the retina and restricting the entry of hazardous molecules. This BRB support of retinal integrity is fundamental, which is illustrated by the fact that its breakdown is associated with vision loss.[76] The BRB is constituted of an inner (iBRB) and outer barrier (oBRB) represented by respectively the tight junctions of the inner retinal vasculature and the RPE

cells in the outer retina (**Figure 2.3**). In the iBRB these tight junctions, also referred to as zonula occludens, are intertwined with adherens and gap junctions into sophisticated junction structures that strictly control paracellular transport.[77] Molecularly, intercellular junctions are constituted of a complex collection of proteins including occludin and claudin proteins.[78] On top of these junctions, the transcellular transport of the iBRB is also restricted thanks to the absence of fenestrations in the endothelial cells as well as the lack of transport vesicles. Together, these features result in a high transendothelial resistance which is comparable to that of the blood-brain-barrier.[79] Next to the primary role of endothelial cells in the iBRB, other retinal cell types also influence the barrier function. Surely, the basal lamina of endothelial cells are connected to the so-called neurovascular unit which involves pericytes, Müller cells, astrocytes and microglia.[79a] Whereas pericytes mainly influence the endothelial cells through the secretion of growth factors,[80] glial cells also offer support through the transfer of nutrients and waste products.[77,81]

For therapeutics to reach the oBRB, they must first escape the choroidal blood flow. Conveniently, in contrast to the capillaries of the inner vasculature, the endothelial cells of the choroidal capillaries are fenestrated allowing leakage of larger molecules like proteins.[82,83] The choriocapillaries therefore represent no bottleneck for the systemic delivery of therapeutics into the eye.[78] Similarly, the Bruch's membrane, which lies in between the choroid and RPE layer, does not restrict macromolecular diffusion into the neuroretina.[78] The choroid-retinal transfer of macromolecules is in fact predominantly limited by the junctional complexes between the RPE cells. Similar to those of the iBRB, these complexes are constituted of an entanglement of tight, gap and adherens junctions.[83] In addition, the uneven distribution of RPE membrane proteins also adds to the function of the oBRB.[78] Fascinatingly, junctional complexes are not static structures yet their strands open and reseal to allow passage of molecules. Indeed, transfer of fluid and its components is limited yet elegantly regulated by several types of transport routes allowing the RPE to perform one of its primary functions i.e. preserving the ion, water and nutrient balance of the retina.[84,85] Next to passive diffusion through the tight junctions, transport routes include active transport by pump proteins and transcytosis by means of invaginating vesicles.[84]

Seeing the strictly regulated transport of endogenous molecules across the BRB, it is not surprising the BRB represents a crucial hurdle for systemic delivery of foreign molecules in the retina. Initial studies with small hydrophilic molecules such as fluorescein have shown limited permeability of the oBRB, where inward diffusion (choroid to retina) is much lower than in the opposite direction.[86–88] It seems that sufficiently small solutes (< 0.4 nm) can diffuse freely through the pores of the junction network while the larger ones (> 0.4 nm) are dependent on the ability of the junctions to break open and close.[79] A systematic study looking into the permeation of differently sized FITC-dextrans up to

80 kDa in isolated bovine RPE-choroid tissue also revealed that the permeability of macromolecules decreases dramatically with increasing size with an insignificant permeability starting from 20 kDa.[88] Since the choroid poses no hurdle for permeation of the size ranges studied, it can be assumed the limitations observed are likely solely attributed to the RPE layer.

In addition to size, other physicochemical features of the entity such as charge and hydrophilicity influence to which extent the oBRB serves as a barrier.[89] The diffusion of ions, and likely therefore also of charged compounds, is hypothesized to be influenced by the charge features of the claudin proteins present in the junctions.[79] Pitkänen et al. tested the permeation of several similarly sized β-blockers in function of their lipophilicity and found that the more lipophilic ones crossed the oBRB substantially more efficiently.[88] Trends regarding physicochemistry of macromolecules that allows permeation of the iBRB are very similar, with hydrophilic substances again having great difficulty in overcoming this barrier.[90] Furthermore, Bellhorn et al. observed that dextrans as small as 3 kDa were unable of entering the retina through the oBRB nor the iBRB.[91] Generally, it is suggested that small hydrophilic compounds migrate through the paracellular network of junctions, while lipophilic molecules benefit from the transcellular route.[88] The iBRB and oBRB exhibit influx transporters for physiological substrates like the glucose transporter and L-type amino acid transporter. Designing drugs that resemble these transporter substrates could therefore be a strategy to enhance delivery across the BRB into the retina. Efflux pumps, on the other hand, work counteractive by shuttling the therapeutic back to the bloodstream.[92] The most well-known efflux pump is likely P-glycoprotein which is present on RPE cells as well as on the endothelial cells of the iBRB.[93,94] Proposed strategies to prevent this shuttling are the design of therapeutics in such a way they are not recognized by efflux pumps, and/or the co-administration of efflux pump inhibitors (e.g. tariquidar or dexverapamil).[92,95]

Besides macromolecules, larger drug delivery vehicles like NPs have also been evaluated on their ability to cross the BRB in vivo - and intriguingly, with some success. In this regard, Kim et al. observed in mice that intravenously administrated gold NPs of 100 nm were excluded while their smaller counterparts of 20 nm were present within the retina.[96] Similarly, AAV 9 vectors have also been reported to efficiently transduct the retina after systemic delivery, especially in the neonatal mouse with less developed vasculature.[97,98] Seeing both particles are likely too large to passively diffuse through the junctional complexes, it is hypothesized that active processes such as transcytosis mediate their transport through the BRB.[96] Plasmid-loaded liposomes of greater size (~85 nm) are also reported to cross the BRB in mice, since gene expression was detected in the RPE as well as the inner retina. Interestingly, these liposomes were decorated with antibodies targeted against the

transferrin receptor present in the BRB causing receptor-mediated transcytosis of the particles across the BRB into the retina.[99]

Similar as observed with the ILM, it is suggested that disease states associated with compromised BRB integrity might make systemic delivery of ocular therapeutics more feasible.[77,100,101] With this in mind, several strategies have been proposed to transiently manipulate the permeability of the BRB, such as the induction of ocular hypotony, treatment with vasoactive compounds or siRNA-mediated downregulation of tight junction proteins.[75,77,102]

Barriers encountered after suprachoroidal administration

Suprachoroidal administration involves injection into the suprachoroidal space (SCS), i.e. the virtual space between the sclera and the choroid (**Figure 2.1**). Under normal conditions this border is not an existent space, but it can open up under the influence of the pressure applied by injection and incorporate fluid volumes up to 200 µl.[100] Strikingly, a study in *ex vivo* porcine eyes revealed that the injected material spreads out across the inner surface of the eye within 8 seconds.[103] Suprachoroidal administration offers the advantage of bypassing several burdensome barriers such as the ILM and the sclera, whereby it often results in higher bioavailability in comparison to IVT injection and periocular administration, respectively.[104] The most promising method to reach the SCS currently investigated is likely the use of microneedles (maximum 1 mm in length), which might find its way to the clinic soon. These microneedles penetrate through the sclera to deliver into the SCS in a safe and minimally invasive way.[105–107] Suprachoroidal injection is rumored to be an ideal route to target the posterior segment. However, depending on the final target tissue several barriers should be taken into account. To reach the retina, both the RPE and the choroid should be successfully passed while for treatment of choroidal diseases (e.g. choroidal neovascularization) only the high choroidal circulation represents a potential hurdle.[1,108,109] Since the RPE has been extensively discussed above we will focus here on the choroid.

Choroid

The choroid is the highly vascularized layer lying between the RPE layer and the sclera, with as primary function the delivery of oxygen and nutrients from the blood flow into the outer retina. The choroidal tissue is approximately 200 µm thick at birth and thins with age.[110,111] Anatomically, the choroid is usually divided into five layers: the Bruch's membrane, the choriocapillary layer, two vascular layers and the suprachoroidea which is closest to the sclera (**Figure 2.4**).[112] The Bruch's membrane contains collagen and elastin and its inner and outer layer is represented by the basement membranes of the RPE cells and choriocapillaries, respectively.[113] The capillaries in the choriocapillary layer are highly fenestrated, allowing the passage of nutrients as well as larger molecules such as proteins.[112] The underlying vascular layers contain small arteries and increasingly

larger blood vessels toward the sclera. Finally, the suprachoroid forms the border between the choroid and the sclera, and contains both collagen fibers and cell types from the stromal tissue such as melanocytes and fibroblasts.[112]

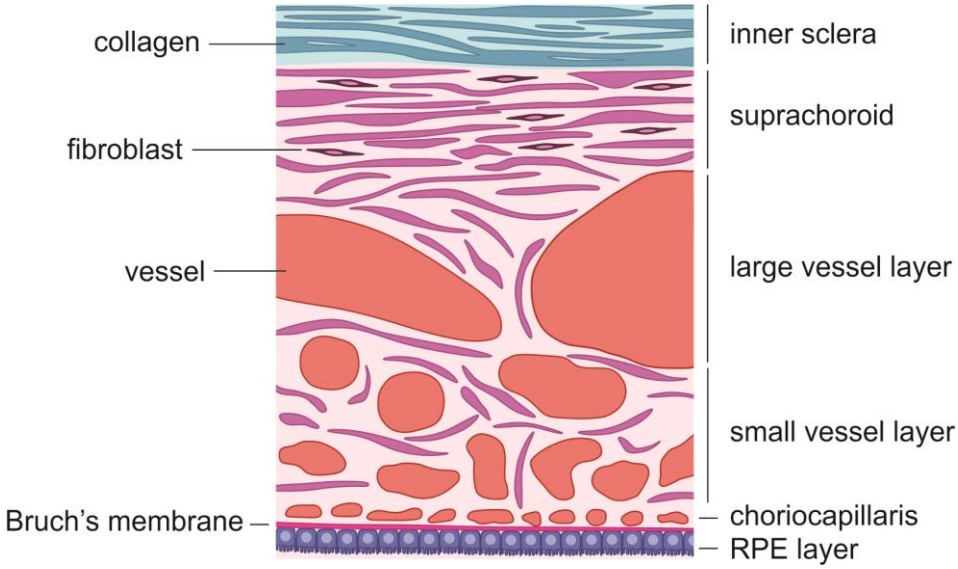

Figure 2.4 | Schematic drawing of the choroid and sclera. The choroid is divided into five different layers. The Bruch's membrane aligning with the retinal pigment epithelium (RPE) layer, the choriocapillaris with fenestrated capillaries, two vascular layers with larger vessels toward the sclera, and the suprachoroid located next to the sclera. The sclera is constituted of collagen bundles, proteoglycans and glycoproteins. The thickness and orientation of the collagen bundles depends on the region in the eye as well as the tissue depth within the sclera. Figure adapted from [112].

Technically, the choroid has two barrier roles. On the one hand it functions as a molecular sieve while on the other hand the choroidal blood flow functions as an important clearance mechanism. Naturally, the ability of certain therapeutics to reach their retinal targets will be defined by their ability to overcome both the static physical barrier as well as the dynamic barrier. Luckily, the barrier roles in relation to the physicochemical characteristics of the compounds are becoming increasingly clear.

The physical permeability of the choroidal tissue has been investigated with small molecules, macromolecules and particles. In case of small molecules, several groups found that injection of sodium fluorescein (NaF) and contrast agents into the SCS leads to the rapid spread of fluid around the SCS.[103,107,114,115] Tyagi *et al*. found that the rate and level of delivery of NaF into the retina after suprachoroidal administration was higher when compared to periocular and IVT injection.[114] As expected, the diffusivity into the posterior segment depends on molecular weight. When FITC-dextrans with a molecular weight of 4 and 40 kDa were injected into the SCS of a rabbit *ex vivo* eye model, the delivery of the 4 kDa molecule in the vitreous and retina was substantially higher compared to its larger counterpart.[115] In the same report, also the permeability of various Beta-

blockers with differing lipophilicity was evaluated. Higher lipophilicity correlated with increased choroidal and retinal delivery, most likely due to the interaction of lipophilic compounds to binding sites in the choroid and retina such as cellular membranes and melanin.[116]

The diffusivity of nano-and microparticles was tested *ex vivo* on porcine tissues.[106] After injecting particles into the SCS using a microneedle, 20 and 100 nm particles were found in the SCS as well as in the sclera, while 500 and 1000 nm particles could not diffuse into other tissues but the SCS. Strikingly, not only the physicochemistry of the therapeutic entity influences its bioavailability, also the injection site at which it is originally deposited can have an impact. In fact, Chiang *et al*. defined another anatomical barrier for the circumferential spread of particles across the SCS that was independent of the particle size, i.e. ciliary arteries. In rabbit eyes they observed that particles injected on one side of the posterior ciliary artery were unable of diffusing to its opposite side.[117]

An additional and likely greater hurdle than the static barrier function of the choroid is its circulation. It is established that the choroidal circulation is extraordinarily high when compared to other organs, this to supply the metabolically active RPE cells with the necessary oxygen and nutrients.[104,114] Many groups have looked into the influence of choroidal circulation on the delivery of drugs in ocular tissues.[100] Many compounds such as fluorescently labeled dextrans of 40 and 250 kDa, bevacizumab and NaF have indeed been found to be rapidly cleared post-injection, usually within hours.[100,107,114,118] In contrast, larger nondegradable particles of 20 nm up to 10 µm in size were detected in the SCS for two months.[107] This lack of clearance is in line with the predicted maximal pore size of the fenestrated choriocapillaries which is estimated to lie between 6 and 12 nm.[119] The above-mentioned observations indicate that sustained release systems such as nano-or microparticles can have great potential since their controlled release might be able to compensate for the swift removal of the therapeutic.[120,121]

Barriers encountered after transscleral administration

Transscleral drug delivery, often referred to as periocular drug delivery, is an umbrella term for different administration routes including subconjunctival, sub-tenon, peribulbar and retrobulbar routes (**Figure 2.1**). While all these routes could be applied to reach the retina, we will not further discuss barriers specific to subconjunctival administration since this chapter primarily focuses on the barriers present at the back of the eye. The exact procedures and injection locations of these techniques are summarized in a review by Raghava *et al*.[122] These type of injections, especially sub-tenon, are already applied in the clinic for e.g. applying local anaesthesia for ocular surgery.[122] The transscleral routes, which are less invasive than IVT injections, take advantage of the large surface area of the sclera.[123,124] Furthermore, relatively large volumes can be administered with a single

injection, with up to 4 ml and 5 ml for sub-tenon and retrobulbar injection, respectively.[122] The periocular route is definitely a valuable one for treatment of diseases of the middle and outer coat of the eye. Its potential for treating retinal diseases is, however, still a matter of debate, as therapeutic concentrations within the retina remain quite low.[125] Therapeutics should indeed overcome static barriers such as the sclera, choroid and the RPE layer, whilst also encountering dynamic barriers like choroidal blood flow and episcleral flow.[124,126] The combination of these various barriers makes periocular delivery a challenge. Since the RPE layer and choroid are already extensively discussed above, we limit our focus in this section on the sclera.

Sclera

The sclera or the white of the eye is the outer opaque layer of the ocular globe that blends into the transparent cornea at the front of the eye. The opacity of the sclera is no coincidence since it prevents internal light scattering to ensure an optimal retinal image.[127] The human scleral thickness is not consistent but averages around 0.5 mm at the limbus to approximately 1 mm at the optic nerve.[127,128] The sclera has several mechanical functions such as general support of the eye, maintaining the shape of the eye during its movement and protecting the eye against external injuries as well as increased internal ocular pressure.[129,130]

Microscopically, several regions can be differentiated from the outside to the inner side of the sclera, including the episclera, the stromal tissue and the lamina fusca.[127] On a molecular level, the sclera is built up from the typical components of connective tissue i.e. collagen, proteoglycans and glycoproteins. The predominant structural protein, collagen type I, forms fibers and fiber bundles with varying thickness and orientation depending on the region and tissue depth.[130] In the episclera, a thin vascularized layer, the collagen fibers connect to the blood vessel walls or the underlying stromal tissue.[127] The outer regions of the stromal tissue contain thinner bundles with lamellar characteristics, while their counterparts in the inner layers of the stroma are generally thicker and orientated in a multitude of directions.[130] Finally, the collagen bundles of the lamina fusca are smaller and strongly intertwine to integrate into the choroidal layer below.[127] Remarkably, similar to the sclera the corneal tissue is also based on collagen fibers, yet the cornea has a highly transparent appearance. This contrast in opacity can be explained by the different ultrastructure of the two tissues: while the collagen fibers of the sclera are quite thick and compactly organized, their corneal counterparts are thinner, strictly longitudinally oriented and more widely separated.[131] Next to collagen fibrils also a small fraction of elastic fibers runs through the scleral tissue which adds to the viscoelastic properties of the tissue.[132] Notably, the sclera is not acellular but contains fibroblasts responsible for the synthesis and turnover of the scleral matrix.[132]

The permeability of the sclera and its barrier role has been extensively described in literature in context of a wide range of compounds ranging from antibiotics to dextrans.[126] Considering the dense structure of the sclera, it represents a physical barrier toward many therapeutics. Successful passage through the complex fiber network has proven to be highly dependent on the molecular weight of the compound, where larger molecules have more trouble diffusing than smaller ones (< 70 kDa).[124,133–137] On the other hand, clearance values for macromolecules are much lower than for smaller molecules.[124] Apart from molecular weight, Ambati *et al.* revealed that molecular radius is an even better predictor of permeability, as globular proteins permeated faster through the sclera than linear dextrans with similar molecular weight.[134] Still, the same molecular radius does not necessarily result in similar permeability coefficients. In fact, Cheruvu *et al.* found that negatively charged solutes permeated across the sclera more effectively than positively charged ones despite their comparable radii.[116] This is a logic consequence of the matrix structure seeing the sclera contains proteoglycans that are negatively charged at physiological pH.[138] Too many negative charges on macromolecules, on the other hand, might also inhibit permeation due to charge repulsion.[124] Next to size and charge also lipophilicity has an influence on scleral permeation, where hydrophilic molecules more readily diffuse through the sclera than lipophilic ones as observed in scleral tissue of multiple species.[89,116,126,139] This is likely due to the aqueous nature of the sclera owing to the hydrated proteoglycans.[126] Importantly, choroidal bioavailability is often also low for hydrophilic molecules since the largest part of the drug that reaches the choroid is likely next cleared by the choroidal blood flow.[126]

Regarding nano-and microparticles, there are only limited reports on penetration of ocular tissues after periocular administration. Amrite *et al*. looked into the influence of particle size on the retention at the injection site by comparing the disposition of 20 nm, 200 nm and 2 µm sized polystyrene particles *in vivo* in rats. Except for a very limited amount of 20 nm particles, no particles were present in the ocular tissues after injection.[140,141] Additionally, 20 nm but not larger particles were rapidly cleared from the injection site, with only 15% remaining one day post-administration.[140] Also in bovine *ex* vivo experiments only 0.46% of the 20 nm particles were able to cross the sclera.[141] Successful delivery of particles to the ocular tissues after periocular administration is therefore dependent on a challenging balance. While smaller particles can penetrate into ocular tissues but are cleared rapidly from the injection site, larger particles are retained but are unable of reaching the retina. Drug delivery strategies concentrating on nano- and microparticles therefore tend to focus on particles as vehicles for sustained delivery.[1,122,142] Besides from particle design, research groups also look into clever modifications of the technique by which it is delivered, like the application of hollow microneedles penetrating into the sclera.[143]

In all cases, it should be noted that the scleral thickness can differ greatly among species which has a direct impact on the permeability of the sclera.[144] In light of this, the study of Nicoli *et al*. serves as a leading example: they found porcine sclera to be twice as thick as human sclera which reflected in the fact that in comparison the permeability of human sclera was up to three times higher.[145] In contrast, the rabbit sclera is approximately twice as thin as the human sclera which yet again should be taken into account when extrapolating results based on this species to the human situation [144]. Similar to the other structures of the eye, aging also affects the sclera which yet again can influence its permeability. Indeed, it has been reported that the hydration of the sclera decreases with age and seeing permeability declines with decreasing hydration this can certainly have an impact on drug distribution.[136,146] The age of the animals used during sclera permeation studies is therefore a factor than can add to experimental variability.

3. IN VITRO AND EX VIVO METHODS TO STUDY BARRIER ROLES

Barrier-specific methods

Methods to study the vitreous

Over the last two decades several methods have been developed to improve our understanding of the vitreous structure and the behavior of therapeutics within it, ranging from rather straightforward *in vitro* methods to more relevant though more complex *ex vivo* techniques. This is likely owing to the advancement of technology in general combined with the integration of the 3R principle regarding animal experiments (reduction, refinement and replacement).[142]

Prior to starting experiments on vitreous, it is important to note that the vitreous structure varies across different species.[9] For example, it is estimated that the collagen content is up to five times lower in bovine vitreous compared to its human counterpart.[7] These species-specific variations should be taken into account since the impact of the vitreous as a barrier could be over-or underestimated in comparison with the human situation.[9] Overall, large animal models such as cow, pig and non-human primates are significantly more representative for the human vitreous structure. Seeing the small volume of vitreous present in the mouse eye, vitreous isolation and quantification of its components is troublesome.[147] Hence, the composition of mouse vitreous is less documented and it is unclear if mice are relevant animal models to test the *in vivo* potential of a drug delivery system. Notably, even within one species the structure of the vitreous can vary: it is well established that the vitreous gel loses its gel-like appearance and liquefies with age, which implies that the migration of therapeutics toward the retina could also be age-dependent.[10]

The most straightforward *in vitro* experiments to study the barrier role of vitreous are performed on isolated vitreous. In the earliest experiments, diffusivity of a fluorescent dye such as fluorescein was measured in the isolated vitreous (often bovine) based on the concentrations measured with a fluorometer.[23,148,149] While most of these studies only considered passive diffusion, Xu *et al.* included the influence of convection by applying a custom-built diffusion cell and numerical modeling.[23] To investigate the barrier role of vitreous for larger structures, like NPs, the use of fluorescence microscopy to evaluate binding of (fluorescent) NPs to vitreous components could be a first preliminary experiment. For more accurate interpretations, the diffusion of fluorescent small molecules as well as NPs in isolated vitreous can also be assessed by Fluorescence Recovery After Photobleaching (FRAP). In this microscopy technique, fluorescent components are permanently bleached in a small area of the vitreous by a high intensity laser. Next, diffusion of surrounding fluorescent molecules into the bleached area causes the recovery of fluorescence, which is measured over time using a low intensity laser. Based on the fluorescence recovery, the diffusion coefficient and fraction of (im)mobile molecules can be precisely calculated.[14,22]

Isolated vitreous can also be used in cell culture experiments. Pitkänen *et al.,* for example, applied a thin layer of freshly isolated bovine vitreous on top of an RPE cell culture after which DNA-complexes were supplemented on top. The following transfection and uptake studies revealed that the presence of vitreous nearly entirely blocked particle uptake and thus gene transfer.[12] Since these *in vitro* methods are very straightforward, they are certainly valuable for providing a first impression whether or not the vitreous hampers the efficiency of a certain therapeutic. However, it is well-known that without the support of the eye the vitreous loses its typical structure due to outflow of hyaluronic acid.[150] Therefore, tests on isolated vitreous could lead to biased results which is the principal limitation of these *in vitro* methods. *Ex vivo* methods on the other hand, are usually more representative for the *in vivo* tissue structures as the vitreous is (partially) maintained in its natural environment.

The *ex vivo* models of Martens *et al*. and Xu *et al.* are ideally suited for studying the drug delivery of larger entities like viral or non-viral gene carriers.[16,21,151] Both models share the same principle: fluorescent NPs are injected in the vitreous of a cadaveric cow eye after which their diffusion is followed by particle tracking microscopy. Tracking each particle in function of time allows to calculate a distribution of diffusion coefficients that is highly representative for the Brownian motion taking place. Though both models are quite similar, the dissection and subsequent set-up are slightly different: while Xu *et al*. disposes the entire anterior part of the eye resulting in an eye-cup and exposure of the vitreous, Martens *et al*. only removes the cornea and lens so that the hyaloid membrane and the rest of the eye remains intact. In the latter model, particles are therefore allowed

to diffuse for 24 h instead of less than an hour in the exposed vitreous. On the other hand, in the system of Martens *et al*. NPs are intravitreally injected unusually close to the hyaloid membrane owing to working distance limitations of the objective lens needed for single particle tracking.[151] Xu *et al*., in contrast, injects the NP suspension in the central vitreous, which is likely more representative for the IVT injections taking place in the clinic.[16] All these *ex vivo* methods are though less straightforward, highly relevant for drug delivery studies since they allow us to study the static barrier functions of tissues from larger more representative animals without proceeding to costly and often unnecessary *in vivo* experiments. It is important to recognize, however, that information on the influence of dynamic barrier roles such as for example the anterior-posterior convective flow, is lost. Furthermore, the above-mentioned assays do not take into account the potential influence of vitreous humor motion during eye rotations on the dispersion of therapeutics in the vitreous.[27] To look into these factors affecting the delivery of a drug (vehicle), *in vivo* studies are still unique and necessary.

Methods to study the blood-retinal barrier

Studies with the goal to investigate the potential of therapeutics to permeate the BRB can be roughly subdivided in two categories: *in vitro* studies based on endothelial or epithelial cell cultures, and *ex vivo* studies based on isolated RPE/choroid tissue in diffusion chambers (discussed in section *Diffusion chambers*). The most straightforward and thus most applied *in vitro* experimental set-up involves the culture of BRB cell types on specialized filter systems of which the most frequently used is the Transwell system. These filters can be coated with e.g. laminin and/or fibronectin to mimic extracellular matrices and allow cells to grow in a polarized fashion.[152] The permeability of macromolecules through the iBRB or oBRB can then be evaluated *in vitro* by quantifying the fraction of macromolecules, applied at the apical side, that crossed the BRB and reached the basal medium at specific time points. This quantification can be done by a diversity of methods ranging from fluorescence measurements with a plate reader to mass spectrometry.[153–157] Naturally, the permeability of the compounds through the blank filter system should also be determined to account for potential barrier properties of the filter itself.[153]

These *in vitro* barrier studies can be performed on immortalized cell lines or primary cultures, where both options have their merits and disadvantages. Whereas cell lines are straightforward to culture and store, and allow comparison of test results between different research groups, they are often not truly representative of the *in vivo* setting, especially when it comes to barrier function.[79] Employing primary cultures, on the other hand, can be troublesome in practical terms owing to complex isolation protocols. Moreover, the isolated cell population is often more heterogeneous which complicates the interpretation of results.[153] Nevertheless, these cultures are regarded as more

representative. It should be noted that finding cell culture conditions that result in the most representative phenotype is known to be a universal challenge.[79,158] Indeed, culture conditions can greatly influence the characteristics of e.g. the RPE layer, which might have an impact on its barrier function. In fact, it is well established that the RPE layer exhibits variations related to species and age, which implies that when working with primary cell cultures animals should be carefully selected.[79] It has furthermore been reported that even within the same RPE layer microenvironments can be distinguished, which can further add to tissue variability.[159] A critical review on the culture options for RPE and influence of culture conditions on its properties has been published recently by Rizzolo *et al*.[79]

Recently, several groups have made progress in the development of more advanced co-cultures of multiple BRB cell types.[160–162] An elegant example of this is the work of Wisniewska-Kruk *et al*. who managed to mimic the iBRB by co-culture of primary endothelial cells, pericytes and astrocytes. In brief, they allowed pericytes and astrocytes to adhere to the bottom of the Transwell filter after which endothelial cells were cultured on top of the filter. After a few days of culture, permeability studies were performed as usual: fluorescent dextrans and other tracers were added to the top compartment after which their presence in the bottom compartment was measured.[162]

General methods for barrier investigation

Retinal explants

The culture of retinal explants is a widely applied method in a variety of ocular studies, especially in fundamental research and retinal drug delivery. Similar to polarized ocular cell types, explants are typically cultured on specialized membranes (e.g. Transwell filters) that allow adding substances below the filter and/or on top of the explant. Except for the commercially available filter systems, this experimental set-up does not require special equipment and is therefore readily accessible for each research group.

Retinal explant culture can help to define to which extent the neural retina or ILM represents a barrier to the diffusion of therapeutics. Interestingly, the orientation of the explant, i.e. PR-side up or down, can be altered depending on the research question investigated.[69,163] To investigate the penetration of intravitreally injected therapeutics into the retina, isolated explants are typically cultured with PR-side down. Even when detaching the vitreous from the retina while dissecting, the ILM usually remains largely intact, especially in larger species such as cow or human. Therefore, therapeutics or drug carriers can be dropped on top of the explant to follow transfer through the ILM into the retina. When looking into subretinal injection there are generally two options: therapeutic entities are applied directly on top of the retinal explants (PR side upwards) on a Transwell insert,[69]

or the therapeutic entities are placed on the filter and covered with the retinal explants (PR side down).[163] After a certain time point (e.g. 24 hours), the penetration of the entity can then be examined by microscopy after preparing cryosections. It should be noted, however, that it is always important to prevent overflow to the other side of the retina when applying a larger volume of therapeutics on top of the retina, since this can result in biased interpretations.

As discussed in **Chapter 3**, we recently developed an *ex vivo* model based on bovine eyes, in which the vitreous remains attached to the ILM and retina during dissection and explant culture, ensuring an intact vitreoretinal interface. After dissection and explant culture, fluorescent therapeutics or drug carriers can be injected into the vitreous after which the extent and route of retinal entry can be defined by confocal microscopy.[164]

Diffusion chambers

While the retinal explants described above allow for valuable estimations of the extent and relative rate at which certain entities penetrate into the retina, studies performed using a diffusion chamber can provide us with accurate absolute diffusional rates. The Ussing chamber, originally developed to look into ion transport across epithelial membranes, has led to the advancement of the understanding of transport of molecules through tissues in many fields including the ocular one.[165,166] In this Ussing chamber system, the studied tissue is mounted in such a way that it forms the physical barrier between two halves of one chamber. One of these halves contains the tested compound, while the second half merely contains a buffer with the same osmolarity and if necessary, antibiotics. After a certain time point (e.g. 24 hours) the rate of diffusion through the tissue can be measured by detecting the compound in the opposite half with for example a spectrophotometer. To monitor the viability and integrity of the studied barrier during these experiments the transepithelial electrical resistance (TEER) can be assessed. This resistance can be measured in a non-invasive way by placing an electrode pair in both halves of the Ussing chamber that can detect voltage and current.[77,89,167] Next to these quantitative measurements, the location of the compounds within the tissue can be examined after the conventional cryosection protocol followed by microscopy. The Ussing diffusion chamber and its variations can be used to study almost every barrier discussed in this chapter. In fact, studies applying a diffusion chamber have been reported on the ILM,[62] retinal tissue,[62,65] the oBRB,[87,88,168] the choroid,[116] and the sclera.[116,169,170] The application of a diffusion chamber indeed offers several advantages. For instance, depending on the barrier you aim to investigate a certain side of the tissue can be directed toward the donor or the receiver chamber. As with the retinal explants described above, changing the orientation of the retina toward the donor chamber for example allows you to focus on the ILM or the PR layer.[62] In case of transscleral administration for retinal targets, a diffusion chamber allows to define for your compound which physical barrier

signifies the dominant hurdle (the choroid or the sclera) simply by mounting scleral tissue with and without choroid in the chamber.[116]

While these experiments can provide us with highly valuable qualitative and quantitative information, certainly for diffusion of macromolecules, they are less accessible since they require uncommon instrumentation that might not be available in every research group. It should also be noted that while the Ussing chamber is a commercially available diffusion system, some groups apply the same principle but make use of a custom-designed set-up.[65]

Perfused eye models

Originally developed in the early 80s for biological studies, the isolated perfused eye model has been optimized in multiple species over the years ranging from cat to human while focus has also switched toward drug delivery.[171–176] In this technique, an entire mammalian eye is isolated after which a ciliary artery is cannulated to supply it with carefully composed perfusion fluid. By means of a peristaltic pump, the eye is then perfused while keeping it moist. Next, pharmacokinetic and drug distribution studies following administration of a therapeutic can be performed by quantification of the therapeutic in the different ocular tissues using mass spectrometry or fluorometry. In addition, examination of tissue cryosections can aid to define the exact (cellular) location of the therapeutic (carrier). Many drug delivery studies have already been done based on this model, usually focusing on intravitreal [174,175,177] or suprachoroidal drug delivery.[106,115,178] Patel *et al*. added an interesting feature to the common *ex vivo* eye model by inserting a cannula connected to an irrigating solution through the optic nerve into the vitreous.[106] In this fashion, they mimicked an elevated intraocular pressure and evaluated its effect on particle delivery by hollow microneedles.

Well-established advantages of this system over *in vivo* experiments are among others: no influence of anaesthesia, no limitation on applied drug concentration and complete control over physiological environment while reducing animal usage.[175] Thanks to the perfusion, the model also allows to look into the influence of clearance mechanisms, like the choroidal circulation, on drug delivery.[178] Nevertheless, it remains a great difficulty to fully mimic the remarkably complex *in vivo* conditions. In addition, the viability of the perfused *ex vivo* eye is limited to around 9 hours which can form a limitation when executing pharmacokinetic studies that require longer timepoints.[174,179]

4. CONCLUSION

In the past decade, a lot of effort of industry and academia has gone to the design of new drug delivery vehicles and advanced administration techniques to treat blinding diseases that find their origin at the back of the eye. Nevertheless, despite this effort and the resulting progress therapeutic efficacy remains limited, especially in case of larger entities such as nucleic acids. This inefficient delivery of therapeutics is usually due to the many physiological barriers encountered by the therapeutic entity. Each administration route to target the posterior segment has it specific barriers, benefits and disadvantages (**Figure 2.1**). For example, while subretinal injection theoretically involves the least barriers, it is at the same time a highly invasive technique. IVT injection, on the other hand, is a highly safe and feasible administration method, but comes with challenging drug delivery barriers such as the vitreous and the ILM. The balance between efficacy and safety therefore remains difficult to maintain. Interestingly, the ideal physicochemical characteristics of a therapeutic (carrier) depend on the barrier it needs to overcome and therefore also on the preferred administration route (**Table 2.1**). The sclera and vitreous are for example more permeable for hydrophilic compounds while the choroid and retina are easier to cross for lipophilic ones. In view of the complexity of the various barriers we encourage drug delivery researchers to systematically explore which physicochemistry (e.g. size, charge and hydrophilicity/hydrophobicity) a therapeutic needs to surmount every barrier of importance for the chosen delivery route. To perform these studies, a whole variety of *in vitro* and *ex vivo* methods is available. *In vitro* studies on ocular cell cultures can be powerful to provide preliminary results on the intrinsic therapeutic potential of new compounds and to evaluate if the vitreous represents an obstacle for transfection. In addition, intelligently designed *ex vivo* experiments can be as valuable as *in vivo* studies – if not more. Indeed, *ex vivo* studies, which are in line with the worldwide resolution to implement the 3R principle, allow to look into tissues of larger animals that have a physiology resembling the human one. It is expected that the increasing knowledge of the exact barrier composition, and especially, the interspecies variability will help to further define which model is most related to the complex *in vivo* human situation by preventing over-or underestimation of species-dependent barrier functions. Finally, it is well established that age and disease can affect the composition and/or the integrity of nearly each barrier discussed in this review. Therefore, the development of standardized *in vitro* and *ex vivo* disease models next to the existing *in vivo* ones could be an important field of research to evaluate the delivery of drugs and carriers to diseased or aged tissues. Overall, we are confident that the increasing barrier knowledge and the proper use of *in vitro* and *ex vivo* methods will continue to boost the design and optimization of drug delivery systems that are successful in treating disease targets at the back of the eye. In light of this philosophy, we have developed a novel *ex vivo* model to thoroughly investigate the barrier role of the vitreoretinal interface, as will be discussed in **Chapter 3**.

	Vitreous (A)	**ILM** (A)	**Retina** (A,B,C,D,E)	**BRB** (B,C,D)	**Choroid** (B,D)	**Sclera** (B)
size	Mesh size ~550 nm [16] 1 µm particles were mobile in vitreous [13]	Mesh size ~ 10 to 25 nm [36] 350 nm particles and 2000 kDa dextran crossed ILM [15,51,52]	Free diffusion is limited to < 76 kDa in fixed human retina [62] Active cellular transport can shuttle larger entities through retina	Solutes < 0.4 nm can freely diffuse through BRB [79] Very low permeability above 20 kDa [88] 20 nm gold particles and 85 nm targeted liposomes crossed BRB [96,99]	40 kDa dextran crossed choroid [115] 20 nm particles delivered in SCS did not reach retina [106]	150 kDa dextran diffuses through rabbit sclera [134,169] Barely penetration of 20 nm polystyrene particles through sclera [140]
charge	Negative [17–20]	Neutral to negative. [15,20,36,52]	Negative [51,68]	N.D.	N.D.	Negative [116]
hydrophilicity	Hydrophilic compounds have longer half-lives [73]	N.D. likely hydrophilic	N.D. likely lipophilic	Lipophilic [88,124]	Lipophilic [115]	Hydrophilic [89,116,126,139]
other features	Coating particles with polymers like PEG or HA can increase diffusion [14,21,22]	Binding to ligands at the ILM influences viral vector passage through the ILM [44,45,47–50]		Targeting for receptors present in BRB cells can facilitate BRB passage [99]		

Table 2.1 | Overview of the preferred physicochemical features necessary to cross the different barriers. A: intravitreal injection; B: transscleral administration; C: systemic injection; D: suprachoroidal administration; E: subretinal injection. N.D. = not defined.

5. REFERENCES

1. Rowe-Rendleman, C. L. *et al.* Drug and gene delivery to the back of the eye: from bench to bedside. *Invest. Ophthalmol. Vis. Sci.* **55,** 2714–30 (2014).

2. Englander, M., Chen, T. C., Paschalis, E. I., Miller, J. W. & Kim, I. K. Intravitreal injections at the Massachusetts Eye and Ear Infirmary: analysis of treatment indications and postinjection endophthalmitis rates. *Br. J. Ophthalmol.* **97,** 460–5 (2013).

3. A. Vasavada, A. Partani, A. Jindal, A. Chakravarti, A.K. Dubey, A. Pathengay, B. Dubey, D. Shukla, I. Singh, K. Duggal , K. Mithal, L. Verma, M. Goyal, M.R. Dogra , NS. Muralidhar, P.M. Shanmugam, P. Bansal, M. Radhika, R. Narayanan, R. Ramanjulu, R.M. Ga, V. *Intravitreal Injections*. (Jaypee Brothers Medical Publishers (P) Ltd., 2014).

4. Thrimawithana, T. R., Young, S. A., Bunt, C. R., Green, C. & Alany, R. G. Drug delivery to the posterior segment of the eye. *Drug Disco* **16,** 59–72 (2011).

4a. Kotterman, M. A. *et al.* Antibody neutralization poses a barrier to intravitreal adeno-associated viral vector gene delivery to non-human primates. *Gene Ther.* **22,** 116–126 (2015).

5. Mains, J. & Wilson, C. G. The Vitreous Humor As a Barrier to Nanoparticle Distribution. *J. Ocul. Pharmacol. Ther.* **29,** 143–50 (2012).

6. Halfter, W., Winzen, U., Bishop, P. N. & Eller, A. Regulation of eye size by the retinal basement membrane and vitreous body. *Investig. Ophthalmol. Vis. Sci.* **47,** 3586–3594 (2006).

7. Le Goff, M. M. & Bishop, P. N. Adult vitreous structure and postnatal changes. *Eye (Lond).* **22,** 1214–22 (2008).

8. Bu, S. C. *et al.* The ultrastructural localization of type II, IV, and VI collagens at the vitreoretinal interface. *PLoS One* **10,** 1–23 (2015).

9. Noulas, A. V., Skandalis, S. S., Feretis, E., Theocharis, D. A. & Karamanos, N. K. Variations in content and structure of glycosaminoglycans of the vitreous gel from different mammalian species. *Biomed. Chromatogr.* **18,** 457–461 (2004).

9a. Forrester, J. V. *et al.* in *The Eye* 1–102.e2 (2016). doi:10.1016/B978-0-7020-5554-6.00001-0

9b. Worst, J. G. F. & Los, L. I. *Cisternal anatomy of the vitreous*. (Kugler Publications, 1995).

10. Tan, L. E. *et al.* Effects of vitreous liquefaction on the intravitreal distribution of sodium fluorescein, fluorescein dextran, and fluorescent microparticles. *Investig. Ophthalmol. Vis. Sci.* **52,** 1111–1118 (2011).

11. Sakamoto, T. *et al.* A vitrectomy improves the transfection efficiency of adenoviral vector-mediated gene transfer to Müller cells. *Gene Ther.* **5,** 1088–97 (1998).

12. Pitkänen, L., Ruponen, M., Nieminen, J. & Urtti, A. Vitreous is a barrier in nonviral gene transfer by cationic lipids and polymers. *Pharm. Res.* **20,** 576–583 (2003).

13. Martens, T. F. *et al.* Measuring the intravitreal mobility of nanomedicines with single-particle tracking microscopy. *Nanomedicine* **8,** 1955–1968 (2013).

14. Peeters, L. *et al.* Vitreous: A barrier to nonviral ocular gene therapy. *Investig. Ophthalmol. Vis. Sci.* **46,** 3553–3561 (2005).

15. Koo, H. *et al.* The movement of self-assembled amphiphilic polymeric nanoparticles in the vitreous and retina after intravitreal injection. *Biomaterials* **33,** 3485–3493 (2012).

16. Xu, Q. *et al.* Nanoparticle diffusion in, and microrheology of, the bovine vitreous ex vivo. *J. Control. Release* **167,** 76–84 (2013).

17. Kim, H., Robinson, S. B. & Csaky, K. G. Investigating the movement of intravitreal human serum albumin nanoparticles in the vitreous and retina. *Pharm. Res.* **26,** 329–337 (2009).

18. Bejjani, R. A. *et al.* Nanoparticles for gene delivery to retinal pigment epithelial cells. *Mol Vis* **11,** 124–132 (2005).

19. Kim, H. & Csaky, K. G. Nanoparticle-integrin antagonist C16Y peptide treatment of choroidal neovascularization in rats. *J. Control. Release* **142,** 286–293 (2010).

20. Sakurai, E., Ozeki, H., Kunou, N. & Ogura, Y. Effect of particle size of polymeric nanospheres on intravitreal kinetics. *Ophthalmic Res.* **33,** 31–6 (2001).

21. Martens, T. F. *et al.* Coating nanocarriers with hyaluronic acid facilitates intravitreal drug delivery for retinal gene therapy. *J. Control. Release* **202,** 83–92 (2015).

22. Sanders, N. N., Peeters, L., Lentacker, I., Demeester, J. & De Smedt, S. C. Wanted and unwanted properties of surface PEGylated nucleic acid nanoparticles in ocular gene transfer. *J. Control. Release* **122,** 226–235 (2007).

23. Xu, J., Heys, J. J., Barocas, V. H. & Randolph, T. W. Permeability and diffusion in vitreous humor: implications for drug delivery. *Pharm. Res.* **17,** 664–669 (2000).

24. Wilson, C. & Tan, L. E. in *Nanostructured Biomaterials for Overcoming Biological Barriers* 173–189 (RSC Publishing Ltd., 2012).

25. Park, J. *et al.* Evaluation of coupled convective-diffusive transport of drugs administered by intravitreal injection and controlled release implant. *J. Control. Release* **105,** 279–295 (2005).

26. Urtti, A. in *Nanostructures Overcoming the Ocular Barrier* 190–204 (2012). doi:10.1039/9781849735292-00190

27. Bonfiglio, A., Repetto, R., Siggers, J. H. & Stocchino, A. Investigation of the motion of a viscous fluid in the vitreous cavity induced by eye rotations and implications for drug delivery. *Phys. Med. Biol.* **58,** 1969–1982 (2013).

28. Modareszadeh, A., Abouali, O., Ghaffarieh, A. & Ahmadi, G. Saccade movements effect on the intravitreal drug delivery in vitreous substitutes: A numerical study. *Biomech. Model. Mechanobiol.* **12,** 281–290 (2013).

29. Halfter, W., Dong, S., Dong, A., Eller, A. W. & Nischt, R. Origin and turnover of ECM proteins from the inner limiting membrane and vitreous body. *Eye (Lond).* **22,** 1207–1213 (2008).

30. Bu, S. C. *et al.* The Ultrastructural Localization of Type II, IV, and VI Collagens at the Vitreoretinal Interface. *PLoS One* **10,** 1–23 (2015).

31. Halfter, W. *et al.* Embryonic synthesis of the inner limiting membrane and vitreous body.

Investig. Ophthalmol. Vis. Sci. **46,** 2202–2209 (2005).

32. Halfter, W., Willem, M. & Mayer, U. Basement membrane-dependent survival of retinal ganglion cells. *Investig. Ophthalmol. Vis. Sci.* **46,** 1000–1009 (2005).

33. Halfter, W., Dong, S., Balasubramani, M. & Bier, M. E. Temporary disruption of the retinal basal lamina and its effect on retinal histogenesis. *Dev. Biol.* **238,** 79–96 (2001).

34. Semeraro, F. *et al.* Current trends about inner limiting membrane peeling in surgery for epiretinal membranes. *J. Ophthalmol.* **2015,** 1–13 (2015).

35. Nakamura, T. *et al.* Ultrastructure of the vitreoretinal interface following the removal of the internal limiting membrane using indocyanine green. *Curr. Eye Res.* **27,** 395–399 (2003).

36. Nishihara, H. Studies on the ultrastructure of the inner limiting membrane of the retina. I. Surface replication study on the inner limiting membrane of the retina. *Nihon. Ganka Gakkai Zasshi* **93,** 429–38 (1989).

37. Henrich, P. B. *et al.* Nanoscale topographic and biomechanical studies of the human internal limiting membrane. *Invest. Ophthalmol. Vis. Sci.* **53,** 2561–2570 (2012).

38. Halfter, W. *et al.* New concepts in basement membrane biology. *FEBS J.* **282,** 4466–4479 (2015).

39. Candiello, J., Cole, G. J. & Halfter, W. Age-dependent changes in the structure, composition and biophysical properties of a human basement membrane. *Matrix Biol.* **29,** 402–410 (2010).

40. Mowat, F. M. *et al.* Tyrosine capsid-mutant AAV vectors for gene delivery to the canine retina from a subretinal or intravitreal approach. *Gene Ther.* **21,** 96–105 (2014).

41. Hellström, M. *et al.* Cellular tropism and transduction properties of seven adeno-associated viral vector serotypes in adult retina after intravitreal injection. *Gene Ther.* **16,** 521–532 (2009).

42. Takahashi, K. *et al.* Improved Intravitreal AAV-Mediated Inner Retinal Gene Transduction after Surgical Internal Limiting Membrane Peeling in Cynomolgus Monkeys. *Mol. Ther.* **25,** 296–302 (2017).

43. Boyd, R. F. *et al.* Photoreceptor-targeted gene delivery using intravitreally administered AAV vectors in dogs. *Gene Ther.* **23,** 223–230 (2016).

44. Dalkara, D. *et al.* Inner limiting membrane barriers to AAV-mediated retinal transduction from the vitreous. *Mol. Ther.* **17,** 2096–102 (2009).

45. Kolstad, K. D. *et al.* Changes in adeno-associated virus-mediated gene delivery in retinal degeneration. *Hum. Gene Ther.* **21,** 571–8 (2010).

46. Vacca, O. *et al.* AAV-mediated gene delivery in Dp71-null mouse model with compromised barriers. *Glia* **62,** 468–476 (2014).

47. Akache, B. *et al.* The 37/67-Kilodalton Laminin Receptor Is a Receptor for Adeno-Associated Virus Serotypes 8, 2, 3, and 9. *J. Virol.* **80,** 9831–9836 (2006).

48. Woodard, K. T., Liang, K. J., Bennett, W. C. & Samulski, R. J. Heparan Sulfate Binding Promotes Accumulation of Intravitreally-Delivered Adeno-Associated Viral Vectors at the

Retina for Enhanced Transduction but Weakly Influences Tropism. *J. Virol.* **90,** 9878–9888 (2016).

49. Boye, S. L. *et al.* The Impact of Heparan Sulfate Binding on Transduction of Retina by rAAV Vectors. *J. Virol.* **90,** JVI.00200-16 (2016).

50. Khabou, H. *et al.* Insight into the mechanisms of enhanced retinal transduction by the engineered AAV2 capsid variant -7m8. *Biotechnol. Bioeng.* **113,** 2712–2724 (2016).

51. Pitkänen, L., Pelkonen, J., Ruponen, M., Rönkkö, S. & Urtti, A. Neural retina limits the nonviral gene transfer to retinal pigment epithelium in an in vitro bovine eye model. *AAPS J.* **6,** article 25 (2004).

52. Bourges, J. L. *et al.* Ocular drug delivery targeting the retina and retinal pigment epithelium using polylactide nanoparticles. *Investig. Ophthalmol. Vis. Sci.* **44,** 3562–3569 (2003).

53. Hauswirth, W. W. *et al.* Treatment of leber congenital amaurosis due to RPE65 mutations by ocular subretinal injection of adeno-associated virus gene vector: short-term results of a phase I trial. *Hum. Gene Ther.* **19,** 979–90 (2008).

54. Acland, G. M. *et al.* Gene therapy restores vision in a canine model of childhood blindness. *Nat. Genet.* **28,** 92–95 (2001).

55. Bennett, J. *et al.* Safety and durability of effect of contralateral-eye administration of AAV2 gene therapy in patients with childhood-onset blindness caused by RPE65 mutations: a follow-on phase 1 trial. *Lancet* **388,** 661–672 (2016).

56. Ghazi, N. G. *et al.* Treatment of retinitis pigmentosa due to MERTK mutations by ocular subretinal injection of adeno-associated virus gene vector: results of a phase I trial. *Hum. Genet.* **135,** 327–343 (2016).

57. Zulliger, R., Conley, S. M. & Naash, M. I. Non-viral therapeutic approaches to ocular diseases: An overview and future directions. *J. Control. Release* **219,** 471–487 (2015).

58. Surace, E. M. & Auricchio, A. Versatility of AAV vectors for retinal gene transfer. *Vision Res.* **48,** 353–359 (2008).

59. Simonelli, F. *et al.* Gene therapy for Leber's congenital amaurosis is safe and effective through 1.5 years after vector administration. *Mol. Ther.* **18,** 643–650 (2009).

60. MacLaren, R. E. *et al.* Retinal gene therapy in patients with choroideremia: Initial fi ndings from a phase 1/2 clinical trial. *Lancet* **383,** 1129–1137 (2014).

61. Igarashi, T. *et al.* Direct comparison of administration routes for AAV8-mediated ocular gene therapy. *Curr. Eye Res.* **38,** 569–77 (2013).

62. Jackson, T. L., Antcliff, R. J., Hillenkamp, J. & Marshall, J. Human retinal molecular weight exclusion limit and estimate of species variation. *Investig. Ophthalmol. Vis. Sci.* **44,** 2141–2146 (2003).

63. Shahar, J. *et al.* Electrophysiologic and retinal penetration studies following intravitreal injection of bevacizumab (Avastin). *Retin. (Philadelphia, Pa)* **26,** 262–269 (2006).

64. Heiduschka, P. *et al.* Penetration of bevacizumab through the retina after intravitreal injection in the monkey. *Investig. Ophthalmol. Vis. Sci.* **48,** 2814–2823 (2007).

65. Tao, Y. *et al.* Diffusion of macromolecule through retina after experimental branch retinal vein occlusion and estimate of intraretinal barrier. *Curr. Drug Metab.* **8,** 151–156 (2007).

66. Naik, R., Mukhopadhyay, A. & Ganguli, M. Gene delivery to the retina: focus on non-viral approaches. *Drug Discov. Today* **14,** 306–315 (2009).

67. Ishikawa, M., Sawada, Y. & Yoshitomi, T. Structure and function of the interphotoreceptor matrix surrounding retinal photoreceptor cells. *Exp. Eye Res.* **133,** 3–18 (2015).

68. Ruponen, M., Ylä-Herttuala, S. & Urtti, A. Interactions of polymeric and liposomal gene delivery systems with extracellular glycosaminoglycans: Physicochemical and transfection studies. *Biochim. Biophys. Acta - Biomembr.* **1415,** 331–341 (1999).

68a. Omri, S. *et al.* The outer limiting membrane (OLM) revisited: Clinical implications. *Clin. Ophthalmol.* **4,** 183–195 (2010).

69. Fradot, M. *et al.* Gene Therapy in Ophthalmology: Validation on Cultured Retinal Cells and Explants from Postmortem Human Eyes. *Hum. Gene Ther.* **22,** 587–593 (2011).

70. Vellonen, K.-S., Soini, E.-M., del Amo, E. M. & Urtti, A. Prediction of ocular drug distribution from systemic blood circulation. *Mol. Pharm.* **13,** 2906–11 (2016).

71. Bressler, N. M. & Bressler, S. B. Photodynamic therapy with verteporfin (Visudyne): impact on ophthalmology and visual sciences. *Invest. Ophthalmol. Vis. Sci.* **41,** 624–628 (2000).

72. Thakur, S. S., Barnett, N. L., Donaldson, M. J. & Parekh, H. S. Intravitreal drug delivery in retinal disease: are we out of our depth? *Expert Opin. Drug Deliv.* **11,** 1575–90 (2014).

73. Urtti, A. in *Nanostructured Biomaterials for Overcoming Biological Barriers* 13 (2012). doi:10.1039/9781849735292-00316

74. Dobrovolskaia, M. A., Aggarwal, P., Hall, J. B. & McNeil, S. E. Preclinical Studies To Understand Nanoparticle Interaction with the Immune System and Its Potential Effects on Nanoparticle Biodistribution. *Mol. Pharm.* **5,** 487–495 (2008).

75. Campbell, M. *et al.* An experimental platform for systemic drug delivery to the retina. *Proc. Natl. Acad. Sci. U. S. A.* **106,** 17817–22 (2009).

76. Cunha-Vaz, J. Blood-Retinal Barrier and Its Relevance in Retinal Disease. *Med. Retin.* **1,** 6–10 (2012).

77. Klaassen, I., Van Noorden, C. J. F. & Schlingemann, R. O. Molecular basis of the inner blood-retinal barrier and its breakdown in diabetic macular edema and other pathological conditions. *Prog. Retin. Eye Res.* **34,** 19–48 (2013).

78. Kaur, C., Foulds, W. S. & Ling, E. A. Blood-retinal barrier in hypoxic ischaemic conditions: Basic concepts, clinical features and management. *Prog. Retin. Eye Res.* **27,** 622–647 (2008).

79. Rizzolo, L. J. Barrier properties of cultured retinal pigment epithelium. *Exp. Eye Res.* **126,** 16–26 (2014).

79a. Busch, S. *et al.* Systemic treatment with erythropoietin protects the neurovascular unit in a rat model of retinal neurodegeneration. *PLoS One* **9,** (2014).

80. Fisher, M. Pericyte signaling in the neurovascular unit. *Stroke* **40,** S13–S15 (2009).

81. Shen, W. *et al.* Conditional Muller Cell Ablation Causes Independent Neuronal and Vascular Pathologies in a Novel Transgenic Model. *J. Neurosci.* **32,** 15715–15727 (2012).

82. Toris, C. D., Pederson, J. E., Tsuboi, S., Gregerson, D. S. & Rice, T. J. Extravascular Albumin Concentration of the Uveo. **31,** 43–53 (1990).

83. Bernstein, M. H. & Hollenberg, M. J. Fine structure of the choriocapillaris and retinal capillaries. *Invest. Ophthalmol. Vis. Sci.* **Dec,** 1016–1025 (1965).

84. Rizzolo, L. J., Peng, S., Luo, Y. & Xiao, W. Integration of tight junctions and claudins with the barrier functions of the retinal pigment epithelium. *Prog. Retin. Eye Res.* **30,** 296–323 (2011).

85. Simó, R., Villarroel, M., Corraliza, L., Hernández, C. & Garcia-Ramírez, M. The retinal pigment epithelium: Something more than a constituent of the blood-retinal barrier-implications for the pathogenesis of diabetic retinopathy. *J. Biomed. Biotechnol.* **2010,** 15 (2010).

86. Tsuboi, S. & Pederson, J. E. Permeability of the isolated dog retinal pigment epithelium to carboxyfluorescein. *Investig. Ophthalmol. Vis. Sci.* **27,** 1767–1770 (1986).

87. Kimura, M., Araie, M. & Koyano, S. Movement of carboxyfluorescein across retinal pigment epithelium-choroid. *Exp. Eye Res.* **63,** 51–6 (1996).

88. Pitkänen, L., Ranta, V. P., Moilanen, H. & Urtti, A. Permeability of retinal pigment epithelium: Effects of permeant molecular weight and lipophilicity. *Investig. Ophthalmol. Vis. Sci.* **46,** 641–646 (2005).

89. Kansara, V. & Mitra, A. K. Evaluation of an ex vivo model implication for carrier-mediated retinal drug delivery. *Curr. Eye Res.* **31,** 415–426 (2006).

90. Russ, P. K., Gaylord, G. M. & Haselton, F. R. Retinal vascular permeability determined by dual-tracer fluorescence angiography. *Ann. Biomed. Eng.* **29,** 638–647 (2001).

91. Bellhorn, R. W. Permeability of blood-ocular barriers of neonatal and adult cats to fluorescein-labeled dextrans of selected molecular sizes. *Invest. Ophthalmol. Vis. Sci.* **21,** 282–290 (1981).

92. Masanori, T., Vadivel, G. & Ken-ichi, H. Systemic Route for Retinal Drug Delivery: Role of the Blood-Retinal Barrier. *Drug Deliv.* **2,** 111–124 (2011).

93. Kennedy, B. G. & Mangini, N. J. P-Glycoprotein expression in human retinal pigment epithelium. *Mol. Vis.* **83,** 422–430 (2002).

94. Greenwood, J. Characterization of a rat retinal endothelial cell culture and the expression of P-glycoprotein in brain and retinal endothelium in vitro. *J. Neuroimmunol.* **39,** 123–132 (1992).

95. Amin, M. L. P-glycoprotein inhibition for optimal drug delivery. *Drug Target Insights* **7,** 27–34 (2013).

96. Kim, J. H., Kim, J. H., Kim, K.-W., Kim, M. H. & Yu, Y. S. Intravenously administered gold nanoparticles pass through the blood-retinal barrier depending on the particle size, and induce no retinal toxicity. *Nanotechnology* **20,** 505101 (2009).

97. Dalkara, D. *et al.* Enhanced gene delivery to the neonatal retina through systemic

administration of tyrosine-mutated AAV9. *Gene Ther.* **19,** 176–181 (2012).

98. Byrne, L. C., Lin, Y. J., Lee, T., Schaffer, D. V & Flannery, J. G. The expression pattern of systemically injected AAV9 in the developing mouse retina is determined by age. *Mol. Ther.* **23,** 290–296 (2015).

99. Zhu, C., Zhang, Y. & Pardridge, W. M. Widespread expression of an exogenous gene in the eye after intravenous administration. *Investig. Ophthalmol. Vis. Sci.* **43,** 3075–3080 (2002).

100. Kim, Y. C., Chiang, B., Wu, X. & Prausnitz, M. R. Ocular delivery of macromolecules. *J. Control. Release* **190,** 172–181 (2014).

101. Singh, S. R. *et al.* Intravenous transferrin, RGD peptide and dual-targeted nanoparticles enhance anti-VEGF intraceptor gene delivery to laser-induced CNV. **16,** 645–659 (2009).

102. Occhiutto, M. L., Freitas, F. R., Maranhao, R. C. & Costa, V. P. Breakdown of the blood-ocular barrier as a strategy for the systemic use of nanosystems. *Pharmaceutics* **4,** 252–275 (2012).

103. Seiler, G. S. *et al.* Effect and distribution of contrast medium after injection into the anterior suprachoroidal space in ex vivo eyes. *Investig. Ophthalmol. Vis. Sci.* **52,** 5730–5736 (2011).

104. Rai, U. D. J. P. *et al.* The suprachoroidal pathway: A new drug delivery route to the back of the eye. *Drug Discov. Today* **20,** 491–495 (2015).

105. Moisseiev, E., Loewenstein, A. & Yiu, G. The suprachoroidal space: From potential space to a space with potential. *Clin. Ophthalmol.* **10,** 173–178 (2016).

106. Patel, S. R., Lin, A. S. P., Edelhauser, H. F. & Prausnitz, M. R. Suprachoroidal drug delivery to the back of the eye using hollow microneedles. *Pharm. Res.* **28,** 166–176 (2011).

107. Patel, S. R. *et al.* Targeted administration into the suprachoroidal space using a microneedle for drug delivery to the posterior segment of the eye. *Investig. Ophthalmol. Vis. Sci.* **53,** 4433–4441 (2012).

108. Einmahl, S. *et al.* Evaluation of a novel biomaterial in the suprachoroidal space of the rabbit eye. *Investig. Ophthalmol. Vis. Sci.* **43,** 1533–1539 (2002).

109. Touchard, E. *et al.* Suprachoroidal Electrotransfer: A Nonviral Gene Delivery Method to Transfect the Choroid and the Retina Without Detaching the Retina. *Mol. Ther.* **20,** 1559–1570 (2012).

110. Ramrattan, R. S. *et al.* Morphometric analysis of Bruch's membrane, the choriocapillaris, and the choroid in aging. *Invest. Ophthalmol. Vis. Sci.* **35,** 2857–2864 (1994).

111. Margolis, R. & Spaide, R. F. A Pilot Study of Enhanced Depth Imaging Optical Coherence Tomography of the Choroid in Normal Eyes. *Am. J. Ophthalmol.* **147,** 811–815 (2009).

112. Nickla, D. L. & Wallman, J. The multifunctional choroid. *Prog. Retin. Eye Res.* **29,** 144–168 (2010).

113. Booij, J. C., Baas, D. C., Beisekeeva, J., Gorgels, T. G. M. F. & Bergen, A. A. B. The dynamic nature of Bruch's membrane. *Prog. Retin. Eye Res.* **29,** 1–18 (2010).

114. Tyagi, P., Kadam, R. S. & Kompella, U. B. Comparison of Suprachoroidal Drug Delivery with

Subconjunctival and Intravitreal Routes Using Noninvasive Fluorophotometry. *PLoS One* **7,** 1–9 (2012).

115. Kadam, R. S., Williams, J., Tyagi, P., Edelhauser, H. F. & Kompella, U. B. Suprachoroidal delivery in a rabbit ex vivo eye model: influence of drug properties, regional differences in delivery, and comparison with intravitreal and intracameral routes. *Mol. Vis.* **19,** 1198–210 (2013).

116. Cheruvu, N. P. S. & Kompella, U. B. Bovine and porcine transscleral solute transport: Influence of lipophilicity and the choroid-Bruch's layer. *Investig. Ophthalmol. Vis. Sci.* **47,** 4513–4522 (2006).

117. Chiang, B., Kim, Y. C., Edelhauser, H. F. & Prausnitz, M. R. Circumferential flow of particles in the suprachoroidal space is impeded by the posterior ciliary arteries. *Exp. Eye Res.* **145,** 424–431 (2016).

118. Olsen, T. W. *et al.* Pharmacokinetics of pars plana intravitreal injections versus microcannula suprachoroidal injections of bevacizumab in a porcine model. *Investig. Ophthalmol. Vis. Sci.* **52,** 4749–4756 (2011).

119. Sarin, H. Physiologic upper limits of pore size of different blood capillary types and another perspective on the dual pore theory of microvascular permeability. *J Angiogenes Res* **2,** 14 (2010).

120. Kompella, U. B., Amrite, A. C., Pacha Ravi, R. & Durazo, S. A. Nanomedicines for back of the eye drug delivery, gene delivery, and imaging. *Prog. Retin. Eye Res.* **36,** 172–198 (2013).

121. Tyagi, P., Barros, M., Stansbury, J. W. & Kompella, U. B. Light-activated, in situ forming gel for sustained suprachoroidal delivery of bevacizumab. *Mol. Pharm.* **10,** 2858–2867 (2013).

122. Raghava, S., Hammond, M. & Kompella, U. B. Periocular routes for retinal drug delivery. *Expert Opin. Drug Deliv.* **1,** 99–114 (2004).

123. Bansal, P., Garg, S., Sharma, Y. & Venkatesh, P. Posterior Segment Drug Delivery Devices: Current and Novel Therapies in Development. *J. Ocul. Pharmacol. Ther.* **32,** 135–44 (2016).

124. Ranta, V. P. *et al.* Barrier analysis of periocular drug delivery to the posterior segment. *J. Control. Release* **148,** 42–48 (2010).

125. Edelhauser, H. F. *et al.* Ophthalmic Drug Delivery Systems for the Treatment of Retinal Diseases: Basic Research to Clinical Applications. *Investig. Opthalmology Vis. Sci.* **51,** 5403 (2010).

126. Kim, S. H., Lutz, R. J., Wang, N. S. & Robinson, M. R. Transport barriers in transscleral drug delivery for retinal diseases. *Ophthalmic Res.* **39,** 244–254 (2007).

127. Watson, P. G. & Young, R. D. Scleral structure, organisation and disease. A review. *Exp. Eye Res.* **78,** 609–623 (2004).

128. Meek, K. M. in *Collagen: Structure and Mechanics* (ed. Fratzl, P.) 359–396 (Springer US, 2008). doi:10.1007/978-0-387-73906-9_13

129. Nguyen, T. D. in *Structure-Based Mechanics of Tissues and Organs* 285–315 (Springer, 2016). doi:10.1007/978-1-4899-7630-7_14

130. Meek, K. M. in *Collagen: Structure and Mechanics* (ed. Fratzl, P.) 359–396 (Springer US, 2008). doi:10.1007/978-0-387-73906-9_13

131. Yamabayashi, S. *et al.* Ultrastructural studies of collagen fibers of the cornea and sclera by a quick-freezing and deep-etching method. *Ophthalmic Res* **23,** 320–329 (1991).

132. Summers Rada, J. A., Shelton, S. & Norton, T. T. The sclera and myopia. *Exp. Eye Res.* **82,** 185–200 (2006).

133. Maurice, D. M. & Polgar, J. Diffusion across the sclera. *Exp. Eye Res.* **25,** 577–582 (1977).

134. Ambati, J. *et al.* Diffusion of High Molecular Weight Compounds through Sclera. *Invest. Ophthalmol. Vis. Sci.* **41,** 1181–5 (2000).

135. Olsen, T. W., Edelhauser, H. F., Lim, J. & Geroski, D. H. Human Scleral Permeability and Surgical Thinning. *Invest. Ophthalmol.* **36,** 1893–1903 (1995).

136. Boubriak, O. a, Urban, J. P., Akhtar, S., Meek, K. M. & Bron, a J. The effect of hydration and matrix composition on solute diffusion in rabbit sclera. *Exp. Eye Res.* **71,** 503–514 (2000).

137. Berezovsky, D. E., Patel, S. R., McCarey, B. E. & Edelhauser, H. F. In vivo ocular fluorophotometry: delivery of fluoresceinated dextrans via transscleral diffusion in rabbits. *Invest. Ophthalmol. Vis. Sci.* **52,** 7038–45 (2011).

138. Murtomäki, L., Vainikka, T., Pescina, S. & Nicoli, S. Drug adsorption on bovine and porcine sclera studied with streaming potential. *J. Pharm. Sci.* **102,** 2264–2272 (2013).

139. Cruysberg, L. P. J. *et al. In Vitro* Human Scleral Permeability of Fluorescein, Dexamethasone-Fluorescein, Methotrexate-Fluorescein and Rhodamine 6G and the Use of a Coated Coil as a New Drug Delivery System. *J. Ocul. Pharmacol. Ther.* **18,** 559–569 (2002).

140. Amrite, A. C. & Kompella, U. B. Size-dependent disposition of nanoparticles and microparticles following subconjunctival administration. *J. Pharm. Pharmacol.* **57,** 1555–63 (2005).

141. Amrite, A. C., Edelhauser, H. F., Singh, S. R. & Kompella, U. B. Effect of circulation on the disposition and ocular tissue distribution of 20 nm nanoparticles after periocular administration. *Mol. Vis.* **14,** 150–60 (2008).

142. Vellonen, K. S. *et al.* A critical assessment of in vitro tissue models for ADME and drug delivery. *J. Control. Release* **190,** 94–114 (2014).

143. Jiang, J., Moore, J. S., Edelhauser, H. F. & Prausnitz, M. R. Intrascleral drug delivery to the eye using hollow microneedles. *Pharm Res* **26,** 395–403 (2009).

144. Maurice, D. M. & Polgar, J. Diffusion across the sclera. *Exp. Eye Res.* **25,** 577–582 (1977).

145. Nicoli, S. *et al.* Porcine sclera as a model of human sclera for in vitro transport experiments: histology, SEM, and comparative permeability. *Mol. Vis.* **15,** 259–66 (2009).

146. Boubriak, O. A., Urban, J. P. G. & Bron, A. J. Differential effects of aging on transport properties of anterior and posterior human sclera. *Exp. Eye Res.* **76,** 701–713 (2003).

147. Skeie, J. M., Tsang, S. H. & Mahajan, V. B. Evisceration of mouse vitreous and retina for proteomic analyses. *J. Vis. Exp.* **50,** 12–14 (2011).

148. Kaier, R. J. & Maurice, D. M. The Diffusion of Fluorescein in the Lens. *Exp. Eye Res.* **3,** 156–165 (1964).

149. Ohtori, A. & Tojo, K. In vivo/in vitro correlation of intravitreal delivery of drugs with the help of computer simulation. *Biol. Pharm. Bull.* **17,** 283–90 (1994).

150. Nickerson, C. S., Park, J., Kornfield, J. A. & Karageozian, H. Rheological properties of the vitreous and the role of hyaluronic acid. *J. Biomech.* **41,** 1840–1846 (2008).

151. Martens, T. F. *et al.* Measuring the intravitreal mobility of nanomedicines with single-particle tracking microscopy. *Nanomedicine (Lond)* **8,** 1955–1968 (2013).

152. Barar, J., Asadi, M., Mortazavi-Tabatabaei, S. A. & Omidi, Y. Ocular Drug Delivery; Impact of in vitro Cell Culture Models. *J. Ophthalmic Vis. Res.* **4,** 238–52 (2009).

153. Shen, J., Cross, S. T., Tang-Liu, D. D. S. & Welty, D. F. Evaluation of an immortalized retinal endothelial cell line as an in vitro model for drug transport studies across the blood-retinal barrier. *Pharm. Res.* **20,** 1357–1363 (2003).

154. Gillies, M. C., Su, T. & Naidoo, D. Electrical resistance and macromolecular permeability of retinal capillary endothelial cells in vitro. *Curr. Eye Res.* **14,** 435–42 (1995).

155. Wisniewska-Kruk, J. *et al.* A novel co-culture model of the blood-retinal barrier based on primary retinal endothelial cells, pericytes and astrocytes. *Exp. Eye Res.* **96,** 181–190 (2012).

156. Garcia-Ramírez, M., Villarroel, M., Corraliza, L., Hernández, C. & Simó, R. in *Permeability Barrier: Methods and Protocols* (ed. Turksen, K.) 179–194 (Humana Press, 2011). doi:10.1007/978-1-61779-191-8_12

157. Campbell, M. & Humphries, P. in *Permeability Barrier: Methods and Protocols* (ed. Turksen, K.) 355–367 (Humana Press, 2011). doi:10.1007/978-1-61779-191-8_24

158. Blenkinsop, T. A., Salero, E., Stern, J. H. & Temple, S. The culture and maintenance of functional retinal pigment epithelial monolayers from adult human eye. *Methods Mol. Biol.* **945,** 45–65 (2013).

159. Burke, J. M. & Hjelmeland, L. M. Mosaicism of the retinal pigment epithelium: seeing the small picture. *Mol. Interv.* **5,** 241–9 (2005).

160. Lupo, G. *et al.* Role of phospholipases A2 in diabetic retinopathy: In vitro and in vivo studies. *Biochem. Pharmacol.* **86,** 1603–1613 (2013).

161. Hamilton, R. D., Foss, A. J. & Leach, L. Establishment of a human in vitro model of the outer blood-retinal barrier. *J.Anat.* **211,** 707–16 (2007).

162. Wisniewska-Kruk, J. *et al.* A novel co-culture model of the blood-retinal barrier based on primary retinal endothelial cells, pericytes and astrocytes. *Exp. Eye Res.* **96,** 181–190 (2012).

163. Pang, J. J. *et al.* Comparative analysis of in vivo and in vitro AAV vector transduction in the neonatal mouse retina: Effects of serotype and site of administration. *Vision Res.* **48,** 377–385 (2008).

164. Peynshaert, K. *et al.* Toward smart design of retinal drug carriers: a novel bovine retinal explant model to study the barrier role of the vitreoretinal interface. *Drug Deliv.* **24,**

1384–1394 (2017).

165. Clarke, L. L. A guide to Ussing chamber studies of mouse intestine. *Am. J. Physiol. Gastrointest. Liver Physiol.* **296,** G1151-66 (2009).

166. Lennernas, H. Animal data: The contributions of the Ussing Chamber and perfusion systems to predicting human oral drug delivery in vivo. *Adv. Drug Deliv. Rev.* **59,** 1103–1120 (2007).

167. Srinivasan, B. *et al.* TEER measurement techniques for in vitro barrier model systems. *J. Lab. Autom.* **20,** 107–126 (2016).

168. Steuer, H., Jaworski, A., Stoll, D. & Schlosshauer, B. In vitro model of the outer blood-retina barrier. *Brain Res. Protoc.* **13,** 26–36 (2004).

169. Ambati, J. *et al.* Transscleral delivery of bioactive protein to the choroid and retina. *Investig. Ophthalmol. Vis. Sci.* **41,** 1186–1191 (2000).

170. Amrite, A. C., Edelhauser, H. F., Singh, S. R. & Kompella, U. B. Effect of circulation on the disposition and ocular tissue distribution of 20 nm nanoparticles after periocular administration. *Mol. Vis.* **14,** 150–60 (2008).

171. Schuurmans, R. P. & Zrenner, E. Responses of the blue sensitive cone system from the visual cortex and the arterially perfused eye in cat and monkey. *Vision Res.* **21,** 1611–1615 (1981).

172. Ripps, H., Mehaffey, L., Siegel, I. M. & Niemeyer, G. Vincristine-induced changes in the retina of the isolated arterially-perfused cat eye. *Exp. Eye Res.* **48,** 771–790 (1989).

173. Gottanka, J., Chan, D., Eichhorn, M., Lütjen-Drecoll, E. & Ethier, C. R. Effects of TGF-β2 in Perfused Human Eyes. *Investig. Ophthalmol. Vis. Sci.* **45,** 153–158 (2004).

174. Koeberle, M. J., Hughes, P. M., Skellern, G. G. & Wilson, C. G. Pharmacokinetics and disposition of memantine in the arterially perfused bovine eye. *Pharm. Res.* **23,** 2781–2798 (2006).

175. Mains, J., Tan, L. E., Wilson, C. & Urquhart, A. A pharmacokinetic study of a combination of beta adrenoreceptor antagonists - In the isolated perfused ovine eye. *Eur. J. Pharm. Biopharm.* **80,** 393–401 (2012).

176. Niemeyer, G. Retinal research using the perfused mammalian eye. *Prog. Retin. Eye Res.* **20,** 289–318 (2001).

177. Mains, J., Wilson, C. G. & Urquhart, A. ToF-SIMS analysis of dexamethasone distribution in the isolated perfused eye. *Investig. Ophthalmol. Vis. Sci.* **52,** 8413–8419 (2011).

178. Abarca, E. M., Salmon, J. H. & Gilger, B. C. Effect of Choroidal Perfusion on Ocular Tissue Distribution After Intravitreal or Suprachoroidal Injection in an Arterially Perfused Ex Vivo Pig Eye Model. *J. Ocul. Pharmacol. Ther.* **29,** 715–722 (2013).

179. Yu, D. Y., Su, E. N., Cringle, S. J. & Yu, P. K. Isolated preparations of ocular vasculature and their applications in ophthalmic research. *Prog. Retin. Eye Res.* **22,** 135–169 (2003).

3

Toward smart design of retinal drug carriers: a novel bovine retinal explant model to study the barrier role of the vitreoretinal interface

An adapted version of this chapter is published as:

Karen Peynshaert[a,b], Joke Devoldere[a,b] , Valérie Forster[c], Serge Picaud[c], Christian Vanhove[d], Stefaan C. De Smedt[a,b], Katrien Remaut[a,b]. Toward smart design of retinal drug carriers: a novel bovine retinal explant model to study the barrier role of the vitreoretinal interface. *Drug Delivery* **24** 1384-1394 (2017).

[a]Lab of General Biochemistry and Physical Pharmacy, Faculty of Pharmaceutical Sciences, Ghent University, Ottergemsesteenweg 460, 9000 Ghent, Belgium.
[b]Ghent Research Group on Nanomedicines, Ghent University, Ottergemsesteenweg 460, 9000 Ghent, Belgium.

[c] Institut de la Vision, INSERM, Université Paris 6, 17 rue Moreau, Paris, France

[d] Department of Respiratory Medicine, Ghent University, 9000 Ghent, Belgium

ABSTRACT

Retinal gene delivery via intravitreal injection is hampered by various physiological barriers present in the eye of which the vitreoretinal (VR) interface represents the most serious hurdle. In this chapter we present a retinal explant model especially designed to study the role of this interface as a barrier for the penetration of vectors into the retina. In contrast to all existing explant models, the developed model is bovine-derived and more importantly, keeps the vitreous attached to the retina at all times to guarantee an intact VR interface. After *ex vivo* intravitreal injection into the living retinal explant, the route of fluorescent carriers across the VR interface can be tracked. By applying two different imaging methods on this model we discovered that the transfer through the VR barrier is size-dependent since 40 nm polystyrene particles are more easily taken up in the retina than 100 and 200 nm sized particles. In addition, we found that removing the vitreous, as commonly done for culture of conventional explants, leads to an overestimation of particle uptake, and conclude that the ultimate barrier to overcome for retinal uptake is undoubtedly the inner limiting membrane. Damaging this matrix resulted in a massive increase in particle transfer into the retina. In conclusion, we have developed a highly relevant *ex vivo* model that maximally mimics the human *in vivo* physiology which can be applied as a representative test set-up to assess the potential of promising drug delivery carriers to cross the VR interface.

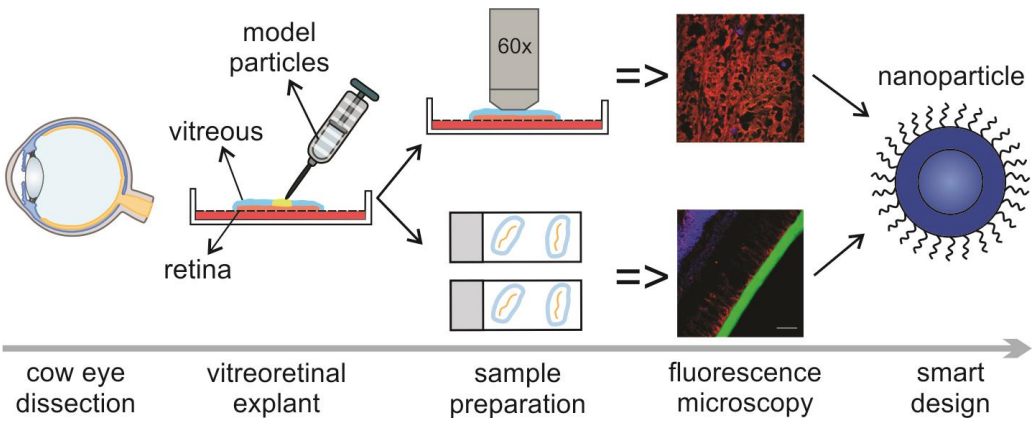

Table of Contents

1. INTRODUCTION

As discussed in **Chapter 2**, there are several administration routes available to reach the back of the eye. Currently, roughly 75 % of clinical trials are based on subretinal injection as gene delivery method.[1] However, subretinal injections are mainly efficient to reach cells surrounding the injection spot, i.e. photoreceptors (PR) or RPE cells. Hence, the majority of retinal gene therapy trials are also focused on treatment of the outer retina. Nevertheless, the inner retina harbors important target cells as well including retinal ganglion cells (RGCs) as target for Leber Hereditary Optic Neuropathy (LHON),[2] Müller cells for neurotrophic strategies,[3] and bipolar and amacrine cells for optogenetic therapy (cfr. **Chapter 1**).[4] It is, however, not at all evident to reach these cell types via subretinal injection.

An alternative method to reach the inner retina is intravitreal (IVT) injection, a technique that is considered safe, minimally invasive and relatively easy to perform.[5] Nonetheless, the transfer of (high molecular weight) drugs and nanosized particles carrying drugs into the retina after IVT injection remains troublesome, primarily because of the presence of the vitreoretinal (VR) interface. **Figure 3.1** shows that this interface consists of three structures: peripheral vitreous, the inner limiting membrane (ILM) and Müller cell endfeet. As discussed in **Chapter 2**, both the vitreous and the ILM represent important drug delivery barriers. Indeed, the vitreous, a transparent gel composed of collagen fibrils filled up with hyaluronic acid, may hamper the mobility of carriers preventing them to reach the retina.[6–8] The ILM has an extracellular matrix structure composed of a collagen IV network intertwined with proteoglycans, laminin and fibronectin.[9,10] It represents a physical border between the vitreous and the retina and functions as a sieve that more than often impedes the transfer of drug carriers into the retina.[11–13] Once drug carriers pass the vitreous and ILM they encounter retinal cells, where the first cell type they face is likely the Müller cell, a glial cell of which the endfeet align with the ILM.

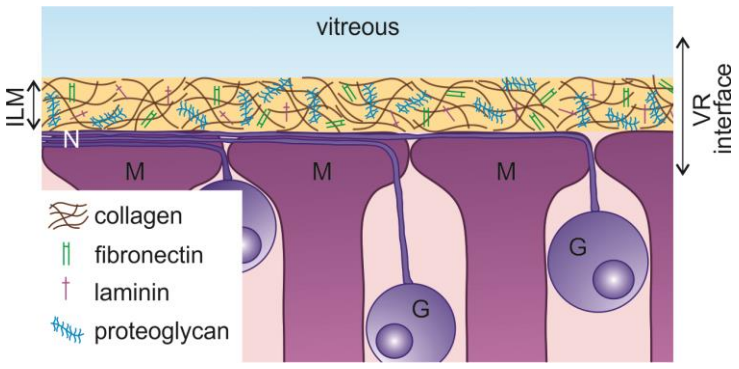

Figure 3.1 | Schematic drawing of the vitreoretinal interface. M: Müller cell; G: Ganglion cell; ILM: inner limiting membrane; VR: vitreoretinal; N: nerve fiber

Aiming for the delivery of nucleic acids in retinal cells, several groups have reported successful penetration of both non-viral as well as viral gene carriers through the entire VR interface of rodents, resulting in gene expression in the retina. In animals larger than rodents, however, IVT injection rarely results in effective gene expression.[11,12,14–17] Interspecies differences greatly hamper the extrapolation of successful IVT therapies in rodents to larger animal models and humans. This is likely because the VR interface is substantially more difficult to overcome in larger species.[18] Indeed, as mentioned in **Chapter 2**, the anatomy of the rodent eye and the structure of its vitreous and ILM is less representative for human physiology.[19,20] As an example, the thickness of the mouse ILM is estimated to be around 100 nm, while a parafoveal thickness of up to 4 µm is measured in human eyes.[21,22] In light of this, some research groups perform drug delivery studies directly on explants of larger species.[23,24] Nevertheless, in these studies the vitreous is separated from the retina so that information regarding the VR interface is lost. Therefore there is an urgent need for models with an intact VR interface based on larger animals since it is expected these will be more representative for the human VR interface. As argued in **Chapter 2**, we are convinced that such relevant *ex vivo* models will become highly useful in research which aims for drug delivery into the retina.

To address this need, we developed an *ex vivo* explant model that is bovine-derived and most importantly, guarantees an intact VR interface by keeping the vitreous attached to the retina at all times. Drugs or drug carriers can be injected *ex vivo* into the vitreous of the VR explant after which their potential to cross the VR interface as well as their transport route into the retina can be examined by microscopy. In this chapter we present the methodology of this novel VR explant and validate its retinal morphology and viability. We furthermore demonstrate the potential of the model in drug delivery research by studying how the size of nanosized polystyrene (PS) nanoparticles (NPs) influences their transport over the VR interface. Finally, we apply the presented model to draw conclusions on the drug delivery barrier role of the separate parts of the VR interface.

2. METHODS

Materials

Carboxylated polystyrene beads (FluoSpheres®) were purchased from Molecular Probes™: 40nm (8795), 100nm (F8800), 200nm (F8809). Dyes for Müller cell and viability staining were obtained from Invitrogen: Hoechst 33342 (H3570), FM® 1-43 (T3163), Mitotracker® Deep Red (M22426), Propidium iodide (P3566). Antibodies against glutamine synthetase (ab73593) and Collagen IV (ab6586) were purchased from Abcam; AlexaFluor® 647 tagged secondary antibody (A27040)

was obtained from Invitrogen. Cell culture materials were mostly acquired from Gibco™: CO_2 Independent medium (18045088), Neurobasal®-A medium (10888022), Advanced DMEM medium (12491023), B-27® supplement (17504044), Penicillin-streptomycin (15140122), L-Glutamine (25030081), GlutaMAX™ Supplement (35050061), Trypsin-EDTA 0,25% (25200072), epidermal growth factor (Sigma, E9644).

Nanoparticle characterization

The hydrodynamic size and zeta potential of the FluoSpheres® are determined using a Malvern Zetasizer Nano (Malvern Instruments, Worcestershire, U.K.). For this purpose the FluoSpheres® are diluted a thousand times in HEPES buffer (25mM, pH 7.2) prior to performing the measurements at 25 °C. Size measurements are done in triplicate with three runs per replicate and presented based on the number distribution. The zeta potentials are calculated from the electrophoretic mobility of the FluoSpheres based on the Henry equation considering the Smoluchowski approximation. Zeta potential measurements are done in triplicate with two runs per replicate.

Dissection and culture of a *conventional* retinal explant

Fresh bovine eyes are obtained from the local slaughterhouse where they are enucleated up to 30 min after the animal is sacrificed. The eyes are transported and kept in ice cold CO_2 independent medium until dissection. After removing all extra-ocular connective tissue and disinfecting the eyes by soaking them in 20% ethanol, the sclera is punctured with a 21G needle around 10 mm below the limbus. This hole next serves as an entry point for the scissors used to bisect the eye. After bisection of the eye, the vitreous is removed and the posterior eye cup is filled with cold CO_2 independent medium. Next, 3 to 4 flaps are cut in the eyecup, preferably along large veins. While the whole structure is submerged in medium, a trephine blade (Beaver®) with 10 mm diameter is used to isolate a circular piece of retina from each flap. The explant is then removed from the eyecup by gently pipetting medium below. Two of these explants are then placed on a dry 75mm Transwell® explant filter after which the explant filter is moistened with explant culture medium (Neurobasal®-A, 1% B-27® supplement, 1% Penicillin-streptomycin, 0,5% L-glutamine) and 10 ml of the same medium is added below the explant filter. Finally, the explants are incubated at 37°C and 5% CO_2.

Dissection and culture of a *vitreoretinal* explant

Our newly developed dissection protocol differs from the conventional one by the preservation of vitreous and an intact ILM during dissection. The preparation of this so-called “vitreoretinal explant” is shown in **Figure 3.2**. Before dissection, isolated bovine eyes are gently warmed by 20 – 30 minutes incubation in CO_2 independent medium at room temperature, a crucial step to

allow smooth separation of the retina from the RPE-choroid layer in step E of the protocol. As for conventional explants, the sclera is punctured with a 21G needle around 10 mm below the limbus (step A). In step B, the eye is bisected so that a posterior eye cup filled with vitreous gel remains. Next, at the rim of the eyecup the retina is gently detached from the choroid using a fine pincet, except at the side of the optic nerve (step C). Then, the vitreous is gently pulled down during which the attached retina should slide along (step D-E). After cutting the optic nerve (step F), the whole tissue is slid with vitreous side upwards into a culture dish of 10cm (Corning) filled with cold CO_2 independent medium. In step G, a scalpel is used to cut up to three pieces of VR explant (up to 1,5 cm^2) from the vitreous side downwards through the retina. Hereby the potentially damaged edges of the retinal tissue are avoided. In step I-K, a plastic Pasteur pipette is used to gently aspire the VR explant and to transfer it to a dry explant filter from a 75mm Transwell® dish (3419, Corning). Excess amounts of vitreous (e.g. lying next to the retina) can then be removed by aspiration of some vitreous using a plastic Pasteur pipette while cutting through the gel with scissors. Finally, 10 ml of supplemented Neurobasal®-A medium is added below the explant filter (Step L) and the VR explant is placed in an incubator with 5% CO_2 at 37°C.

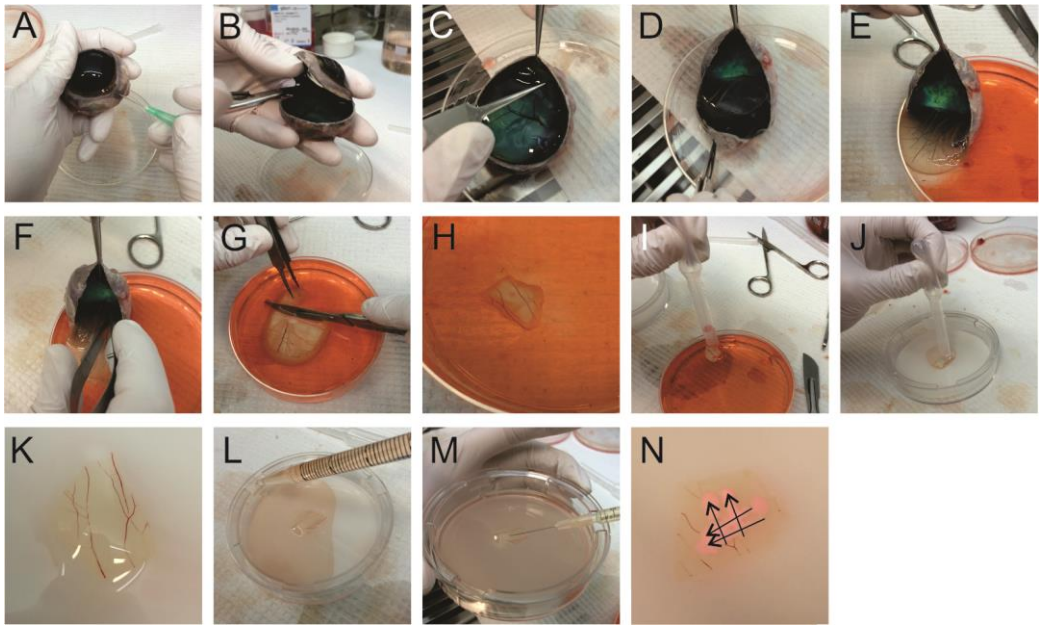

Figure 3.2 | Step-by-step overview of the dissection protocol to culture a bovine vitreoretinal explant.

Ex vivo intravitreal injection of nanoparticles

Immediately after explant dissection, carboxylated PS beads ($1,42*10^{15}$ NPs/ml) are injected (using a 30G needle) in the vitreous layer covering the retina. Multiple injections (about 50 µL per injection) within one VR explant are performed. The injections are done 'horizontally' to avoid direct transfer of NPs into the retina (**Figure 3.2**, M). As shown in step N each IVT injection

typically resulted in an 'injection band' (arrows) containing a high concentration of (fluorescent) beads. Following injection the beads then diffuse through the vitreous toward the retina. Since IVT injection is not possible in conventional retinal explants (as there is no remaining vitreous), 25 µl of the carboxylated PS beads is applied on top of the explants. All explants are incubated with the PS beads at 37°C for 24 hours.

Explant staining, fixation and "direct imaging"

Explants are stained by the injection of a mixture of dyes in the vitreous covering the retina, followed by incubation at 37°C for 2 hours. Nuclei are stained with 10 µg/ml Hoechst, lipid membranes with 20 µg/ml FM-43 and Müller cells with 2 µM Mitotracker Deep red following the protocol of Uckermann *et al.*[25]. To evaluate retinal cell viability, a mixture of Propidium Iodide and Hoechst is added to the explant culture medium below the explant filter resulting in a final concentration of 10 µg/ml for both dyes. After dye incubation the explants are fixed by replacing the explant culture medium with 4% paraformaldehyde (in PBS) during 2 hours at 4°C. After fixation, the fixative is replaced by PBS for imaging.

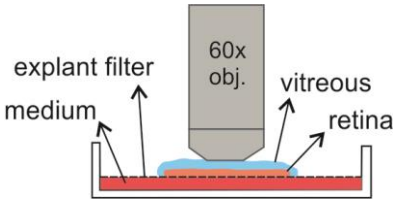

Figure 3.3 | Schematic drawing of the set-up applied for "direct imaging" of the vitreoretinal explant.

Fixed *ex vivo* explants are imaged with a confocal microscope (C1-si, Nikon) directly or after preparing cryosections (see below). For "direct imaging", a 60x water dipping objective (NIR, Apo) with a large working distance (2,8 mm) is pushed on top of the vitreous which allows to image from the vitreous until the ganglion cell layer (**Figure 3.3**).

Explant cryosectioning and immunohistochemistry

After fixation, the fixative below the explant filter is removed and replaced by 30% sucrose and incubated overnight at 4°C. After snap freezing the samples in Tissue-Tek® O.C.T. (Sakura) with liquid nitrogen, 14 µm sections are cut with a cryostat (Leica).

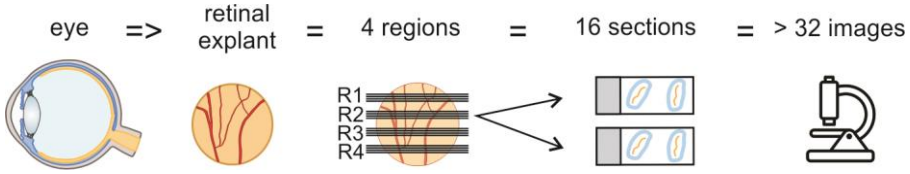

Figure 3.4 | Workflow applied for cryosectioning of the retina and cryosection imaging.

For reliability of our results we applied the workflow drawn in **Figure 3.4**: 16 sections are analyzed per retina, resulting from 4 distinct retina regions. These retinal sections are permeabilized with 0,1% Triton for 5 min prior to a 1 hour incubation at room temperature with 5% goat serum in PBS as a blocking step. Next, sections are incubated overnight at 4°C with 1:200 rabbit antibody against Collagen IV. Finally, after a 1 hour incubation at room temperature with goat anti-rabbit Alexafluor 647 conjugated secondary antibody and 10 µg/ml Hoechst, the sections are mounted with Vectashield (Vector Laboratories) and prepared for imaging. The cryosection imaging is done with a confocal microscope (C1-si, Nikon) using a 10x objective (CFI Plan Apochromat, Nikon) and a 60x water objective (NIR Apo, Nikon).

Uptake of nanoparticles by the retina: cryosection image processing for semi-quantitative analysis

To analyse the uptake of the PS beads by the retina, following the workflow presented in **Figure 3.4**, (minimally) two images are taken per retinal section, resulting in at least 32 images per retinal explant. Image analysis is done with FIJI (NIH) as follows: using the Polygon Tool a region of interest (ROI) is drawn around the retinal area below the ILM. Then, the area outside this ROI, i.e. above the ILM, is colored black using the 'clear tool' so only particles present within the ROI (retina) would be counted. The number of particles within the ROI is counted using the 'analyze particles' tool. Finally, the surface area of the ROI is measured by applying the 'measure' tool in the ROI manager so that the number of counted particles can be recalculated per 1000 μm^2. Based on these results, the various sections are categorized in three categories i.e. samples containing a low (< 10), higher (10-30) or very high (> 30) amount of particles per 1000 μm^2.

3. RESULTS

Vitreoretinal explant morphology and viability

The VR explant differs from the conventional explant by the presence of an intact VR interface. Despite this seemingly small difference, the search for a dissection protocol suitable to obtain the VR explant was intensive. The dissection protocol as presented in **Figure 3.2** resulted in an explant that keeps a layer of vitreous attached to the retina. Next, we visualized the ganglion cell layer (GCL) and nerve fiber layer (NFL) of the VR explant by staining for Müller cells and lipid membranes. **Figure 3.5** shows that a large portion of this layer is taken in by a patchwork of Müller cell endfeet (red color) separated by lipid membranes (green color). Nerve fibers run unidirectional through these patchworks, while other dye-less cell types such as RGCs are randomly scattered within this layer.

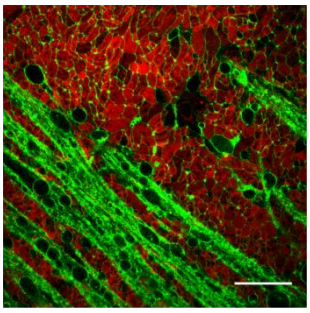

Figure 3.5 | Confocal view of the GCL/NFL layer as obtained through "direct imaging" (Figure 3.3). Müller cells (red) are stained with Mitotracker Deep Red, lipid membranes and nerve fibers (green) with FM-43. Scale bar: 20 µm.

When we compare the morphology of the bovine GCL/NFL layer with the morphology of Mitotracker-stained tissue of others species as presented in literature (**Figure 3.6**), the morphology of the bovine GCL/NFL layer highly relates to that of the human retina. Interestingly, bovine vitreous also has a similar structure as human vitreous and has therefore been frequently applied in *ex vivo* models developed for IVT drug delivery studies.[7,20,26–28]

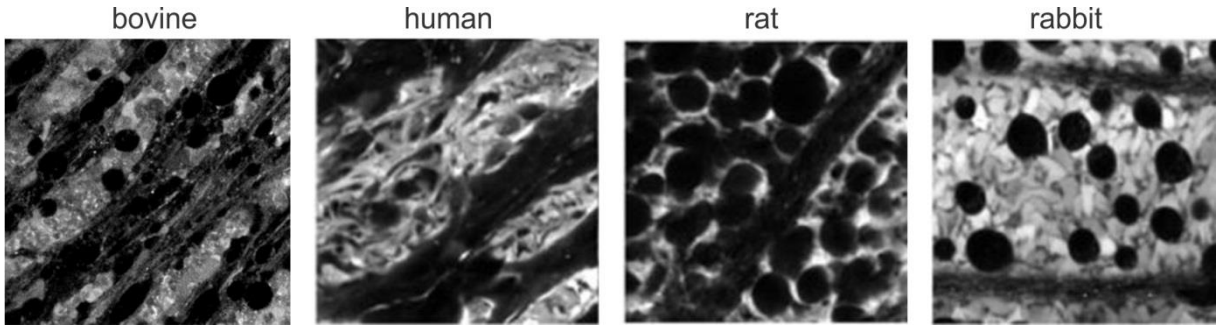

Figure 3.6 | Confocal view of the GCL/NFL layer of different species stained for Müller cells. Bovine retinal tissue was stained by Mitotracker Deep Red (own data); human, rat and rabbit tissues were stained with Mitotracker Orange, data taken from [25].

Next, we aimed to assess if the dissection protocol and explant culture conditions maintain the integrity and viability of the various retinal layers. VR explants were stained with the nuclear label Hoechst to identify the various layers and check gross retinal morphology. Also, the cell-impermeable (red) dye Propidium Iodide (PI) was added to identify cell viability. The cryosections in **Figure 3.7** show that the architecture of the retina is nicely preserved and all retinal layers can be easily distinguished. In addition, a layer of vitreous gel is clearly attached at the side of the ILM as indicated by the arrows. Also note that the number of PI-positive cells is very limited at both time points from which we conclude that the explant is viable for at least 48 hours.

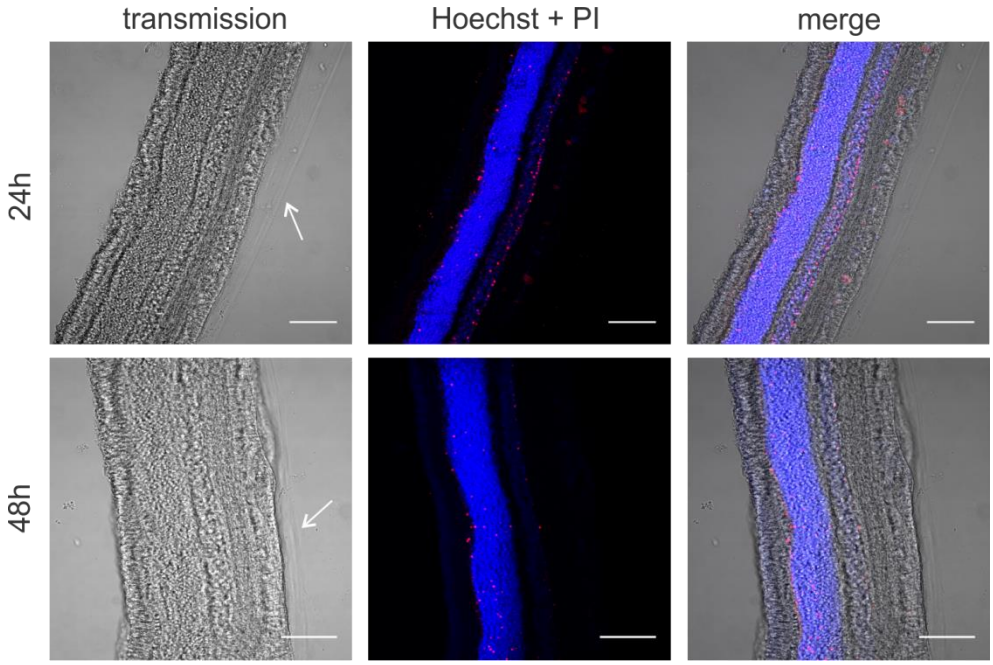

Figure 3.7 | Cryosections showing gross morphology and tissue viability of vitreoretinal explants. Nuclei are stained with Hoechst (blue), dead cells are stained with propidium iodide (PI, red). Arrows indicate the vitreous layer. Scale bar: 100 µm.

Influence of nanoparticle size on the transfer through the vitreoretinal interface studied by direct imaging of the VR explant

Following the successful characterization of the morphology and viability of the VR explant, we applied the model to study, for the first time, the size dependent penetration of polystyrene (PS) beads over the intact VR interface of a large animal. The three selected sizes of the PS beads correlate with the sizes of (intravitreally injected) gene carriers currently under investigation for the treatment of retinal diseases: 40 nm ranges at the upper size limit of viral vectors, while the 100 and 200 nm sized beads represent the size of most common non-viral vectors. **Table 3.1** represents the size and zeta-potential (a measure for the surface charge) of the carboxylated PS beads dispersed in HEPES buffer, as measured by DLS. As expected, the particle sizes were highly reproducible and all particles were negatively charged due to the carboxylated surface. This negative charge is of importance since negatively charged entities are known to diffuse well through the vitreous, increasing their potential to reach the retina.

	size (nm)	zeta potential (mV)
40 nm	37 (± 0.4)	-14 (± 0.4)
100 nm	90 (± 0.4)	-30 (± 0.8)
200 nm	205 (± 1.2)	-39 (± 0.4)

Table 3.1 | Size and zeta-potential of the carboxylated PS beads in HEPES buffer as measured by DLS (n=3).

As described above, the PS beads were administered into the VR explant by multiple 50 µl *ex vivo* IVT injections. 24 Hours post injection, the transfer of the NPs from the vitreous into the retina was investigated using the direct imaging method. Here, a water dipping objective is gently pushed on top of the vitreous to image the vitreous and NFL/GCL layer (**Figure 3.3**). **Figure 3.8A** demonstrates the transfer of green PS beads through the VR interface into the NFL/GCL layer (of which the Müller cell endfeet are stained in red). Our data shows that only 40 nm particles can be spotted in the retina, while 100 nm and 200 nm NPs do not appear in the NFL/GCL layer. Note that, on the micro-scale, the position of the retina as it occurs in **Figure 3.8** is not entirely flat. Therefore, images were often taken in which the vitreous (right top side) appears bright green as it is heavily loaded with green PS beads, while the rest of the image displays Müller cell endfeet and nerve fibers. Remarkably, 40 nm particles that were able of crossing the VR interface tended to selectively co-localize with the Mitotracker-stained Müller cells. Indeed, 40 nm PS beads were only present in the mosaic of red islands representing Müller cells, though not in the blood vessels, nerve fibers or dye-less cells representing other retinal cell types (**Figure 3.8B**).

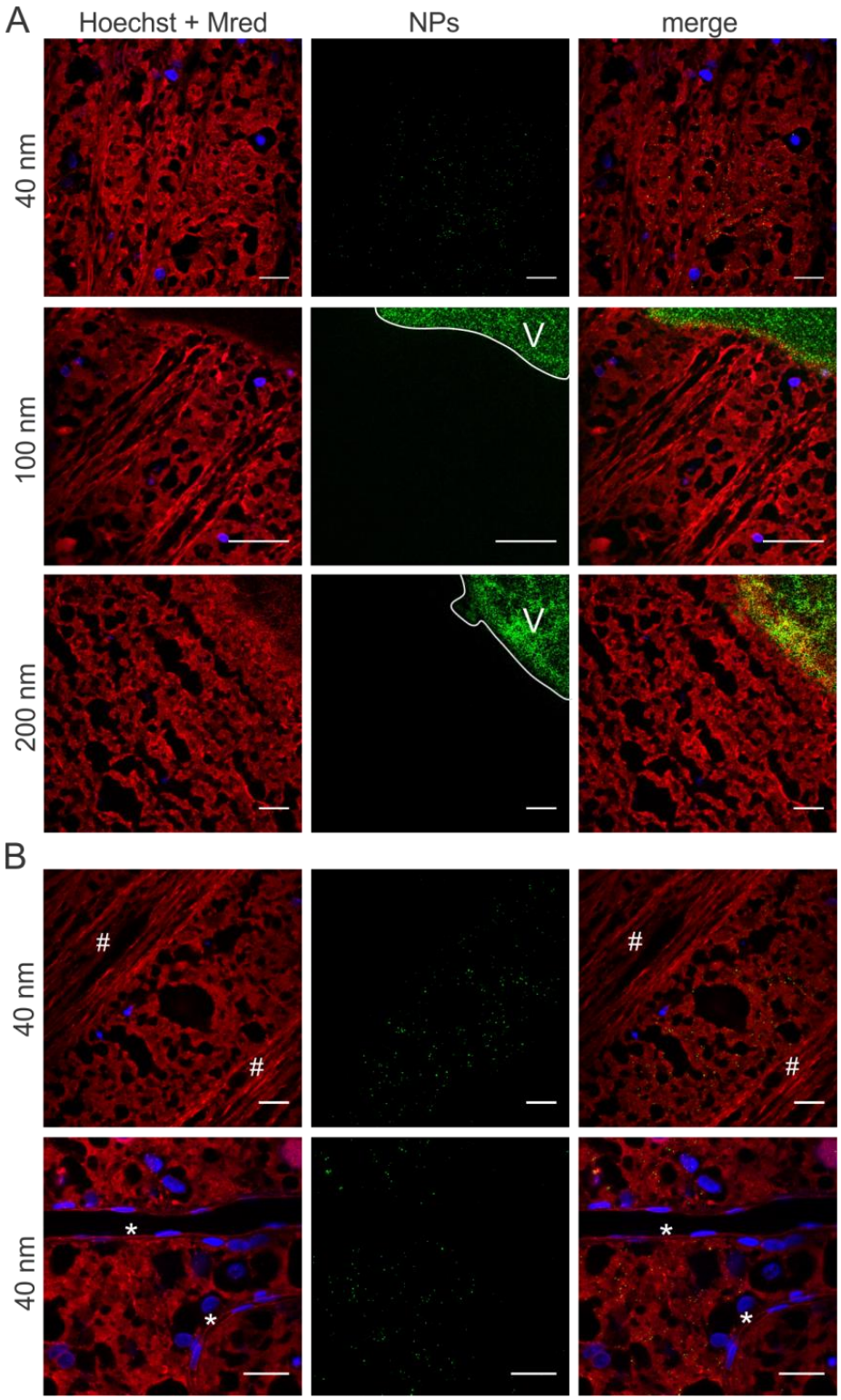

Figure 3.8 | Transfer of (green) PS beads through the VR interface, as visualized by "direct imaging" (Fig. 3.3). Müller cells (red) are stained with Mitotracker Deep Red, cell nuclei (blue) with Hoechst. **A**) 40 nm particles enter the Müller cells, 100 and 200 nm particles remain in the vitreous (indicated with "V"). Scale bar: 25µm. For optimal contrast we refer the reader to the pdf version. **B**) Co-localization of 40 nm PS beads (green) with Müller cells. Asterisks (*) indicate blood vessels, number signs (#) indicate nerve fibers. Scale bar: 25 µm.

Influence of nanoparticle size on the transfer through the vitreoretinal interface studied by cryosection imaging of the vitreoretinal explant

We further investigated the uptake of differently sized PS beads in the VR explant by cryosection imaging. Considering our interest in the VR interface, we visualized the ILM by staining it with (red) antibodies against Collagen IV. Typically this resulted in images as presented in **Figure 3.9**, where the vitreous, which appears as bright green due to the high number of PS beads, nicely aligns with the intact ILM. Based on these images, we estimated the thickness of the ILM to be around 2 µm, which correlates well with the average thickness of fixed human ILM (~ 2-4 µm) reported before.[21,22]

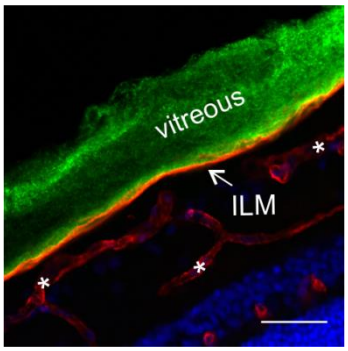

Figure 3.9 | Cryosection image of a bovine VR explant. Green: 100 nm polystyrene beads injected in the vitreous; Red: ILM stained for collagen, which also stains retinal blood vessels (*); Blue: Hoechst staining of nuclei. Scale bar 50 µm.

To rule out any bias, cryosection preparation was performed complying with the workflow drawn in **Figure 3.4** followed by image processing, resulting in at least 32 images that were analyzed per replicate of a given NP size. We opted for this systematic and objective approach based on the initial observation that NP uptake often greatly varied between different explants and even between different locations within one explant. **Figure 3.10B** shows the number of NPs that penetrated in the retina, subdivided in categories of low (< 10 NPs), intermediate (10-30 NPs) and high (> 30 NPs) penetration per 1000µm^2 of retina. The size-dependent uptake of the PS beads confirms the trend observed in **Figure 3.8**. Indeed, the majority of sections originating from explants incubated with 40 nm NPs contain a large amount of beads inside the retina (**Figure 3.10B**, black bar) while the opposite is true for the 100 and 200 nm sized NPs. **Figure 3.10A** shows representative images of the most occurring situation for each particle size i.e. high (> 30 NPs/1000µm^2 as seen with 40 nm NPs), low (10-30 NPs/1000 µm² as observed with 100 nm NPs) and medium (< 10 NPs/1000µm^2 for 200 nm NPs) penetration. Also on these images, the high VR transfer into the retina of 40 nm beads in comparison with the larger particles is clearly noticeable.

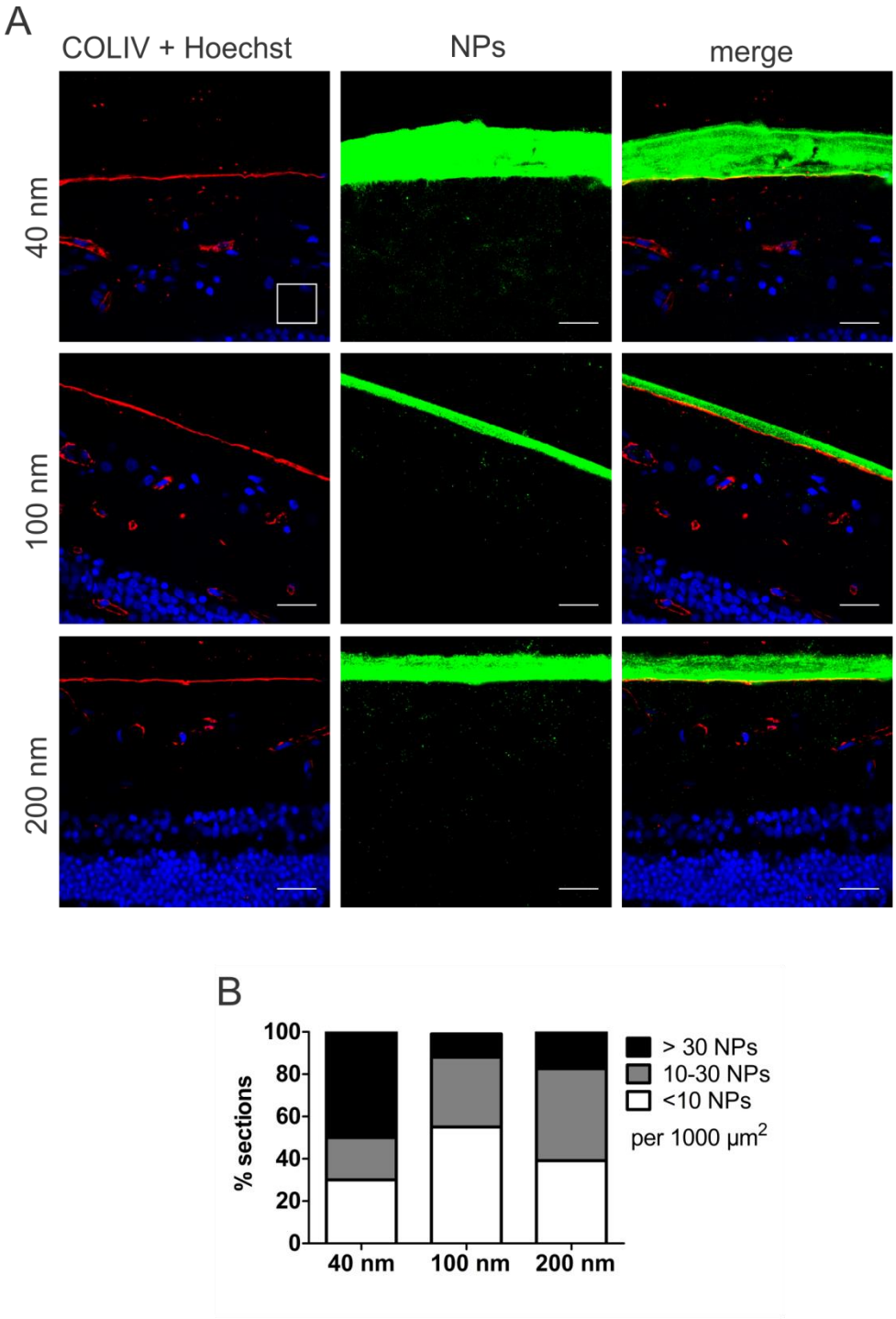

Figure 3.10 | Transfer of (green) PS beads through the VR interface, as visualized by cryosection imaging. **A**) Representative cryosection images showing the transport of PS beads through the vitreoretinal interface, 24 h after injecting the PS beads in the vitreous of the VR explant. ILM and blood vessels are stained by anti-collagen antibodies (red), nuclei (blue) with Hoechst, particles are shown in green. Note that the contrast in the middle panel is enhanced to optimally visualize the PS beads, while the brightness of the PS beads is reduced in the right panel to illustrate the perfect alignment of the vitreous and ILM. The scale square in the top left image represents 1000 µm^2 (31,6 µm x 31,6 µm). Scale bar: 31,6 µm. **B**) Semi-quantitative analysis of transport of PS beads through the VR interface after 24 h incubation. (n = 3)

Relevance of the vitreous and ILM as drug delivery barriers

To illustrate the importance of an *ex vivo* model that keeps the entire VR interface intact we have compared the transport of 100 nm sized PS beads into the retina using respectively our VR explants and conventional explants without vitreous. As can be derived from **Figure 3.11B**, the transfer of particles into the retina observed using conventional explants was clearly higher. In fact, the fraction of sections containing > 30 NPs per 1000 μm^2 nearly tripled (11 to 31%). We furthermore observed that absence of vitreous allowed larger particle aggregates to enter the retina (**Figure 3.11A, - vitreous**). In view of these observations, it is evident that tearing off the vitreous significantly affects the transport of NPs into the retina which may result in an inaccurate estimation of the potential of NPs to cross the VR interface. To further explore to which extent the ILM is a transport barrier for NPs we purposely sought for spots in the retinal sections with a compromised ILM. It has indeed been reported before that the ILM can be severely damaged by tearing of the vitreous.[29] A typical image of this case is shown in **Figure 3.11A (-ILM)** where the ILM is absent in the center of the image, a condition which clearly results in unusually high NP transport.

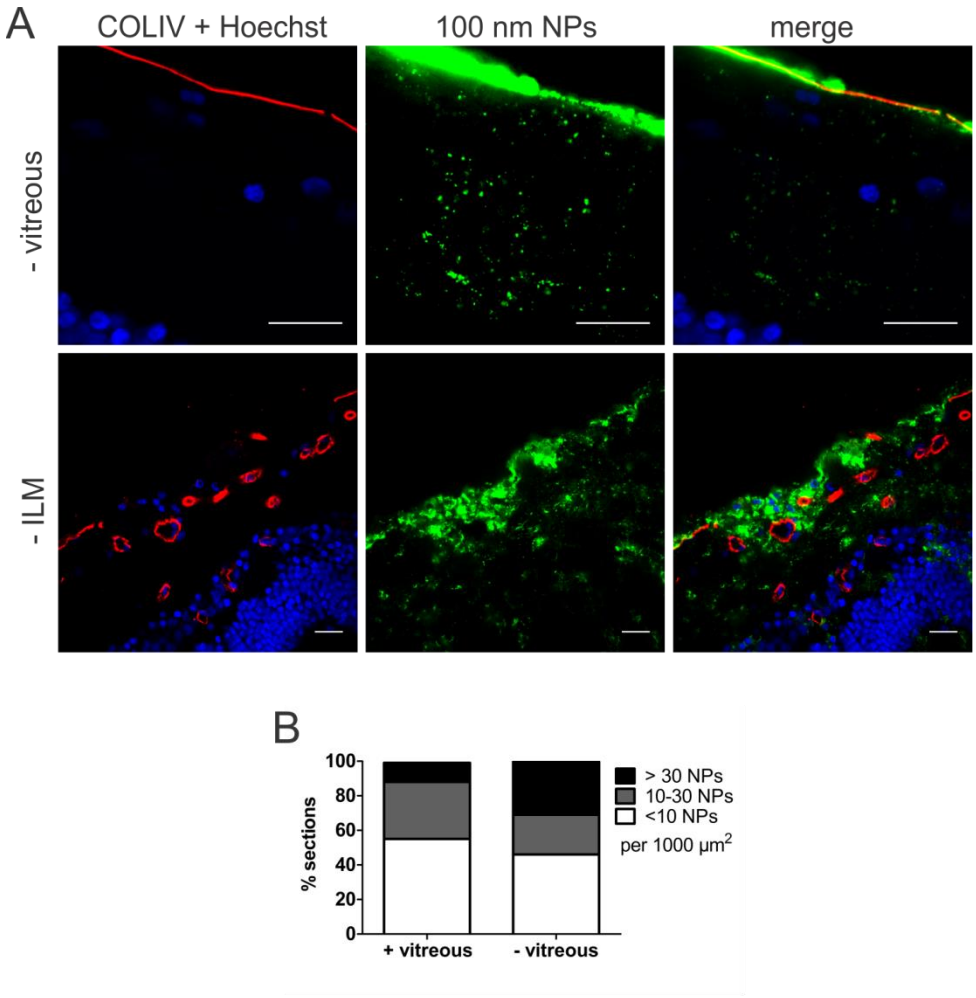

Figure 3.11 | Transfer of 100 nm PS beads in explants with compromised barriers. **A)** Representative cryosection images showing the transport of 100 nm sized PS beads into the retina, 24 h after applying the beads on the explants. Top row: no vitreous, bottom row: no ILM. ILM and blood vessels (red) are stained by anti-COLIV antibodies, nuclei (blue) with Hoechst, particles are shown in green. Scale bar: 20 µm. **B)** Semi-quantitative analysis of 100 nm PS bead uptake in vitreoretinal explants compared to conventional explants without vitreous (n = 3).

4. DISCUSSION

IVT injection is globally a daily employed administration technique for the delivery of therapeutics to the retina, such as anti-VEGF medication or antibiotics. For the delivery of gene carriers, on the other hand, subretinal injection is clinically the most investigated technique, especially for targeting PRs or RPE cells in the outer retina. We, and others, however strongly believe IVT injection can be a worthy alternative for gene delivery to the retina, especially when (widespread) expression over the inner retinal tissue should be obtained.[8,30] Yet, to ensure effective gene therapy after IVT injection, gene carriers have to pass the VR interface before reaching the retina. As extensively discussed in **Chapter 2**, three parts of this VR interface can be considered as a hurdle: peripheral vitreous, the ILM and Müller cell endfeet (**Figure 3.1**). Strikingly, gene carriers often efficiently overcome these hurdles in small animal *in vivo* studies,

usually on rodents, though this success is rarely extrapolated to larger animal models like pigs.[18] Based on our knowledge on interspecies differences in ocular anatomy and barrier structure this does not entirely come as a surprise: the combination of the smaller volume of vitreous (5 – 20 µl),[31] its more liquid composition and the reduced ILM thickness make the VR interface in mice hardly representative for the human situation.[32] For this reason several research groups focus on the culture of large animal retinal explants, however, this usually implies detachment of the vitreous gel so information on the VR interface is lost.[23,24] We therefore aimed to bridge the gap between these *ex vivo* models and the eventual *in vivo* situation in large animals and humans, by developing a novel *ex vivo* explant model based on bovine eyes that maintains the entire VR interface intact. We show that our VR explant remains viable for at least two days and its morphology is rather human-like (**Figure 3.6-3.7)**. We furthermore demonstrate that our model is ideally suited to study the penetration of particles across the VR interface into the retina after IVT injection.

Conveniently, our VR explant model allows for two ways of imaging, where both ways have their merits. The direct imaging method (**Figure 3.3**) is faster, less labour-intensive and requires for less tissue manipulation which results in optimal integrity of the whole tissue. The observable tissue depth is however limited to the ganglion cell layer. On the other hand, cryosection preparation and imaging is rather labour-intensive but gives a full cross-section of all retinal layers and allows to stain for a plethora of markers by immunostaining (**Figure 3.4**).

As highlighted in **Chapter 2** working *ex vivo* comes with several advantages, which is why we purposely opted for this approach. Firstly, highly relevant drug delivery studies can be performed on representative large animal species such as pig, cow or even human donor eyes; this without the high costs that accompany the care and housing of larger species as required for *in vivo* studies. Secondly, *ex vivo* assays are convenient and accessible: eyes can be easily obtained from local slaughterhouses, and only basic cell culture and dissection materials are required to culture our VR model, making it feasible for every researcher. Finally, the application of *ex vivo* assays is in line with the worldwide aim to implement the 3R principle (replacement, reduction and refinement), originally introduced by Russell and Burch as guidelines for more ethical and less use of laboratory animals.[33]

To demonstrate the value and functionality of our VR explant for drug delivery we looked into the size-dependent transfer of NPs through the VR interface into the retina. To this end, we decided to use commercially available carboxylated polystyrene beads, since these particles are highly fluorescent, well characterized and monodisperse as confirmed by our DLS measurements (**Table 3.1**). Furthermore, these particles have potential to penetrate into the retina after IVT

injection as: 1) the NP sizes are lower than the estimated mesh size of the vitreal collagen network (550 nm) [20] 2) negatively charged particles exhibit ideal vitreal mobility and do not aggregate in the vitreous,[20,34–37] and 3) in contrast to positively charged particles, negatively charged ones have been reported before to cross the ILM.[11,12] As anticipated, the PS beads did effectively enter the retina and more importantly, a clear size-dependent trend was noticeable using both imaging methods (**Figure 3.8 and 3.10)**: 40 nm PS beads more easily entered the retina from the vitreous than 100 and 200 nm sized beads. It is essential to note that for a given particle size, the number of NPs that crossed the VR interface varied greatly between different retinal explants and even for different locations within the same retinal explant. For this reason the retinal section data were presented as a distribution rather than only showing the most occurring observation. A potential explanation for this variety in uptake within and between VR explants is that the ILM thickness varies depending on the retinal region,[10] as well as on the age of the animal.[9,38] In addition, although the same particle concentration and injection volumes were injected into the vitreous of the various VR explants, the injection location and the thickness of the vitreous layer largely determine the actual NP concentrations across the vitreous and the retina.

Once NPs passed the VR interface, they were generally located in the inner retinal layers, which is in line with the rationale of exploring IVT injection as a valuable strategy for gene therapy, primarily for targeting cell types in the inner retina. Using the direct imaging method we further observed that 40 nm particles co-localized specifically with Müller cell endfeet (**Figure 3.8B**), an observation also made by Koo *et al*. with human serum albumin based NPs in rats.[11,34] Since the Müller cell endfeet abut in the ILM, these cells are likely the first ones particles encounter after IVT injection. Also our *in vitro* uptake studies demonstrate that bovine primary Müller cells efficiently endocytose polystyrene beads (data not shown). Unfortunately, we were unable to confirm a clear co-localisation of NPs and Müller cells using cryosection imaging.

Interestingly, while 100 nm sized particles had difficulty crossing the VR interface in our hands, some reports discuss the easy entry of larger particles into the retina.[11,34,39,40] Koo *et al*. for example found 350 nm sized negatively charged human serum albumin particles to enter the retina in rats after IVT injection.[11] Similarly, neutral polylactide particles of the same size were reported to accumulate at the ILM followed by smooth penetration into the rat retina as well.[39] Also solid lipid nanoparticles of 230 nm resulted in efficient transfection across nearly all retinal layers after IVT injection in mice.[40] It should be noted, however, that all these observations were made in rodents, which could account for the contrast with our data obtained in bovine eyes.

To illustrate the importance of preserving the VR interface and to explore the barrier role of the vitreous, we have investigated the uptake of 100 nm sized NPs in conventional explants without vitreous. Removing the vitreous had a positive effect on retinal uptake, since the fraction of retinal sections containing high amounts of NPs increased and larger NP aggregates were able to enter the inner layers of the retina (**Figure 3.11A and B**). Notably, the vitreous does not represent a major barrier for these negatively charged 100 nm PS beads since they are known to have good vitreal mobility [41]. We therefore expect the effect of vitreous removal to be more pronounced for positively charged particles that are obstructed by their interaction with the negatively charged components of the vitreous,[7,11,20,34,41,42] and for particles that are larger than the mesh size of the vitreal network (~550 nm).[20] Next to losing information on the barrier function of the vitreous for a particular NP, tearing off the vitreous also influences the barrier function of the ILM. In fact, Russell *et al*. found that vitreous separation commonly results in ILM breaks, ILM evulsion and sporadically even loss of inner retinal layers in cynomolgus monkeys.[29] An example of ILM separation upon vitreous removal can be seen in **Figure 3.11A**, a condition that clearly results in massive NP uptake in the retina. A similar observation was made by Gan *et al.* who witnessed enhanced penetration of liponanoparticles through the disintegrated ILM of rats suffering from uveitis when compared to healthy rats.[13] Also, Dalkara *et al.* witnessed enhanced retinal transduction by viral vectors following mild enzymatic digestion of the ILM.[43] Considering these observations and the spectacular contrast in retinal delivery seen between a retina with and without the ILM in this chapter, it is obvious that the ILM is a crucial barrier for gene therapy. Surely, it functions as a sieve that defines the type and number of particles presented to the inner retinal cells.

The significant role of the vitreous and ILM as a barrier for drug delivery and the influence of vitreous removal on the integrity of both of them again highlights the necessity of the model presented in this chapter. Certainly, our bovine-derived VR explant could be highly valuable as a relevant set-up to assess if promising particles, showing favorable *in vitro* results, are competent in crossing the different hurdles connected to the VR interface. However, despite its value, some general remarks can be made. It should be noted that by isolating the vitreous along with the retina, the vitreous loses the natural support of the eyecup, causing a partial collapse of the vitreal collagen network.[44] While potential (unwanted) interactions of particles with the vitreal components will still be detected in our model, we refer the reader to other advanced models, such as the one developed by our research group, when exact diffusional rates of fluorescent particles in intact vitreous are to be determined.[26] Along the same line, the vitreous volume in which nanoparticles are injected in the vitreoretinal explant is significantly lower than in case of a clinical intravitreal injection. When evaluating therapeutic carriers applying our model it is

therefore important to estimate a dose that is as much as possible corrected for the diffusion that needs to take place prior to arrival of carriers at the retina. Secondly, while the VR explant greatly mimics the *in vivo* situation, certain dynamic processes present in the living eye are not taken into account such as clearance mechanisms, potential immune reactions, and the anterior-posterior flow present in the vitreous.[27]The currently available *ex vivo* system that most closely resembles the *in vivo* situation, is the perfused eye model (cfr. **Chapter 2**). In this approach, an entire eye is isolated, cannulated and perfused, keeping the eye globe perfectly intact.[45,46] This eye integrity is highly beneficial, although it comes with the disadvantage that these perfused eyes are only viable for a limited time (~ 9 hours). In contrast, our VR explant remains viable for at least 2 days, making it more suitable to evaluate retinal uptake of carriers after IVT injection. For long-term follow up of gene carriers, however, *in vivo* studies remain indispensable as for example retinal gene expression usually only reveals itself after 2 weeks.[14,47]

5. CONCLUSION

For future research we argue that further detailed characterization of the properties and composition of the vitreous and ILM across species could help to identify which models are the most suited for IVT drug delivery studies with the retina as main target. Thanks to the valuable research performed on especially developed large animal models we have the knowledge to smartly design vectors able of overcoming the vitreous as a barrier. In contrast, owing to the diversity of vectors studied on a variety of species the physicochemical requirements to efficiently cross the ILM is way less coherent. Well-designed systematic studies into which particle properties do result in successful retinal entry from the vitreous could therefore form a sound foundation for future design of 'the' optimal gene carrier administered by IVT injection. We are strongly convinced that advanced *ex vivo* models, such as the one presented in this chapter could have great significance in reaching this goal. Surely, our VR explant is currently the most representative *ex vivo* model on the market that is viable for a sufficiently long time to study carrier uptake. Moreover, our *ex vivo* approach is readily accessible, relatively cheap and transferrable to other large species like pig or human.

6. ACKNOWLEDGEMENTS

This work was funded by the Institute for the Promotion of Innovation through Science and Technology in Flanders, Belgium (IWT-Vlaanderen) and by an award granted by Funding for Research in Ophthalmology (FRO). We would like to thank the kind people of Flanders Meat Group in Zele who provided us with freshly enucleated cow eyes even on busy days.

7. REFERENCES

1. Bennett, J. Taking Stock of Retinal Gene Therapy: Looking Back and Moving Forward. *Mol. Ther.* **25,** 1076–1094 (2017).

2. Boye, S. E., Boye, S. L., Lewin, A. S. & Hauswirth, W. W. A comprehensive review of retinal gene therapy. *Mol. Ther.* **21,** 509–19 (2013).

3. Gauthier, R., Joly, S., Pernet, V., Lachapelle, P. & Di Polo, A. Brain-derived neurotrophic factor gene delivery to muller glia preserves structure and function of light-damaged photoreceptors. *Invest. Ophthalmol. Vis. Sci.* **46,** 3383–3392 (2005).

4. Busskamp, V., Picaud, S., Sahel, J. a & Roska, B. Optogenetic therapy for retinitis pigmentosa. *Gene Ther.* **19,** 169–175 (2012).

5. Englander, M., Chen, T. C., Paschalis, E. I., Miller, J. W. & Kim, I. K. Intravitreal injections at the Massachusetts Eye and Ear Infirmary: analysis of treatment indications and postinjection endophthalmitis rates. *Br. J. Ophthalmol.* **97,** 460–5 (2013).

6. Le Goff, M. M. & Bishop, P. N. Adult vitreous structure and postnatal changes. *Eye (Lond).* **22,** 1214–22 (2008).

7. Peeters, L. *et al.* Vitreous: A barrier to nonviral ocular gene therapy. *Investig. Ophthalmol. Vis. Sci.* **46,** 3553–3561 (2005).

8. Da Costa, R. *et al.* A novel method combining vitreous aspiration and intravitreal AAV2/8 injection results in retina-wide transduction in adult mice. *Investig. Ophthalmol. Vis. Sci.* **57,** 5326–5334 (2016).

9. Halfter, W., Dong, S., Dong, A., Eller, A. W. & Nischt, R. Origin and turnover of ECM proteins from the inner limiting membrane and vitreous body. *Eye (Lond).* **22,** 1207–1213 (2008).

10. Bu, S. C. *et al.* The ultrastructural localization of type II, IV, and VI collagens at the vitreoretinal interface. *PLoS One* **10,** 1–23 (2015).

11. Koo, H. *et al.* The movement of self-assembled amphiphilic polymeric nanoparticles in the vitreous and retina after intravitreal injection. *Biomaterials* **33,** 3485–3493 (2012).

12. Pitkänen, L., Pelkonen, J., Ruponen, M., Rönkkö, S. & Urtti, A. Neural retina limits the nonviral gene transfer to retinal pigment epithelium in an in vitro bovine eye model. *AAPS J.* **6,** article 25 (2004).

13. Gan, L. *et al.* Hyaluronan-modified core-shell liponanoparticles targeting CD44-positive retinal pigment epithelium cells via intravitreal injection. *Biomaterials* **34,** 5978–5987 (2013).

14. Mowat, F. M. *et al.* Tyrosine capsid-mutant AAV vectors for gene delivery to the canine retina from a subretinal or intravitreal approach. *Gene Ther.* **21,** 96–105 (2014).

15. Hellström, M. *et al.* Cellular tropism and transduction properties of seven adeno-associated viral vector serotypes in adult retina after intravitreal injection. *Gene Ther.* **16,** 521–532 (2009).

16. Boyd, R. F. *et al.* Photoreceptor-targeted gene delivery using intravitreally administered AAV vectors in dogs. *Gene Ther.* **23,** 223–230 (2016).

17. Takahashi, K. *et al.* Improved Intravitreal AAV-Mediated Inner Retinal Gene Transduction after Surgical Internal Limiting Membrane Peeling in Cynomolgus Monkeys. *Mol. Ther.* **25,** 296–302 (2017).

18. Trapani, I., Banfi, S., Simonelli, F., Surace, E. M. & Auricchio, A. Gene therapy of inherited retinal degenerations: prospects and challenges. *Hum. Gene Ther.* **26,** 193–200 (2015).

19. The Lasker/IRRF Initiative for Innovation in Vision Science. Restoring vision to the blind: Gene therapy for vision loss: the road ahead. *Transl. Vis. Sci. Technol.* **3,** 5 (2014).

20. Xu, Q. *et al.* Nanoparticle diffusion in, and microrheology of, the bovine vitreous ex vivo. *J. Control. Release* **167,** 76–84 (2013).

21. Henrich, P. B. *et al.* Nanoscale topographic and biomechanical studies of the human internal limiting membrane. *Invest. Ophthalmol. Vis. Sci.* **53,** 2561–2570 (2012).

22. Halfter, W. *et al.* New concepts in basement membrane biology. *FEBS J.* **282,** 4466–4479 (2015).

23. Fradot, M. *et al.* Gene Therapy in Ophthalmology: Validation on Cultured Retinal Cells and Explants from Postmortem Human Eyes. *Hum. Gene Ther.* **22,** 587–593 (2011).

24. Kobuch, K. *et al.* Maintenance of adult porcine retina and retinal pigment epithelium in perfusion culture: Characterisation of an organotypic in vitro model. *Exp. Eye Res.* **86,** 661–668 (2008).

25. Uckermann, O. *et al.* Selective Staining by Vital Dyes of Müller Glial Cells in Retinal Wholemounts. *Glia* **45,** 59–66 (2004).

26. Martens, T. F. *et al.* Measuring the intravitreal mobility of nanomedicines with single-particle tracking microscopy. *Nanomedicine* **8,** 1955–1968 (2013).

27. Xu, J., Heys, J. J., Barocas, V. H. & Randolph, T. W. Permeability and diffusion in vitreous humor: implications for drug delivery. *Pharm. Res.* **17,** 664–669 (2000).

28. Käsdorf, B. T., Arends, F. & Lieleg, O. Diffusion Regulation in the Vitreous Humor. *Biophys. J.* **109,** 2171–2181 (2015).

29. Russell, S. R. What We Know (and Do Not Know) About Vitreoretinal Adhesion. *Retina* **32,** S181–S186 (2012).

30. Ochakovski, G. A., Bartz-Schmidt, K. U. & Fischer, M. D. Retinal Gene Therapy: Surgical Vector Delivery in the Translation to Clinical Trials. *Front. Neurosci.* **11,** 1–7 (2017).

31. Lebrun-Julien, F. *et al.* Excitotoxic Death of Retinal Neurons In Vivo Occurs via a Non-Cell-Autonomous Mechanism. *J. Neurosci.* **29,** 5536–5545 (2009).

32. Skeie, J. M. & Mahajan, V. B. Proteomic interactions in the mouse vitreous-retina complex. *PLoS One* **8,** 1–14 (2013).

33. Russell, W. M. S. & Burch, R. L. The principles of humane experimental technique. *Princ. Hum. Exp. Tech.* (1959).

34. Kim, H., Robinson, S. B. & Csaky, K. G. Investigating the movement of intravitreal human serum albumin nanoparticles in the vitreous and retina. *Pharm. Res.* **26,** 329–337 (2009).

35. Bejjani, R. A. *et al.* Nanoparticles for gene delivery to retinal pigment epithelial cells. *Mol*

Vis **11,** 124–132 (2005).

36. Sakurai, E., Ozeki, H., Kunou, N. & Ogura, Y. Effect of particle size of polymeric nanospheres on intravitreal kinetics. *Ophthalmic Res.* **33,** 31–6 (2001).

37. Martens, T. F. *et al.* Coating nanocarriers with hyaluronic acid facilitates intravitreal drug delivery for retinal gene therapy. *J. Control. Release* **202,** 83–92 (2015).

38. Candiello, J., Cole, G. J. & Halfter, W. Age-dependent changes in the structure, composition and biophysical properties of a human basement membrane. *Matrix Biol.* **29,** 402–410 (2010).

39. Bourges, J. L. *et al.* Ocular drug delivery targeting the retina and retinal pigment epithelium using polylactide nanoparticles. *Investig. Ophthalmol. Vis. Sci.* **44,** 3562–3569 (2003).

40. Apaolaza, P. S. *et al.* Structural recovery of the retina in a retinoschisin-deficient mouse after gene replacement therapy by solid lipid nanoparticles. *Biomaterials* **90,** 40–49 (2016).

41. Martens, T. F. *et al.* Measuring the intravitreal mobility of nanomedicines with single-particle tracking microscopy. *Nanomedicine (Lond)* **8,** 1955–1968 (2013).

42. Pitkänen, L., Ruponen, M., Nieminen, J. & Urtti, A. Vitreous is a barrier in nonviral gene transfer by cationic lipids and polymers. *Pharm. Res.* **20,** 576–583 (2003).

43. Dalkara, D. *et al.* Inner limiting membrane barriers to AAV-mediated retinal transduction from the vitreous. *Mol. Ther.* **17,** 2096–102 (2009).

44. Nickerson, C. S., Park, J., Kornfield, J. A. & Karageozian, H. Rheological properties of the vitreous and the role of hyaluronic acid. *J. Biomech.* **41,** 1840–1846 (2008).

45. Mains, J., Tan, L. E., Wilson, C. & Urquhart, A. A pharmacokinetic study of a combination of beta adrenoreceptor antagonists - In the isolated perfused ovine eye. *Eur. J. Pharm. Biopharm.* **80,** 393–401 (2012).

46. Mains, J., Wilson, C. G. & Urquhart, A. ToF-SIMS analysis of dexamethasone distribution in the isolated perfused eye. *Investig. Ophthalmol. Vis. Sci.* **52,** 8413–8419 (2011).

47. Wassmer, S. J., Carvalho, L. S., György, B., Vandenberghe, L. H. & Maguire, C. A. Exosome-associated AAV2 vector mediates robust gene delivery into the murine retina upon intravitreal injection. *Sci. Rep.* **7,** 45329 (2017).

4

Influence of pathogenic stimuli on Müller cell transfection by lipoplexes

This chapter contains unpublished data:

Karen Peynshaert[a,b], Joke Devoldere[a,b] , Stefaan De Smedt[a,b], Katrien Remaut[a,b]

[a]Lab of General Biochemistry and Physical Pharmacy, Faculty of Pharmaceutical Sciences, Ghent University, Ottergemsesteenweg 460, 9000 Ghent, Belgium. [b]Ghent Research Group on Nanomedicines, Ghent University, Ottergemsesteenweg 460, 9000 Ghent, Belgium.

ABSTRACT

Neuroprotection is a mutation-independent therapeutic strategy that seeks to enhance the survival of neuronal cell types through delivery of neuroprotective factors. The Müller cell, a glial cell type appreciated for its unique morphology and neuroprotective functions, could be regarded as an ideal target for this strategy by functioning as a secretion platform within the retina following uptake of a transgene of our choice. In this *in vitro* study we aimed to investigate the capability of Müller cells to take up a standard liposomal vector (i.e. lipofectamine 2000) and process its pDNA or mRNA cargo into GFP protein. By doing so, we found that mRNA lipoplexes outperformed pDNA lipoplexes in Müller cell transfection. We furthermore explored the Müller cell's performance in stressful circumstances by examining lipoplex-induced transfection efficiency and cytotoxicity in hypoxic, hyperglycemic and oxidatively stressed cells – conditions linked to diabetic retinopathy and glaucoma. None of the stress factors substantially altered GFP expression in Müller cells. Interestingly, hyperglycemia seemed to have a protective effect against lipoplex-induced toxicity while hypoxia and oxidative stress led to a slightly higher toxicity. In conclusion, our study indicates that mRNA-lipoplexes have potential in transfecting Müller cells in healthy as well as diseased conditions.

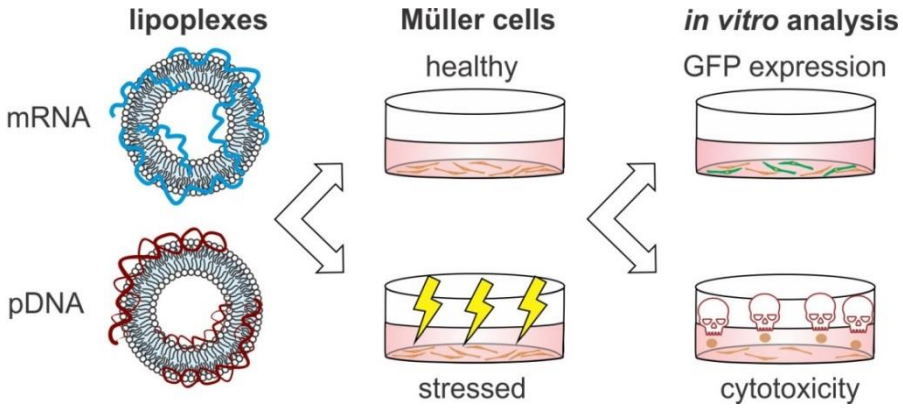

Table of contents

1. INTRODUCTION

As mentioned in **Chapter 1**, Müller cells are a dominant glial cell type in the retina and provide support to their surrounding neurons through a myriad of functions. On top of this natural neuroprotective behavior, Müller cells also exhibit several beneficial properties which render them ideal targets for gene transfer. Indeed, their exceptional radial morphology allows them to interact with each neuronal cell type while their endfeet, which abut in the ILM, make the Müller cell a reachable target via IVT injection. In contrast to neurons and photoreceptors (PRs), Müller cells are furthermore remarkably resistant to stress allowing them to survive in advanced stages of retinal diseases.[1,2] Based on these advantageous characteristics, we, and others, believe that the Müller cell could play a prominent role in ocular neuroprotection by performing as a secretion platform within the retina (cfr. **Chapter 1**).[1,3,4] In this strategy, illustrated in **Figure 4.1**, gene vectors carrying genes encoding for neuroprotective factors are delivered to Müller cells after which they secrete the factors into their surroundings, thus enhancing neuron survival.

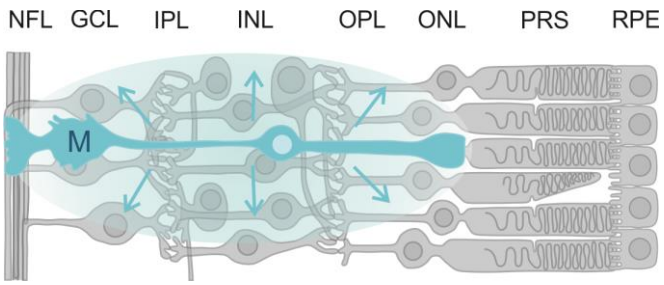

Figure 4.1 | The Müller cell as a secretion platform for neurotrophic factors. M: Müller cell; NFL: nerve fiber layer; GCL: ganglion cell layer; IPL: inner plexiform layer; INL: inner nuclear layer; OPL: outer plexiform layer; ONL: outer nuclear layer; PRS: photoreceptors.

This concept was already explored in the 90's by Di Polo *et al*. who applied IVT injected viral vectors carrying a transgene of brain-derived neurotrophic factor (BDNF) to Müller cells in axotomized rats. More importantly, the expression of BDNF that followed led to the prolonged survival of the injured retinal ganglion cells (RGCs).[5] Several research groups performed similar studies with viral vectors, resulting in extended survival of RGCs in glaucoma animal models by expression of ciliary neurotrophic factor (CNTF),[6,7] as well as delay of retinal degeneration in retinitis pigmentosa by glial cell-derived neurotrophic factor (GDNF) expression.[1] Although all these successes were achieved with viral vectors, the high production cost and associated safety issues connected to viruses still remain a concern. Consequently, there has been a growing interest toward nanoparticle-based technology (NPs) for retinal gene therapy partly due to their high payload, easy surface modification and relatively straightforward scale-up (cfr. **Chapter 1**).[8] Among non-viral particles, the most extensively researched particle is undoubtedly the liposome.[8–11] Lipid mixtures, usually containing cationic and neutral lipids, can bind negatively

charged nucleic acids (NAs), forming lipid-NA complexes called lipoplexes (**Figure 4.2**). The packaging of NAs in these lipoplexes substantially enhances transfection efficiency by protecting the NAs from degradation and enhancing cellular uptake and endosomal escape due to their interaction with the cellular and endosomal membranes, resulting in efficient NA cargo release into the cytosol.[8,12] The liposomal transfection agent applied in our study is Lipofectamine 2000 (LF2000), a universally applied commercial carrier in *in vitro* studies.

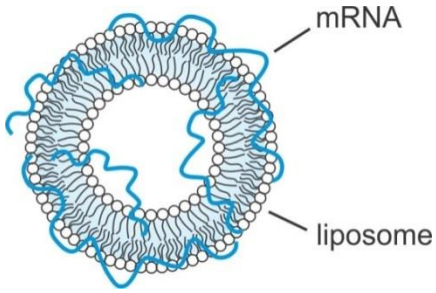

Figure 4.2 | Schematic drawing of a mRNA-loaded lipoplex.

In this study we have focused on pDNA as well as mRNA as therapeutic genes. The use of pDNA is well-established in the field of retinal gene therapy due to its stability and long-term expression. Surely, nearly all reports on non-viral transfection in retinal cells are based on plasmid DNA.[13] Exploring mRNA as therapeutic gene therefore might seem as an unconventional choice. The predominant disadvantage of applying mRNA is evidently its transient expression which renders mRNA useful for only a few specific applications. However, its stability and immunogenicity can be positively tuned by the incorporation of naturally occurring modified nucleosides.[14] This enhanced stability and reduced immunogenicity can both result in a prolonged expression of the mRNA - as confirmed by our group (data not shown). In context of retinal disease, mRNA might have an important advantage over the commonly applied pDNA: it exerts its function in the cytosol which implies that, in contrast to pDNA, transfection efficiency is not dependent on cell division. This is a relevant asset when targeting the adult retina since many retinal cell types, including the Müller cells, are post-mitotic.

Neuroprotection has been proposed as a treatment strategy for glaucoma and diabetic retinopathy, two leading causes of vision loss which we briefly discussed in **Chapter 1**.[15–20] We therefore wished to explore the influence of stress factors associated with these retinopathies on Müller cell transfection. We selected three pathological conditions that are easily simulated *in vitro*. As a first stress factor we have selected oxidative stress since this anomaly has been detected in several experimental (animal) models of glaucoma as well as diabetic retinopathy.[21–23] We further selected hyperglycemia since this is the fundamental cause of diabetic retinopathy

and elevated glucose levels are known to engender a variety of metabolic abnormalities and oxidative stress.[23] Finally, we chose hypoxia as a stress factor since diabetic retinopathy is correlated with decreased retinal blood flow [24] and hypoxic tissue has also been detected in glaucomatous eyes.[25,26]

Taken together, in this preliminary study we explored the readiness of Müller cells to take up lipoplexes and process their NA cargo into proteins. We furthermore sought to compare the expression profiles of mRNA and pDNA in healthy Müller cells and assess the therapeutic potential of mRNA. Finally, we examined if pathogenic stimuli, as present in diseased retinal tissue, could influence the transfection efficiency and/or toxicity induced by lipoplexes *in vitro*.

2. METHODS

Cell culture

Immortalized human Müller cells (MIO-M1) were a kind gift from Astrid Limb (Institute of Ophthalmology, University College London, London U.K.).[27] The MIO-M1 cells were cultured using DMEM GlutaMAX™ with low glucose (Gibco®, Paisly, UK) supplemented with 10% fetal bovine serum (Hyclone®, Cramilton, UK), 1% L-glutamine (Gibco®, Paisly, UK) and 2% penicillin – streptomycine solution (Gibco®, Paisly, UK). Cells were passaged at 80% confluency and incubated at 37°C with 5.0% CO_2.

Plasmid purification and mRNA synthesis

gWIZ GFP (Promega, Leiden, The Netherlands) was amplified in transformed E. Coli bacteria and isolated from this bacteria suspension using a Qiafilter Plasmid Giga Kit (Qiagen, Venlo, The Netherlands). pDNA concentration was determined on a NanoDrop 2000c (Thermo Fisher Scientific, Rockford, IL, USA) and adjusted to a final concentration of 1 µg/µl with HEPES buffer (20 mM, pH 7.2). GFP mRNA was produced by in vitro transcription from gWIZ GFP plasmids. The plasmids were purified using a QIAquick PCR purification kit (Qiagen, Venlo, The Netherlands) and linearized using SpeI restriction enzymes (Promega, Leiden, The Netherlands). Linearized plasmids were used as templates for the in vitro transcription reaction using the T7 mMessage mMachine kit (Ambion, Life Technologies, Ghent, Belgium). The resulting capped mRNAs were purified using a RNeasy Mini kit (Qiagen, Venlo, The Netherlands). The mRNA concentration was determined on a NanoDrop 2000c and adjusted to a concentration of 1 µg/µl as done for pDNA.

Lipoplex preparation

The lipoplexes were prepared according to the manufacturer's protocol applying a ratio of 1:3 (µg pDNA/mRNA to µL reagent). Briefly, the transfection agent Lipofectamine™2000 (Invitrogen) was diluted in OptiMEM and was left to incubate for 10 minutes at room temperature. The pDNA or mRNA (stock 1µg/µL) was prepared by diluting it in OptiMEM after which it was added in an equal volume to the diluted transfection reagent. After a 5 min incubation allowing for complexation of the NAs with Lipofectamine, the lipoplexes were ready for use.

Lipoplex characterization

The hydrodynamic size and zeta potential of the lipoplexes were determined using a Malvern Zetasizer Nano (Malvern Instruments, Worcestershire, U.K.). For this purpose the lipoplexes were diluted in HEPES buffer prior to performing the measurements at 25 °C. Size measurements were done in triplicate with three runs per replicate and presented based on the number distribution. The zeta potentials were calculated from the electrophoretic mobility based on the Henry equation considering the Smoluchowski approximation. Zeta potential measurements were done in triplicate with two runs per replicate.

Nanoparticle incubation

Müller cells were seeded in a 24 well plate at a cell density of 10.000 cells per well applying 500 µl of medium per well. After 5 days of culture, 100 µl of the lipoplexes, prepared using the standard protocol in OptiMEM, was added to the cells and allowed to incubate for 24 hours at 37°C.

Stress incubation

Müller cells were exposed to stress factors for 48 hours in total: 24 hours prior to lipoplex incubation and during the 24 h lipoplex incubation. To induce oxidative stress, cells were exposed to 75 µM Tert-butyl hydroxyperoxide (TBHP, 458139**,** Sigma-Aldrich, USA). To mimic hypoxia, the cell-containing well plates were placed in an incubator with 2% O_2 (instead of 21%) at 37°C and 5% CO_2. To generate hyperglycemia, glucose (G8644**,** Sigma-Aldrich, USA) was added to the cell culture medium to reach a final concentration of 25mM. Note that basic Müller cell culture medium (DMEM GlutaMAX™) already contains 5 mM of glucose.

Flow cytometry

All flow cytometry experiments were performed on 24 well plates. After stress and/or lipoplex treatment, cell culture medium was removed and cells were washed once with 500 µl PBS. Next, the cells were detached by applying 300 µl of 0.25% Trypsin-EDTA (Gibco®, Paisly, UK) after which the trypsin was neutralized by adding 500 µl of cell culture medium. This cell suspension was transferred to FACS tubes followed by a centrifugation step of 5 min at 300g. Then, the

supernatant was removed and the cells were re-suspended in FACS buffer (1% FBS, 0.1% sodium azide in PBS-). After performing this wash cycle twice, the cells were re-suspended in 300 µl FACS buffer and measured with a CytoFLEX™ (Beckman Coulter, Nederland). Data analysis was done with Flowjo software (Tree Star Inc.).

MTT cell viability

Müller cells were seeded in a 24 well plate at a cell density of 10.000 cells per well and cultured for 5 days. After stress and/or NP treatment the medium was removed and the cells were washed once with PBS (Gibco®, Paisly, UK). Next, fresh cell culture medium containing 5 mg/ml of MTT reagent (Sigma-Aldrich, USA) was added to the cells and incubated for 3 h at 37°C. After this incubation step, the medium was carefully removed and the formazan crystals were dissolved by incubation with 100% DMSO on a shaker for 1 h at room temperature. Finally, the absorbance was measured at 590 nm and 690 (background) with an Envision plate reader (Perkin Elmer, Zaventem, Belgium). The percentage of viability was then calculated by comparison with untreated cells representing 100% viability.

Statistical analysis

All experiments were analyzed for statistical significance with a one or two-way ANOVA followed by the Bonferroni post hoc test to estimate significance between treated groups, or followed by the Dunnett post hoc test when compared to an untreated group. The results were considered as statistically significant if $p < 0.05$. The number of asterisks in the figures indicate the statistical significance as follows: *p<0.05; **p<0.01; ***p<0.001. All statistical analysis was performed with Graphpad Prism 5 software (San Diego, CA). Values are reported as the mean with Standard Error (SEM).

3. RESULTS

Nanoparticle characterization

Figure 4.3 shows that pDNA and mRNA complexes had a similar size in HEPES buffer i.e. ~600 nm. Their zeta potential, a measure for their surface charge, were both negative though differed significantly: pDNA lipoplexes had a zeta potential of around -10 mV while their mRNA counterparts exhibited a zeta potential of – 25 mV. This overall negative charge could be explained by the fact that the positively charged LF is neutralized by its complexation with the negatively charged NAs. Despite the significant difference in charge between both lipoplexes, their uptake was similar in MIO-M1 cells (data not shown).

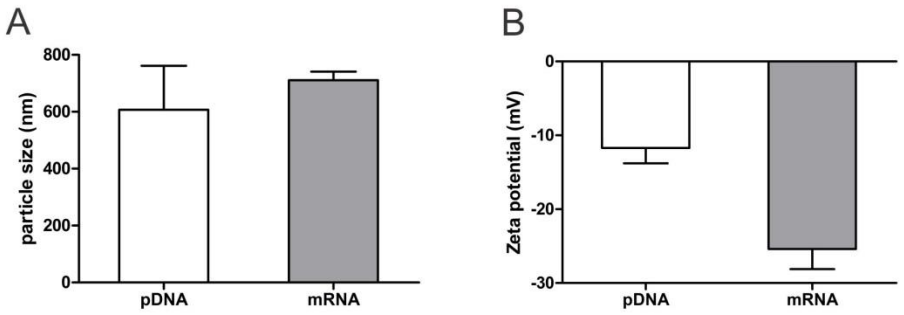

Figure 4.3 | Characterization of lipofectamine 2000 – NA complexes by dynamic light scattering. A) size B) zeta-potential. Error bars represent the SEM (n ≥ 3).

Transfection of healthy Müller cells by mRNA and pDNA-lipoplexes

To explore the potential difference in gene expression profile generated by pDNA and mRNA we exposed Müller cells to a dose range of NA-loaded lipoplexes from 0.2 to 1 µg for 24 hours. As shown in **Figure 4.4A**, the transfection efficiency with NPs containing mRNA was remarkably higher than for pDNA, with transfection maxima of 81 (± 3%) and 21 (±1 %) respectively. While a dose-dependent increase in transfection efficiency is apparent for pDNA between 0.2 µg to 0.4 µg, the transfection potential of mRNA did not augment significantly after 0.2 µg. Furthermore, while a seemingly downward trend is visually observed at highest dosages for pDNA, this effect is not significant.

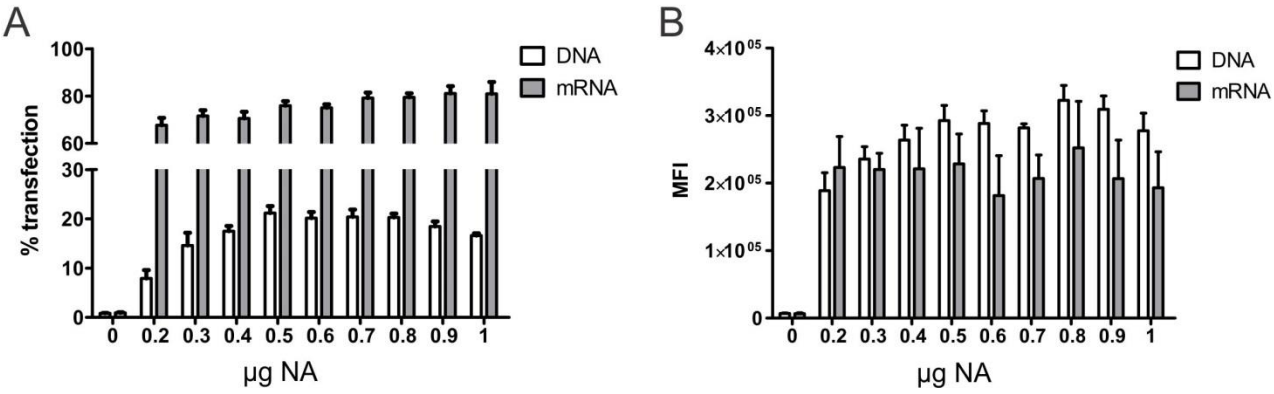

Figure 4.4 | Transfection of healthy Müller cells by mRNA and pDNA lipoplexes. A) Transfection efficiency B) mean fluorescence intensity (MFI). Error bars represent the SEM (n≥5).

Interestingly, despite the great contrast in transfection efficiency between the two types of NA, the mean fluorescence intensity (MFI) of the cell populations are situated in the same range for all dosages for both NAs (**Figure 4.4B**). Similar to the trend observed in transfection efficiency,

pDNA does elicit a significant dose-dependent increase in MFI between 0.2 and 0.5 µg while no significant changes in MFI are observed with mRNA for dosages higher than 0.2 µg.

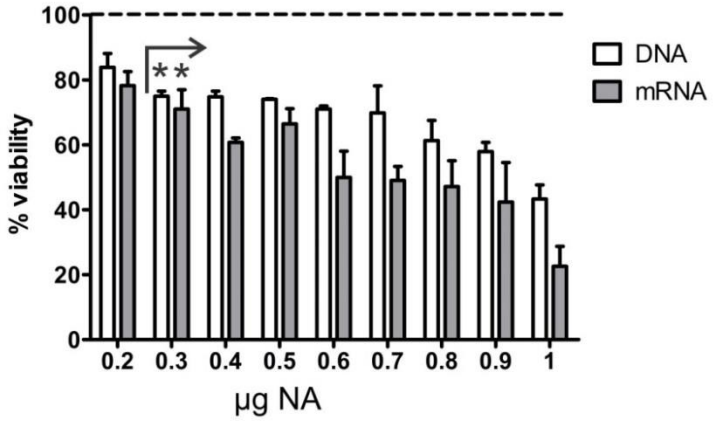

Figure 4.5 | Müller cell viability following transfection with DNA or mRNA lipoplexes. Both NPs induce significant cytotoxicity starting from a dose of 0.3 µg. Error bars represent the SEM (n≥3).

Exposure of cells to NPs more than often leads to cellular stress and/or toxicity (cfr. **Chapter 5**).[28] To investigate the possible toxic effect of the lipoplexes on the Müller cells we have performed an MTT viability assay after 24 hour exposure to the NPs. As shown in **Figure 4.5**, both particles elicit a dose-dependent reduction in cell viability with significant toxicity initiating from a dose of 0.3 µg (± 30% cell death). However, no significant contrast between pDNA and mRNA was detected at any dose. We can conclude that pDNA lipoplexes are less efficient but equally toxic transfection agents compared to mRNA lipoplexes. In light of this, we further investigated the influence of stress on Müller cell transfection with the most promising transfection agent, i.e. the mRNA lipoplexes.

Transfection of stressed Müller cells by mRNA lipoplexes

To investigate the influence of retinal disease on the lipoplex-induced transfection efficiency and cytotoxicity of Müller cells we exposed MIO-M1 cells to noxious stimuli *in vitro*. Oxidative stress was represented by incubation with TBHP, an organic peroxide that is frequently applied in cell culture studies. It causes oxidative stress by its decomposition in unstable alkoxyl and peroxyl radicals which next react with cellular components.[29] To simulate diabetic retinopathy we exposed the cells to 25 mM of glucose, a concentration established in literature.[30–32] Finally, cells were exposed to 2% of O_2 instead of 21 % to imitate hypoxia. For all stress factors, cells were exposed to the stress for 24 hours prior to performing a 24 hour incubation with lipoplexes under stress conditions. This implies that the Müller cells were exposed to the noxious stimuli for 48 hours before the assay readout. To look into the potential cytotoxicity induced by the stress

factors itself we have assessed cell viability with the MTT assay after 48 hour exposure to each stress factor separately. As shown in **Figure 4.6A**, 48 hour exposure to hyperglycemia provoked a small but insignificant increase in cell viability. Hypoxia did not result in any toxicity, while 75 µM TBHP elicited a drop in cell viability to 67% (± 4).

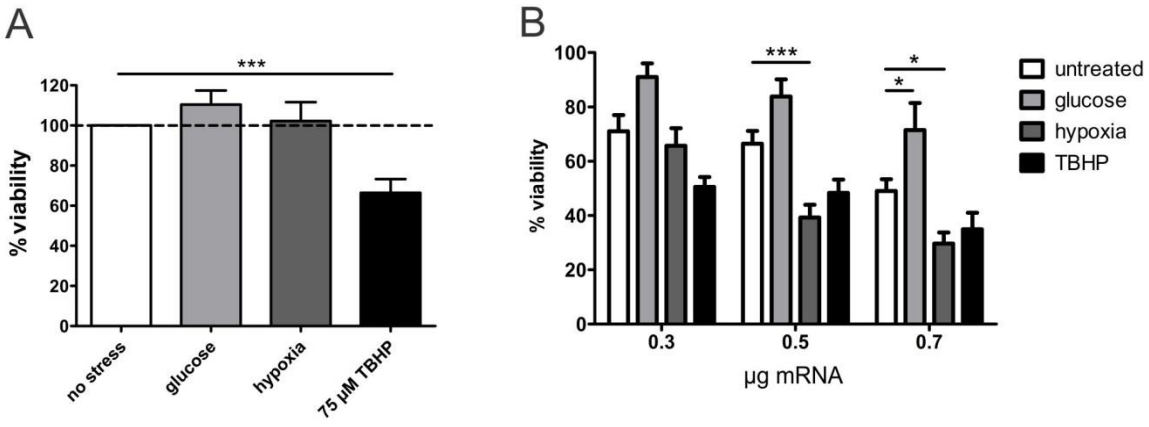

Figure 4.6 | Müller cell viability after exposure to stress factors as measured by the MTT assay. A) Viability after 48 h exposure to noxious stimuli alone. B) Viability following transfection with mRNA in stressed cells. Error bars represent the SEM (n≥3).

Also the combined toxicity of the mRNA lipoplexes and the stressful environment was assessed (**Figure 4.6B**). Interestingly, the viability of cells incubated with lipoplexes increased when combined with hyperglycemia. At a dose of 0.7 µg cell viability even augmented from 49% (± 4) to 71% (± 10) without and with hyperglycemia. Compared to hyperglycemia, hypoxia had the opposite effect: viability of NP treated cells was significantly reduced upon exposure to a hypoxic environment, from 65 % (±5) to 40% (±5) and from 49% (±4) to 30% (±4) for a dose of 0.5 and 0.7 µg, respectively. Treatment with TBHP, leading to moderate toxicity in untreated cells, did not significantly affect NP-mediated cytotoxicity.

To look into the efficacy of lipoplexes to transfect stressed Müller cells we selected three dosages (0.3; 0.5; 0.7 µg) to identify possible dose-dependent trends. 0.7 µg was chosen as the highest dose since this elicited a 50 % reduction in cell viability in healthy conditions. **Figure 4.7** presents the percentage of transfected Müller cells as well as their MFI in healthy and stressed conditions. Though not significant, hypoxia seems to lead to a reduction in transfection efficiency as well as MFI. Furthermore, hyperglycemic conditions and oxidative stress do not significantly alter transfection efficiency nor the GFP expression per cell.

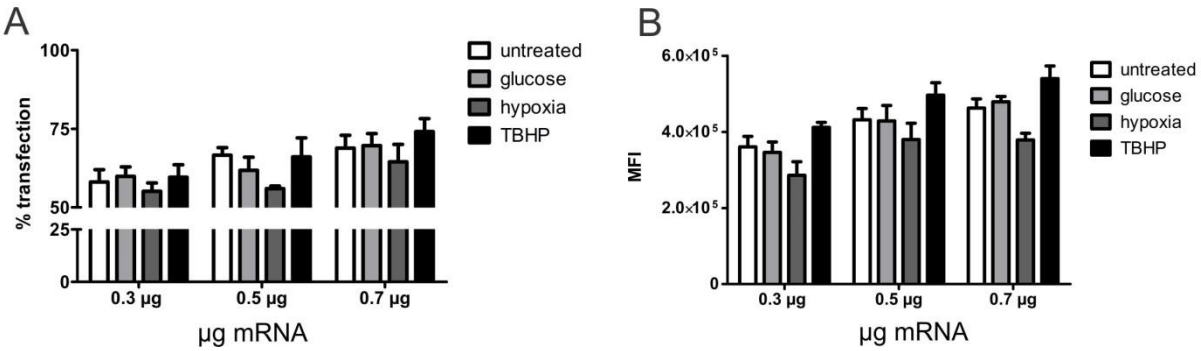

Figure 4.7 | Transfection in Müller cells exposed to pathogenic stimuli. A) transfection efficiency B) MFI. Error bars represent the SEM (n≥3).

4. DISCUSSION

In this preliminary study we aimed to get an impression on NP-induced gene expression in *in vitro* cultured Müller cells. To this end we applied the most straightforward set-up: a commercial lipid carrier (LF2000) loaded with GFP-encoding NAs in an easy-to-culture Müller cell line. This was a purposeful choice since, rather than looking for an ideal drug delivery carrier, we sought to examine general trends in Müller cell behavior toward NPs and/or stress.

Comparison of Müller cell transfection and cytoxicity induced by mRNA and pDNA lipoplexes

Characterization of the lipoplexes showed that mRNA and pDNA particles have a similar size which is rather large for a liposomal carrier, i.e. ~600 nm. Despite this similar size their zeta potential did differ, although both types of lipoplexes were clearly negatively charged (**Figure 4.3**). Still, both lipoplexes were taken up at similar levels in Müller cells (data not shown).

This comparable uptake did not result in similar levels of transfection efficiency. In contrast, mRNA-containing lipoplexes led to a 4 fold higher transfection efficiency in comparison to pDNA particles (**Figure 4.4A**). This great discrepancy is undoubtedly partly attributed to the basic difference in working mechanism and site of action between mRNA and pDNA: while pDNA requires transfer into the nucleus and transcription into mRNA, the GFP-encoding mRNA can be instantly translated into protein in the cytosol. Considering pDNA needs cell division to cross the nuclear envelope, it is likely that the rather slow division of MIO-M1 cells adds to the low transfection efficiency after 24 hours. Longer incubation times (≥ 48 hours) might therefore lead to a higher percentage of transfected cells. Nevertheless, it should be noted that the Müller cells in the adult retina are usually in a post-mitotic state which does not play in favor of pDNA. Once transfected the degree of expression per cell (MFI) was found to be similar for mRNA and pDNA. Overall, mRNA therefore achieves a more beneficial expression profile since the MFI is as high as

for pDNA though the number of GFP-expressing cells is substantially higher. Notably, we did not look into the duration of expression which is expected to be longer for pDNA.

Next to efficacy, toxicity is an important parameter to consider when evaluating the potential of nanocarriers. To estimate particle-induced acute cytotoxicity we made use of the widely applied MTT assay. This assay revealed a rise in cytotoxicity with increasing dose for both lipoplexes (**Figure 4.5**). Based on the literature we expect this toxicity to be mainly attributed to the growing amount of lipid carrier rather than the nucleic acid fraction. Indeed, while liposomal carriers are often presented as relatively safe,[11,33] several studies report on *in vitro* and *in vivo* toxicity induced by liposomes fabricated with cationic lipids.[34,35] No significant difference in cell viability was detected between mRNA and pDNA-based lipoplexes. This observation is in line with our hypothesis that toxicity is caused by the lipid fraction, since the amount of lipid applied to the cells is exactly the same for both lipoplex formulations. When taking both protein expression and toxicity into account, we can conclude that mRNA is the preferred NA for transfection of Müller cells since low dosages of mRNA lipoplexes produced high transfection efficiency with limited cytotoxicity.

Influence of noxious stimuli on transfection efficiency and toxicity of mRNA-lipoplexes

As a next step we performed the very same experiments evaluating lipoplex-induced transfection efficacy and toxicity yet under influence of hyperglycemia, hypoxia and oxidative stress.

Hyperglycemia

Hyperglycemia was generated by culture of Müller cells in medium containing 25 mM of glucose. In cells exposed to hyperglycemia for 48 hours, a slight increase in cell viability was observed though this effect was not significant (**Figure 4.6A**). Interestingly, cell viability was also higher for all lipoplex dosages in glucose-treated cells compared to untreated ones, yet the difference in viability was only significant for the highest lipoplex dose (**Figure 4.6B**). It therefore seems that hyperglycemic conditions boost the survival of Müller cells exposed to lipoplexes and thus have a protective effect. Enhanced Müller cell viability under influence of elevated glucose levels *in vitro* has been noticed before by Vellanki *et al*. They hypothesize that hyperglycemia provokes augmented entry of calcium in Müller cells which next stimulates cell proliferation.[32] In addition, studies in different cell types have shown that also other pathways can enhance cell proliferation as a response to hyperglycemia.[36] It indeed seems logical that an increase in nutrient availability can stimulate the metabolism and simultaneously the proliferation of cells. Following this hypothesis an increase in the number of transfected cells could be expected, though this was not

detected. Notably, it is well-established that the diabetic retina is characterized by Müller cell gliosis which usually involves Müller proliferation.[37,38] It is important to recognize that while these *in vitro* results indicate that hyperglycemia is beneficial, Müller cell gliosis and enhanced proliferation is *in vivo* accompanied by many Müller cell alterations of which some can have a harmful effect on the retina.[38,39] Hyperglycemia did not influence transgene expression since the number of GFP transfected cells and the MFI of the transfected cells was comparable to cells in normoglycemia (**Figure 4.7**). We can conclude that hyperglycemia influences Müller cell survival, yet does not affect the cell's ability to take up and process foreign mRNA.

Hypoxia

Exposure of Müller cells to hypoxia for 48 hours did not cause any cytotoxicity compared to cells cultured in normoxic conditions (**Figure 4.6A**). The same observation was made by Zhang et al. who did not detect significant apoptosis in hypoxic rat primary Müller cells.[40] On the other hand, we should note that a hypoxic gaseous environment of 2% does not guarantee similar low oxygen levels will be reached in the cell culture medium.[40a] It is therefore possible that the cells did not experience hypoxia which could account for the lack of cytotoxicity we have observed. Still, based on the fact that the energy metabolism of Müller cells is largely based on glycolysis rather than the highly oxygen-dependent process of respiration, we did not expect hypoxia-induced cytotoxicity.[41] It is furthermore well-established that hypoxia can trigger the autophagy pathway,[42] as observed in multiple retinal cell types such as retinal ganglion cells,[43] PRs [44] and Müller cells.[45] As will be explained in **Chapter 5**, autophagy is a cytoprotective pathway meant to enhance cell survival, and is activated upon exposure to a wide range of stress factors, including hypoxia.[46,47] The lack of Müller cell death in response to hypoxia might therefore be due to the naturally adapted energy metabolism of the Müller cell in combination with its ability to upregulate autophagy when needed. However, for higher dosages (≥ 0.5 µg) the combined treatment of hypoxia and lipoplexes did lead to significant toxicity (**Figure 4.6B**). More importantly, the drop in cell viability was more substantial compared to lipoplex treatment alone. This observation was rather unanticipated considering the lack of cytotoxicity observed in hypoxic Müller cells. Yet, while the Müller cell can compensate for the hypoxia-induced stress, the addition of NP-elicited stress clearly exceeds the Müller cell's ability to adapt, ultimately resulting in cell death. We therefore assume that the basic metabolism of the Müller cell is not highly oxygen-dependent, yet the coping mechanisms it upregulates to endure the lipoplexes, likely is. The Müller cell death following co-treatment might be mediated by autophagy and/or by apoptosis. The latter is a cell death pathway that is activated by hypoxia,[48] as well as by our lipoplexes at doses above 0.7 µg (data not shown). This implies that, while autophagy could

prevent cell death in hypoxic cells, the combined treatment with lipoplexes might allow apoptosis to take the upper hand. Müller cells might also die from overactivation of the autophagy pathway. Indeed, next to hypoxia, Lipofectamine 2000 as well as liposomes have been reported to induce genuine autophagy.[49,50] As discussed in **Chapter 5**, this overactivation might lead to excessive self-digestion eventually resulting in the observed cytotoxicity. Finally, there is a highly complex interplay between autophagy and apoptosis where both processes directly and/or indirectly influence each other (cfr. **Chapter 5**).[48,51] It is therefore likely that both pathways play a role in the cell death observed by co-treatment of lipoplexes and hypoxia. When examining the data on transfection efficiency and level of gene expression (MFI) we can distinguish a clear but insignificant trend: for each dose tested, the transfection efficiency and MFI is slightly lower for hypoxia-treated cells than for cells kept in normoxia (**Figure 4.7**). Since liposomes are known to enter the cell via endocytosis, an active uptake process, this trend could be due to decreased uptake of the lipoplexes in hypoxic conditions.[52,53] On the other hand, lipoplex uptake could be similar in both conditions but the translation of mRNA into the GFP protein might be affected by oxygen deprivation as stated by Andreev *et al*.[54] Nevertheless, repetition of this data as well as further studies (e.g. cellular uptake) are necessary to define a conclusive trend and identify its underlying causes. Overall, we can summarize that hypoxia intensifies lipoplex-induced cytotoxicity but does not greatly affect the efficacy of the lipoplexes.

Tert-butylhydroperoxide

A 48 hour incubation with 75 µM of TBHP evoked significant Müller cell death (**Figure 4.6A**). Ostensibly this does not seem to correlate well with other reports in the field, since exposure to the peroxide H_2O_2 did not affect MIO-M1 cells,[55] and only elicited very limited apoptosis in rat primary Müller cells.[40] In fact, we also applied H_2O_2 as an inducer of oxidative stress during our initial experiments and did not observe any cytotoxicity even at concentrations above 1500 µM (data not shown). We therefore decided to continue our studies with TBHP based on the following facts: 1) H_2O_2 is rapidly degraded and is eliminated from cell culture medium within the hour at concentrations around 100 µM,[56] and 2) in contrast to H_2O_2, TBHP was found to evoke consistent cellular stress and was thus proposed as a more suited compound for studies investigating oxidative stress.[29] It is well-established that generation of ROS and the associated oxidative stress can cause cellular damage on multiple levels including e.g. lipid peroxidation and DNA damage (cfr. **Chapter 5**).[29] Consequently, the TBHP-induced cytotoxicity in Müller cells observed in our experiment is in line with these findings. Co-treatment of TBHP and lipoplexes did provoke more cytotoxicity than lipoplex treatment alone for all dosages tested, although the effect was never significant (**Figure 4.6B**). Seeing the separate treatments each evoked

substantial cell death we did anticipate the combined treatment to be even more harmful. It could therefore be valuable to repeat this experiment to allow us to conclude a definite trend. In spite of the extensive stress and accompanying cytotoxicity elicited by co-treatment of lipoplexes and TBHP, the transfection efficiency and MFI in TBHP-treated cells was similar compared to untreated cells (**Figure 4.7**). This is a hopeful outcome for our neuroprotective strategy since it seems that regardless of cellular toxicity, the surviving cells are able of maintaining a high rate of transgene expression.

5. CONCLUSION

The principal goal of this study was to explore the potential of mRNA and pDNA as a therapeutic for neuroprotection in healthy and diseased Müller cells. Here, we found that mRNA lipoplexes outperformed DNA lipoplexes in Müller cell transfection since both the number of transfected cells as well as the level of GFP expression was higher. To further examine the potential of mRNA in this context, future experiments should determine the transience of the mRNA-induced GFP expression since this is an important requirement for the neuroprotective strategy. Remarkably, none of the stress factors applied, greatly influenced the transfection efficiency or the MFI induced by mRNA lipoplexes. We did observe that hypoxia and oxidative stress sensitized Müller cells to lipoplex toxicity while hyperglycemic conditions had the opposite effect. Naturally, the experimental set-up applied in this chapter is elementary since diseases usually lead to multifactorial changes in the cellular environment and the influence of surrounding cell types is absent in the Müller monoculture. Future experiments could therefore focus on confirming these trends in more complex systems such as non-dividing Müller cells and/or retinal explants. Since both diabetic retinopathy and glaucoma are chronic diseases, the influence of longer exposures to stress should also be evaluated. Nevertheless, these preliminary observations support the strategy to apply Müller cells as secretion platforms in the diseased retina since this suggests that, despite a stressful environment, Müller cells would be able of processing NPs and expressing the transgene of our choice.

6. ACKNOWLEDGEMENTS

I would like to thank my colleague Joke Devoldere for providing me with the characterization data presented in this paper. Students Frederik Philips and Fauve Vergauwe are greatly acknowledged for the experimental work presented in this chapter. Thomas Martens is acknowledged for the liposome figure.

7. REFERENCES

1. Dalkara, D. *et al.* AAV mediated GDNF secretion from retinal glia slows down retinal degeneration in a rat model of retinitis pigmentosa. *Mol. Ther.* **19,** 1602–8 (2011).

2. Bringmann, A. *et al.* Cellular signaling and factors involved in Müller cell gliosis: neuroprotective and detrimental effects. *Prog. Retin. Eye Res.* **28,** 423–51 (2009).

3. Gauthier, R., Joly, S., Pernet, V., Lachapelle, P. & Di Polo, A. Brain-derived neurotrophic factor gene delivery to muller glia preserves structure and function of light-damaged photoreceptors. *Invest. Ophthalmol. Vis. Sci.* **46,** 3383–3392 (2005).

4. Greenberg, K. P., Geller, S. F., Schaffer, D. V. & Flannery, J. G. Targeted transgene expression in Müller glia of normal and diseased retinas using lentiviral vectors. *Investig. Ophthalmol. Vis. Sci.* **48,** 1844–1852 (2007).

5. Di Polo, A., Aigner, L. J., Dunn, R. J., Bray, G. M. & Aguayo, A. J. Prolonged delivery of brain-derived neurotrophic factor by adenovirus-infected Müller cells temporarily rescues injured retinal ganglion cells. *Proc. Natl. Acad. Sci. U. S. A.* **95,** 3978–83 (1998).

6. Pease, M. E. *et al.* Effect of CNTF on retinal ganglion cell survival in experimental glaucoma. *Invest. Ophthalmol. Vis. Sci.* **50,** 2194–200 (2009).

7. van Adel, B. a, Kostic, C., Déglon, N., Ball, A. K. & Arsenijevic, Y. Delivery of ciliary neurotrophic factor via lentiviral-mediated transfer protects axotomized retinal ganglion cells for an extended period of time. *Hum. Gene Ther.* **14,** 103–115 (2003).

8. Adijanto, J. & Naash, M. I. Nanoparticle-based technologies for retinal gene therapy. *Eur. J. Pharm. Biopharm.* **95,** 353–367 (2015).

9. Martens, T. F. *et al.* Coating nanocarriers with hyaluronic acid facilitates intravitreal drug delivery for retinal gene therapy. *J. Control. Release* **202,** 83–92 (2015).

10. Martens, T. F. *et al.* Effect of hyaluronic acid-binding to lipoplexes on intravitreal drug delivery for retinal gene therapy. *Eur. J. Pharm. Sci.* **103,** 27–35 (2017).

11. Bozzuto, G. & Molinari, A. Liposomes as nanomedical devices. *Int. J. Nanomedicine* **10,** 975–999 (2015).

12. Du, J. D., Fong, W.-K., Caliph, S. & Boyd, B. J. Lipid-based drug delivery systems in the treatment of wet age-related macular degeneration. *Drug Deliv. Transl. Res.* **6,** 781–792 (2016).

13. Zulliger, R., Conley, S. M. & Naash, M. I. Non-viral therapeutic approaches to ocular diseases: An overview and future directions. *J. Control. Release* **219,** 471–487 (2015).

14. Devoldere, J., Dewitte, H., De Smedt, S. C. & Remaut, K. Evading innate immunity in nonviral mRNA delivery: Don't shoot the messenger. *Drug Discov. Today* **21,** 11–25 (2016).

15. Matteucci, A. *et al.* Neuroprotection by rat Müller glia against high glucose-induced neurodegeneration through a mechanism involving ERK1/2 activation. *Exp. Eye Res.* **125,** 20–9 (2014).

16. Hernández, C., Dal Monte, M., Simó, R. & Casini, G. Neuroprotection as a therapeutic target for diabetic retinopathy. *Curr. Diab. Rep.* **16,** 29 (2016).

17. Jindal, V. Neurodegeneration as a Primary Change and Role of Neuroprotection in Diabetic Retinopathy. *Mol. Neurobiol.* **51,** 878–884 (2015).

18. Foxton, R. H. *et al.* VEGF-A is necessary and sufficient for retinal neuroprotection in models of experimental glaucoma. *Am. J. Pathol.* **182,** 1379–1390 (2013).

19. Wilson, a M. & Di Polo, a. Gene therapy for retinal ganglion cell neuroprotection in glaucoma. *Gene Ther.* **19,** 127–136 (2012).

20. Hanumunthadu, D., Dehabadi, M. H. & Cordeiro, M. F. Neuroprotection in glaucoma: Current and emerging approaches. *Expert Rev. Ophthalmol.* **9,** 109–123 (2014).

21. Ferreira, S. M. *et al.* Time Course Changes of Oxidative Stress Markers in a Rat Experimental Glaucoma Model. *Investig. Opthalmology Vis. Sci.* **51,** 4635 (2010).

22. Chrysostomou, V., Rezania, F., Trounce, I. A. & Crowston, J. G. Oxidative stress and mitochondrial dysfunction in glaucoma. *Curr. Opin. Pharmacol.* **13,** 12–15 (2013).

23. Kowluru, R. A. & Chan, P.-S. Oxidative Stress and Diabetic Retinopathy. *Exp. Diabetes Res.* **2007,** 1–12 (2007).

24. Arjamaa, O. & Nikinmaa, M. Oxygen-dependent diseases in the retina: Role of hypoxia-inducible factors. *Exp. Eye Res.* **83,** 473–483 (2006).

25. Tezel, G. & Wax, M. B. Hypoxia-inducible factor 1alpha in the glaucomatous retina and optic nerve head. *Arch. Ophthalmol.* **122,** 1348–56 (2004).

26. Zhu, Y., Zhang, Y., Ojwang, B. A., Brantley, M. A. & Gidday, J. M. Long-term tolerance to retinal ischemia by repetitive hypoxic preconditioning: Role of HIF-1?? and heme oxygenase-1. *Investig. Ophthalmol. Vis. Sci.* **48,** 1735–1743 (2007).

27. Limb, G., Salt, T., Munro, P., Moss, S. & Khaw, P. In vitro characterization of a spontaneously immortalized human Muller cell line (MIO-M1). *Invest. Ophthalmol. Vis. Sci.* **43,** 864–869 (2002).

28. Peynshaert, K. *et al.* Exploiting Intrinsic Nanoparticle Toxicity: The Pros and Cons of Nanoparticle-Induced Autophagy in Biomedical Research. *Chem. Rev.* **114,** 7581–7609 (2014).

29. Alía, M., Ramos, S., Mateos, R., Bravo, L. & Goya, L. Response of the antioxidant defense system to tert-butyl hydroperoxide and hydrogen peroxide in a human hepatoma cell line (HepG2). *J. Biochem. Mol. Toxicol.* **19,** 119–128 (2005).

30. Tien, T. *et al.* High Glucose Induces Mitochondrial Dysfunction in Retinal Müller Cells: Implications for Diabetic Retinopathy. *Invest. Ophthalmol. Vis. Sci.* **58,** 2915–2921 (2017).

31. Kusner, L. L., Sarthy, V. P. & Mohr, S. Nuclear translocation of glyceraldehyde-3-phosphate dehydrogenase: a role in high glucose-induced apoptosis in retinal Müller cells. *Investig. Ophthalmol. Vis. Sci.* **45,** 2543–2548 (2004).

32. S, V., A, F., Y, A., BS, B.-O. & AT, T. High Glucose and Glucose Deprivation Modulate Müller Cell Viability and VEGF Secretion. *Int. J. Ophthalmol. Eye Sci.* **4,** 178–183 (2016).

33. Miki, H. *et al.* Liposomes and nanotechnology in drug development: Focus on neurological targets. *Int. J. Nanomedicine* **8,** 951–960 (2013).

34. Lv, H., Zhang, S., Wang, B., Cui, S. & Yan, J. Toxicity of cationic lipids and cationic polymers

in gene delivery. *J. Control. Release* **114,** 100–109 (2006).

35. Knudsen, K. B. *et al.* In vivo toxicity of cationic micelles and liposomes. *Nanomedicine Nanotechnology, Biol. Med.* **11,** 467–477 (2015).

36. Lopez, R. *et al.* Hyperglycemia enhances the proliferation of non-tumorigenic and malignant mammary epithelial cells through increased leptin/IGF1R signaling and activation of AKT/mTOR. *PLoS One* **8,** (2013).

37. Astrid Limb, G. & Jayaram, H. Regulatory and pathogenic roles of m??ller glial cells in retinal neovascular processes and their potential for retinal regeneration. *Exp. Approaches to Diabet. Retin.* **20,** 98–108 (2009).

38. Bringmann, A. & Wiedemann, P. Müller glial cells in retinal disease. *Ophthalmologica* **227,** 1–19 (2011).

39. Bringmann, A. *et al.* Cellular signaling and factors involved in Müller cell gliosis: neuroprotective and detrimental effects. *Prog. Retin. Eye Res.* **28,** 423–51 (2009).

40. Zhang, X., Feng, Z., Li, C. & Zheng, Y. Morphological and migratory alterations in retinal Müller cells during early stages of hypoxia and oxidative stress. *Neural Regen. Res.* **7,** 31–5 (2012).

40a. Wenger, R., Kurtcuoglu, V., Scholz, C., Marti, H. & Hoogewijs, D. Frequently asked questions in hypoxia research. *Hypoxia* **5,** 35–43 (2015).

41. Winkler, B. S., Arnold, M. J., Brassell, M. A. & Puro, D. G. Energy Metabolism in Human Retinal Müller Cells. **44,** 735–745 (2000).

42. Kroemer, G., Marino, G. & Levine, B. Autophagy and the Integrated Stress Response. *Mol. Cell* **40,** 280–293 (2010).

43. Lin, W. & Kuang, H. Oxidative stress induces autophagy in response to multiple noxious stimuli in retinal ganglion cells. **10,** 1692–1701 (2014).

44. Shelby, S. J. *et al.* Hypoxia inducible factor 1α contributes to regulation of autophagy in retinal detachment. *Exp. Eye Res.* **137,** 84–93 (2015).

45. Fung, F. K. C., Law, B. Y. K. & Lo, A. C. Y. Lutein attenuates both apoptosis and autophagy upon cobalt (II) chloride-induced hypoxia in rat Muller cells. *PLoS One* **11,** 1–19 (2016).

46. Mazure, N. M. & Pouysségur, J. Hypoxia-induced autophagy: Cell death or cell survival? *Curr. Opin. Cell Biol.* **22,** 177–180 (2010).

47. Kumar, H. & Choi, D.-K. Hypoxia Inducible Factor Pathway and Physiological Adaptation: A Cell Survival Pathway? *Mediators Inflamm.* **2015,** 1–11 (2015).

48. Li, M., Tan, J., Miao, Y., Lei, P. & Zhang, Q. The dual role of autophagy under hypoxia-involvement of interaction between autophagy and apoptosis. *Apoptosis* **20,** 769–777 (2015).

49. Roberts, R. *et al.* Autophagy and formation of tubulovesicular autophagosomes provide a barrier against nonviral gene delivery. *Autophagy* **9,** 13–14 (2013).

50. Man, N., Chen, Y., Zheng, F., Zhou, W. & Wen, L. P. Induction of genuine autophagy by cationic lipids in mammalian cells. *Autophagy* **6,** 449–454 (2010).

51. Rubinstein, A. D. & Kimchi, A. Life in the balance - a mechanistic view of the crosstalk between autophagy and apoptosis. *J Cell Sci* **125,** 5259–5268 (2012).

52. Jain, S. *et al.* Gold nanoparticle cellular uptake, toxicity and radiosensitisation in hypoxic conditions. *Radiother. Oncol.* **110,** 342–347 (2014).

53. Chen, E. *et al.* Oxygen microenvironment affects the uptake of nanoparticles in head and neck tumor cells. *Proc. SPIE* **31,** 1133–1136 (2013).

54. Andreev, D. E. *et al.* Oxygen and glucose deprivation induces widespread alterations in mRNA translation within 20 minutes. *Genome Biol.* **16,** 90 (2015).

55. Toft-Kehler, A. K. *et al.* Oxidative Stress-induced dysfunction of Müller cells during starvation. *Investig. Ophthalmol. Vis. Sci.* **57,** 2721–2728 (2016).

56. Gülden, M., Jess, A., Kammann, J., Maser, E. & Seibert, H. Cytotoxic potency of H2O2 in cell cultures: impact of cell concentration and exposure time. *Free Radic. Biol. Med.* **49,** 1298–305 (2010).

5

A general introduction to nanoparticles, nanotoxicology and nanoparticle-mediated changes in autophagy

This chapter is part of two literature reviews published as :

Karen Peynshaert[a,b], Bella B. Manshian[c], Freya Joris[a,b], Kevin Braeckmans[a,b], Stefaan C. De Smedt[a,b], Jo Demeester[a,b], Stefaan Soenen[c]. Exploiting intrinsic nanoparticle toxicity: the pros and cons of nanoparticle-induced autophagy in biomedical research. *Chemical Reviews* **114** 7581-7609 (2014).

Freya Joris[a,b], Bella B. Manshian[c], Karen Peynshaert[a,b], Stefaan C. De Smedt[a,b], Kevin Braeckmans[a,b,d], Stefaan J. Soenen[c]. Assessing nanoparticle toxicity in cell-based assays: influence of cell culture parameters and optimized models for bridging the in vitro–in vivo gap. *Chemical Society Reviews* **42** 8339–8359 (2013).

[a]Lab of General Biochemistry and Physical Pharmacy, Faculty of Pharmaceutical Sciences, Ghent University, B9000 Ghent, Belgium.

[b]Ghent Research Group on Nanomedicine, Ghent University, B9000 Ghent, Belgium.

[c]Biomedical MRI Unit/MoSAIC, Department of Imaging and Pathology, Catholic University of Leuven, Faculty of Medicine, B3000- Leuven

[d]Centre for Nano- and Biophotonics, Ghent University, B9000 Ghent, Belgium

ABSTRACT

In the middle of the biomedical nanotechnology boom, the self-digestion process of autophagy increasingly gained attention as researchers gradually discovered its relevance within the cell as well as its connection to cancer. Surely, by 2000 autophagy was rumored to become “the new apoptosis”, i.e. a process playing key roles in human pathophysiology. Logically, it was not long before nanotoxicological researchers were triggered by this fascinating pathway as well, which led to many studies exploring the influence of nanomedicines on this process – including **Chapter 6** of this thesis. As an introduction to this study, a primary aim of this chapter is therefore to introduce you to nanomedicine, nanotoxicology and the autophagy pathway. In this regard, we will discuss the most widely investigated nanoparticles (NPs) for biomedical applications, the common mechanisms of NP toxicity and the autophagy pathway along with available methods to study it. Finally, we will provide a look into the mechanisms by which NPs can affect the autophagy pathway in addition to an overview of the most interesting studies investigating NP-autophagy interactions where we attempt to link NP physicochemistry to its effect on autophagy.

Table of Contents

1. NANOMEDICINE

While the concept of nanotechnology was introduced earlier, the technical inventions made in the 1980's led to many discoveries that truly launched the 'nano' field. Indeed, it became increasingly clear that by miniaturization materials can acquire unique physical, chemical and/or optical properties. Examples of such interesting properties include *a)* the superparamagnetic nature of iron oxide nanoparticles (NPs),[1] *b)* the very high fluorescent brightness and excellent photostability of Quantum Dots,[2] *c)* the localized surface plasmon resonance effect of silver or gold NPs,[3] and *d)* the high rigidity of carbon nanotubes.[4] Even though these materials were initially developed for industrial use, the same properties had also awoken the interest of the medical and biological communities, since these properties can be harnessed to create novel and powerful therapeutic and/or diagnostic tools. As such, nanomedicine was born as the scientific discipline in which these NPs are utilized for medical purposes. NPs certainly exhibit many advantageous features that can be exploited to solve some principal issues present in conventional medicine. Firstly, NPs enable the delivery of poorly soluble therapeutics and provide protection against their degradation. Additionally, their design can be tailored based on the desired target and delivery mode (e.g. controlled release). Decoration of the NP surface with targeting moieties can furthermore enhance target specificity and bioavailability when compared to conventional drugs. Yet, the most unique and powerful aspect of NPs is perhaps their multimodality which allows to apply one particle for both diagnostic as well as therapeutic purposes.[5]

These promising aspects of NPs have led to an incredible boost in the number of engineered NPs, their fine-tuning, and explored applications. As an indication of the expansion of the nano field, it was estimated that almost 10 % of all articles indexed in Web of Science in 2016 involved nanotechnology.[6] Generally, NPs can be divided into two categories i.e. soft and hard NPs. Soft NPs are mostly investigated for delivery purposes, while hard NPs are researched for diagnostics or novel types of therapy.[5] Here, we will briefly describe the various types of NPs currently used in or explored for clinical settings, mainly in the field of cancer therapy (**Figure 5.1**). The principal focus will lie on introducing the different types of materials, a short description of their most important properties and an overview of their current and potential future applications.

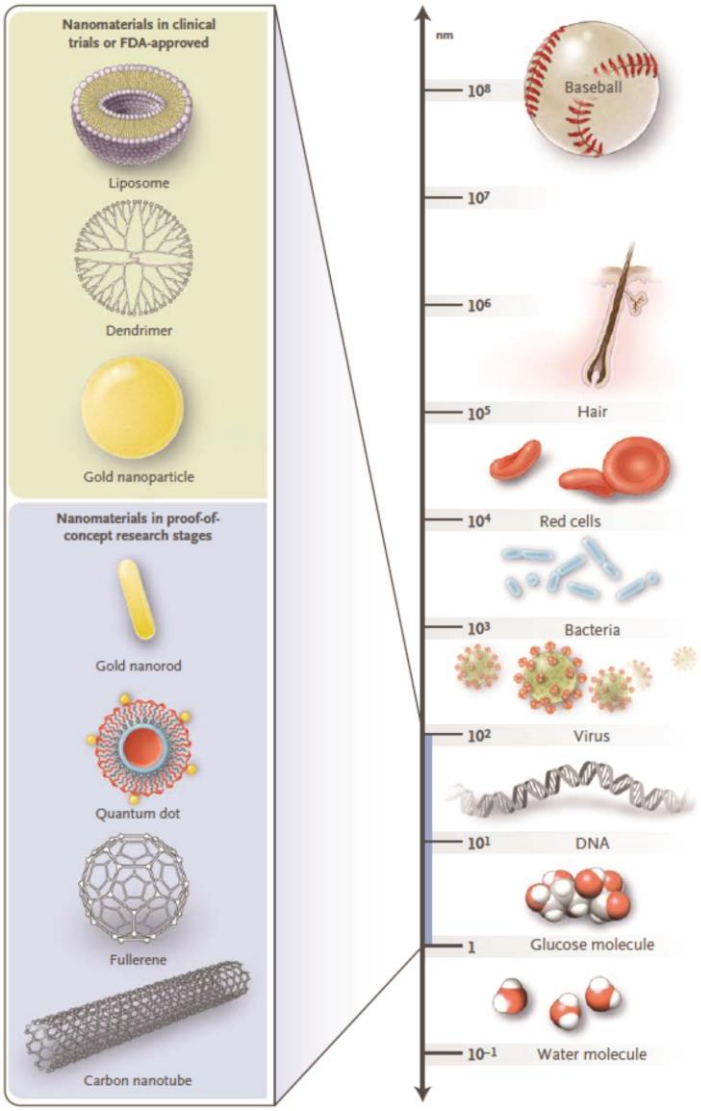

Figure 5.1 | Commonly investigated nanoparticles for medicine. Figure taken from [7]

Soft nanoparticles

Soft NPs can be roughly subdivided into two principal categories being lipid-based and polymer-based particles. Lipid-based particles are usually organized into liposomal structures, originally discovered by Bangham and colleagues in 1965.[8] The most basic **liposome** is made up of an inner aqueous compartment that is separated from the outer aqueous compartment by a single lipid bilayer, though many different types of liposomes can be synthesized with varying size and/or number of lipid bilayers (**Figure 5.2**). Drugs can be enclosed either within the aqueous central cavity (for hydrophilic compounds) or embedded within the lipid layers (for hydrophobic compounds). Conveniently, the variety of lipids (e.g. neutral, negatively or positively charged) and potential incorporation of proteins or other lipophilic compounds allows easy fine-tuning of the liposomal composition and surface chemistry.[9] This surface can be further functionalized with various smart ligands such as those presented in **Figure 5.2**. For clinical use, a common

surface molecule is poly(ethylene glycol) (PEG) as it reduces opsonization of the liposomes by immune components and proteins by which it increases blood circulation time through impeding liposomal clearance by the reticuloendothelial system.[10] For improved targeting, several targeting ligands such as antibodies can be decorated on the surface of the liposome. As such, a great number of liposomal systems have been generated and put into clinical trials in combination with various therapeutic agents, mostly anti-cancer drugs.[11,12] A full overview of the newer lipid-based vesicles can be found here [13].

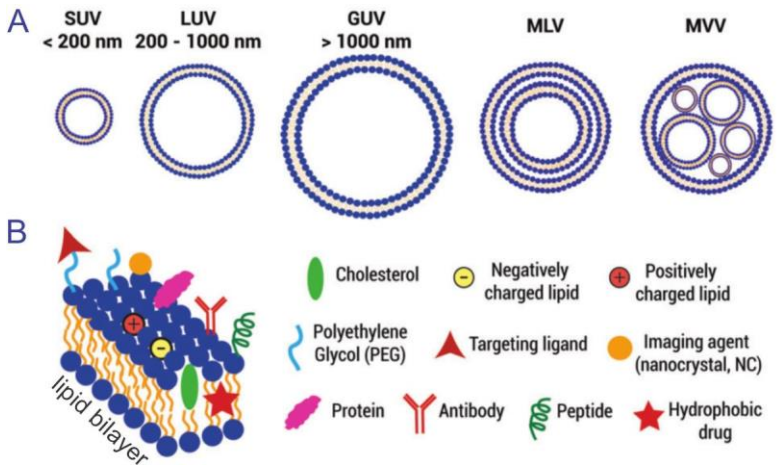

Figure 5.2 | Schematic representation of lipid-based vesicles. A) Lipid vesicles can be classified depending on their size and lamellarity. SUV: small unilamellar vesicle; LUV: large unilamellar vesicle; GUV giant unilamellar vesicle; MLV: multilamellar vesicle; MVV: multivesicular vesicle. B) Structure of the lipid bilayer and overview of the functionalization possibilities. Figure taken from [13].

Next to lipid-based formulations, **polymer-based NP**s are also frequently employed as delivery systems especially for anti-cancer drugs. Similar to lipid-based carriers, the advances in chemical research have led to the discovery of a wide variety of different polymers that allow to smartly tailor the size, composition and surface functionality of polymer NPs.[5] Furthermore, their drug release can be regulated through controlled degradation of the polymers or by stimulus activation such as pH change, offering many exciting possibilities for clinical applications. Both natural and synthetic polymers can be used for drug delivery, many of which have been optimized to present high levels of biocompatibility.[14] Co-polymers comprised of a hydrophilic and lipophilic block are applied to form polymeric micelles, since these block co-polymers automatically form core-shell structures in aquaous surroundings. These vehicles with size range from 20 to 100 nm are therefore ideal for the transport and delivery of more hydrophobic anti-cancer agents.[15] Consequently, many of the formulations investigated in clinical trials consist of polymeric micelles, either untargeted or bestowed with an antibody against a specific marker and containing hydrophobic compounds such as Paclitaxel or Cisplatin.[14]

A special type of polymeric NPs are **dendrimers** (**Figure 5.1**). These are hyperbranched globular structures known for their high monodispersity and large drug payload.[16] Drugs can be loaded into the interior part of the dendrimer or can be attached to the many surface groups at the periphery of the particle. Dendrimers are mainly studied for their drug delivery capacities, where research has been mainly focusing on anti-cancer agents and anti-viral treatment.[17]

Hard nanoparticles

Hard NPs represent a wide variety of compounds, including metal, metaloxide, semiconductor and carbon particles that are characterized by unique properties.[18] Many chemical linking strategies are also available that allow the conjugation of chemical drugs, fluorophores or small compounds to these hard NPs in order to further enhance their application range. Given these exciting properties, hard NPs are currently receiving a lot of attention in view of possible biomedical applications.

Metaloxide NPs are a broad collection of materials with many different applications. For example, titanium dioxide (TiO_2) NPs are often used in pharmaceutical tablets because of their whitening effect, zinc oxide (ZnO) NPs are commonly added to sunscreens for their high UV absorbance and iron oxide NPs (IONPs; Fe_2O_3 or Fe_3O_4) are investigated in clinical settings as magnetic resonance imaging (MRI) contrast agents due to their superparamagnetic nature.[19,20] Cerium oxide (CeO_2) NPs are also gaining attention since they can possibly be implemented to scavenge oxide radicals and prevent radical-mediated cell damage owing to their potent antioxidant capacity.[21]

Metal NPs such as silver (Ag) or gold (Au) are increasingly being explored for clinical applications as delivery vehicles, diagnostic and/or therapeutic agents.[22,23] Both Ag and Au NPs can be made in a variety of shapes and sizes through various chemical synthesis routes. AgNPs are widely used in consumer goods such as deodorants due to their potent antibacterial properties.[23] Similarly, the same properties have led to their use in wound dressing. **AuNP** applications involve mostly diagnostic and photothermal therapies which are both based on their surface plasmon resonance (SPR) effect.[24] This effect enhances the absorbance and scattering properties of the AuNPs dependent on the wavelength applied. Seeing these optical features can be tuned by varying NP size and shape, an immense diversity of AuNPs have been developed ranging from gold nanorods to nanocages (**Figure 5.1**).[25] A leading example of enhanced drug delivery based on AuNPs is laser-induced photoporation, a technique our research group has gained expertise in. Here, AuNPs are irradiated by a short laser pulse by which the AuNPs heat up. The resulting evaporation of the water surrounding the AuNP surface creates an explosive vapour nanobubble. This bubble formation and subsequent collapse results in local high-pressure shock waves that

can locally disrupt their surroundings. Applying this photoporation method, our group has succeeded in the controlled intracellular delivery of macromolecules through the formation of transient openings in the cell membrane.[26,27]

Other interesting materials are **Quantum Dots** (QDs), which consist of a semiconductor core with a narrow bandgap made up of elements from groups 12 and 16 (CdSe, CdTe, ZnS) or groups 13 and 15 (InP, GaN) (**Figure 5.1**). For imaging purposes, these QDs offer many possibilities as their size-dependent broad excitation spectra and narrow emission spectra enable efficient multiplexing.[28] However, many research groups, including ours (cfr. **Chapter 6**) have reported on the toxic effects of QDs or the heavy metals they contain which severely impedes their progress into clinical applications. Novel formulations such as Cd^{2+}-free QDs are therefore being considered, but more research is needed before these materials can be used in clinical trials.[29]

A last widely investigated class is **carbon-based materials** which amongst other materials includes fullerenes, carbon nanotubes and graphene (**Figure 5.1**). While these materials are mostly developed for industrial purposes, their exceptional properties have also been investigated for biomedical applications. As an example, their capacity to absorb near-infrared (NIR) light could be beneficial for *in* vivo imaging since NIR has shown to penetrate tissues more efficiently. Their outstanding tensile strength, on the other hand, is researched to enhance the mechanical strength of scaffold materials. Also the drug delivery field could benefit from these materials considering their straightforward functionalization and ability to adsorb biomacromolecules (e.g. DNA).[30]

2. NANOTOXICOLOGY

The high interest in using NPs for medical applications and their increasing use in various technological applications and consumer goods (e.g. clothing and food products) has raised high concerns on their possible impact on human and environmental health. Indeed, due to the pertaining uncertainties concerning the potential danger of NPs and the lack of appropriate legislation, the nanotechnology industry is facing significant setbacks in their attempt to implement NPs in a clinical setting.[31] It is therefore of vital importance to carefully characterize the toxicity of these NPs to enable the field of nanotechnology to fulfill some of its truly exciting possibilities in many aspects of human life. In view of this, the increasing production and use of NPs has led to the instilment of another scientific discipline: nanotoxicology.[32] **Nanotoxicology** is referred to as the study on interactions between NPs and biological systems with an emphasis on establishing a relationship, if any, between the physicochemical properties of the NP and the toxicological responses.[33] Although the area of nanotoxicology was initially a small niche within

the field of particle and fiber inhalation studies, the field has rapidly expanded to become an important stand-alone scientific discipline, encompassing multiple domains such as *in vitro*, *in vivo*, environmental and human toxicology.[34] It is crucial that nanotoxicology is regarded as a distinct category of toxicology since standard toxicity assays, initially developed for the evaluation of chemical substances, are often inadequate for nanotoxicity assessment. This can be attributed to the different mechanisms leading to nanocytotoxicity, the specific behavior of the NPs in culture media and the possible interference of NPs with various toxicity assays.[35–38] Therefore the classical toxicity-testing paradigm needs to be optimized to be applicable for nanosafety evaluation.

Generally, higher levels of toxicity are observed for NPs in comparison to their bulk material,[33,39] which is attributed to the higher surface area to volume ratio, possible surface reactivity and susceptibility to NP degradation and ion leaching.[40,41] In addition, most chemicals induce cell damage through interactions with specific biomolecules, whereas a single NP may cause cytotoxicity *via* a combination of adverse events. A true general paradigm on how NPs evoke cell injury remains to be elucidated. However, it can be stated that cytotoxicity can be evoked *via* 4 distinct categories of events: (i) effects related to induction of reactive oxygen species (ROS), (ii) effects due to direct interactions of the NPs with biomolecules, (iii) effects from leached ions and (iv) effects related to the protein corona.

Nel *et al.* have put **ROS induction** forward as one of the main mechanisms through which inorganic NPs induce cytotoxicity, as this effect has been observed in a multitude of *in vivo* and *in vitro* studies.[34,40,42–44] It is proposed that ROS can be induced either through intrinsic ROS generating properties of the NP or cell-mediated ROS generation. In the latter category, NPs can interfere with the anti-oxidative defense mechanism by reducing the activity of the anti-oxidative defense enzymes.[45] Furthermore NPs can activate several signaling pathways through interaction with cell surface receptors.[46] Hereby stress-dependent signaling pathways are activated which alter gene expression of the anti-oxidant response element, leading to ROS overproduction.[47] In addition, NPs can cause increased ROS production in the mitochondria through interference with the respiratory chain.[47,48] Finally, several NPs are capable of activating NADPH oxidase, thereby inducing ROS production.[49] In the first category (intrinsic ROS generating properties), NPs are intrinsically capable of generating ROS through the presence of reactive surface groups or surface bound radicals.[40] In addition, transition metals present on the surface or leached from the NP in the acidic environment of the endo-lysosomes can generate ROS *via* Fenton chemistry.[40,46] Overall, ROS induction can be a consequence of a single or a combination of the abovementioned events. Furthermore, Nel *et al.* proposed a tired response

of the cells to elevated ROS levels which has been confirmed in *in vitro* and *in vivo* studies for different NPs. In general limited ROS levels induce an anti-oxidative response, medium ROS levels evoke a proliferative and inflammatory response and persistently high levels of oxidative stress induce apoptotic and necrotic signaling pathways.[40]

The induction of ROS can have a multitude of downstream effects. Indeed, ROS is known to induce general cell damage, as it can interact with DNA, proteins, lipids and organelles.[40] First, oxidative DNA damage influences gene expression or can induce mutagenesis or apoptosis in case of insufficient repair mechanisms.[50] Secondly, proteins can be activated or inactivated as a consequence of ROS presence.[51] ROS can furthermore cause actin stress fiber formation and therefore alter the cell's morphology, motility and adhesion.[52,53] Persistent ROS induction will trigger a stress response leading to the production of cytokines and the induction of an inflammatory response. If ROS is not neutralized in a timely fashion, a feed-forward loop keeps stimulating both ROS and cytokine production leading to immunotoxicity.[40] Due to lipid peroxidation, membranes can be damaged, which in turn leads to malfunctioning organelles. Indeed, the mitochondria, endoplasmatic reticulum (ER) and lysosomes are reported to suffer from ROS.[54] This secondary ROS damage can in turn lead to downstream effects such as altered signaling and a perturbed calcium homeostasis. [54] In addition, both ER stress and lysosomal destabilization can induce autophagy and an inflammatory response.[55]

The second main mechanism through which NPs induce adverse effects is by **direct interaction with biomolecules**, such as DNA, proteins and lipids, which in turn leads to downstream effects. Notably, most ROS-related events may also occur through direct NP-biomolecule interactions. For instance, NPs can alter gene expression *via* interactions with signal transduction pathways, interference with epigenetic gene regulation or the transcriptional or translational machinery through their perinuclear localisation.[50,56,57] In addition, very small NPs with a diameter below 5 nm may directly interact with DNA and alter its expression.[58] Studies furthermore show that NPs can interact with components of the cytoskeleton thereby potentially altering cell morphology as well as signal transduction.[59–61] In addition, NPs were shown to interfere with receptor-ligand interactions and signalling pathways.[62] Comparable to ROS-induced damage, NPs are capable of damaging membranes and organelles such as the mitochondria and lysosomes. This may in turn evoke autophagy or an inflammatory response.[56,63] Finally, NPs are also capable of directly evoking ER stress, which in turn leads to autophagy, increased calcium levels and potentially inflammation or apoptosis.[63,64]

The third general element causing NPs to induce toxicity is their susceptibility to **degradation**. Depending on the uptake mechanisms and subsequent trafficking many NPs end up in the acidic

and degrading environment of the lysosomes.[46,65] This environment can cause degradation or even dissolution of the NP, resulting in the leaching of free ions or an increase in reactive surface groups.[46] The following impact on the cell's wellbeing depends on the chemical composition of the NP. For cadmium (Cd)-containing QDs, for example, the leaching of highly toxic Cd^{2+}-ions is considered to be the main cause of any observed toxicity.[66,67] It has been shown for several NPs that the induced toxicity is more severe for the nanoparticulate form than its ionic counterpart. This is called the "Trojan Horse effect" as it can likely be attributed to a more efficient uptake of the NP through endocytosis compared to the free ionic form which consequently leads to elevated intracellular ionic concentrations.[56]

Finally, it is known that NPs avidly bind serum proteins to their surface, creating a **protein corona**.[68] The nature of this corona depends on the NPs physicochemical properties and the composition of the microenvironment (e.g. cell culture media) surrounding the NPs.[33,69] The binding of serum proteins to the NP surface is an important determinant in how the cells 'see' the NPs and therefore influences NP uptake and toxicity.[68,70,71] Additionally, proteins incorporated in this corona can undergo conformational changes because of which the cell may recognize them as an antigen and initiate an immune response.[32,39] An immune response can furthermore be triggered by direct interactions of NPs with immune cells, complement activation and facilitation of antigen-specific hypersensitivity reaction through interactions with T lymphocytes or the release of chemokines and cytokines.[72]

As mentioned earlier in this chapter, there is growing evidence that a wide variety of NPs are able of influencing **autophagy** in a diversity of cell types, implying that also autophagy changes might be a common cellular response toward NP uptake. Prior to examining this phenomenon, the next section will introduce the autophagy pathway, its involvement in cell death and available methods to study this intriguing process.

3. AUTOPHAGY

The efficient degradation of intracellular materials is of vital importance to ensure cytoplasmic quality control and guard cellular homeostasis. This degradation can occur via multiple cellular pathways including autophagy. Autophagy is a collective term for various selective and non-selective processes comprising microautophagy, chaperone-mediated autophagy and macroautophagy. Microautophagy involves the formation of lysosomal invaginations resulting in a direct and non-specific sequestration of cytosolic components following breakdown.[73] In case of chaperone-mediated autophagy, which is a highly specific process, unfolded proteins are recognized and bound by a chaperone complex, resulting in their translocation into the lysosome

lumen.[74] However, in most cases and also in this chapter the designation 'autophagy' refers to the process of macroautophagy.

Macroautophagy, or simply autophagy is an evolutionarily conserved process that is coordinated by key proteins encoded by autophagy-related genes, i.e. Atg genes. It warrants cytoplasmic quality control through the degradation of excessive or damaged cytoplasmic components such as organelles or aggregated proteins. It is usually present at a basal level but can be induced as a cytoprotective mechanism in case of cell stress. For instance, during starvation autophagy aids to overcome the food drop by degrading and recycling less essential cytoplasmic materials.

Autophagy process

The process of autophagy initiates with the synthesis of a phagophore that, while sequestering cytoplasmic cargo, elongates and closes to form a double-membraned autophagosome (**Figure 5.3**). During the creation of this autophagosome, cytoplasmic microtubule-associated protein 1 light chain 3 (LC3-I) is activated by lipidation, forming LC3-II, and incorporated into the autophagosomal membrane. Next, the autophagosome fuses with a lysosome that supplies the acidic pH and enzymes for degradation of the cargo carried by the autophagosome. Alternatively, a lysosome can merge with an amphisome, i.e. the end product of an endosome-autophagosome fusion. In this way, also newly ingested material can be targeted for degradation by autophagy. In the resulting vesicle, the auto(phago)lysosome, the cargo is degraded after which the resulting macromolecules are transported into the cytoplasm by permeases. Hereby the necessary energy and/or building blocks for the *de novo* synthesis of cellular components are provided. Since during this step also the inner membrane of the autolysosome is degraded, the LC3-II within the vesicle is lysed while the LC3-II on the outside is recycled back to LC3-I. The overall process from autophagosome maturation to its degradation is often referred to as autophagy flux (**Figure 5.3**).[75,76]

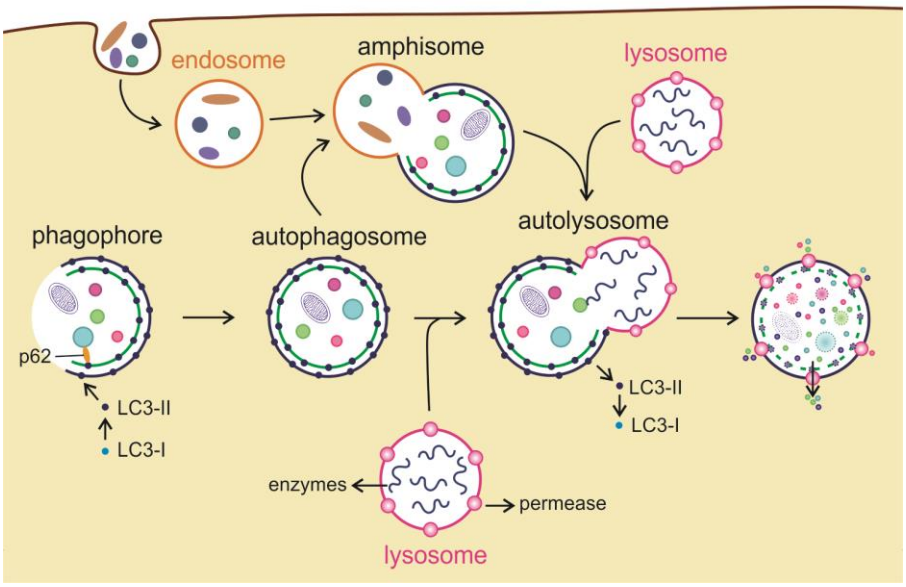

Figure 5.3 | Overview of the mechanistic steps of autophagy. Figure adjusted from [75].

A key aspect of autophagy is the ability to engulf a portion of the cytoplasm by which it selectively removes certain proteins, pathogens or complete organelles such as mitochondria. This cargo selectivity is mediated by the protein p62 that, due to its multiple binding domains, can create a direct link between LC3 and components targeted for autophagy.[77] As will be discussed later, p62 is selectively degraded by autophagy and is therefore frequently used as a marker for autophagy flux.[78,79] The most reported and actively studied pathways known to coordinate the level of autophagy are focused around the convergence point mammalian target of rapamycin complex 1 (mTORC1), a serine/threonine kinase that can directly tune autophagy through its interaction with multiple Atg proteins that are essential for autophagy initiation. On the other hand mTORC1 can indirectly stimulate autophagy via TFEB, a transcription factor that upon activation translocates to the nucleus where it promotes transcription of lysosomal and autophagic genes. The phosphorylation status of mTORC1 itself depends on the action of multiple upstream mediators of which the activity is driven by the nutrient level and energy status of the cell.[80] Indeed, besides performing its housekeeper functions at a basal level, autophagy also serves as a cytoprotective pathway upon activation by triggers that represent a certain form of stress. For example, nutrient starvation leads to autophagy upregulation, promoting the breakdown of less essential cellular components to macromolecules ready to be recycled.[81] Invading pathogens can also stimulate autophagy leading to their selective removal.[82] Additionally, oxidative stress elicited by ROS formation, can also give rise to autophagy, hereby promoting the degradation of the ROS-damaged organelles, typically mitochondria. As mitochondria are the predominant sources of ROS and are also sensitive to ROS-induced damage, they are seen as the main regulators of ROS-induced autophagy.[83]

Autophagic cell death

The process of autophagy has generally been labeled as a pro-survival pathway, however, it has been argued that excessive self-digestion can result in autophagic cell death (ACD).[84] Albeit not abundant, there are some studies that report on autophagy performing a pro-death role - as revised in a review by Shen *et al*.,[85] which has led to the generation of the term ACD. On the other hand, ACD has long been relatively unexplored, which resulted in different interpretations and considerable misuse of the term. The process of cell death is indeed often very complex and during its progress, damaged cells typically display various markers representative of different cell death pathways such as apoptosis and autophagy. Although morphological changes typical for autophagy can often be observed, it remains unclear whether autophagy is a true killer, a mere side phenomenon accompanying death or rather an unsuccessful attempt to save the cell.[85,86]

In order to overcome these issues, the definition of ACD has evolved from merely comprising morphological changes (i.e. autophagic vacuoles) to a list of clear biochemical requirements drafted by the Nomenclature Committee on Cell Death.[87] In line with this, Shen *et al.* argue the term ACD is only justified when the observations made meet the following standards: *1)* cell death must be apoptosis-independent, *2)* autophagy inhibition, preferably by the knockdown of minimum two relevant Atg genes,[87] prevents the observed cell death and *3)* an increase in autophagy flux is detected.[85] Specialists agree that on top of the above-mentioned criteria, ACD must be a separate death pathway that stands alone, and cases by which autophagy promotes other cell death pathways (e.g. apoptosis) must be excluded.[88,89] In conclusion, it is important for any researcher to understand that autophagy in itself can either be pro-survival or pro-death and that the co-occurrence of cell death and autophagy does not automatically imply that autophagy in itself is leading to cell death. Interestingly, however, NPs have been introduced as potential inducers of autophagy as well as ACD as will be discussed later on in this chapter.[90]

Over the last decade it has gradually been revealed that autophagy and apoptosis are interconnected at several levels. Autophagy can influence apoptosis by direct interaction of autophagy proteins with the apoptotic machinery, by autophagic degradation of apoptotic factors and/or by providing a platform for caspase activation. Likewise, apoptotic proteins can affect autophagy through interaction with and/or caspase-mediated cleavage of its proteins. It is thus proposed autophagy can induce cell death by *1)* the dismantling of the cell through self-digestion and *2)* the promotion of apoptosis.[91] The cellular decision to activate a certain cell death pathway is likely to depend on the cellular stresses involved; yet, given its role in damage control it is suggested that autophagy affects the onset of cell death. For example, when

autophagy is dysfunctional or not able to restore the ATP level, apoptosis or necrosis is initiated.[92] It is important to note that cell death is a dynamic phenomenon and multiple cell death types are often co-observed within the same cell.[93]

Methods to study autophagy

As a result of the increasing interest in autophagy, multiple methods have been developed in the past years to detect various autophagic markers. The most widely examined markers are LC3, p62 and mTOR. The following section presents a short overview of the most extensively used methods to detect these markers. For a complete overview of available methods we refer the reader to [94].

Initially, transmission **electron microscopy** (TEM) used to be the only key technique to detect autophagy, and it still remains an important method today as it can provide highly detailed ultrastructural information like autophagosomal cargo and potential inclusion of NPs (**Figure 5.4**).[95] TEM allows detection of the distinct steps of the process based on the specific morphology of the autophagic organelles; yet, since autophagy is a dynamic process identifying these structures can be troublesome and thus requires special expertise.[96]

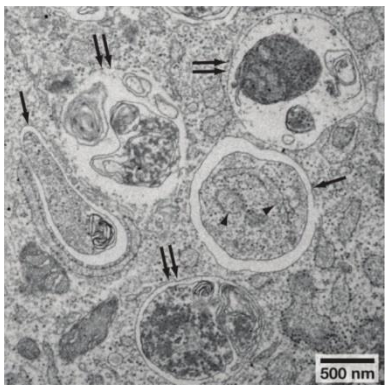

Figure 5.4 | TEM image of starved mouse fibroblasts. Arrows indicate double-membraned autophagosomes, and double arrows indicate autolysosomes/amphisomes. Arrowheads designate endoplasmic reticulum debris as autophagosomal cargo. Image taken from [97].

To date, LC3, which is selectively incorporated into autophagic membranes, has been the most specific and therefore also the most analyzed autophagy marker. It is indeed well established that autophagosomes can be visualized by **fluorescence microscopy** by antibody staining for LC3 or transfection of cell cultures with the GFP-LC3 construct. Accordingly, LC3 is usually diffusely scattered throughout the cytoplasm while autophagosomal accumulation can be identified as distinct puncta (**Figure 5.5**).[98–100] Since upon incorporation into the autophagosome LC3-I is conjugated with phosphatidylethanolamine to form LC3-II, LC3's molecular weight differs sufficiently to cause a visible mobility shift on **Western Blot** gels. Hence, changes in the amount

of autophagosomes – which corresponds to the ratio of LC3-II/LC3-I – can also be detected by Western blotting.[101]

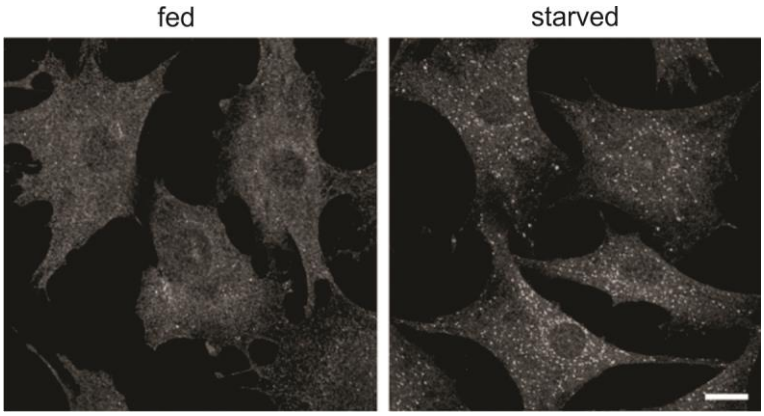

Figure 5.5 | Immunofluorescent labeling of endogenous LC3 in fed and starved mouse fibroblasts. Figure taken from [100]

We must emphasize that these methods are based on static measurements of autophagosome accumulation and therefore do not allow to differentiate between the induction of autophagy or an impaired autophagy flux since both result in higher numbers of autophagosomes. An impaired **autophagy flux** can readily be determined by the above-mentioned LC3 Western Blot experiment in the presence of lysosomal protease inhibitors (e.g. pepstatin A) or buffers (e.g. chloroquine, ammonium chloride) that inhibit LC3-II degradation. If the amount of LC3-II remains the same in the presence and absence of the inhibitor it can be concluded that the increased level of LC3-II is likely the result of an autophagy flux blockage. Alternatively, if the level of LC3-II further exceeds in presence of lysosomal inhibitors, the initially observed LC3-II accumulation is due to autophagy upregulation. [101] Autophagy flux can also be evaluated based on other Western Blot experiments such as GFP-LC3 cleavage. Since GFP is relatively resistant to lysosomal hydrolysis the amount of free GFP can be detected as a measure of autophagosome degradation.[97] In addition to LC3, an increase in the level of p62 can also indicate a potential blockage of autophagy flux.[78] The turnover of autophagosomes into autolysosomes can be visualized by means of autophagosome-lysosome colocalization studies using LC3-labeling and lysosomal markers (e.g. LAMP-1 or LysoTracker®).[99] This maturation can be assessed microscopically as well as via **flow cytometry** using for instance, an mRFP-GFP tandem fluorescent-tagged LC3 (tfLC3). As GFP is pH-sensitive and more prone to quenching than mRFP, the various autophagic vesicles can be distinguished through their different fluorescence signal; autophagosomes will show both signals (i.e. yellow) while after lysosomal fusion GFP is quenched and thus autolysosomes can be identified as mRFP-positive vesicles.[102,103] Flow

cytometry can also be applied to determine the total fluorescence intensity of GFP-LC3 as a measure of autophagic activity.[104]

Another approach could be to evaluate the activity of mTOR and its interacting proteins. This is usually examined to study the effect of various stimuli (including NPs) on the status of autophagy and/or the mechanism behind an observed induction or inhibition. Since the activity of these proteins depends on their phosphorylation status, Western Blotting by means of phospho-specific antibodies is the favored method. In this way the activity of mTOR can be measured directly by analyzing its phosphorylation level or indirectly by determining the activity of its substrates (e.g. p70S6K) or upstream mediators (e.g. Akt).[105] Whereas *in vitro* detection of autophagy has seen a positive progress over the past years, *in vivo* methods are not yet thoroughly developed. As a consequence *in vivo* monitoring of autophagy remains limited, although there are some methods being suggested such as imaging tissue samples of transgenic mice expressing fluorescently tagged LC3 or staining of tissue sections with LC3-antibodies.[106]

When evaluating the influence of NPs on autophagy it is essential to include controls that help to reliably verify and interpret observed changes in autophagic activity. There are multiple **autophagy-modulating chemicals** and conditions widely used in autophagy research. The most extensively applied chemical inducer is rapamycin, which directly inhibits mTORC1 and thus stimulates autophagy.[107] More natural stimuli of autophagy are serum starvation and amino acid deprivation, which can be used as a positive control in studies with the aim of identifying autophagy inducers (e.g. NPs).[97] 3-Methyladenine (3-MA) and Wortmannin are both known to negatively regulate autophagy through inhibition of phosphatidylinositol-3 kinase (PI3K),[108] and are commonly used to identify the role of autophagy in NP-induced cell death. Furthermore, chemicals that influence lysosomal activity by alkalinization of its acidic lumen (e.g. chloroquine)[109] or inhibition of lysosomal enzymes (e.g. pepstatin A) can inhibit autophagosome-lysosome fusion and/or block the breakdown of the sequestered cargo in the autolysosome. These type of chemicals can be applied to mimic disruptions in autophagy flux. It is important to note that these chemicals can influence other cellular processes that can indirectly affect autophagy. It is therefore recommended to combine chemical modulation with other approaches such as genetic inhibition or functional knockdown of relevant Atg genes.[97,99]

In conclusion, to study the complex and dynamic process of autophagy a number of different assays and detection techniques are required to accurately and reliably link certain effects to the modulation of autophagy. It is however necessary to comprehend that assays based on autophagosome detection not necessarily provide information on the status of autophagy flux.

Also, since each of the above-described methods has its advantages and flaws, we advise to combine several assays when evaluating autophagy - as we have done in **Chapter 6**.

4. NANOPARTICLE-INDUCED AUTOPHAGIC CHANGES

Over the last decade, an increasing number of nanotoxicological studies have reported on the ability of diverse types of NPs to modulate autophagy in various cell types.[63] Even more, it has been suggested that autophagic changes might be a common cellular response to NP uptake.[110] Since autophagy is essential to maintain cellular homeostasis, these findings could have great toxicological impact. In fact, insufficient or defective autophagy is argued to lie at the origin of multiple pathologies including cancer,[111–113] neurodegenerative diseases,[114,115] myopathies,[116] autoimmune diseases[117] and metabolic diseases.[118] Unfortunately, this may also imply that NPs capable of disrupting autophagy may result in or contribute to the development of these pathologies. In the context of disease, it is pivotal to appreciate the complexity of the autophagic process and that the impact of autophagy induction or inhibition on cell or animal physiology can vary and is often ambiguous. For example, autophagy induction can have beneficial effects on healthy cells by boosting their survival capacity or enhancing immune reactivity by improved presentation of antigens in dendritic cells,[119,120] but also on diseased cells by ameliorated clearance of dysfunctional organelles or protein aggregates in myopathies or neurodegenerative diseases.[121–124] On the other hand, uncontrolled induction of autophagy could lead to massive cell death and organ failure.[125] Apart from toxicological effects, the induction of autophagy could aid the cell to overcome NP-associated stress, as such lowering NP-associated toxicity. Yet, its induction might also hamper the functionality of NPs, for instance, by enclosing and degrading drug loaded nanocarriers or fluorescent NPs in autophagosomes in this way reducing their efficacy.[126–128]

Considering these observations, it is relevant to define the influence of NPs on autophagy from a toxicological as well as from a therapeutic point of view. In the following section we therefore seek to summarize the underlying mechanisms by which NPs can affect autophagy.

Mechanisms of nanoparticle-induced autophagic changes

As visualized in **Figure 5.6,** NPs can enter the autophagy pathway via multiple routes, yet they all initiate with endocytosis**.**

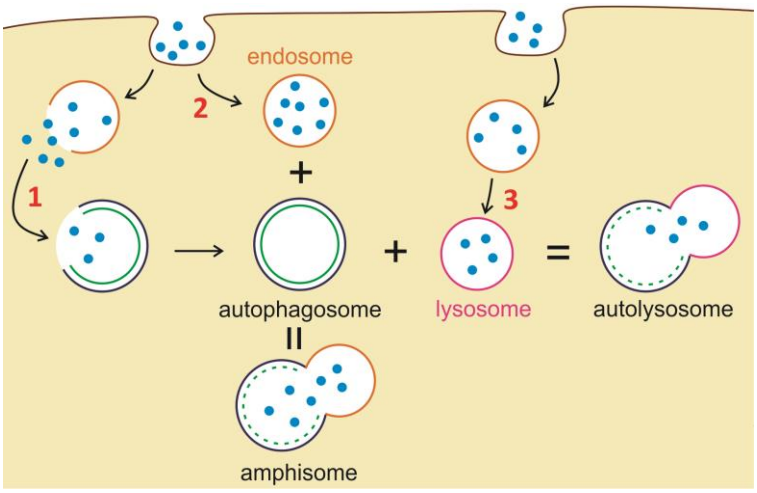

Figure 5.6 | Routes via which NPs can enter the autophagic pathway. 1) NPs able of escaping the endosome (e.g. by proton sponge effect) can be captured by autophagosomes 2) Following endocytosis, the NPs are enclosed in endosomes that next fuse with autophagosomes to form amphisomes. 3) NPs that move further down the endocytic pathway can end up in lysosomes that next fuse with autophagosomes.[129]

Similar to entry routes, NPs can affect the autophagy pathway through various mechanisms. As explained earlier in this chapter, one of the key mechanisms by which NPs elicit cellular toxicity is by formation of ROS. This **ROS formation** can next damage the entire cytoplasmic environment including organelles, proteins and lipids. As a result, autophagy will be activated to attempt to restore this stressful situation by removal of the respective components. Mitochondria are specifically sensitive to ROS and are therefore often specifically removed by autophagy (i.e. mitophagy). It is important to note that not only the secondary effects of ROS (e.g. mitochondrial damage) but also increased levels of ROS as such are able of tuning the level of autophagy by altering the activity of different intracellular signaling molecules.[130–132] Autophagy has been shown to be regulated by different types of ROS, and ROS-mediated autophagy is involved in various pathologies, including cancer.[131] Since metal-oxide particles and heavy metal-containing NPs are generally more prone to inducing oxidative stress, those may have high autophagy-modulating properties.[131]

Since the majority of NPs enter the cell through endocytosis, the lysosomes are also frequently a target for their toxicity. NPs can cause **lysosomal dysfunction** by alkalinization of its lumen, NP overload, oxidative damage to lysosomes or cytoskeleton disruption.[129,133,134] These dysfunctions can indirectly upregulate autophagy as a mechanism for the cell to compensate for insufficient degradative capacity. The signaling link between lysosomal sensing of stress and autophagy is effected by Transcription Factor EB (TFEB), a main regulator of the Coordinated Lysosomal Expression and Regulation (CLEAR) network.[135] Upon starvation and lysosomal stress TFEB will detach from the sensing machinery present on the lysosome and translocate to the nucleus

where it will boost the transcription of lysosomal and autophagic genes.[136] For this reason, non-degradable NPs (for instance Au NPs) or formulations containing compounds that cannot be efficiently metabolized (e.g. cationic lipids) that are taken up by endocytosis at high doses are more likely to result in autophagy disruption.

NPs can also **directly influence autophagy-related signaling** pathways or gene expression of relevant autophagy genes.[129] It has further been hypothesized that **NPs can be directed toward autophagic degradation** in a manner similar to pathogens and cytoplasmic material.[128] In practice, this involves NP ubiquitination and binding of p62 which links the NPs to the autophagic machinery.[137–139] Accordingly, autophagy induction might be a way to try to eliminate these foreign particles.

Impact of nanoparticles on autophagy

In this section we provide an overview of the most interesting reports on NP-mediated autophagy alterations. At the same time, we aim to link specific physicochemical characteristics to the autophagic response of the cell.

Influence of hard nanoparticles on autophagy

Gold Nanoparticles

Several research groups have shown alterations in autophagic activity upon treatment with different types of Au NPs. Ma *et al.* demonstrated an Au NP-mediated mTOR-independent accumulation of autophagosomes owing to a blockage of autophagosome degradation. The lysosomal impairment elicited by these gold particles, demonstrated by lysosomal enlargement and alkalinization, probably accounts for this blockage. Interestingly, in line with the observed **size-dependent** uptake, larger particles (50 nm) were more potent autophagy flux disruptors compared to their smaller equivalents (10 and 25 nm). We could indeed hypothesize that larger NPs can have a greater effect on the lysosomal degradative potential than a large number of smaller particles which can be more readily degraded. Besides size preliminary results further uncovered a potential **charge-dependent** autophagy response with more autophagosome accumulation upon treatment with positively charged NP compared to equally sized negative ones.[140] Certainly, it is well-known that positively charged NPs are more able to destabilize or permeabilize the lysosomal membrane than negative ones.

Several groups reported on autophagy stimulation triggered by oxidative stress induced by Au NPs. FBS-coated Au NPs generated significant signs of oxidative stress in human lung fibroblasts, a probable cause of the simultaneously observed autophagosome accumulation.[141] Oxidative stress was also detected in oral cancer cells in the presence of iron core-gold shell particles

(Fe@Au), although this was not the primary cause of NP toxicity. Notably, these particles provoked different levels of autophagy in cancerous and benign cells which further led to the hypothesis that the concurrently observed selective growth inhibition is caused by a different reaction of the cancerous and healthy mitochondria toward the induced stress.[142] NPs of comparable composition, i.e. gold-coated iron oxide NPs, also activated autophagy in lung cancer cells.[142]

Iron oxide nanoparticles

Analogous to the Fe@Au NPs, bare IONPs selectively induced cytotoxicity in lung cancer cells while causing a minor decrease in cell viability in normal lung fibroblasts. The origin of this differential toxicity was suggested to be oxidative stress and subsequent autophagy upregulation via the AMPK-Akt-mTOR pathway, which was supported by the observed mitochondrial damage and ATP depletion.[143] Bare IONPs also provoked oxidative stress in macrophages and human cerebral endothelial cells, although we argue that the proposed autophagy induction stated by the authors conflicts with the increased levels of p62.[143,144] Magnetite (Fe_3O4) particles were shown to enhance autophagosome levels through lysosomal impairment and mitochondrial damage.[145] Remarkably, an elegant study of Huang *et al*. demonstrated that IONPs elicited a rise in autophagosomes in a **dispersity-dependent** manner: aggregated particles induced substantial autophagic disruption while well-dispersed particles did not.[146] Comparable to **size-related** effects, the accumulation of large NP aggregates in the endosomes and/or lysosomes could be responsible for lysosomal impairment and at the same time autophagosome accumulation.

Quantum Dots

QDs of multiple compositions have been put forward as autophagy activators. Again, the changes in autophagy are regularly put forth as a response to oxidative stress.[136,147–150] As an illustration COOH-functionalized CdSe/ZnS QDs were able to provoke ROS-dependent LC3-II accumulation. Here, a ROS scavenger as well as 3-MA enhanced cell death indicating autophagy served as a protective mechanism against QD cytotoxicity.[151] The latter finding is in contrast with a study conducted with similar COOH-conjugated CdTe QDs where 3-MA reduced cytotoxicity, suggestive of a pro-death role for autophagy.[150] Graphene QDs along with streptavidine-coated core-shell ones were found to induce autophagy which in case of the streptavidin-coated QDs could be abrogated by antioxidant treatment.[149] For the graphene QDs, ROS-dependency was also suggested, yet this was not experimentally demonstrated.[148] Neibert *et al*. discovered that treatment with uncapped CdTe QDs significantly activated TFEB, which they identify as a cellular attempt to remove the damaged cytoplasmic material generated by QD treatment.[136] Interestingly, Seleverstov *et al.* reported on a **size-dependent** effect where smaller QDs modulated autophagy more extensively than their larger counterparts.[147] This seems in contrast

with the previously discussed studies where larger particles consistently elicited a higher autophagic response. However, the total surface area of smaller QDs is substantially higher than for larger ones owing to their higher surface over volume ratio.[152] This higher surface area could then result in raised levels of oxidative stress that in turn can influence autophagy. This aspect of size versus surface area clearly illustrates that it is often hard to predict the impact of NPs and their modifications on NP-cell interactions. It is therefore relevant to systematically investigate the influence of QD physicochemistry on their induced cellular effects. To this end, we have examined the impact of QD surface coating on the lysosomal and autophagic pathway, which we will discuss in **Chapter 6.**

Carbon-based nanoparticles

Various types of carbon-based NPs have been shown to alter autophagy. For instance, carboxyl functionalized carbon nanotubes (CNTs) affected autophagy in an mTOR dependent manner in A549 cells, conversely, differently functionalized particles (with poly(m-aminobenzenesulphonic acid or PEG) did not. Even so potential differences in uptake by the different CNTs were not examined, this does suggest that **surface group characteristics** may influence the impact of NPs on autophagy modulation. Interestingly, besides restoring cell viability *in vitro,* pre-treatment with 3-MA partly abrogated NP-mediated lung inflammation in mice indicating a role for autophagy in lung toxicity.[153]

Furthermore, a detailed study of Wan *et al.* demonstrated that acid-functionalized CNTs and graphene oxides caused autophagosome accumulation by compromised autophagy flux in primary murine peritoneal macrophages. The underlying mechanism was clarified by means of LysoTracker staining and FITC-dextran labeling of NP treated cells, which revealed decreased lysosomal quantity and lysosomal membrane damage, respectively.[154] Surely, as described above, it is well established lysosomal health strongly influences autophagy.[129] It is noteworthy that, despite their comparable chemical composition and surface functionalization, CNT and graphene oxides affected autophagy to a different extent. This suggests **physical characteristics** might also influence autophagy modulation, yet a more thorough study is necessary to substantiate this. [154] Fullerenes have been correlated with autophagy induction as well as dysfunction. [154] For example, fullerene (C60) and Neodymium functionalized fullerenes (C60(Nd)) are presented as autophagy inducers,[155,156] while Johnson-Lyles *et al.* suggest fullenerol NPs can disturb autophagy at high concentration. They hypothesize the observed NP-mediated cytoskeleton disruption results in autophagy dysfunction and consequently ATP depletion.[157]

Other hard nanoparticles

A study describing the autophagic response of A549 cells and macrophages toward diversely shaped silica (SiO_2) NPs reported that the cell type but not the **geometry** of the particles shaped this response.[158] Also with silica particles a **size-dependent** autophagy response has been observed: 40 and 60 nm sized particles elevated autophagosome levels while 200 nm sized ones did not.[159]

A great variety of rare-earth element based NPs were described to induce authentic autophagy in HeLa cells.[155,160–163] Among these studies there was a remarkable example of how **surface group characteristics** can influence the autophagy-inducing potential of a NP. This was presented by Zhang *et al.,* who were able to adapt the level of induction upon treatment with lanthanide-based upconversion NPs by coating them with different peptides.[160] Another interesting example of **size-dependent** autophagy alteration was reported with neodymium oxide particles where non-nanoscale particles elicited less of an autophagic response.[164]

Not only surface characteristics but also **chemical composition** has been brought forward as a way of tuning autophagy: treatment of HeLa cells with Nickel-Cobalt NPs with different molar concentrations of both components revealed that the higher the Ni component, the more potent the impact on cytotoxicity and autophagy. [165]

Influence of soft nanoparticles on autophagy

Compared to the substantial amount of literature describing metallic NP-induced autophagy, the evidence for polymeric and lipid particles remains rather limited. However, several reports indicate that also these materials are capable of modulating autophagy.

Liposomes

Induction of autophagy has been observed in HeLa cells upon treatment with dioleoyltrimethylammonium propane (DOTAP), a cationic lipid commonly used as a transfection agent. The results not only suggest that DOTAP enhances autophagosome formation but also demonstrate that the induction is mTOR-independent.[166] The autophagy activation may be caused by the fact that DOTAP is a synthetic lipid and the cell undergoes problems degrading it. As a result, the cell aims to increase its total degradative capacity by the induction of autophagy. Naturally, the fact that transfection agents as such are able of enhancing autophagy casts doubt on observations made in transfected cells, particularly if autophagy is the process examined. At the same time, this implies that inhibition of autophagy might aid to improve transfection efficiency. The latter hypothesis was corroborated by Roberts *et al.* who found that cationic liposomes were delivered to the autophagic pathway through endosome-autophagosome fusion, indicative of a cellular attempt to eliminate the foreign material. In addition, gene delivery and

expression was remarkably enhanced in autophagy-defective Atg5$^{-/-}$ cells.[127] Interestingly, treatment with un**charge**d lipids (i.e. dioleoylphosphatidylethanolamine; DOPE) failed to alter autophagy.[166] A finding that is in contrast with the ability of neutral PEGylated C6-ceramide nanoliposomes to activate fully functional autophagy in liver HepG2 cells.[167]

Polymeric nanoparticles

Autophagy modulation was observed upon treatment of macrophages with positively charged polymer (Eudragit RS) particles. In this case TEM showed significant localization of particles inside or in contact with mitochondria. Furthermore, substantial signs of oxidative stress were observed. The authors thus propose that the cell aims to remove the damaged mitochondria by triggering autophagy.[168]

Cationic polyamidoamine (PAMAM) dendrimers of multiple generations (G3 to G8) have been proposed to induce autophagy in A549 lung cancer cells with involvement of the mTOR pathway. However, it was not specified if the increased level of LC3, assessed by microscopy and Western Blotting, was caused by an enhanced on-rate or decreased off-rate of autophagosomes, therefore, an autophagy blockage cannot be excluded.[169] As PAMAM dendrimers have been reported to cause lysosomal alkalinization,[170] potentially resulting in lysosomal impairment, a blockage of flux is rather likely. On the other hand it has been put forth that these dendrimers can affect mTOR activity during their endocytic uptake; the observed autophagy alteration could thus be a combination of multiple effects. Intriguingly, comparable with the conflicting findings obtained with differently charged lipids, anionic G5.5 PAMAM particles did not affect autophagic activity. Together, these data suggest that **charge** may have an impact on the autophagy-inducing potential of NPs, however, without any uptake comparison between the various particles it cannot be excluded that this is merely because of differences in uptake efficiency.

5. CONCLUSION

In general, the field of nanotechnology is greatly expanding, increasing the public's exposure to NPs at a fast pace. Since many of these (in)organic NPs have been proposed to be capable of altering autophagy, and since autophagy dysfunction itself is associated with multiple pathologies (e.g. neurodegenerative diseases), it is of vital medical and toxicological importance to determine the effect of NPs on autophagy and its consequences. To efficiently address this potential danger more in-depth research is necessary to determine the role of autophagy in these pathologies and at the same time the mechanisms by which NPs are able of altering this process. Throughout this chapter several NP properties were put forth as probable influencing factors on NP-mediated autophagy deregulation, including size, charge and chemical

composition. For most NPs, the extent of autophagy is presumably determined by a complex interplay of these different parameters. In general, the wide variety of NPs and used cell types makes it difficult to draw any broad conclusions. There is therefore a great need for more systematic studies that will aid the design of NPs that do not affect autophagy at all or can be tuned to induce autophagy to our advantage. In **Chapter 6** we aim to contribute to this objective by looking into the influence on autophagy of two identical particles that only differ in their surface modification.

6. REFERENCES

1. Laurent, S. *et al.* Magnetic iron oxide nanoparticles: synthesis, stabilization, vectorization, physicochemical characterizations, and biological applications. *Chem. Rev.* **108,** 2064 (2008).

2. Michalet, X. *et al.* Quantum dots for live cells, in vivo imaging, and diagnostics. *Science* **307,** 538–44 (2005).

3. Saha, K., Agasti, S. S., Kim, C., Li, X. & Rotello, V. M. Gold nanoparticles in chemical and biological sensing. *Chem. Rev.* **112,** 2739–2779 (2012).

4. De Volder, M. F. L., Tawfick, S. H., Baughman, R. H. & Hart, A. J. Carbon nanotubes: present and future commercial applications. *Science (80-.).* **339,** 535–539 (2013).

5. Chen, G., Roy, I., Yang, C. & Prasad, P. N. Nanochemistry and Nanomedicine for Nanoparticle-based Diagnostics and Therapy. *Chem. Rev.* **116,** 2826–2885 (2016).

6. StatNano. Ranking of Countries in Nanotechnology Publications in 2016. 3–6 (2017). at <http://statnano.com/news/57105>

7. Kim, B. Y. S., Rutka, J. T. & Chan, W. C. . Nanomedicine. *N. Engl. J. Med.* **363,** 2434–43 (2010).

8. Bangham, A. D., Standish, M. M. & Watkins, J. C. Diffusion of univalent ions across the lamellae of swollen phospholipids. *J. Mol. Biol.* **13,** IN26-IN27 (1965).

9. Al-Jamal, W. T. & Kostarelos, K. Liposomes: From a clinically established drug delivery system to a nanoparticle platform for theranostic nanomedicine. *Acc. Chem. Res.* **44,** 1094–1104 (2011).

10. Hatakeyama, H., Akita, H. & Harashima, H. The Polyethyleneglycol Dilemma: Advantage and Disadvantage of PEGylation of Liposomes for Systemic Genes and Nucleic Acids Delivery to Tumors. *Biol. Pharm. Bull.* **36,** 892–899 (2013).

11. Schütz, C. A., Juillerat-Jeanneret, L., Mueller, H., Lynch, I. & Riediker, M. Therapeutic nanoparticles in clinics and under clinical evaluation. *Nanomedicine* **8,** 449–467 (2013).

12. Sercombe, L. *et al.* Advances and challenges of liposome assisted drug delivery. *Front. Pharmacol.* **6,** 1–13 (2015).

13. Grimaldi, N. *et al.* Lipid-based nanovesicles for nanomedicine. *Chem. Soc. Rev.* **45,** 6520–6545 (2016).

14. Biswas, S., Kumari, P., Lakhani, P. M. & Ghosh, B. Recent advances in polymeric micelles for anti-cancer drug delivery. *Eur. J. Pharm. Sci.* **83,** 184–202 (2016).

15. Shi, M., Lu, J. & Shoichet, M. S. Organic nanoscale drug carriers coupled with ligands for targeted drug delivery in cancer. *J. Mater. Chem.* **19,** 5485 (2009).

16. Nanjwade, B. K., Bechra, H. M., Derkar, G. K., Manvi, F. V. & Nanjwade, V. K. Dendrimers: Emerging polymers for drug-delivery systems. *Eur. J. Pharm. Sci.* **38,** 185–196 (2009).

17. Pandita, D., Poonia, N., Kumar, S., Lather, V. & Madaan, K. Dendrimers in drug delivery and targeting: Drug-dendrimer interactions and toxicity issues. *J. Pharm. Bioallied Sci.* **6,** 139 (2014).

18. Dreaden, E. C., Austin, L. A., Mackey, M. A. & El-Sayed, M. A. Size matters: gold nanoparticles in targeted cancer drug delivery. *Ther. Deliv.* **3,** 457–478 (2012).

19. Hilger, I. & Kaiser, W. a. Iron oxide-based nanostructures for MRI and magnetic hyperthermia. *Nanomedicine* **7,** 1443–1459 (2012).

20. Mornet, S., Vasseur, S., Grasset, F. & Duguet, E. Magnetic nanoparticle design for medical diagnosis and therapy. *J. Mater. Chem.* **14,** 2161–2175 (2004).

21. Pagliari, F. *et al.* Cerium oxide nanoparticles protect cardiac progenitor cells from oxidative stress. *ACS Nano* **6,** 3767–3775 (2012).

22. Daraee, H. *et al.* Application of gold nanoparticles in biomedical and drug delivery. *Artif. Cells, Nanomedicine, Biotechnol.* **44,** 410–422 (2016).

23. Wong, K. K. Y. & Liu, X. Silver nanoparticles—the real 'silver bullet' in clinical medicine? *Med. Chem. Commun.* **1,** 125–131 (2010).

24. Amendola, V., Pilot, R., Frasconi, M., Maragò, O. M. & Iatì, M. A. Surface plasmon resonance in gold nanoparticles: a review. *J. Phys. Condens. Matter* **29,** 203002 (2017).

25. Skrabalak, S. E., Au, L., Lu, X., Li, X. & Xia, Y. Gold nanocages for cancer detection and treatment. *Nanomedicine (Lond).* **2,** 657–668 (2007).

26. Xiong, R. *et al.* Comparison of Gold Nanoparticle Mediated Photoporation: Vapor Nanobubbles Outperform Direct Heating for Delivering Macromolecules in Live Cells. *ACS Nano* **8,** 6288–6296 (2014).

27. Xiong, R. *et al.* Cytosolic Delivery of Nanolabels Prevents Their Asymmetric Inheritance and Enables Extended Quantitative in Vivo Cell Imaging. *Nano Lett.* **16,** 5975–5986 (2016).

28. Chan, W. C. . *et al.* Luminescent quantum dots for multiplexed biological detection and imaging. *Curr. Opin. Biotechnol.* **13,** 40–46 (2002).

29. Xu, G. *et al.* New Generation Cadmium-Free Quantum Dots for Biophotonics and Nanomedicine. *Chem. Rev.* **116,** 12234–12327 (2016).

30. Cha, C., Shin, S. R., Annabi, N., Dokmeci, M. R. & Khademhosseini, A. Carbon-based nanomaterials: Multifunctional materials for biomedical engineering. *ACS Nano* **7,** 2891–2897 (2013).

31. Oberdörster, G. Safety assessment for nanotechnology and nanomedicine: Concepts of nanotoxicology. *J. Intern. Med.* **267,** 89–105 (2010).

32. Donaldson, K. Nanotoxicology. *Occup. Environ. Med.* **61,** 727–728 (2004).

33. Fischer, H. C. & Chan, W. C. Nanotoxicity: the growing need for in vivo study. *Curr. Opin. Biotechnol.* **18,** 565–571 (2007).

34. Oberdörster, G., Oberdörster, E. & Oberdörster, J. Nanotoxicology: An emerging discipline evolving from studies of ultrafine particles. *Environ. Health Perspect.* **113,** 823–839 (2005).

35. Donaldson, K. Resolving the nanoparticles paradox. *Nanomedicine* **1,** 229–234 (2006).

36. Kroll, A., Pillukat, M. H., Hahn, D. & Schnekenburger, J. Interference of engineered nanoparticles with in vitro toxicity assays. *Arch. Toxicol.* **86,** 1123–1136 (2012).

37. Monteiro-Riviere, N. A., Inman, A. O. & Zhang, L. W. Limitations and relative utility of screening assays to assess engineered nanoparticle toxicity in a human cell line. *Toxicol. Appl. Pharmacol.* **234,** 222–235 (2009).

38. Magdolenova, Z., Lorenzo, Y., Collins, A. & Dusinska, M. Can Standard Genotoxicity Tests be Applied to Nanoparticles? *J. Toxicol. Environ. Heal. Part A* **75,** 800–806 (2012).

39. El-Ansary, A. & Al-Daihan, S. On the Toxicity of Therapeutically Used Nanoparticles: An Overview. *J. Toxicol.* **2009,** 1–9 (2009).

40. Nel, A., Xia, T., Mädler, L. & Li, N. Toxic potential of materials at the nanolevel. *Science (80-.).* **311,** 622–627 (2006).

41. Duffin, R., Tran, L., Brown, D., Stone, V. & Donaldson, K. Proinflammogenic Effects of Low-Toxicity and Metal Nanoparticles In Vivo and In Vitro: Highlighting the Role of Particle Surface Area and Surface Reactivity. *Inhal. Toxicol.* **19,** 849–856 (2007).

42. Park, E. J. & Park, K. Oxidative stress and pro-inflammatory responses induced by silica nanoparticles in vivo and in vitro. *Toxicol. Lett.* **184,** 18–25 (2009).

43. Chen, B. *et al.* In vitro evaluation of cytotoxicity and oxidative stress induced by multiwalled carbon nanotubes in murine RAW 264.7 macrophages and human A549 lung cells. *Biomed. Environ. Sci.* **24,** 593–601 (2011).

44. Soenen, S. J., De Cuyper, M., De Smedt, S. C. & Braeckmans, K. *Investigating the toxic effects of iron oxide nanoparticles*. *Methods in Enzymology* **509,** (Elsevier Inc., 2012).

45. Freyre-Fonseca, V. *et al.* Titanium dioxide nanoparticles impair lung mitochondrial function. *Toxicol. Lett.* **202,** 111–119 (2011).

46. Soenen, S. J. *et al.* Cellular toxicity of inorganic nanoparticles: Common aspects and guidelines for improved nanotoxicity evaluation. *Nano Today* **6,** 446–465 (2011).

47. Feng, X. *et al.* Central nervous system toxicity of metallic nanoparticles. *Int. J. Nanomedicine* **10,** 4321–4340 (2015).

48. Xie, Y. *et al.* Size-dependent cytotoxicity of Fe3O4 nanoparticles induced by biphasic regulation of oxidative stress in different human hepatoma cells. *Int. J. Nanomedicine* **11,** 3557–3570 (2016).

49. Wilhelmi, V. *et al.* Zinc Oxide Nanoparticles Induce Necrosis and Apoptosis in Macrophages in a p47phox- and Nrf2-Independent Manner. *PLoS One* **8,** e65704 (2013).

50. Singh, N. *et al.* NanoGenotoxicology: The DNA damaging potential of engineered nanomaterials. *Biomaterials* **30,** 3891–3914 (2009).

51. Hussain, S. *et al.* in *Advances in Experimental Medicine and Biology* 111–134 (Springer, Dordrecht, 2014). doi:10.1007/978-94-017-8739-0_7

52. Naumanen, P., Lappalainen, P. & Hotulainen, P. Mechanisms of actin stress fibre assembly. *J. Microsc.* **231,** 446–454 (2008).

53. Buyukhatipoglu, K. & Clyne, A. M. Superparamagnetic iron oxide nanoparticles change endothelial cell morphology and mechanics via reactive oxygen species formation. *J. Biomed. Mater. Res. Part A* **96A,** 186–195 (2011).

54. Brookes, P. S., Yoon, Y., Robotham, J. L., Anders, M. W. & Sheu, S.-S. Calcium, ATP, and ROS: a mitochondrial love-hate triangle. *AJP Cell Physiol.* **287,** C817–C833 (2004).

55. Yu, K.-N. *et al.* Titanium Dioxide Nanoparticles Induce Endoplasmic Reticulum Stress-Mediated Autophagic Cell Death via Mitochondria-Associated Endoplasmic Reticulum Membrane Disruption in Normal Lung Cells. *PLoS One* **10,** e0131208 (2015).

56. Hussain, S. *et al.* in 111–134 (Springer, Dordrecht, 2014). doi:10.1007/978-94-017-8739-0_7

57. Pisanic, T. R., Blackwell, J. D., Shubayev, V. I., Fiñones, R. R. & Jin, S. Nanotoxicity of iron oxide nanoparticle internalization in growing neurons. *Biomaterials* **28,** 2572–2581 (2007).

58. Gu, Y. J. *et al.* Nuclear penetration of surface functionalized gold nanoparticles. *Toxicol. Appl. Pharmacol.* **237,** 196–204 (2009).

59. Soenen, S. J. *et al.* Cytotoxic Effects of Gold Nanoparticles: A Multiparametric Study. *ACS Nano* **6,** 5767–5783 (2012).

60. Wu, Y.-L. *et al.* Biophysical Responses upon the Interaction of Nanomaterials with Cellular Interfaces. *Acc. Chem. Res.* **46,** 782–791 (2012).

61. Tay, C. Y. *et al.* Nanoparticles Strengthen Intracellular Tension and Retard Cellular Migration. *Nano Lett.* **14,** 83–88 (2014).

62. Comfort, K. K., Maurer, E. I., Braydich-Stolle, L. K. & Hussain, S. M. Interference of Silver, Gold, and Iron Oxide Nanoparticles on Epidermal Growth Factor Signal Transduction in Epithelial Cells. *ACS Nano* **5,** 10000–10008 (2011).

63. Peynshaert, K. *et al.* Exploiting Intrinsic Nanoparticle Toxicity: The Pros and Cons of Nanoparticle-Induced Autophagy in Biomedical Research. *Chem. Rev.* **114,** 7581–7609 (2014).

64. Christen, V. & Fent, K. Silica nanoparticles and silver-doped silica nanoparticles induce endoplasmatic reticulum stress response and alter cytochrome P4501A activity. *Chemosphere* **87,** 423–434 (2012).

65. Free, P. *et al.* Cathepsin L digestion of Nanobioconjugates upon endocytosis. *ACS Nano* **3,** 2461–2468 (2009).

66. Soenen, S. J., Demeester, J., De Smedt, S. C. & Braeckmans, K. The cytotoxic effects of polymer-coated quantum dots and restrictions for live cell applications. *Biomaterials* **33,**

4882–4888 (2012).

67. Mahto, S. K., Park, C., Yoon, T. H. & Rhee, S. W. Assessment of cytocompatibility of surface-modified CdSe/ZnSe quantum dots for BALB/3T3 fibroblast cells. *Toxicol. Vitr.* **24,** 1070–1077 (2010).

68. Cedervall, T. *et al.* Understanding the nanoparticle-protein corona using methods to quantify exchange rates and affinities of proteins for nanoparticles. *Proc. Natl. Acad. Sci.* **104,** 2050–2055 (2007).

69. Maiorano, G. *et al.* Effects of Cell Culture Media on the Dynamic Formation of Protein−Nanoparticle Complexes and Influence on the Cellular Response. *ACS Nano* **4,** 7481–7491 (2010).

70. Lynch, I., Salvati, A. & Dawson, K. A. Protein-nanoparticle interactions: What does the cell see? *Nat. Nanotechnol.* **4,** 546–547 (2009).

71. Mahmoudi, M., Laurent, S., Shokrgozar, M. A. & Hosseinkhani, M. Toxicity Evaluations of Superparamagnetic Iron Oxide Nanoparticles: Cell 'Vision' *versus* Physicochemical Properties of Nanoparticles. *ACS Nano* **5,** 7263–7276 (2011).

72. Dobrovolskaia, M. A., Shurin, M. & Shvedova, A. A. Current understanding of interactions between nanoparticles and the immune system. *Toxicol. Appl. Pharmacol.* **299,** 78–89 (2016).

73. Li, W., Li, J. & Bao, J. Microautophagy: lesser-known self-eating. *Cell. Mol. Life Sci.* **69,** 1125–1136 (2012).

74. Kaushik, S. & Cuervo, A. M. Chaperone-mediated autophagy: a unique way to enter the lysosome world. *Trends Cell Biol.* **22,** 407–417 (2012).

75. Klionsky, D. J. Autophagy: from phenomenology to molecular understanding in less than a decade. *Nat. Rev. Mol. Cell Biol.* **8,** 931–937 (2007).

76. Peynshaert, K. *et al.* Coating of Quantum Dots strongly defines their effect on lysosomal health and autophagy. *Acta Biomater.* **48,** 195–205 (2017).

77. Pankiv, S. *et al.* p62/SQSTM1 binds directly to Atg8/LC3 to facilitate degradation of ubiquitinated protein aggregates by autophagy. *J. Biol. Chem.* **282,** 24131–24145 (2007).

78. Bjorkoy, G. *et al.* in *Methods in Enzymology: Autophagy in Mammalian Systems, Vol 452, Pt B* (ed. Klionsky, D. J.) **452,** 181–197 (Elsevier Academic Press Inc, 2009).

79. Komatsu, M. & Ichimura, Y. Physiological significance of selective degradation of p62 by autophagy. *FEBS Lett.* **584,** 1374–1378 (2010).

80. Jung, C. H., Ro, S.-H., Cao, J., Otto, N. M. & Kim, D.-H. mTOR regulation of autophagy. *FEBS Lett.* **584,** 1287–1295 (2010).

81. Kroemer, G., Marino, G. & Levine, B. Autophagy and the Integrated Stress Response. *Mol. Cell* **40,** 280–293 (2010).

82. Deretic, V. Autophagy in immunity and cell-autonomous defense against intracellular microbes. *Immunol. Rev.* **240,** 92–104 (2011).

83. Scherz-Shouval, R. & Elazar, Z. Regulation of autophagy by ROS: physiology and pathology. *Trends Biochem. Sci.* **36,** 30–38 (2011).

84. Tsujimoto, Y. & Shimizu, S. Another way to die: autophagic programmed cell death. *Cell Death Differ.* **12,** 1528–1534 (2005).

85. Shen, H. M. & Codogno, P. Autophagic cell death Loch Ness monster or endangered species? *Autophagy* **7,** 457–465 (2011).

86. Denton, D., Nicolson, S. & Kumar, S. Cell death by autophagy: facts and apparent artefacts. *Cell Death Differ.* **19,** 87–95 (2012).

87. Galluzzi, L. *et al.* Molecular definitions of cell death subroutines: Recommendations of the Nomenclature Committee on Cell Death 2012. *Cell Death Differ.* **19,** 107–120 (2012).

88. Clarke, P. G. H. & Puyal, J. Autophagic cell death exists. *Autophagy* **8,** 867–869 (2012).

89. Shen, S., Kepp, O. & Kroemer, G. The end of autophagic cell death? *Autophagy* **8,** 1–3 (2012).

90. De Stefano, D., Carnuccio, R. & Maiuri, M. C. Nanomaterials Toxicity and Cell Death Modalities. *J. Drug Deliv.* **2012,** (2012).

91. Rubinstein, A. D. & Kimchi, A. Life in the balance - a mechanistic view of the crosstalk between autophagy and apoptosis. *J Cell Sci* **125,** 5259–5268 (2012).

92. Loos, B., Engelbrecht, A. M., Lockshin, R. A., Klionsky, D. J. & Zakeri, Z. The variability of autophagy and cell death susceptibility: Unanswered questions. *Autophagy* **9,** 1270–1285 (2013).

93. Loos, B. & Engelbrecht, A. M. Cell death: a dynamic response concept. *Autophagy* **5,** 590–603 (2009).

94. Klionsky DJ, Abdelmohsen K, Abe A, Abedin MJ, Abeliovich H, Acevedo Arozena A, Adachi H, Adams CM, Adams PD, Adeli K, Adhihetty PJ, Adler SG, Agam G, Agarwal R, Aghi MK, Agnello M, Agostinis P, Aguilar PV, Aguirre-Ghiso J, Airoldi EM, Ait-Si-Ali S, Akemat, Z. S. Guidelines for use and interpretation of assays for monitoring autophagy (3rd edition). *Autophagy* **12,** 1–222 (2016).

95. Eskelinen, E.-L., Reggiori, F., Baba, M., Kovacs, A. L. & Seglen, P. O. Seeing is believing The impact of electron microscopy on autophagy research. *Autophagy* **7,** 935–956 (2011).

96. Eskelinen, E.-L. To be or not to be? Examples of incorrect identification of autophagic compartments in conventional transmission electron microscopy of mammalian cells. *Autophagy* **4,** 257–260 (2008).

97. Mizushima, N., Yoshimori, T. & Levine, B. Methods in Mammalian Autophagy Research. *Cell* **140,** 313–326 (2010).

98. Kabeya, Y. *et al.* LC3, a mammalian homologue of yeast Apg8p, is localized in autophagosome membranes after processing. *EMBO J.* **19,** 5720–5728 (2000).

99. Klionsky, D. J. *et al.* Guidelines for the use and interpretation of assays for monitoring autophagy. *Autophagy* **8,** 445–544 (2012).

100. Kimura, S., Fujita, N., Noda, T. & Yoshimori, T. in *Methods in Enzymology: Autophagy in Mammalian Systems, Vol 452, Pt B* (ed. Klionsky, D. J.) **452,** 1–12 (2009).

101. Mizushima, N. & Yoshimori, T. How to interpret LC3 immunoblotting. *Autophagy* **3,** 542–545 (2007).

102. Kimura, S., Noda, T. & Yoshimori, T. Dissection of the autophagosome maturation process by a novel reporter protein, tandem fluorescent-tagged LC3. *Autophagy* **3,** 452–460 (2007).

103. Hundeshagen, P., Hamacher-Brady, A., Eils, R. & Brady, N. R. Concurrent detection of autolysosome formation and lysosomal degradation by flow cytometry in a high-content screen for inducers of autophagy. *BMC Biol.* **9,** 38 (2011).

104. Shvets, E., Fass, E. & Elazar, Z. Utilizing flow cytometry to monitor autophagy in living mammalian cells. *Autophagy* **4,** 621–628 (2008).

105. Ikenoue, T., Hong, S. & Inoki, K. in *Methods in Enzymology: Autophagy in Mammalian Systems, Vol 452, Pt B* (ed. Klionsky, D. J.) **452,** 165–180 (2009).

106. Mizushima, N., Yamamoto, A., Matsui, M., Yoshimori, T. & Ohsumi, Y. In vivo analysis of autophagy in response to nutrient starvation using transgenic mice expressing a fluorescent autophagosome marker. *Mol. Biol. Cell* **15,** 1101–1111 (2004).

107. Ravikumar, B. *et al.* Inhibition of mTOR induces autophagy and reduces toxicity of polyglutamine expansions in fly and mouse models of Huntington disease. *Nat. Genet.* **36,** 585–595 (2004).

108. Wu, Y.-T. *et al.* Dual Role of 3-Methyladenine in Modulation of Autophagy via Different Temporal Patterns of Inhibition on Class I and III Phosphoinositide 3-Kinase. *J. Biol. Chem.* **285,** 10850–10861 (2010).

109. Yoon, Y. H. *et al.* Induction of Lysosomal Dilatation, Arrested Autophagy, and Cell Death by Chloroquine in Cultured ARPE-19 Cells. *Invest. Ophthalmol. Vis. Sci.* **51,** 6030–6037 (2010).

110. Zabirnyk, O., Yezhelyev, M. & Seleverstov, O. Nanoparticles as a novel class of autophagy activators. *Autophagy* **3,** 278–281 (2007).

111. Mizushima, N., Levine, B., Cuervo, A. M. & Klionsky, D. J. Autophagy fights disease through cellular self-digestion. *Nature* **451,** 1069–1075 (2008).

112. Rosenfeldt, M. T. & Ryan, K. M. The multiple roles of autophagy in cancer. *Carcinogenesis* **32,** 955–963 (2011).

113. Maes, H., Rubio, N., Garg, A. D. & Agostinis, P. Autophagy: shaping the tumor microenvironment and therapeutic response. *Trends Mol. Med.* **19,** 428–446 (2013).

114. Stern, S. T. & Johnson, D. N. Role for nanomaterial-autophagy interaction in neurodegenerative disease. *Autophagy* **4,** 1097–1100 (2008).

115. Nixon, R. A. The role of autophagy in neurodegenerative disease. *Nat. Med.* **19,** 983–997 (2013).

116. Gottlieb, R. A. & Mentzer, R. M. Autophagy During Cardiac Stress: Joys and Frustrations of Autophagy. *Annu. Rev. Physiol.* **72,** 45–59 (2010).

117. Levine, B., Mizushima, N. & Virgin, H. W. Autophagy in immunity and inflammation. *Nature* **469,** 323–335 (2011).

118. Rubinsztein, D. C., Codogno, P. & Levine, B. Autophagy modulation as a potential therapeutic target for diverse diseases. *Nat. Rev. Drug Discov.* **11,** 709–730 (2012).

119. Luo, Y. H. *et al.* Cadmium-based quantum dot induced autophagy formation for cell survival via oxidative stress. *Chem. Res. Toxicol.* **26,** 662–673 (2013).

120. Li, H. Y., Li, Y. H., Jiao, J. & Hu, H. M. Alpha-alumina nanoparticles induce efficient autophagy-dependent cross-presentation and potent antitumour response. *Nat. Nanotechnol.* **6,** 645–650 (2011).

121. Hara, T. *et al.* Suppression of basal autophagy in neural cells causes neurodegenerative disease in mice. *Nature* **441,** 885–889 (2006).

122. Komatsu, M. *et al.* Loss of autophagy in the central nervous system causes neurodegeneration in mice. *Nature* **441,** 880–884 (2006).

123. Cheung, Z. H. & Ip, N. Y. Autophagy deregulation in neurodegenerative diseases - recent advances and future perspectives. *J. Neurochem.* **118,** 317–325 (2011).

124. Pickford, F. *et al.* The autophagy-related protein beclin 1 shows reduced expression in early Alzheimer disease and regulates amyloid beta accumulation in mice. *J. Clin. Invest.* **118,** 2190–9 (2008).

125. Kunapuli, S., Rosanio, S. & Schwarz, E. R. 'How Do Cardiomyocytes Die?' Apoptosis and Autophagic Cell Death in Cardiac Myocytes. *J. Card. Fail.* **12,** 381–391 (2006).

126. Vercauteren, D. *et al.* Dynamic colocalization microscopy to characterize intracellular trafficking of nanomedicines. *ACS Nano* **5,** 7874–7884 (2011).

127. Roberts, R. *et al.* Autophagy and formation of tubulovesicular autophagosomes provide a barrier against nonviral gene delivery. *Autophagy* **9,** 667–682 (2013).

128. Remaut, K., Oorschot, V., Braeckmans, K., Klumperman, J. & De Smedt, S. C. Lysosomal capturing of cytoplasmic injected nanoparticles by autophagy: An additional barrier to non viral gene delivery. *J. Control. Release* **195,** 29–36 (2014).

129. Stern, S. T., Adiseshaiah, P. P. & Crist, R. M. Autophagy and lysosomal dysfunction as emerging mechanisms of nanomaterial toxicity. *Part. Fibre Toxicol.* **9,** (2012).

130. Scherz-Shouval, R. & Elazar, Z. Regulation of autophagy by ROS: Physiology and pathology. *Trends Biochem. Sci.* **36,** 30–38 (2011).

131. Lee, J., Giordano, S. & Zhang, J. Autophagy, mitochondria and oxidative stress: cross-talk and redox signalling. *Biochem. J.* **441,** 523–540 (2012).

132. Scherz-Shouval, R. *et al.* Reactive oxygen species are essential for autophagy and specifically regulate the activity of Atg4. *Embo J.* **26,** 1749–1760 (2007).

133. Wang, F. *et al.* Time resolved study of cell death mechanisms induced by amine-modified polystyrene nanoparticles. *Nanoscale* **5,** 10868–76 (2013).

134. Settembre, C. *et al.* TFEB Links Autophagy to Lysosomal Biogenesis. *Science (80-.).* **332,** 1429–1433 (2011).

135. Settembre, C. *et al.* A lysosome-to-nucleus signalling mechanism senses and regulates the lysosome via mTOR and TFEB. *Embo J.* **31,** 1095–1108 (2012).

136. Neibert, K. D. & Maysinger, D. Mechanisms of cellular adaptation to quantum dots - the role of glutathione and transcription factor EB. *Nanotoxicology* **6,** 249–262 (2012).

137. Hundeshagen, P., Hamacher-Brady, A., Eils, R. & Brady, N. R. Concurrent detection of autolysosome formation and lysosomal degradation by flow cytometry in a high-content screen for inducers of autophagy. *Bmc Biol.* **9,** (2011).

138. Brancolini, G., Kokh, D. B., Calzolai, L., Wade, R. C. & Corni, S. Docking of Ubiquitin to Gold Nanoparticles. *ACS Nano* **6,** 9863–9878 (2012).

139. Liu, K.-K. *et al.* Ubiquitin-coated nanodiamonds bind to autophagy receptors for entry into the selective autophagy pathway. *Autophagy* **13,** 187–200 (2017).

140. Ma, X. *et al.* Gold Nanoparticles Induce Autophagosome Accumulation through Size-Dependent Nanoparticle Uptake and Lysosome Impairment. *ACS Nano* **5,** 8629–8639 (2011).

141. Li, J. J., Hartono, D., Ong, C.-N., Bay, B.-H. & Yung, L.-Y. L. Autophagy and oxidative stress associated with gold nanoparticles. *Biomaterials* **31,** 5996–6003 (2010).

142. Wu, Y.-N. *et al.* The selective growth inhibition of oral cancer by iron core-gold shell nanoparticles through mitochondria-mediated autophagy. *Biomaterials* **32,** 4565–4573 (2011).

143. Khan, M. I. *et al.* Induction of ROS, mitochondrial damage and autophagy in lung epithelial cancer cells by iron oxide nanoparticles. *Biomaterials* **33,** 1477–1488 (2012).

144. Park, E.-J. *et al.* ERK pathway is activated in bare-FeNPs-induced autophagy. *Arch. Toxicol.* **88,** 323–336 (2014).

145. Zhang, X. *et al.* Iron oxide nanoparticles induce autophagosome accumulation through multiple mechanisms: Lysosome impairment, mitochondrial damage, and ER stress. *Mol. Pharm.* **13,** 2578–2587 (2016).

146. Huang, D., Zhou, H. & Gao, J. Nanoparticles modulate autophagic effect in a dispersity-dependent manner. *Sci. Rep.* **5,** 14361 (2015).

147. Seleverstov, O. *et al.* Quantum dots for human mesenchymal stem cells labeling. A size-dependent autophagy activation. *Nano Lett.* **6,** 2826–2832 (2006).

148. Markovic, Z. M. *et al.* Graphene quantum dots as autophagy-inducing photodynamic agents. *Biomaterials* **33,** 7084–7092 (2012).

149. Chen, L. *et al.* The role of elevated autophagy on the synaptic plasticity impairment caused by CdSe/ZnS quantum dots. *Biomaterials* **34,** 10172–10181 (2013).

150. Wu, J., Chen, Q., Liu, W., Zhang, Y. & Lin, J.-M. Cytotoxicity of quantum dots assay on a microfluidic 3D-culture device based on modeling diffusion process between blood vessels and tissues. *Lab Chip* **12,** 3474–3480 (2012).

151. Luo, Y.-H. *et al.* Cadmium-Based Quantum Dot Induced Autophagy Formation for Cell Survival via Oxidative Stress. *Chem. Res. Toxicol.* **26,** 662–673 (2013).

152. Soenen, S. J. H. & De Cuyper, M. Assessing iron oxide nanoparticle toxicity in vitro: current status and future prospects. *Nanomedicine* **5,** 1261–1275 (2010).

153. Liu, H.-L. *et al.* A functionalized single-walled carbon nanotube-induced autophagic cell death in human lung cells through Akt–TSC2-mTOR signaling. *Cell Death Dis.* **2,** e159 (2011).

154. Wan, B. *et al.* Single-walled carbon nanotubes and graphene oxides induce autophagosome accumulation and lysosome impairment in primarily cultured murine peritoneal macrophages. *Toxicol. Lett.* **221,** 118–127 (2013).

155. Wei, P., Zhang, L., Lu, Y., Man, N. & Wen, L. C60(Nd) nanoparticles enhance chemotherapeutic susceptibility of cancer cells by modulation of autophagy. *Nanotechnology* **21,** 495101 (2010).

156. Zhang, Q. *et al.* Autophagy-mediated chemosensitization in cancer cells by fullerene C60 nanocrystal. *Autophagy* **5,** 1107–17 (2009).

157. Johnson-Lyles, D. N. *et al.* Fullerenol cytotoxicity in kidney cells is associated with cytoskeleton disruption, autophagic vacuole accumulation, and mitochondrial dysfunction. *Toxicol. Appl. Pharmacol.* **248,** 249–258 (2010).

158. Herd, H. L., Malugin, A. & Ghandehari, H. Silica nanoconstruct cellular toleration threshold in vitro. *J. Control. Release* **153,** 40–48 (2011).

159. Li, Q. *et al.* Cytotoxicity and autophagy dysfunction induced by different sizes of silica particles in human bronchial epithelial BEAS-2B cells. *Toxicol. Res. (Camb).* **5,** 1216–1228 (2016).

160. Zhang, Y. *et al.* Tuning the autophagy-inducing activity of lanthanide-based nanocrystals through specific surface-coating peptides. *Nat. Mater.* **11,** 817–26 (2012).

161. Yu, L., Lu, Y., Man, N., Yu, S.-H. & Wen, L.-P. Rare Earth Oxide Nanocrystals Induce Autophagy in HeLa Cells. *Small* **5,** 2784–2787 (2009).

162. Wei, P.-F. *et al.* Accelerating the clearance of mutant huntingtin protein aggregates through autophagy induction by europium hydroxide nanorods. *Biomaterials* **35,** 899–907 (2014).

163. Hussain, S. *et al.* Cerium Dioxide Nanoparticles Induce Apoptosis and Autophagy in Human Peripheral Blood Monocytes. *ACS Nano* **6,** 5820–5829 (2012).

164. Chen, Y., Yang, L., Feng, C. & Wen, L.-P. Nano neodymium oxide induces massive vacuolization and autophagic cell death in non-small cell lung cancer NCI-H460 cells. *Biochem. Biophys. Res. Commun.* **337,** 52–60 (2005).

165. Dong, L. *et al.* Tuning Magnetic Property and Autophagic Response for Self-Assembled Ni-Co Alloy Nanocrystals. *Adv. Funct. Mater.* **23,** 5930–5940 (2013).

166. Man, N., Chen, Y., Zheng, F., Zhou, W. & Wen, L. P. Induction of genuine autophagy by cationic lipids in mammalian cells. *Autophagy* **6,** 449–454 (2010).

167. Adiseshaiah, P. P. *et al.* Synergistic combination therapy with nanoliposomal C6-ceramide and vinblastine is associated with autophagy dysfunction in hepatocarcinoma and colorectal cancer models. *Cancer Lett.* **337,** 254–265 (2013).

168. Eidi, H. *et al.* Drug delivery by polymeric nanoparticles induces autophagy in macrophages. *Int. J. Pharm.* **422,** 495–503 (2012).

169. Li, C. *et al.* PAMAM Nanoparticles Promote Acute Lung Injury by Inducing Autophagic Cell Death through the Akt-TSC2-mTOR Signaling Pathway. *J. Mol. Cell Biol.* **1,** 37–45 (2009).

170. Thomas, T. P. *et al.* Cationic poly(amidoamine) dendrimer induces lysosomal apoptotic

pathway at therapeutically relevant concentrations. *Biomacromolecules* **10,** 3207–14 (2009).

6

Coating of Quantum Dots strongly defines their effect on lysosomal health and autophagy

An adapted version of this chapter is published as:

Karen Peynshaert[a,b], Stefaan J. Soenen[c], Bella B. Manshian[c], Shareen H. Doak[e], Kevin Braeckmans[a,d], Stefaan C. De Smedt[a,b], Katrien Remaut[a,b]. Coating of Quantum Dots strongly defines their effect on lysosomal health and autophagy. *Acta Biomaterialia* **48** 195-205 (2017)

[a]Lab of General Biochemistry and Physical Pharmacy, Faculty of Pharmaceutical Sciences, Ghent University, Ottergemsesteenweg 460, B9000 Ghent, Belgium. [b]Ghent Research Group on Nanomedicines, Ghent University, Ottergemsesteenweg 460, B9000 Ghent, Belgium.

[c]Biomedical MRI Unit/MoSAIC, Department of Imaging and Pathology, Catholic University of Leuven, Faculty of Medicine, UZ Herestraat 49 Box 7003, B3000- Leuven

[d]Centre for Nano- and Biophotonics, Ghent University, B9000 Ghent, Belgium.

[e] Institute of Life Science, College of Medicine, Swansea University, Singleton Park, Swansea, SA2 8PP Wales

ABSTRACT

In **Chapter 5** we explained that autophagy dysfunction has been proposed to lie at the root of multiple diseases including cancer. We therefore consider it crucial from a toxicological point of view to investigate if nanoparticles (NPs) that are developed for biomedical applications interfere with this cellular process. Here, we study the highly promising 'gradient alloyed' quantum dots (QDs) that differ from conventional ones by their gradient core composition which allows for better fluorescent properties. We carefully examined the toxicity of two identical gradient alloyed QDs, differing only in their surface coatings, namely 3-mercaptopropionic acid (MPA) and polyethylene glycol (PEG). Next to more conventional toxicological endpoints like cytotoxicity and oxidative stress, we examined the influence of these QDs on the autophagy pathway. Our study shows that the cellular effects induced by QDs on HeLa cells were strongly dictated by the surface coat of the otherwise identical particles. MPA-coated QDs proved to be highly biocompatible as a result of lysosomal activation and ROS reduction, two cellular responses that help the cell to cope with nanoparticle-induced stress. In contrast, PEGylated QDs were significantly more toxic due to increased ROS production and lysosomal impairment. This impairment next resulted in autophagy dysfunction which likely added to their toxic effects. Taken together, our study shows that coating QDs with MPA is a better strategy than PEGylation for long term cell tracking with minimal cytotoxicity.

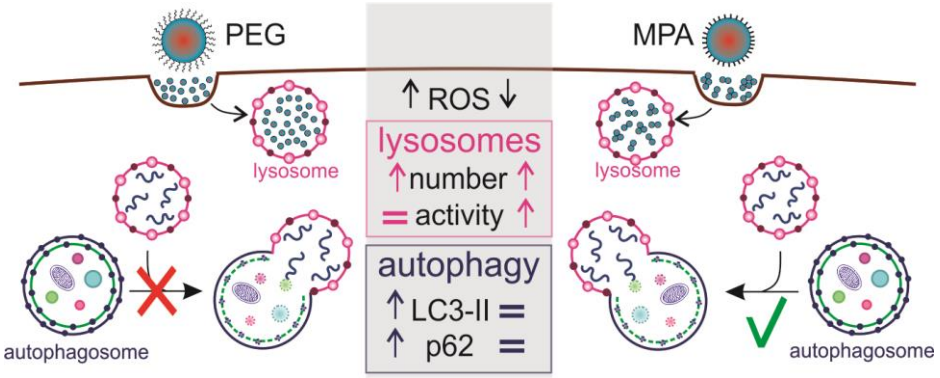

Table of Contents

1. INTRODUCTION

As introduced in **Chapter 5**, nanotechnology is a rapidly evolving field with a growing potential for a wide range of applications. These applications naturally require the design of highly functional though biocompatible nanoparticles (NPs). Among the most extensively investigated NPs for biomedical imaging applications are Quantum Dots (QDs), semiconductor nanocrystals with a size ranging from 2 to 100 nm.[1] They possess supremely advantageous optical properties including a very high and stable fluorescence intensity that is strongly resistant to photobleaching.[2] In addition, they are known for their broad excitation spectrum and narrow emission profile enabling efficient multiplexing.[3] Based on these features QDs have been promoted as eminent materials for *in vivo* and *in vitro* biomedical applications such as tumor visualization and intracellular trafficking.[1,4–6]

With the aim to enhance the biocompatibility and optical properties of the conventional core-shell QDs, many QD designs and compositions have been investigated. Recently, gradient alloyed (GA) QDs were developed (**Figure 6.1**).[7] The gradient structure ensures that instead of the usual size-tunable emission of conventional QDs, the emission spectra of GA-QDs can be subtly altered by adjusting their chemical composition.[8,9] This solves issues related to size limitation sometimes occurring in biological labeling and allows multiplexing of QDs without size-related changes in sensitivity.[8,10]

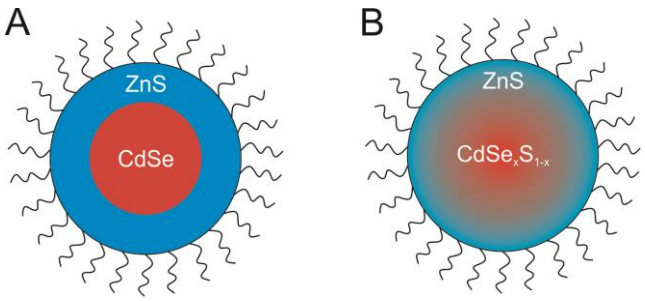

Figure 6.1 | Schematic design of a core-shell QD (A) and a gradient alloyed QD (B). A conventional core-shell QD exists of a metal core enveloped by an inorganic shell and a coating that renders them water-soluble and allows for further conjugation.[11] In case of gradient alloyed QDs, the defined core-shell interface within the QD is replaced by a gradient composition.

Despite their excellent properties, the translation of QDs in general toward biomedical applications is limited, mainly due to concerns about their toxicity. It is widely established that this toxicity, at least *in vitro*, is mainly attributed to the leaching of toxic cadmium ions and the formation of reactive oxygen species (ROS) that can induce secondary toxic effects such as DNA damage and apoptosis (cfr. **Chapter 5**).[12–16] To avoid these toxic pathways, several groups are attempting to develop a more biocompatible QD core by synthesizing e.g. cadmium-free QDs.[17,18]

However, next to core composition, the surface chemistry of the QD can greatly influence toxicity by affecting its cellular interactions.

As extensively discussed in **Chapter 5**, several research groups have recently reported that various types of NPs can modulate (macro)autophagy.[19,20] Autophagy is a highly conserved catabolic process essential for maintaining cellular homeostasis (**Figure 6.2**). It is usually present at a basal level in every cell where it functions as a cytoplasmic housekeeper for organelle and protein quality control. In addition, autophagy serves as a cytoprotective process that is induced to support the cell in stressful conditions such as starvation or oxidative stress.[21] Autophagy perturbations have been associated with the pathogenesis of multiple diseases including cancer, neurodegeneration and liver disease.[22–24] To date, the exact influence of cellular NP exposure on the autophagic process remains unclear. Various studies have reported clear induction of autophagy, resulting in cell death,[19] whereas others have described an inhibition on autophagosome clearance, which can also result in cell death.[25] The direct induction of cell death through the autophagy process however remains a topic of debate, as autophagy is mainly a self-preservation process and any alterations observed during cell death could simply be the result of secondary unrelated bystander effects of the cell trying to recover (cfr. **Chapter 5**).[26] In line with the latter view, it has been suggested that the induction of autophagy could be beneficial, as the overall toxicity of NPs could be reduced by the protective effects of autophagy.[27,28]

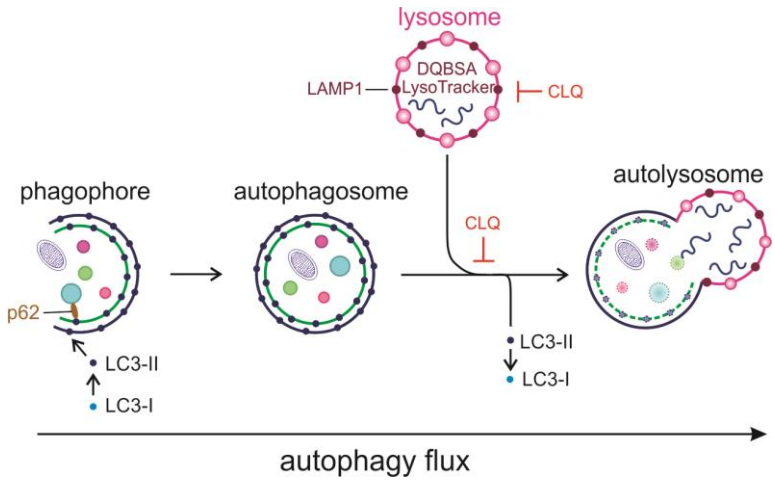

Figure 6.2 | Overview of lysosomal and autophagosomal markers investigated in this study. As lysosomal markers we made use of: LAMP-1, a membrane protein selective for lysosomes;[29] LysoTracker, a dye that primarily accumulates in lysosomes; and Derivatively Quenched Bovine Serum Albumn (DQ BSA), a dye that enters the cell via endocytosis and is therefore selectively degraded by the lysosomal pathway [30]. To check for changes in autophagy we examined LC3, a protein selectively incorporated into the autophagosomal membrane, and p62 which is a protein that links LC3 to autophagosomal cargo. Since the buffer chloroquine (CLQ) induces lysosomal alkalinization we applied it throughout our study to mimick lysosomal impairment. Since this lysosomal impairment causes a block in autophagosome-lysosome fusion further down the line, we also used CLQ as a positive control for autophagosomal accumulation.[31]

Considering the impact of autophagy induction and inhibition as described above, we believe it is critical to characterize the influence of NPs on autophagy from a nanotoxicological point of view.[19] However, despite abundant reports on NP-modulated autophagy, only a few studies exist related to QDs, where especially little attention has been paid to the potential harm induced by the highly promising GA-QDs.[32] In addition**,** many of those studies are limited to one type of coating or lack data on intracellular uptake as debated in **Chapter 5**.[19]

In this chapter we look into the influence of QD surface chemistry on the toxicity and its underlying causes by comparing two types of QDs that only differ in their coating. We opted for polyethylene glycol (PEG) as a coating since this is the most commonly applied coating strategy in biomedical applications to reduce unspecific protein binding and prevent aggregation. In addition, PEGylation is known to increase the blood circulation time of particles by preventing NP uptake by the reticuloendothelial system.[33–35] As a second coating strategy we selected the short ligand 3-mercaptopropionic acid (MPA) based on previous reports that observed limited toxicity with this coating.[29–31] We therefore wanted to analyze this promising observation further with a special focus on autophagy since the influence of MPA coating on this pathway remains unexplored so far. To this end, we examined the aggregation profile, cellular uptake, cytotoxicity and associated ROS levels of QDs, and studied their effect on lysosomes and autophagosomes - the two most essential organelles of the autophagy pathway (**Figure 6.2**).

2. METHODS

Materials

Two types of spherically shaped Gradient Alloy Quantum Dots were purchased from Mesolight LLC (Little Rock, Arkansas, USA). Both types have a gradient $CdSe_xS_{1-x}$ core surrounded by a ZnS shell. (**Figure 6.1**). The GA-QDs only differ in their surface coating: one particle is coated with polyethylene glycol (PEG) with terminating carboxyl groups while the other one is coated with 3-mercaptopropionic acid (MPA). Both QDs have an emission maximum at 580nm and exhibit very similar quantum yields, i.e. 60% for PEG-QDs and 65% for MPA-QDs. All QD dispersions were diluted from the original colloidal suspensions that were stored in H_2O with a concentration of 10 µM for PEGylated QDs (stored at pH 7) and 15 µM for MPA-coated QDs (stored at pH 11). LC3-, p62-, actin and LAMP-1-antibodies were purchased from Cell Signaling (Beverly, USA); secondary AlexaFluor® tagged antibodies, LysoTracker®, DQ™ red BSA and CellROX® were purchased from Molecular Probes™ (Invitrogen, Belgium).

Nanoparticle characterization

The hydrodynamic size and zeta potential of the QDs were determined using a Malvern Zetasizer Nano (Malvern Instruments, Worcestershire, U.K.). For this purpose the QDs were diluted to a concentration of 20 nM in HEPES buffer or Phosphate buffer saline (PBS) prior to performing the measurements at 25 °C. The refractive index was set to 2.56 based on the QD manufacturer's protocol (Mesolight). Size measurements were done in triplicate with three runs per replicate and presented based on the number distribution. The zeta potentials were calculated from the electrophoretic mobility based on the Henry equation considering the Smoluchowski approximation. Zeta potential measurements were done in triplicate with two runs per replicate. The stability of both QDs in cell culture media was assessed with Single Particle Tracking. For these measurements 20nM of PEG-QDs and 125nM of MPA-QDs were incubated in cell culture medium for 24 h at room temperature. After this incubation the samples were further diluted in cell culture medium (by gently pipetting) and transferred to a microscopy slide. Next, we recorded 30 movies of 5 seconds of the diffusing particles using a Sweptfield Confocal Microscope (Nikon® Eclipse T*i*) equipped with a 60× (1.40 NA) oil immersion objective (Nikon®). After movie acquisition the trajectories of the particles were calculated using image processing software. Out of these trajectories the diffusion coefficient per particle was determined which was next converted into a size distribution. A detailed description of this technique and its benefits can be found here [39].

Cell culture

The cervical epithelial cancer cell line HeLa was purchased from ATCC (CCL-2). The stable GFP-LC3 HeLa cell line was a kind gift from Prof. Felix Randow (MRC Laboratory of Molecular Biology, Cambridge, UK). Both cell types were cultured using DMEM/F12 cell culture media (Gibco®, Paisly, UK) supplemented with 10% fetal bovine serum (Hyclone®, Cramilton, UK), 1% L-glutamine (Gibco®, Paisly, UK) and 2% penicillin – streptomycine solution (Gibco®, Paisly, UK). Cells were passaged at 80% confluency and incubated at 37°C with 5.0% CO_2.

MTT cell viability

Cells were seeded in a 96 well plate at a cell density of 20.000 cells per well. After QD treatment the medium was removed and the cells were washed twice with PBS (Gibco®, Paisly, UK). Next, fresh medium containing 5 mg/ml of MTT reagent (Sigma-Aldrich, USA) was added to the cells and incubated for 3 h at 37°C. Following this incubation, the medium was carefully removed and the formazan crystals were dissolved by incubation with DMSO on a shaker for 1 h. Finally, the absorbance was measured at 590 nm and 690 (background) with an Envision plate reader (Perkin Elmer, Zaventem, Belgium). The percentage of viability was then calculated by comparison with

untreated cells representing 100% viability. To check for potential interference of the QDs with the MTT assay absorbance was also measured for several controls. The positive control (cells treated for 15 min with 0,1% Triton X-100) was compared to cells treated with QDs followed by incubation with Triton X-100. Also, culture medium containing QDs and incubated with MTT reagent was compared to culture medium only incubated with MTT reagent. In both cases, no significant change in the assay readout was detected between the controls.

Cellular uptake, oxidative stress, lysosomal and autophagy markers measured by flow cytometry.

All autophagy-related studies were performed in accordance to the guidelines published by Klionsky *et al*.[40]. All flow cytometry experiments were at least performed in triplicate. For this purpose cells were seeded in a 24 well plate at a density of 60.000 cells per well. The general protocol was as follows: after 24 h of incubating the cells with QDs in full cell culture medium, the medium was removed after which a washing step with PBS was performed. Next, the cells were detached with 300 µl of 0.25% Trypsin-EDTA (Gibco®, Paisly, UK), followed by neutralizing the trypsin with 500 µl of cell culture medium and transferring the cell suspension to FACS tubes. The samples were next centrifuged at 300g for 5 min, the supernatant was removed, and the cells were resuspended in FACS buffer. This wash cycle was performed two times. Finally, the cells were resuspended in 300 µl of FACS buffer prior to analyzing them with a FACScalibur flow cytometer (BD, Erembodegem, Belgium). Data acquisition was performed with BD CellQuest™ software while the data analysis was done with Flowjo software (Tree Star Inc). The staining protocols for the respective experiments are described below.

Cellular uptake. HeLa cells were incubated with 400 µl of medium containing the respective concentrations of QDs for 24 h. After this the flow cytometry protocol as described above was executed.

LysoTracker® staining. This dye, which stains all lysosomal vesicles, was used to estimate QD-induced changes in total lysosomal content. Cells were exposed to QDs for 24 h or to 50 µM of chloroquine for 4h. After a washing step with PBS, cells were incubated with 100 nM of LysoTracker Red® DND-99 for 30 min at 37°C.

DQ™ Red BSA staining. This dye, which is degraded by the lysosomal pathway, was used to estimate QD-induced changes in the degradative capacity of lysosomes. After a 24 h incubation with QDs and a washing step with PBS the cells were treated with 10 µg/ml DQ BSA for 3 h at 37°C, allowing the endocytic uptake of the fluorescent BSA. Chloroquine-treated and starved

cells were pre-incubated for 1 h with 50 µM chloroquine or serum-free medium prior to co-incubation with DQ BSA so that the total treatment was each time 4 h.

CellROX® staining. Cells were exposed to QDs for 24 h. After a washing step with PBS, cells were incubated with 5 µM of CellROX® Deep Red for 30 min at 37°C.

GFP-LC3 detection. This protocol was based on a method described by Eng *et al.*[41] Hela cells stably expressing GFP-LC3 were seeded in a 24 well plate with a density of 60.000 cells per well. The general flow cytometry protocol was followed except for the first washing step which was performed with 0.05% saponin (Sigma-Aldrich, USA) instead of PBS. This special washing step ensures that only the LC3 present on autophagosomal membranes, which is insoluble, remains intact. After the saponin washing step, two wash cycles with PBS were executed after which the samples were analyzed.

Immunofluorescence staining for LAMP-1 and LC3

For these experiments 100.000 cells were seeded in a 35 mm microscopy dish, left to adhere overnight and were then treated with QDs for 24 h, or with chloroquine or serum-free medium for 4 h. After a washing step with PBS, the cells were fixed using 2% paraformaldehyde (Sigma-Aldrich, USA) for 15 min. Next, the fixative was removed and the cells were washed three times with PBS. The cells were next permeabilized by a 15 min incubation with 0.5% Tween 20 (Sigma-Aldrich, USA) in PBS. After removing the permeabilization agent the cells were washed three times with blocking buffer (5% goat serum in PBS), after which they were incubated with blocking buffer for 15 min. Adequately diluted primary rabbit antibodies were then applied to the cells and incubated for 1 h. After washing three times with blocking buffer, the cells were incubated with Goat anti-Rabbit Alexafluor® 647 antibodies (Life Technologies, Invitrogen, Belgium) for 1 h. After two final washing steps with PBS, the samples were kept in Vectashield antifade medium (Vector Laboratories, USA) at 4°C until imaging. All the steps of the immunostaining protocol were performed at room temperature. The samples were visualized with a Sweptfield Confocal microscope (Nikon, Belgium) using a 60x oil Plan Apo objective (Nikon, Belgium). Post-image processing of the images was done using ImageJ/FIJI software (NIH).

Western Blot

For this experiment 750.000 cells were seeded in a T25 flask. After treatment, the cell medium was removed and the cells were washed twice with ice cold PBS and harvested by scraping. The cell suspension was then centrifuged for 8 min at 1100 rpm at 4°C. The supernatant was removed and the cell pellet was resuspended in RIPA buffer (Sigma-Aldrich, USA) supplemented

with protease inhibitors (Sigma-Aldrich, USA). This suspension was next centrifuged at 10 000 g for 10 min at 4°C after which the supernatants were collected and kept at -80°C until use. Protein concentrations were determined using the DC™ Protein Assay (BD, Erembodegem, Belgium). For Western blotting equal amounts of protein were loaded on a 12% SDS-PAGE gel and transferred onto a PVDF membrane (BD, Erembodegem, Belgium). After the transfer the blots were blocked with 5% bovine serum albumin (Sigma-Aldrich, USA) for 1 h at room temperature after which they were incubated overnight at 4°C with the designated primary antibodies diluted in blocking buffer. Next, the blots were incubated with HRP-conjugated secondary antibody (Cell Signaling, USA) for 1 h at room temperature. Finally the blots were visualized using the Bio-Rad ImmunStar™ WesternC™ chemiluminescent kit (Biorad) on a VersaDoc™ Imaging System (Biorad).

Statistical Analysis

All experiments were analyzed for statistical significance with a one-way ANOVA followed by the Bonferroni post hoc test to estimate significance between treated groups, or followed by the Dunnett post hoc test when compared to an untreated group. The results were considered as statistically significant if $p < 0.05$. The number of asterisks in the figures indicate the statistical significance as follows: *p<0.05; **p<0.01; ***p<0.001. All statistical analysis was performed with Graphpad Prism 5 software (San Diego, CA).

3. RESULTS

Quantum Dot characterization

As described in **Figure 6.3**, DLS measurements showed that both QDs exhibit similar size (∼20 nm) and zeta potential (∼ -22 mV) in HEPES buffer. A negative zeta potential could be expected for both QDs since MPA is a strong acid and the PEG chains have carboxyl end groups. To characterize the QDs in an ion-rich solution (similar to cell medium) we examined their size and zeta potential in PBS. In this buffer, the PEGylated QDs remain stable (∼20 nm), while the MPA-coated ones form aggregates (**Figure 6.3A**). As expected, exposure to cell culture medium elicited a similar trend as in PBS: PEGylated QDs show an uniform size distribution while MPA-QDs clearly aggregate as indicated by their very broad size distribution (**Figure 6.3B**). In PBS the charge of PEGylated QDs is neutralized to -10 mV while MPA-coated QDs exhibit similar charge as in HEPES buffer, being -22 mV (**Figure 6.3C**).

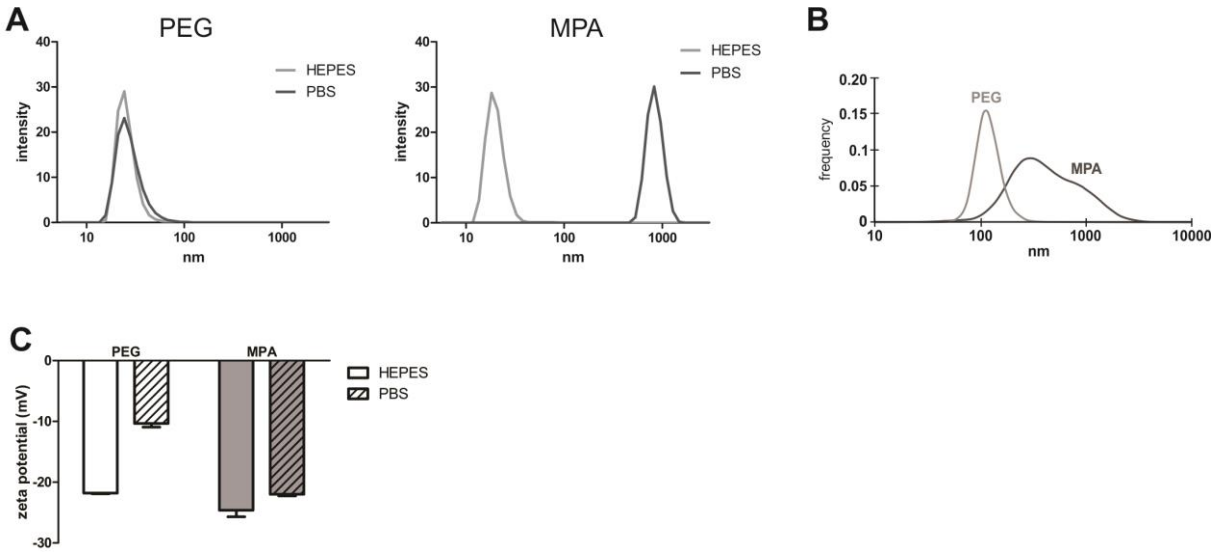

Figure 6.3 | Quantum dot characterization. A) QD size measured in HEPES and PBS by DLS; B) QD size measured in full medium by SPT, C) zeta-potential of the QDs in HEPES and PBS as measured by DLS. Error bars represent the SEM.

Uptake and intracellular localization of Quantum Dots

Uptake experiments (**Figure 6.4**) showed that PEGylated QDs are easily taken up at low concentrations, though the uptake does reach a plateau around 40 nM and decreases at concentrations above 60 nM. In contrast, MPA QDs are only efficiently taken up starting from a concentration of 80 nM, and their uptake increases proportionally to the administered dose. In order to study the intracellular effects later on, we continued our study with dosages of the two types of QDs that should result in comparable intracellular concentrations. Considering the similar quantum yield of both QDs we compared dosages that gave an identical average fluorescence intensity per cell, i.e. 20 nM PEG QDs and 125 nM MPA QDs, as well as 50 nM of PEG QDs and 175 nM of MPA QDs. As discussed in more detail later, **Figure 6.6** shows that both QDs accumulate in the perinuclear region and co-localize strongly with lysosomes, indicating that both particles are taken up by endocytosis.

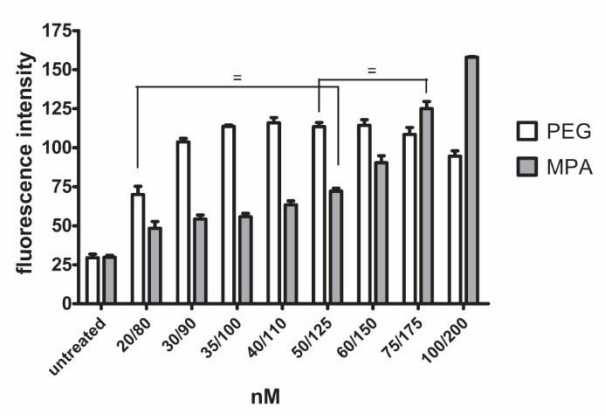

Figure 6.4 | Uptake of QDs in HeLa cells. Uptake was determined by flow cytometry after 24h of QD exposure in full medium (n=3). The x-axis denotes the QD dosage: for PEGylated QDs this ranges from 20 to 100nM, while for MPA-coated QDs this ranges from 80 to 200nM. PEGylated QDs are easily taken up at low concentrations though uptake reaches a maximum around 40 nM. MPA-coated QDs are taken up proportionally with increasing dosage, though are only taken up efficiently at higher concentrations. 20 nM of PEGylated QDs leads to similar intracellular fluorescence levels as 125 nM of MPA-coated QDs. Similarly, incubation with 50 nM of PEGylated QDs results in similar intracellular fluorescence levels as 175 nM of MPA-coated QDs. Error bars represent the SEM.

Quantum Dot-induced acute toxicity and oxidative stress

QD-induced cytotoxicity was determined based on reduction in cellular enzymatic activity. This was tested using the common MTT viability assay after a QD incubation of 24 h for a concentration range up to 200 nM. As shown in **Figure 6.5A**, MPA QDs did not evoke significant toxicity over the tested concentration range. In contrast, PEGylated QDs clearly elicited a dose dependent toxicity with a significant decrease in cell viability ranging from 80.6% (± 1.8) viability at 50 nM to 33.7% (± 1.2) viability at 200 nM. Next to enzymatic activity, we also determined cytotoxicity based on cell membrane rupture by measuring propidium iodide uptake which gave identical results (data not shown). The level of ROS, a measure for oxidative stress, was determined by incubation of QD treated cells with CellROX®, a dye that becomes fluorescent after oxidation by ROS. As shown in **Figure 6.5B**, a 24 h exposure of HeLa cells to PEGylated QDs gave rise to significantly higher levels of ROS: 123 (±4.3)% for 20 nM and 135 (±4.0)% for 50 nM. Remarkably, in case of MPA QDs the oxidative stress level decreased, as the ROS levels were significantly reduced to 85 (±4.5)% and 76 (± 5.1)% for 125 nM and 175 nM respectively.

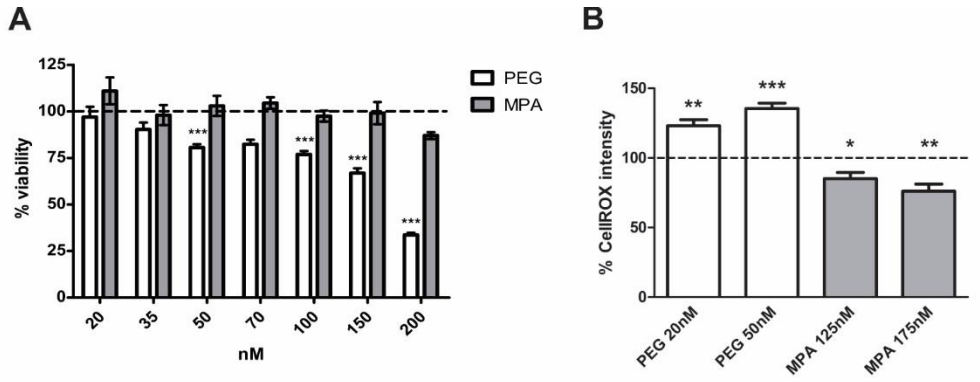

Figure 6.5 | Quantum dot induced acute toxicity and oxidative stress. PEGylated QDs induce cytotoxicity and oxidative stress, MPA-coated QDs are non-toxic up to 200 nM and reduce oxidative stress. (A) relative viability compared to untreated cells (100%) determined by the MTT assay (n=6). (B) relative level of CellROX intensity compared to untreated cells (100%) determined by flow cytometry (n=6). Error bars represent the SEM.

Impact of Quantum Dots on lysosomal health

Until recently the lysosome was merely considered as the waste bag of the cell, since it degrades and recycles the content delivered to the lysosomal compartment following endocytosis or autophagy. However, thanks to recent reports further elucidating its functions, the lysosome is now more and more perceived as an essential organelle for protecting the cell's homeostasis.[42] To our interest, its activity is also crucial to ensure a functional autophagy pathway (**cfr.** Chapter 5). Therefore, we evaluated the effect of QDs on lysosomal abundance and functionality by examining several markers (as indicated in **Figure 6.2**).

As a first indication, we incubated QD treated cells with the lysosome-staining dye LysoTracker and followed its intensity with flow cytometry as a measure for the amount and/or size of the lysosomal network.[43] As a positive control we treated HeLa cells with 50 µM of chloroquine for 4 h since it is widely established that this buffer elicits alkalinization of the lysosomal lumen which next evokes lysosomal swelling.[44] As shown in **Figure 6.6A**, this treatment indeed led to an almost twofold increase (194 ±14%) in LysoTracker intensity. A 24 h incubation with 20 and 50 nM PEGylated QDs resulted in an even more substantial increase up to 240 (±15)% and 248 (± 24)% respectively. The rise in LysoTracker intensity for the MPA coated QDs was not as spectacular as for their PEGylated counterparts though a significant dose-dependent effect was apparent: 125 nM led to 162 (± 14)% while 175 nM gave rise to 220 (± 26)%.

To support this data we performed confocal microscopy on cells stained for LAMP-1, a lysosomal membrane marker.[29] As illustrated in **Figure 6.6B** some lysosomes of chloroquine-treated cells appeared as swollen compared to those of untreated cells which supports the rise in LysoTracker intensity seen with flow cytometry. Instead, confocal images show that the increase in

LysoTracker intensity in QD-treated cells seems rather due to an increase in the number of lysosomes. Moreover, we noticed there was a strong co-localization between lysosomes and both types of QDs, illustrating that both QDs were taken up by endocytosis and thus efficiently delivered to the lysosomal compartment.

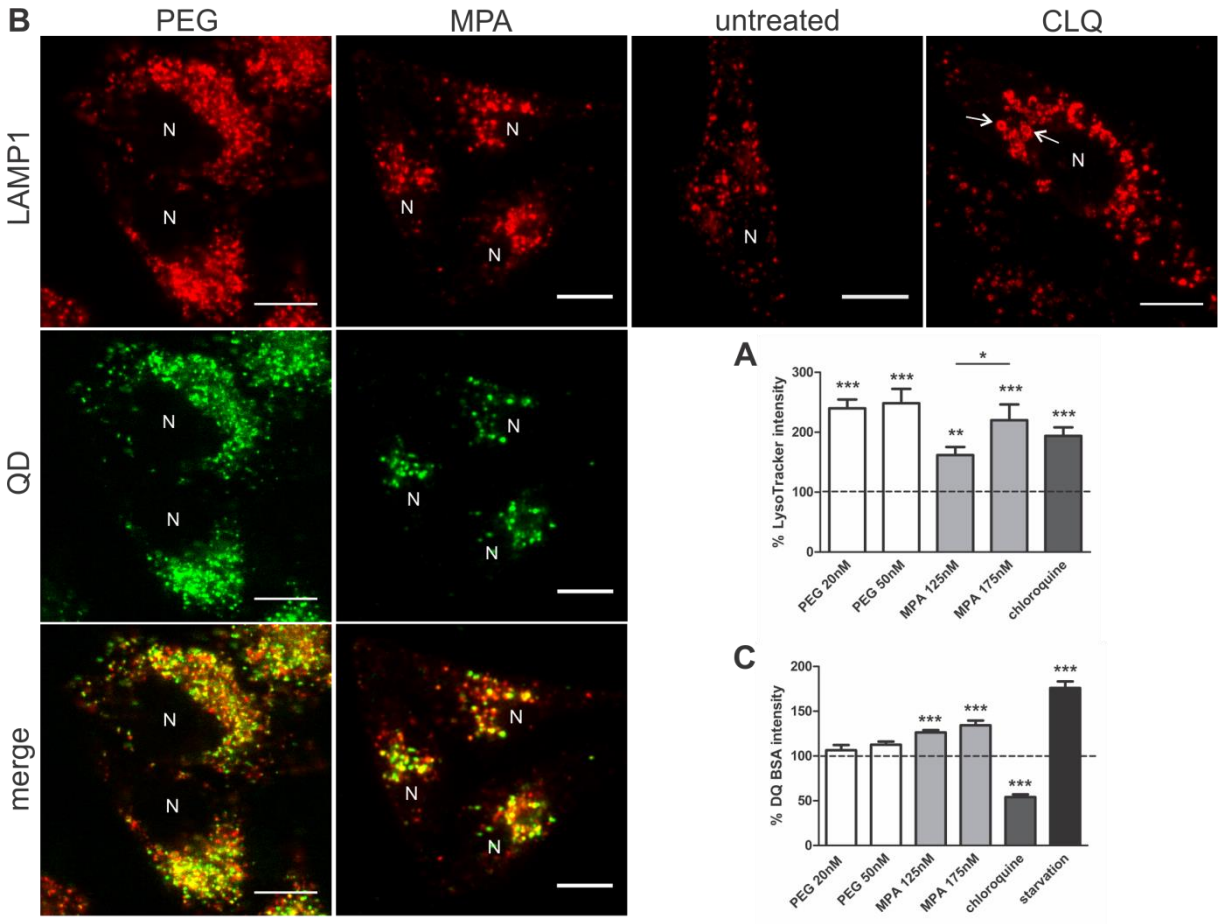

Figure 6.6 | Impact of Quantum Dots on lysosomal health. PEGylated QDs induce lysosomal impairment, while MPA-coated ones cause lysosomal activation. (A) relative level of LysoTracker intensity compared to untreated cells (100%) determined by flow cytometry (n=4). (B) Confocal microscopy on LAMP-1 immunostained cells after 24h of exposure to 50 nM PEGylated QDs, 175 nM of MPA-coated QDs or 4 h of 50 µM chloroquine (CLQ). N indicates the nucleus, arrows indicate swollen lysosomes. Scale bar: 20 µm. (C) relative level of DQ BSA intensity compared to untreated cells (100%) determined by flow cytometry (n=4). Error bars represent the SEM.

Finally, we examined the functionality of lysosomes of cells exposed to QDs, *i.e*. their ability of degrading lysosomal content. To this end, HeLa cells were incubated with the DQ BSA dye which consists of BSA proteins that are heavily labeled with fluorescent dyes so that a strong quenching effect takes place. Upon (lysosomal) degradation of DQ BSA into smaller fragments, this quenching effect is abolished, resulting in a bright fluorescent signal. In other words, an increase in fluorescence represents an increase in lysosomal protein degradation. As a positive control for increased lysosomal activity, cells were incubated for 4 h with serum-free medium to mimic starvation. **Figure 6.6C** demonstrates that this treatment indeed gave rise to a substantial

increase in DQ BSA fluorescence (176 ±14%). This in stark contrast to chloroquine-treated cells where the protein degradation capacity was almost halved (54 ±2.9%). This is not surprising since it has repeatedly been reported that starvation and chloroquine result in upregulation of lysosomal activity and lysosomal impairment, respectively.[45,46] Indeed, the alkalinization of lysosomal pH induced by chloroquine inhibits the degradative enzymes that are in need of an acidic environment. On the other hand, starvation stimulates lysosomal activity and autophagy as the cell attempts to compensate for the nutrient deficit.[31,47] For the QDs, the effect on lysosomal degradation strongly depended on the type of coating. No substantial change in degradation was observed upon treatment with PEGylated QDs. MPA QDs, however, did significantly enhance DQ BSA fluorescence intensity up to 134 (± 5.4)% with 175 nM. This signifies that MPA-QD uptake results in a starvation-like activation of lysosomal degradative capacity.

Impact of Quantum Dots on autophagy

Next, we focused on the most important organelle of the autophagy pathway *i.e* the autophagosome. The most widely investigated marker for autophagosomes is the protein LC3, which is present as two forms within the cell: the unactivated form, LC3-I, which is present in the cytosol and the active form LC3-II that is incorporated into the autophagosomal membrane (**Figure 6.2**). Consequently, the autophagy pathway can be studied by following the processing of LC3. To reliably interpret changes in autophagy we inspected LC3 by multiple techniques (cfr. **Chapter 5**), including (i) flow cytometry on HeLa cells stably expressing GFP-LC3 and (ii) western blotting on autophagosomal markers. As a first indication the level of GFP-LC3 was quantified by flow cytometry in a stably transfected GFP-LC3 HeLa cell line. When autophagosomes fuse with lysosomes the GFP will be quenched by the acidic pH.[31,48] The fluorescence intensity level of GFP is therefore proportional to the amount of autophagosomes. Furthermore, the saponin extraction included in the sample preparation ensures that only the membrane-bound LC3 contributes to the detected signal.[41] A 4 h incubation with 50 µM of chloroquine was applied as a positive control for autophagosome accumulation throughout all autophagy experiments. The lysosomal impairment caused by chloroquine leads to a block in autophagosome-lysosome fusion which results in the accumulation of large autophagosomes positive for LC3-II (**Figure 6.2**).[31] Indeed, as shown in **Figure 6.7A**, chloroquine treatment resulted in more than a three-fold increase in GFP-LC3 fluorescence intensity compared to untreated cells (342 ±60%). Interestingly, the highest concentration of PEGylated QDs also elicited a significant increase in GFP-LC3 (175 ±26%) while MPA QD treatment did not.

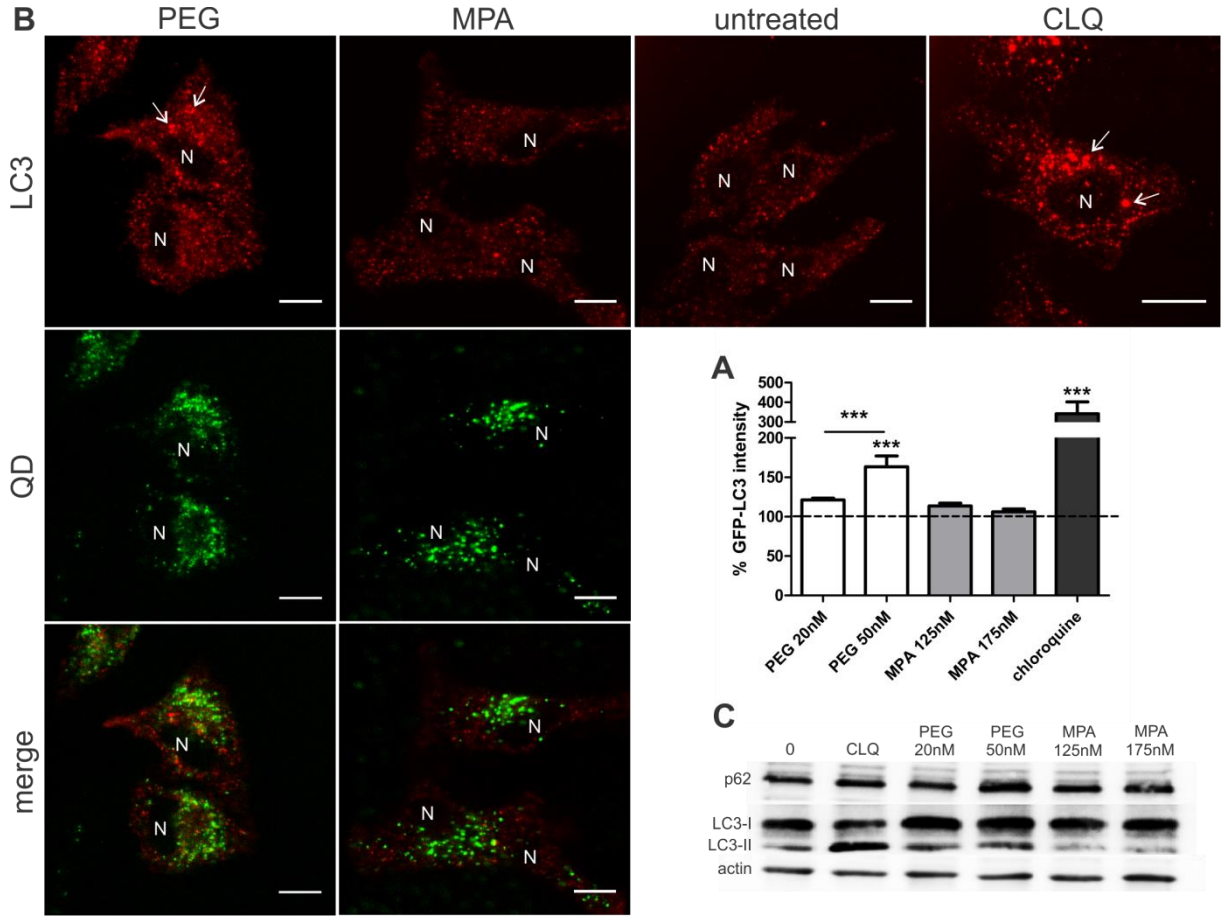

Figure 6.7 | Impact of Quantum Dots on autophagy. PEGylated QDs induce autophagy dysfunction, MPA-coated QDs do not influence autophagic markers. (A) relative level of GFP-LC3 intensity compared to untreated cells (100%) determined by flow cytometry (n=6). Error bars represent the SEM. (B) Confocal microscopy on LC3-immunostained cells after 24h incubation of 50 nM PEGylated QDs, 175 nM of MPA-coated QDs or 4 h of 50 µM chloroquine (CLQ). N indicates the nucleus, arrows indicate large autophagosomes. Scale bars: 20µm (C) Western blot on autophagic markers LC3 and p62.

To support this data we performed confocal microscopy on HeLa cells stained for LC3 after treatment with PEG QDs, MPA QDs or chloroquine. Here, the confocal images in **Figure 6.7B** show that chloroquine-treated cells contain some larger autophagosomes compared to untreated cells while in case of PEG QD treatment the total autophagosomal content seemed higher. In contrast, MPA QD treatment did not appreciably affect autophagosomal abundance nor size. It should be noted that for both QDs there was little co-localization with autophagosomes. Since the QDs are not present in the cytosol the only way of entering the autophagy pathway would be via fusion of autophagosomes with QD-containing lysosomes. Seeing the lack of co-localization we can conclude that these fusion events do not take place.

As mentioned in **Chapter 5**, the level of p62 is often studied to determine if the overall autophagy pathway is entirely functional. Since p62 is solely degraded by autophagy, a rise or fall of its protein level compared to the untreated condition corresponds with an autophagy blockade or upregulation respectively.[49] **Figure 6.7C** shows the protein levels of p62 and LC3 as

determined by Western blotting. Interestingly, the level of p62 was higher for cells treated with 50 nM of PEGylated QDs. As expected based on our observations by microscopy and flow cytometry, a higher level of LC3-II was spotted upon incubation with PEGylated QDs at 50 nM. The rise in LC3-II induced by chloroquine was even more pronounced. In contrast, no change in both markers was detected upon incubation of HeLa cells with MPA-coated QDs.

4. DISCUSSION

In this chapter we apply a step-by-step approach to carefully examine the toxicity of QDs coated with two commonly applied surface ligands. Our data clearly accentuates that the choice of coating is crucial for the degree and mechanisms of toxicity induced by QDs on cells: while MPA coated QDs were highly biocompatible, PEGylated QDs were severely toxic at higher concentrations. A detailed investigation of the ROS production, lysosomal health and autophagy pathway gave some insight in the intracellular mechanisms that could account for these observations.

MPA coated QDs

Coating of QDs with the short ligand MPA was not sufficient to protect the particles from aggregation in buffer or cell culture medium. The aggregated particles were taken up efficiently, though only at higher concentrations. This could be expected since it has been observed before that NP agglomeration has a negative impact on cellular uptake.[50–52] It is therefore likely that we need a higher dosage of MPA-coated QDs to reach similar intracellular fluorescence levels as PEGylated QDs because only the smaller NPs of the dispersion of MPA-QDs are able of entering the cells.[53] Interestingly, Albanese *et al.* stated that the effect of particle aggregation on uptake might be cell-type dependent: gold nanoparticle aggregation led to a reduced uptake in HeLa cells while for a melanoma cell type the opposite was true.[51] In any case, despite the efficient uptake of MPA-QDs, they did not inflict any toxicity on HeLa cells. This biocompatibility corresponds with the findings of Nagy et al. who did not detect any cell death in primary human lung cells upon exposure to differently sized MPA-coated QDs, though they did not show any uptake data.[37] Soenen *et al.*, however, did detect significant toxicity with MPA-coated QDs starting from 50 nM.[32] This difference with our data may be attributed to differences in aggregation: their MPA-QDs form smaller aggregates, which could lead to more efficient uptake and consequently toxicity at lower concentrations. This hypothesis was confirmed *in vivo* in mice where aggregated MPA-QDs exhibited less toxicity than their unaggregated counterparts.[54] On the other hand, the discrepancy in toxicity could also be derived from cell type dependent effects.[55,56]

The most recognized mechanism of QD-induced toxicity is the production of ROS.[57] Shifting ROS levels can indeed lead to a variety of secondary effects such as changes in cell signaling and DNA damage.[16] In addition, ROS and oxidative stress are associated with multiple cell death pathways and have been identified as important regulators of autophagy (cfr. **Chapter 5**).[58–60] Strikingly, incubation with MPA-coated QDs led to a significant reduction in ROS levels (**Figure 6.5B**)**.** Though this observation was unexpected, an NP-induced reduction in ROS has been reported before.[61] Specifically regarding QDs, studies have until now only reported that there is a lack of ROS induction by MPA-coated QDs.[37,38]

Apart from ROS levels, we looked further into the impact of QD exposure on lysosomal health and autophagy. As a first step we evaluated the influence of QDs on the number and size of lysosomes. Here we found that treatment of HeLa cells with MPA-coated QDs elicited a significant expansion of the lysosomal compartment as indicated by the substantially increased levels of LysoTracker. This type of enlargement is a commonly reported phenomenon and has been described for various NPs including ZnO NPs, fullerenol NPs, polystyrene NPs and QDs.[27,62–64] Interestingly, the increase in lysosomal content was accompanied by a rise in cellular degradation capacity, which is an indication for lysosomal activation. A boost in protein degradation was also observed by Chen *et al.* who, similar to our findings, detected an increase in LysoTracker staining and DQ BSA degradation upon treatment of human cerebral microvascular endothelial cells with aluminum NPs.[65] In addition, Kenzaoui *et al*. observed lysosomal activation induced in brain-derived endothelial cells by multiple NPs such as iron oxide NPs and silica NPs.[66] This kind of lysosomal activation, as caused by our MPA-coated QDs, is often accompanied by a similar activation of autophagy. However, the unaltered level of p62 and LC3 indicates that the autophagy pathway is fully functional though at a basal level. Similar to autophagy induction, this QD-induced lysosomal activation likely aids the cell in overcoming stress. In combination with the reduced oxidative stress, this could explain the lack of toxicity we observed upon exposure of HeLa cells to these QDs. Our findings thus confirm that MPA-coated QDs are quite biocompatible. Furthermore, our group recently reported that cells labeled with GA-QDs can be tracked 1.5 times longer than conventional core-shell QDs.[32] In conclusion, the combination of this excellent functionality and biocompatibility makes these MPA-coated GA-QDs very well suited for cell labeling applications.

PEGylated QDs

Unlike MPA coated QDs, PEGylated QDs do not agglomerate in ion-rich media, most likely due to the steric hindrance imparted by the PEG-chains which prevents particle-particle interactions.[67] As Pelaz *et al.* stated, PEGylation more than often leads to a reduction in cellular uptake which is

likely attributed to the lack of protein adsorption at the particle surface.[68] On the other hand, the colloidal stability of our particles likely supports their uptake as stated before by Kirchner *et* al.[53,69] Indeed the smaller and more neutral PEGylated QDs were clearly taken up more efficiently (even at lower extracellular concentrations) than the larger negatively charged MPA-coated QDs. Starting from 60 nM, however, the uptake of PEGylated QDs shows a downward trend. An explanation for this decrease in uptake might be the saturation of surface receptors essential for QD uptake, since it has been described before that neutral to negatively charged QDs are actively internalized by a variety of saturable endocytosis pathways including clathrin- and caveolae-mediated endocytosis.[70,71] Upon investigation of the intracellular location of both QDs we indeed found that after 24h they co-localize strongly with LAMP-1 stained lysosomes implying they are taken up via endocytosis. The decreased uptake of PEGylated QDs upon treatment with higher concentrations could also stem from QD-induced toxicity, as cytotoxicity tests revealed that PEGylated QDs were significantly toxic starting from 50 nM.

Regarding QDs, a common strategy to prevent ROS induction is to limit the dissolution of cadmium ions from their core by the application of a surface coating.[53] Clearly, high density PEGylation is not sufficient to prevent ROS production since exposure to 50 nM of PEGylated QDs significantly raised the level of ROS in HeLa cells. Since this observation correlates well with the cell death seen at this concentration, we suggest this ROS production is at least partly responsible for the observed cytotoxicity. In addition, these findings correspond well with the many reports on QD-induced cell death associated with oxidative stress.[13,32,72] In any case, the difference in toxicity observed between the PEG- and MPA-coated QDs demonstrates that the type of surface functionalization can have a marked influence on the toxicity and ROS production of QDs. This observation was also made by Nagy *et al*., who observed less QD-induced toxicity with shorter negatively charged surface ligands compared to longer ligands - in our case represented by MPA and PEG respectively.[37]

With regard to the lysosomes, PEGylated QDs resulted in an enlargement of the lysosomal compartment. Interestingly, despite the fact that PEGylated QDs gave rise to a more than twofold increase in LysoTracker, the degradation of DQ BSA did remain unchanged. We therefore suspect that at least a part of these lysosomes exhibit limited or no proteolytic activity and thus these QDs lead to lysosomal impairment. Lysosomal impairment is a frequently described mechanism of toxicity in cells exposed to various NPs as summarized in a review by Stern et al.[73] The most extensively reported mechanism of lysosomal impairment involves lysosome membrane permeabilization. However, considering the high LysoTracker dye loading and LAMP-1 staining showing normal lysosomal morphology, we believe that in our case the

lysosomal membrane is intact. We therefore hypothesize that the mechanism underlying this impairment could be lysosomal overload as has previously been reported for several particles such as smoke particulates.[73,74] Another mechanism that could contribute to the lack of degradation taking place within the lysosomes could be oxidative damage inflicted on the lysosomal enzymes by ROS produced during QD lysis.[73] By any means, lysosomal dysfunction is undeniably a toxic parameter worth of investigation since it forms the basis of lysosomal storage disorders, a group of degenerative diseases that affect the nervous and musculoskeletal systems. In addition, lysosomal malfunction can give rise to an autophagy blockade through impaired autophagosome-lysosome fusion, a hypothesis we investigated further.[75]

When looking into autophagosomal markers, treatment of HeLa cells with 50 nM of PEGylated QDs resulted in an elevation of LC3, indicative of an accumulation of autophagosomes. Since the p62 protein level was also increased, we conclude that the accumulation of LC3 derives from a reduction in autophagosomal turn-over rather than autophagy induction. In other words, the autophagy pathway is not fully functional but blocked at its later stage i.e. at autophagosome-lysosome fusion. Since no co-localization of QDs with autophagosomes was observed (**Figure 6.7**), we conclude from this collection of data that PEGylated QDs induce autophagosome accumulation through lysosomal impairment. This theory is in line with observations made by Ma *et al*. who detected compromised degradation capacity induced by endocytosed AuNPs and consequently defective autophagosome-lysosome fusion in normal rat kidney cells.[25] An impaired autophagy flux was also hypothesized by Wang *et al.* who witnessed an increase in the volume of acidic compartments and LC3-II levels upon exposure of human brain astrocytoma cells to polystyrene particles.[64] In addition, the same conclusion was drawn based on similar observations in kidney cells treated with fullerenol NPs.[63] At first sight our findings do seem in contrast with recent observations made by Huang *et al* who saw that NPs modulate autophagy in a dispersity-dependent manner where aggregated NPs induced severe autophagic effects while well-dispersed NPs did not.[76] Our study indicates that MPA-QDs, which aggregate severely in extracellular medium, do not exert major effects on the autophagy pathway while our unaggregated PEGylated QDs clearly do. However, within the cell this phenomenon might be the opposite: as stated before it is likely that the large MPA-QD aggregates are not internalized by the cell while the smaller PEGylated QDs are taken up very efficiently and likely accumulate, and possibly aggregate massively inside the endo- and lysosomes. According to Huang *et al*. this high uptake and intracellular accumulation of NPs can next modulate autophagy, which is in line with our observations. Since autophagy usually encourages survival, especially in cells undergoing stress, it is not surprising that when this function is lost, cytotoxicity becomes inevitable.[77] Our PEGylated QDs induce oxidative stress that undoubtedly leads to damaged cytoplasmic material.

Where usually autophagy aids in the removal of these materials, this coping mechanism is now absent. The autophagy blockade combined with oxidative stress is therefore likely the underlying source of the QD-induced cytotoxicity we observed. This disrupted autophagy flux is a serious observation since this can lead to the accumulation of protein aggregates and damaged cytoplasmic organelles. This buildup of cytoplasmic waste can subsequently provoke genomic instability and tissue degeneration, which in turn has a huge impact on physiology.[22] Surely, autophagy dysfunction is linked with the onset of many diseases including cancer, neurodegenerative and inflammatory diseases.[22,78]

However, autophagy perturbation should not be regarded as threatening per se. Actually, in distinct cases it can be manipulated to our advantage. Recent reports have stated that inducing autophagy malfunction might be an ideal strategy to wipe out (resistant) cancer cells. It seems some types of cancer are highly dependent on autophagy for their survival, since autophagy allows them to overcome stressors like starvation, hypoxia and even chemotherapy.[19,24] Blocking this cytoprotective process would in this case thus lead to their demise. In fact, the anti-cancer activity of chloroquine, a chemical we use as a positive control for autophagy blockade, is currently investigated in multiple clinical trials.[79,80] In this regard, the effects induced by PEGylated QDs might allow us to combine diagnosis by tumor imaging with anti-cancer therapy. In conclusion, the oxidative stress and autophagy blockade caused by these PEGylated GA-QDs has detrimental effects for the cell, however, in cases where these effects are desirable like in anti-cancer therapy, these particles could be valuable.

5. CONCLUSION

The primary goal of this study was to define the toxicity and its origins of MPA-coated and PEGylated QDs with a special emphasis on the autophagy pathway. We observed that despite the fact the two studied QDs are completely identical except for their surface coating, their cellular effects induced in HeLa cells were remarkably different (summarized in **Figure 6.8**). This implies that rather than QD composition, the surface chemistry primarily defines the functionality and toxicity of the QD. Based on our results we conclude that MPA-coated QDs are highly biocompatible, where the lysosomal activation and ROS reduction induced by these QDs likely rescues the cell from potentially NP-induced toxic effects. In this respect, MPA-coated QDs seem promising candidates for cellular labeling. However, since this study is limited by its focus on ROS and autophagy, future research should involve screening for other toxic factors such as DNA damage. As expected, the PEGylated QDs proved to be more resistant to aggregation resulting in efficient cell labeling. However, these QDs exhibited significant toxicity owing to their

capacity to induce ROS production and autophagy malfunction through lysosomal impairment. Considering these toxic defects, the PEGylated QDs do not seem suitable for biomedical applications except for when autophagy dysfunction is actually desirable e.g. in anti-cancer therapy. In this regard, it could be valuable to investigate if combination therapy using a common chemotherapeutic and this QD might enhance the elimination of therapy-resistant cancer cells. Generally, our study highlights the importance of surface chemistry when it comes to nanotoxicology as well as the relevance of lysosomal and autophagy dysfunction as a NP-induced toxicity mechanism.

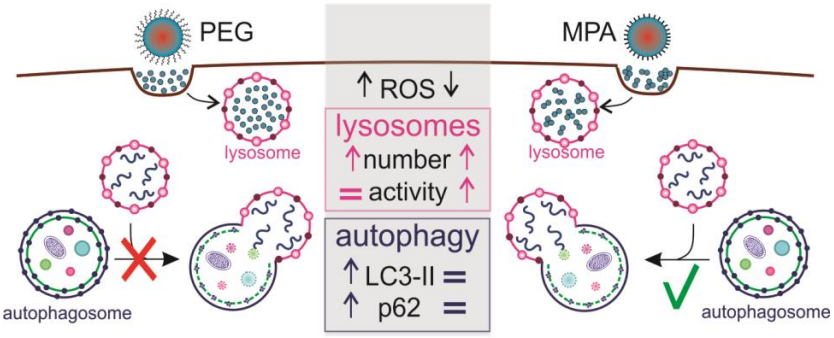

Figure 6.8 | Overview of the distinct cellular effects of GA QDs coated with PEG or MPA.

6. ACKNOWLEDGEMENTS

This project was funded by the Institute for the Promotion of Innovation through Science and Technology in Flanders, Belgium (IWT – Vlaanderen). SJS is supported by the FWO-Vlaanderen. We acknowledge Prof. Felix Randow for providing the GFP-LC3 labeled HeLa cell line. We would also like to thank professor Dieter Deforce for the use of the VersaDoc™ Imaging System. Student Alexander Ryckaert is acknowledged for his experimental work that contributed to this chapter.

7. REFERENCES

1. Doane, T. L. & Burda, C. The unique role of nanoparticles in nanomedicine: imaging, drug delivery and therapy. *Chem. Soc. Rev.* **41,** 2885–2911 (2012).
2. Zhao, M.-X. & Zeng, E.-Z. Application of functional quantum dot nanoparticles as fluorescence probes in cell labeling and tumor diagnostic imaging. *Nanoscale Res. Lett.* **10,** 171 (2015).
3. Chan, W. C. W. *et al.* Luminescent quantum dots for multiplexed biological detection and imaging. *Curr. Opin. Biotechnol.* **13,** 40–46 (2002).
4. Hessel, C. M. *et al.* Copper selenide nanocrystals for photothermal therapy. *Nano Lett.* **11,** 2560–6 (2011).
5. Samir, T. M., Mansour, M. M. H., Kazmierczak, S. C. & Azzazy, H. M. E. Quantum dots:

heralding a brighter future for clinical diagnostics. *Nanomedicine (Lond).* **7,** 1755–69 (2012).

6. Probst, C. E., Zrazhevskiy, P., Bagalkot, V. & Gao, X. Quantum dots as a platform for nanoparticle drug delivery vehicle design. *Adv Drug Deliv Rev* **65,** 703–718 (2013).

7. Bae, W. K. *et al.* Controlled alloying of the core-shell interface in CdSe/CdS quantum dots for suppression of Auger recombination. *ACS Nano* **7,** 3411–9 (2013).

8. Bailey, R. E. & Nie, S. Alloyed semiconductor quantum dots: tuning the optical properties without changing the particle size. *J. Am. Chem. Soc.* **125,** 7100–6 (2003).

9. Maikov, G. I., Vaxenburg, R., Sashchiuk, A. & Lifshitz, E. Composition-Tunable Optical Properties with Alloy Components. *ACS Nano* **4,** 6547–6556 (2010).

10. Mesolight Inc. at <http://www.mesolight.com/e/list.php?classid=23>

11. Michalet, X. *et al.* Quantum dots for live cells, in vivo imaging, and diagnostics. *Science* **307,** 538–44 (2005).

12. Tsoi, K. M., Dai, Q., Alman, B. A. & Chan, W. C. W. Are quantum dots toxic? Exploring the discrepancy between cell culture and animal studies. *Acc. Chem. Res.* **46,** 662–671 (2012).

13. Lovrić, J., Cho, S. J., Winnik, F. M. & Maysinger, D. Unmodified cadmium telluride quantum dots induce reactive oxygen species formation leading to multiple organelle damage and cell death. *Chem. Biol.* **12,** 1227–34 (2005).

14. Al-Ali, A. *et al.* Quantum dot induced cellular perturbations involving varying toxicity pathways. *Toxicol. Res. (Camb).* **4,** 623–633 (2015).

15. Chen, N. *et al.* The cytotoxicity of cadmium-based quantum dots. *Biomaterials* **33,** 1238–44 (2012).

16. Yong, K. T. *et al.* Nanotoxicity assessment of quantum dots: from cellular to primate studies. *Chem. Soc. Rev.* **42,** 1236–1250 (2013).

17. Pons, T. *et al.* Cadmium-free CuInS2/ZnS quantum dots for sentinel lymph node imaging with reduced toxicity. *ACS Nano* **4,** 2531–8 (2010).

18. Soenen, S. J. *et al.* Cytotoxicity of Cadmium-Free Quantum Dots and Their Use in Cell Bioimaging. *Chem. Res. Toxicol.* **27,** 1050–1059 (2014).

19. Peynshaert, K. *et al.* Exploiting Intrinsic Nanoparticle Toxicity: The Pros and Cons of Nanoparticle-Induced Autophagy in Biomedical Research. *Chem. Rev.* **114,** 7581–7609 (2014).

20. Remaut, K., Oorschot, V., Braeckmans, K., Klumperman, J. & De Smedt, S. C. Lysosomal capturing of cytoplasmic injected nanoparticles by autophagy: An additional barrier to non viral gene delivery. *J. Control. Release* **195,** 29–36 (2014).

21. Li, L., Chen, Y. & Gibson, S. B. Starvation-induced autophagy is regulated by mitochondrial reactive oxygen species leading to AMPK activation. *Cell. Signal.* **25,** 50–65 (2013).

22. Levine, B. & Kroemer, G. Autophagy in the pathogenesis of disease. *Cell* **132,** 27–42 (2008).

23. Menzies, F. M., Fleming, A. & Rubinsztein, D. C. Compromised autophagy and neurodegenerative diseases. *Nat. Rev. Neurosci.* **16,** 345–357 (2015).

24. White, E. The role for autophagy in cancer. *J. Clin. Invest.* **125,** 42–6 (2015).

25. Ma, X. *et al.* Gold Nanoparticles Induce Autophagosome Accumulation through Size-

Dependent Nanoparticle Uptake and Lysosome Impairment. *ACS Nano* **5,** 8629–8639 (2011).

26. Kroemer, G. & Levine, B. Autophagic cell death: the story of a misnomer. *Nat. Rev. Mol. Cell Biol.* **9,** 1004–1010 (2008).

27. Neibert, K. D. & Maysinger, D. Mechanisms of cellular adaptation to quantum dots - the role of glutathione and transcription factor EB. *Nanotoxicology* **6,** 249–262 (2012).

28. Luo, Y. H. *et al.* Cadmium-based quantum dot induced autophagy formation for cell survival via oxidative stress. *Chem. Res. Toxicol.* **26,** 662–673 (2013).

29. Eskelinen, E.-L., Tanaka, Y. & Saftig, P. At the acidic edge: emerging functions for lysosomal membrane proteins. *Trends Cell Biol.* **13,** 137–145 (2003).

30. Slattery, C. *et al.* In vivo visualization of albumin degradation in the proximal tubule. *Kidney Int.* **74,** 1480–6 (2008).

31. Mizushima, N., Yoshimori, T. & Levine, B. Methods in Mammalian Autophagy Research. *Cell* **140,** 313–326 (2010).

32. Soenen, S. J. *et al.* The performance of gradient alloy quantum dots in cell labeling. *Biomaterials* **35,** 7249–58 (2014).

33. Hatakeyama, H., Akita, H. & Harashima, H. The Polyethyleneglycol Dilemma: Advantage and Disadvantage of PEGylation of Liposomes for Systemic Genes and Nucleic Acids Delivery to Tumors. *Biol. Pharm. Bull.* **36,** 892–899 (2013).

34. Jokerst, J. V, Lobovkina, T., Zare, R. N. & Gambhir, S. S. Nanoparticle PEGylation for imaging and therapy. *Nanomedicine (Lond).* **6,** 715–28 (2011).

35. Lipka, J. *et al.* Biodistribution of PEG-modified gold nanoparticles following intratracheal instillation and intravenous injection. *Biomaterials* **31,** 6574–81 (2010).

36. Kirchner, C. *et al.* Cytotoxicity of colloidal CdSe and CdSe/ZnS nanoparticles. *Nano Lett.* **5,** 331–8 (2005).

37. Nagy, A. *et al.* Comprehensive Analysis of the effects of CdSe quantum dot size, surface charge, and functionalization on primary human lung cells. *ACS Nano* **6,** 4748–4762 (2012).

38. Nagy, A. *et al.* Functionalization-Dependent Induction of Cellular Survival Pathways by CdSe Quantum Dots in Primary Normal Human Bronchial Epithelial Cells. *ACS Nano* **7,** 8397–8411 (2013).

39. Braeckmans, K. *et al.* Sizing Nanomatter in Biological Fluids by Fluorescence Single Particle Tracking. *Nano Lett.* **10,** 4435–4442 (2010).

40. Klionsky DJ, Abdelmohsen K, Abe A, Abedin MJ, Abeliovich H, Acevedo Arozena A, Adachi H, Adams CM, Adams PD, Adeli K, Adhihetty PJ, Adler SG, Agam G, Agarwal R, Aghi MK, Agnello M, Agostinis P, Aguilar PV, Aguirre-Ghiso J, Airoldi EM, Ait-Si-Ali S, Akemat, Z. S. Guidelines for use and interpretation of assays for monitoring autophagy (3rd edition). *Autophagy* **12,** 1–222 (2016).

41. Eng, K. E., Panas, M. D., Hedestam, G. B. K. & McInerney, G. M. A novel quantitative flow cytometry-based assay for autophagy. *Autophagy* **6,** 634–641 (2010).

42. Appelqvist, H., Waster, P., Kagedal, K. & Ollinger, K. The lysosome: from waste bag to potential therapeutic target. *J. Mol. Cell Biol.* **5,** 214–226 (2013).

43. Neun, B. W. & Stern, S. T. Monitoring lysosomal activity in nanoparticle-treated cells.

Methods Mol Biol **697,** 207–212 (2011).

44. Solomon, V. R. & Lee, H. Chloroquine and its analogs: a new promise of an old drug for effective and safe cancer therapies. *Eur. J. Pharmacol.* **625,** 220–33 (2009).

45. Zhou, J. *et al.* Activation of lysosomal function in the course of autophagy via mTORC1 suppression and autophagosome-lysosome fusion. *Cell Res.* **23,** 508–23 (2013).

46. Li, M. *et al.* Suppression of Lysosome Function Induces Autophagy via a Feedback Down-regulation of MTOR Complex 1 (MTORC1) Activity. *J. Biol. Chem.* **288,** 35769–35780 (2013).

47. Settembre, C. *et al.* TFEB Links Autophagy to Lysosomal Biogenesis. *Science (80-.).* **332,** 1429–1433 (2011).

48. Bampton, E. T. W., Goemans, C. G., Niranjan, D., Mizushima, N. & Tolkovsky, A. M. The dynamics of autophagy visualized in live cells - From autophagosome formation to fusion with endo/lysosomes. *Autophagy* **1,** 23–36 (2005).

49. Bjørkøy, G. *et al.* p62/SQSTM1 forms protein aggregates degraded by autophagy and has a protective effect on huntingtin-induced cell death. *J. Cell Biol.* **171,** 603–14 (2005).

50. Manshian, B. B. *et al.* Genotoxic capacity of Cd/Se semiconductor quantum dots with differing surface chemistries. *Mutagenesis* **31,** 97–106 (2016).

51. Albanese, A. & Chan, W. C. W. Effect of Gold Nanoparticle Aggregation on Cell Uptake and Toxicity BT - ACS Nano. *ACS Nano* **5,** 5478–5489 (2011).

52. Chithrani, B. D., Ghazani, A. A. & Chan, W. C. W. Size and Shape Dependence of Nanoparticles on Cellular Uptake. *Nano* **668,** 662–668 (2006).

53. Kirchner, C. *et al.* Cytotoxicity of colloidal CdSe and CdSe/ZnS nanoparticles. *Nano Lett.* **5,** 331–338 (2005).

54. Loginova, Y. F. *et al.* Biodistribution of intact fluorescent CdSe/CdS/ZnS quantum dots coated by mercaptopropionic acid after intravenous injection into mice. *J. Biophotonics* **5,** 848–859 (2012).

55. Joris, F. *et al.* Assessing nanoparticle toxicity in cell-based assays: influence of cell culture parameters and optimized models for bridging the in vitro–in vivo gap. *Chem. Soc. Rev.* **42,** 8339–8359 (2013).

56. Sohaebuddin, S. K., Thevenot, P. T., Baker, D., Eaton, J. W. & Tang, L. Nanomaterial cytotoxicity is composition, size, and cell type dependent. *Part. Fibre Toxicol.* **7,** 22 (2010).

57. Winnik, F. M. & Maysinger, D. Quantum Dot Cytotoxicity and Ways To Reduce It. *Acc Chem Res* **46,** 672–680 (2013).

58. Chen, Y., McMillan-Ward, E., Kong, J., Israels, S. J. & Gibson, S. B. Oxidative stress induces autophagic cell death independent of apoptosis in transformed and cancer cells. *Cell Death Differ.* **15,** 171–182 (2008).

59. Galluzzi, L. *et al.* Molecular definitions of cell death subroutines: Recommendations of the Nomenclature Committee on Cell Death 2012. *Cell Death Differ.* **19,** 107–120 (2012).

60. Scherz-Shouval, R. *et al.* Reactive oxygen species are essential for autophagy and specifically regulate the activity of Atg4. *Embo J.* **26,** 1749–1760 (2007).

61. Harris, G. *et al.* Iron oxide nanoparticle toxicity testing using high-throughput analysis and high-content imaging. *Nanotoxicology* **9 Suppl 1,** 87–94 (2015).

62. Hackenberg, S. *et al.* Nanoparticle-induced photocatalytic head and neck squamous cell carcinoma cell death is associated with autophagy. *Nanomedicine* **20,** 1–13 (2013).

63. Johnson-Lyles, D. N. *et al.* Fullerenol cytotoxicity in kidney cells is associated with cytoskeleton disruption, autophagic vacuole accumulation, and mitochondrial dysfunction. *Toxicol. Appl. Pharmacol.* **248,** 249–258 (2010).

64. Wang, F. *et al.* Time resolved study of cell death mechanisms induced by amine-modified polystyrene nanoparticles. *Nanoscale* **5,** 10868–76 (2013).

65. Chen, L., Zhang, B. & Toborek, M. Autophagy Is Involved In Nanoalumina-Induced Cerebrovascular Toxicity. *Nanomedicine Nanotechnology, Biol. Med.* **9,** 212–221 (2012).

66. Kenzaoui, B. H., Bernasconi, C. C., Guney-Ayra, S. & Juillerat-Jeanneret, L. Induction of oxidative stress, lysosome activation and autophagy by nanoparticles in human brain-derived endothelial cells. *Biochem. J.* **441,** 813–821 (2012).

67. Sperling, R. A. & Parak, W. J. Surface modification, functionalization and bioconjugation of colloidal inorganic nanoparticles. *Philos. Trans. R. Soc. A Math. Phys. Eng. Sci.* **368,** 1333–1383 (2010).

68. Pelaz, B. *et al.* Surface Functionalization of Nanoparticles with Polyethylene Glycol: Effects on Protein Adsorption and Cellular Uptake. *ACS Nano* **9,** 6996–7008 (2015).

69. Soenen, S. J. *et al.* The cellular interactions of PEGylated gold nanoparticles: Effect of PEGylation on cellular uptake and cytotoxicity. *Part. Part. Syst. Charact.* **31,** 794–800 (2014).

70. Nagy, A. *et al.* Contrast of the Biological Activity of Negatively and Positively Charged Microwave Synthesized CdSe/ZnS Quantum Dots. *Chem. Res. Toxicol.* **24,** 2176–2188 (2011).

71. Zhang, L. W. & Monteiro-Riviere, N. A. Mechanisms of quantum dot nanoparticle cellular uptake. *Toxicol. Sci.* **110,** 138–55 (2009).

72. Lovrić, J. *et al.* Differences in subcellular distribution and toxicity of green and red emitting CdTe quantum dots. *J. Mol. Med. (Berl).* **83,** 377–85 (2005).

73. Stern, S. T., Adiseshaiah, P. P. & Crist, R. M. Autophagy and lysosomal dysfunction as emerging mechanisms of nanomaterial toxicity. *Part. Fibre Toxicol.* **9,** (2012).

74. De Stefano, D., Carnuccio, R. & Maiuri, M. C. Nanomaterials Toxicity and Cell Death Modalities. *J. Drug Deliv.* **2012,** 1–14 (2012).

75. Settembre, C. *et al.* A block of autophagy in lysosomal storage disorders. *Hum. Mol. Genet.* **17,** 119–29 (2008).

76. Huang, D., Zhou, H. & Gao, J. Nanoparticles modulate autophagic effect in a dispersity-dependent manner. *Sci. Rep.* **5,** 1–10 (2015).

77. Moore, M. N. Autophagy as a second level protective process in conferring resistance to environmentally-induced oxidative stress. *Autophagy* **4,** 254–256 (2008).

78. Jones, S. A., Mills, K. H. G. & Harris, J. Autophagy and inflammatory diseases. *Immunol. Cell Biol.* **91,** 250–8 (2013).

79. Loaiza-Bonilla, A. *et al.* Phase II trial of autophagy inhibition using hydroxychloroquine (HCQ) with FOLFOX/bevacizumab in the first-line treatment of advanced colorectal cancer. *J. Clin. Oncol.* **33,** 3614–3614 (2015).

80. Molenaar, R. J. *et al.* Study protocol of a phase IB/II clinical trial of metformin and

chloroquine in patients with IDH1-mutated or IDH2-mutated solid tumours. *BMJ Open* **7,** e014961 (2017).

7

Broader international context, relevance and future perspectives

Karen Peynshaert[a,b]

[a]Lab of General Biochemistry and Physical Pharmacy, Faculty of Pharmaceutical Sciences, Ghent University, Ottergemsesteenweg 460, 9000 Ghent, Belgium.
[b]Ghent Research Group on Nanomedicines, Ghent University, Ottergemsesteenweg 460, 9000 Ghent, Belgium.

ABSTRACT

The content of this thesis is subdivided into two main categories, yet both categories share a common topic i.e. nano. The first purpose of this chapter is therefore to review the recent progress and future goals of nano in context of toxicology and retinal gene therapy. On the other hand, since nano is in practice not as successful as initially anticipated, we will also highlight the predominant issues that currently limit nano to progress to the clinic along with conceptual guidelines that could help the field to advance (more) efficiently. Finally, having these guidelines in mind, we look into non-viral retinal gene delivery as a case study and attempt to envision how this research area should proceed.

Table of Contents

1. CURRENT STATE OF THE ART AND FUTURE GOALS

Retinal gene therapy

Retinal gene therapy has seen astounding progress on many levels over the last 20 years. Our insight in the biology of the retina and pathophysiology of retinal diseases has indeed incredibly expanded. Moreover, since the discovery of the first blinding genetic defects in the 1980's more than 250 disease-causing genes have been identified (**Figure 7.1**)**.** This is partly attributed to the further development and decreasing costs of next-generation sequencing which stimulated the genetic screening of patients by academic and commercial centers.[1,2] While in the 90's diagnosis was solely based on phenotypical features like retinal fundus imaging and classic visual acuity tests, the advances in genetic testing as of today allows earlier diagnosis and prognosis of inherited retinal diseases, and importantly, enables phenotype-genotype linking.[1–3] The identification of these genes further led to the discovery of a collection of naturally occurring animal models of retinal disease. In addition, thanks to the progress made in producing targeted mutations and gene knockouts, a wide variety of engineered animal models of diverse species has been added to this collection.[3,4]

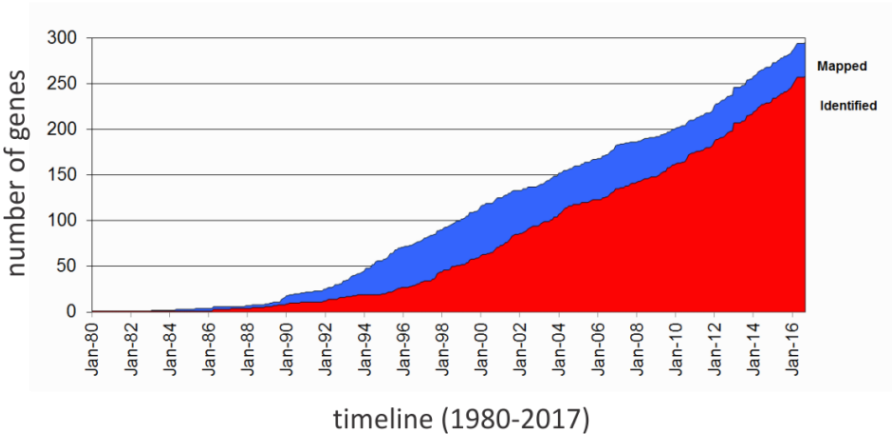

Figure 7.1 | Mapped and identified retinal disease genes from 1980-2017. Taken from [5]

The increasing insight into inherited retinal disease and its causative mutations together with the growing number of available *in vivo* disease models provided a solid foundation for the progression of retinal gene therapy with recombinant viruses as key players. Here, adeno-associated viral vectors (AAV) are by far the most successful and therefore most applied ones for retinal gene transfer.[3] Our ability of engineering their capsids has further improved their therapeutic power by tuning of their cellular specificity, onset of gene expression and extracellular interactions.[6] In view of the pre-clinical success of AAV vectors (especially type 2), the majority of clinical trials involve subretinal injection of these vectors for gene augmentation strategies. Two target genes connected to loss-of-function mutations predominate the clinical

trials, i.e. CHM which causes choroideremia and RPE65, which is linked to Leber Congenital Amaurosis (LCA). In context of the latter disease, Spark therapeutics' AAV2 vector Voretigene Neparvovec was recently recommended for approval by the U.S. Food and Drug Administration (FDA).[7] As the first gene therapy to reach this stage in the U.S. this signifies a great leap forward for treatment of retinal dystrophies. A full overview of completed and ongoing clinical trials can be found here[3,8].

As discussed in **Chapter 1 and 5**, nanomedicines have several advantages over viral vectors, yet, in contrast to the successes achieved with viral vectors, non-viral ones are until now lagging behind when it comes to efficacy of retinal gene transfer. However, while no nanomedicines have reached the clinical stage thus far, some interesting pre-clinical results have been reported on. An example of an elegantly designed nanoparticle (NP) was given by Rajala *et al*. who synthesized lipid-protamine-DNA NPs that were further functionalized with a cell-penetrating peptide and a nuclear localization signaling peptide. This combination proved to be effective since subretinal injection of these particles in RPE65 knockout mice led to a substantial improvement in ERG response as well as photoreceptor integrity.[9] Another example of a successful lipid-based carrier is the solid lipid nanoparticles (SLN) as described by Apaolaza *et al*.[10] SLN's are composed of a solid lipid core surrounded by a surfactant and can be functionalized with smart ligands such as hyaluronic acid (HA). Interestingly, the retina's of Rhs1-deficient mice bearing symptoms of X-linked juvenile retinoschisis showed improved structural integrity after IVT injection of HA-functionalized SLN's.[10] The group of Muna Naash has been working on so-called compacted DNA particles, where DNA is folded into DNase-resistant nanostructures by applying PEG-substituted polylysine. These particles have shown beneficial results in several disease models, including mice knocked out for RPE65, RHO (RP) and ABCA4 (Stargardt's disease).[11–14] These studies demonstrate that it is worthwhile to proceed our research into the potential of nanomedicines for retinal gene therapy even though their efficacy until now does not match that of viral vectors. Nevertheless, there are some challenges to be met for nano to truly advance in the field of retinal gene therapy as will be discussed later in this chapter.

Despite the fact that the progress in retinal gene therapy over the last 20 years is immense, there are still issues to be tackled and challenging goals to aim for. A fundamental aim at the moment is the attempt to **increase the number of disease targets**.[8] Current clinical trials are predominantly limited to gene augmentation strategies that aim to compensate for loss-of-function mutations.[3] However, this gene augmentation strategy may not provide relief for patients suffering from inherited retinal diseases based on gain-of-function mutations.[8,15] To

treat these cases, other gene-specific therapeutic strategies are being researched of which the most eminent one is gene editing technology (e.g. CRISPR/Cas9). As mentioned in **Chapter 1**, this approach involves gene-specific adjustment of the genome and comes with the advantage that the therapeutic effect is expected to be lifelong.[16] As an example of this approach, Bakondi *et al*. were able to prevent retinal degeneration and improve visual function in rats suffering from autosomal dominant RP by selectively ablating the RHO gene using the CRISPR/Cas9 gene editing technology.[17] A concern that for now limits the clinical translation of CRISPR/Cas9 is potential off-target cleaving which could induce unintended mutations.[18] However, seeing the worldwide excitement about gene editing and effort dedicated to it, we are convinced the strategy will be further fine-tuned in order to prevent off-target effects. The complexity of inherited retinal disease and the great number of genes involved furthermore highlights the need for mutation-independent approaches which are able of treating a retinal disease irrespective of the mutation, if any. As already briefly touched upon in **Chapter 1**, optogenetics is an example of such an approach. Many studies in small laboratory animals have demonstrated its feasibility, and one phase I/II clinical trial has been registered so far. The first outcomes of this dose-escalation study were encouraging since no inflammation or ocular adverse effects were observed in the low dose cohort of patients diagnosed with advanced retinitis pigmentosa.[18a] The primary obstacle preventing optogenetics to become clinically successful is likely the fact that the intensity of light required to trigger the neuronal cells lies above the safety threshold. This obstacle is directly connected to the inherent light sensitivity of the opsins expressed in the target neuronal cells together with the high level of opsin expression needed. Remarkably, Chaffiol *et al*. very recently confirmed the feasibility of optogenetics in cynomolgus macaques, and more importantly, managed to acquire light responses with light intensities below the safety threshold for retinal illumination. To this end, they made use of an ultra light-sensitive version of channelrhodopsin[19] combined with an optimized promotor able of inducing high expression in RGCs, their target cell type.[20] We are convinced that these promising preclinical outcomes and the fine-tuning of gene expression lying at the root of this success will pave the way for the clinical development of optogenetics. Another mutation-independent approach is neuroprotection, of which we have already discussed the concept and recent progress in **Chapter 4**. Another restricting factor for AAV-mediated gene augmentation therapy that should be overcome is their **limited cargo capacity** which is not sufficient for some diseases caused by large genes (e.g. ABCA4 in Stargardt disease). Several options are therefore investigated including lentiviral vectors (which have almost twice as much capacity compared to AAV), dual vector systems and of course, nanomedicines.[8]

Since the efficacy of retinal gene therapy is highly dependent on the delivery of therapeutic genes to the target site, future research should definitely focus on **enhancing the delivery of gene carriers** to the retina. As extensively discussed in **Chapter 2**, many physiological barriers hinder the efficient delivery into the retina and hence their induced transgene expression. Here, the density of the retina clearly poses a problem since subretinal injection rarely induces strong expression in inner retinal layers while IVT injection has trouble delivering carriers to the outer layers. Considering the advantages IVT injection has over subretinal administration, many research groups put effort in improving the delivery of their non-viral and viral carriers after IVT injection by adjusting the surface characteristics of the carriers.[21] Next to optimizing the delivery based on these delivery routes, other administration routes have emerged that remain relatively unexplored and deserve more attention in the future such as periocular and suprachoroidal administration (cfr. **Chapter 2**). In addition, progress in surgical delivery such as robot-assisted surgery could enhance the efficiency as well as the safety of retinal gene delivery.[22]

Finally, future research should continue to look into **alternatives for retinal gene therapy**, which could aid to restore or improve vision of patients suffering from inherited as well as acquired retinal degeneration. An alternative strategy that is explored at the moment is the use of stem cells, which amongst other sources can be embryo-derived or induced from patient derived cells.[23] These cells can be manipulated to differentiate into retinal cell types like photoreceptor cells or RPE cells, after which they can be transplanted into the retinal tissue. Diseases currently investigated for this type of therapy include RP, AMD and Stargardt's macular dystrophy.[23] Some clinical trials, which primarily focus on evaluating safety, have been completed showing promising results.[24] Next to these advanced biological strategies also technological progress can help patients suffering from vision loss. An example of a technology-based device is the Argus II retinal prosthesis. Here, a camera in the patient's glasses captures the surroundings, transforms this signal and sends it to an array of electrodes implanted in the patient's eye. Next, this array electrically stimulates the remaining retinal cells which can next signal this information to the brain.[25] While this Argus II offers limited improvement of visual acuity, other prosthesis systems are being tested preclinically that are expected to ameliorate vision to a greater extent.[26,27]

Nanomedicine and nanotoxicology

In view of the many advantageous properties NPs possess (cfr. **Chapter 5**), the scientific community was strongly convinced that **nanomedicine** would completely transform the diagnosis and treatment of a variety of diseases. So far, the potential of nanomedicines has mainly been studied for the treatment of cancer. It was indeed rumored that nano would outperform the efficacy and safety of the currently available anti-cancer therapies. However,

despite the overwhelming amount of preclinical data and proof-of-concept studies, the translation of NPs toward the clinic has been disappointing. While nano is still expected to have an impact on the medicinal field, the enthusiasm of the public about its potential is slightly tempered in light of the absence of clinical success. Many of the NPs are halted in Phase 3 trials since they fail to improve treatment compared to the standard therapies. Remarkably, this is not that surprising considering the analysis made by Wilhelm *et al*.: careful scrutiny of the available literature on intravenous delivery of NPs to tumors revealed that merely 0,7% of the injected dose truly reached the tumour (**Figure 7.2**).[28] Moreover, the authors state that the median delivery efficiency did not improve over 10 years.

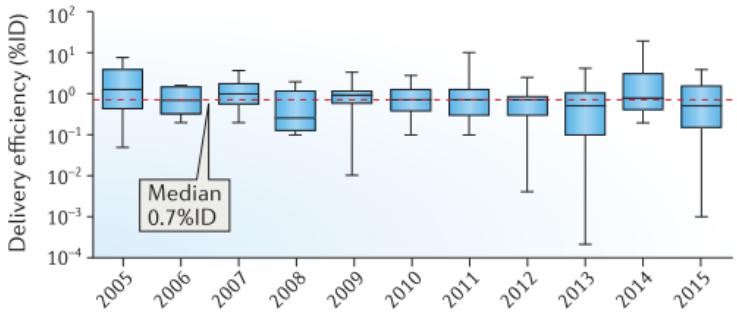

Figure 7.2 | Nanoparticle delivery efficiency (expressed as percentage of injected dose) to solid tumor after intravenous injection. Analysis based on 232 datasets published in 2005-2015. Figure taken from [28].

Nevertheless, some NPs have received FDA-approval or are being evaluated in clinical trials at the moment; an overview of the NP systems that have reached these stages can be found in **Figure 7.3**.[29] The majority of approved nanomedicines are liposomes encapsulating cytotoxic agents such as Doxorubicin (Myocet™) and Daunorubicin (DaunoXome™).[30] Interestingly, the clinical benefit of most approved anti-cancer nanomedicines has been improved safety rather than enhanced efficacy.[30,31] The overall future goal of nanomedicine in context of anti-cancer therapy is therefore rather straightforward: make it live up to its promises. Also for other applications, such as retinal gene therapy, nanoparticles still face many hurdles on the road to the clinic. Some drastic changes in nanoparticle development and evaluation will therefore likely be needed to turn nanomedicine into a success story. Surely, we are convinced that a few fundamental issues lie at the root of the lack of clinical translation, which we will discuss later in this chapter.

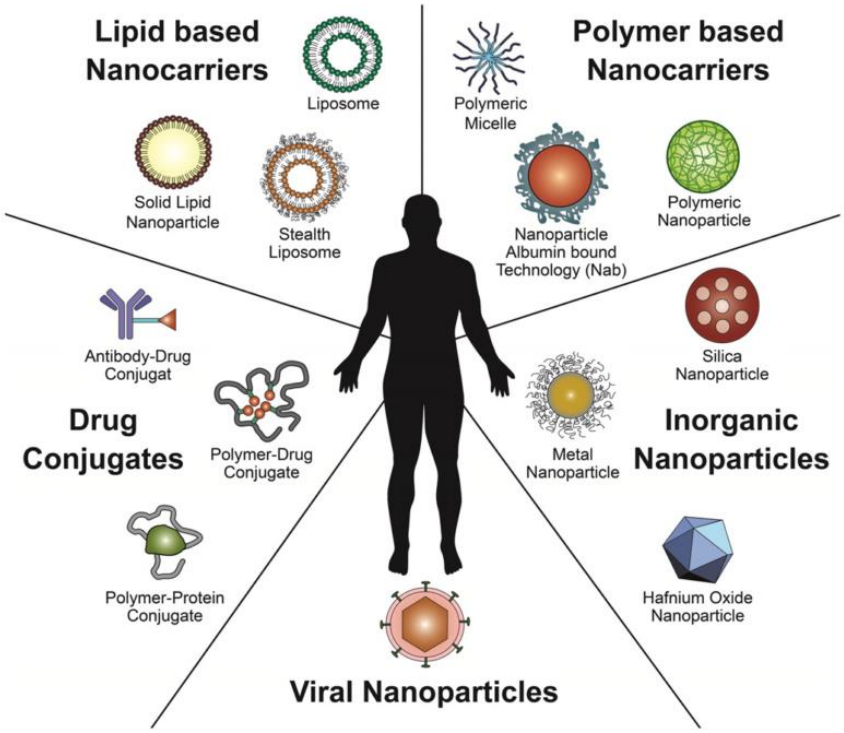

Figure 7.3 | Schematic overview of nanoparticle types that have been approved or are in clinical trials. Figure taken from [29].

In the past 20 years a myriad of NPs have been toxicologically evaluated in a multitude of cell types and models which has led to the discovery of a few commonly observed toxicological mechanisms that many NPs share (cfr. overview in **Chapter 5**). Initially, **nanotoxicology** advanced slowly due to the absence of appropriate toxicological assays for evaluation of NPs, although it became soon clear that by changing the physicochemistry of a NP its elicited cellular effects could vary – as we have confirmed in **Chapter 6**. This insight led to the development of NP characterization tools which proved to be fundamental for the progression of the field. This characterization initially primarily focused on basic NP parameters like size and surface charge. Then, the discovery came that the protein corona, a layer of proteins that surrounds the NP when it is exposed to biological fluids, truly defines the biological identity of a NP and therefore dictates the interactions with its environment.[32] Up to today, this concept has encouraged the field to continue their efforts to come up with novel characterization methods to analyze the composition and morphology of this complex protein layer and its influence on NP physicochemistry.[33] In addition, rather than one clear toxicity mechanism, it was found that NPs can provoke cellular changes via various pathways. In response to this phenomenon the field evolved its methodology from rather basic cytotoxicity assays to a more multiparametric approach.[34] The field has generally matured greatly over the last decade, with overall a high number of available tools to assess NPs and their interactions *in vitro* and *in vivo*. With the

increasing number of complex NP being developed for biomedical applications significant effort is now dedicated to developing high-throughput and high-content systems.[35]

2. ISSUES & CHALLENGES LIMITING OUR PROGRESS IN NANO

The fact that nano is a booming field is likely an understatement since the number of publications has increased dramatically over the years. Nevertheless, despite the exploding number of studies, the nano field does not progress at the expected pace. In this section we will discuss two considerable issues applied to nanotoxicology and non-viral retinal gene therapy that we believe need to be challenged in order to make nano prosperous.

Inefficient enthusiasm

Along with the interest in nanotechnology, nanotoxicology became a hot topic as proven by the 7-fold raise in number of publications discussing toxicity of NPs in a decade (from 1250 in 2007 to 8700 in 2017, according to Web Of Science). Since in context of retinal diseases nanomedicines have more limited applications and are relatively unexplored, the issues related to 'inefficient enthusiasm' as discussed below are primarily connected to nanotoxicology.

The enthusiasm elicited by the discovery of the special properties of NPs encouraged many researchers to jump into the nano field which led to an explosion of publications. Especially in nanotoxicology, a seemingly **endless variety of NPs** have been evaluated in an equally **large collection of cell types**. Due to the novelty of the field and limited experience with NPs, the initial studies, often published in high impact journals, lacked sufficient characterization and/or uptake data which led to questionable outcomes. Moreover, many of the results directly contradict each other: nearly each type of NP (IONP, AuNP, CNT,…) has led to positive and negative biological responses based on a myriad of underlying mechanisms. This stimulating enthusiasm indeed generates a massive amount of data, however, at the same time it works counterproductive since this makes it hard to filter out the most relevant studies. Literature reviews such as **Chapter 2** and **Chapter 5** can assist in this, yet the diversity of NPs and their coatings as well as cell types studied make it **problematic to draw broad conclusions**. Truthfully, the relevance of many publications is limited to the publication itself since the results cannot be extrapolated to other cell types or even NPs of the same type. This is not only owing to inefficient study design, but also due to the **inherent difficulty of studying and synthesizing NPs**: altering one aspect of a NP (e.g. size) inevitably leads to changes in many other features of the NP which in their turn affect its interaction with the biological environment. Next to the variation in NPs and biological models, also the immense diversity of methods applied to examine NP-induced effects hamper the reliability and extrapolation of toxicological data. Up to now, there

are **no official standardized toxicity protocols** specifically set up for NPs, although the need for it is well-established worldwide. Some promising steps forward in this regard are taken by the U.S-based National Institute of Standards and Technology (NIST) who have set up reproducible and validated protocols for physicochemistry measurements that should allow more direct comparisons between laboratories.[36] They furthermore manufactured several reference NPs (e.g. Au and Ag NPs) with the aim to improve the reliability of nanotoxicological assessments.[32,37] A last issue that hinders us to predict the *in vivo* toxicity elicited by NP exposure is the **contrast in dose and exposure time between toxicity studies and real life**. Indeed, besides the matter that the dose metric (surface charge/particles per volume/mass per volume/…) remains to be decided on, the majority of *in vitro* studies are based on short-term exposure to unrealistically high NP doses while real life NP exposure is expected to be low dosages for a longer term. Dosimetry complications are also inherently associated to the concept nano: NPs can agglomerate, aggregate and dissolve, making it hard to predict to which concentrations of particles or its ions a cell is exposed.[38,39]

The above-mentioned nano concerns are also present in the field of retinal gene therapy, although to a lesser extent. Seeing the field is less broad and the number of available retinal cell types is limited (in great contrast with nanotoxicology), studies are usually performed on a relevant cell type (e.g. RPE cells). On the other hand, nearly all *in vitro* studies on nanomedicines are performed on the widely distributed epithelial ARPE-19 cell even when the final application is IVT injection where it would be more preferable to focus on inner layer cell types (e.g. Müller cells).[40,41] In addition, the leap from *in vitro* to *in vivo* is more quickly undertaken than in nanotoxicology which implies that doses are faster updated to *in vivo* settings. The key parameter to define after administration of gene carriers *in vivo* is the retinal gene expression (often GFP) for which a couple of standard methods are available that are widely applied in the field. Nevertheless, it remains challenging to define conclusions when going over the various studies because of the variety of NPs that have been tested on different species.

While a few issues written above are inherently connected to the concept of nano, we are convinced some issues can be resolved by drafting a **project design** while having the final application in mind at every stage of the project. In this way, not only the project but also the respective NP will be rationally designed. By clearly specifying the target tissue some fundamental choices can be made, including: 1) most relevant experimental models (e.g. cell type), 2) characterization experiments (e.g. in vitreous/ in blood), 3) selection of dosages at relevant human exposure levels. In addition, it might be useful to take a few steps back and perform **systematic studies on simple NPs** that only vary in 1 physicochemical feature. This

would allow us to link NP physicochemistry to cellular effects in a more straightforward manner. Furthermore, the creation of elegantly **structured databases** could help to define more general trends in nanotoxicology and retinal drug delivery. Per publication included in the database all data could be catalogued such as detailed physicochemical information of each NP as well as the cellular effects and cell models investigated. In fact, quite recently the 'eNanoMapper' has been created, a database funded by the European commission that is meant to enhance the utilization of data and in this way support effective European nanotechnology research.[42] The database indeed enhances data sharing and provides a basis for advanced analysis like computational modeling. In the same category, we believe **literature reviews** can be helpful since they can provide an overview of existing studies and more importantly, attempt to create order in the chaos. Finally, study outcomes are largely defined by the models investigated throughout the experiments. The limitations and challenges regarding the applied **experimental models** will be extensively debated later in this chapter.

The many studies focusing on the influence of NPs on autophagy summarized in our **literature review** (**Chapter 5**) is a perfect example of the concerns mentioned above. Besides some guidelines which are updated every few years,[43] there are no standardized assays or minimal requirements implemented that define how to examine the effect of NPs on autophagy. Many researchers hence falsely conclude a certain NP induces or inhibits autophagy. On the other hand, while we specifically looked for studies that do aim to link effects on autophagy to specific physicochemical traits of NPs (e.g. positively & negatively charged materials), uptake data is often absent which impedes us to attribute intracellular effects to particle physicochemistry. Aware of the arguments above and with the intention to give a good example we performed a **systematic study** aimed to look into the interaction of QDs with autophagy as reliable as we could master in **Chapter 6**. To this end, we looked into the aggregation status of the two QDs who only differ in surface coating in water, PBS and full cell culture medium. We furthermore attempted to cancel out the differences in endocytosis when interpreting autophagic effects by measuring the uptake of both QDs and examining their intracellular effects at similar intracellular dosages. Finally, we applied multiple methods to investigate the changes in lysosomal and autophagosomal status, ensuring unbiased results. Our study is however not flawless since we established our assessment of intracellular effects on dosages determined by *in vitro* cytotoxicity assays rather than expected *in vivo* doses, and like many nanotoxicologists looked into short-term exposure. Also, while HeLa cells can be practical in view of the amount of data available in literature, this is therapeutically not the most relevant cell type.

Similar to Chapter 5, the **literature review** presented in **Chapter 2** sought to look for links between NP physicochemistry and NP behavior but in context of retinal drug delivery. Again, this proved not to be very straightforward, especially since the studies discussed were performed in different species and it is well-established that ocular barrier properties are highly species-dependent. In **Chapter 3** we aimed to contribute to elucidating the ILM barrier properties by performing a **systematic study** in our newly developed vitreoretinal explant by examining the behavior of **simple polystyrene beads** with different sizes. This was a purposeful choice since we wanted to focus on the potential links between physicochemistry and NP behavior rather than finding a therapeutic carrier in a trial-and-error manner. Still, while we had the intention to purely look into size-related effects, the surface charge of the beads changed along with the size. It is therefore possible that the varying penetration of the beads into the retina was also influenced by the surface charge.

Seeing **Chapter 4** is a preliminary study that, rather than optimizing a NP design, looked for intracellular effects of a commonly applied design, the chapter is limited to essential experiments and thus does not take the above-mentioned guidelines into account. For example, the extrapolation of cellular observations made in a 2D Müller monoculture to Müller cell response in retinal tissue is debatable. Characterization and compexation of the lipoplexes should furthermore be performed in presence of vitreous to estimate the NP physicochemistry and stability when administered by IVT injection. Also, while the experiments in that study are restricted to 24 hours, longer exposure times should be evaluated to look into Müller cell responses.

Missing models that matter

The minimal ability to extrapolate *in vitro* results to *in vivo* or clinical observations is an important topic of debate in both research fields discussed in this thesis. A notable example hereof in nanotoxicology regards QDs: while numerous publications have indicated severe cytotoxicity induced by a variety of QDs *in vitro*, a pilot study where QDs were intravenously injected in primates revealed no significant acute toxicity.[44] Similarly, many NPs for retinal drug/gene delivery are optimized in 2D cell monocultures until favorable results are obtained, yet next fail to deliver when relevant *in vivo* models come into play. The key issues in nanotoxicology and retinal drug delivery regarding models are thus very similar although they manifest themselves in a slightly different manner. In light of the ocular model-related content of **Chapter 2** and **Chapter 3** we will primarily focus this section on retinal delivery of NPs.

When performing experiments on 2D cell monocultures it is of importance to realize that these models bear little resemblance to the complexity of the clinical situation[30] which is a direct

consequence of several well-established shortcomings, including: lack of intercellular communication, lack of a 3D environment, lack of heterogeneity, absence of extracellular barriers and the presence of cell-type dependent effects.[45] These weaknesses more than often result in biased information since in case of nanotoxicology these shortcomings generally result in an overestimation of NP toxicity while in retinal drug delivery it leads to an overestimation of the therapeutic potential of NPs. In nanotoxicology, there is a substantial number of cell types available depending on the expected NP exposure route which translates into the fact that these type of studies dwell for a long time in the *in vitro* stage. This is in great contrast to retinal NP delivery where the restricted number of available retinal cell types pushes ocular researchers to switch more quickly to *in vivo* experiments. These studies are primarily performed in mice, which, as thoroughly discussed in **Chapter 2**, is not an ideal species for projects aiming to design an effective NP.

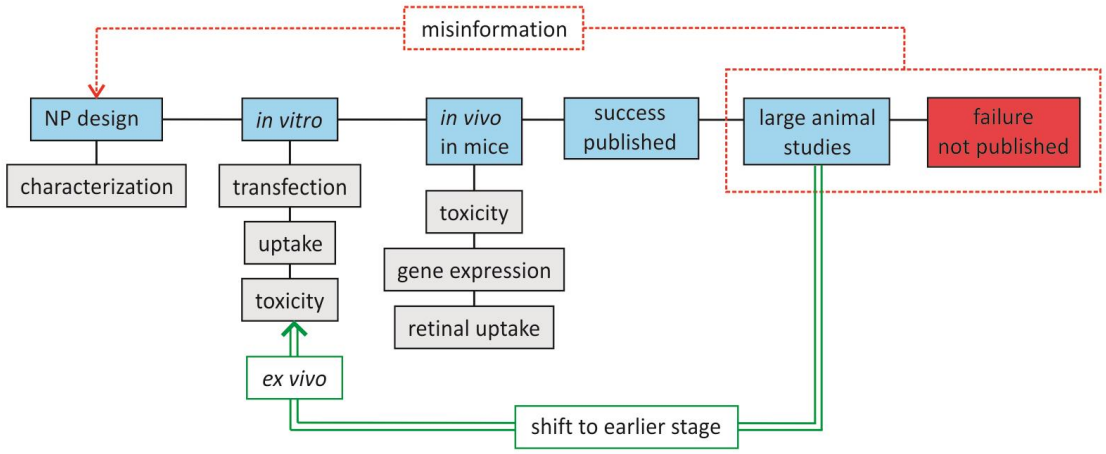

Figure 7.4 | Diagram of the vicious circle characteristic of non-viral retinal delivery research.

As illustrated in **Figure 7.4**, the current *in vitro* – *in vivo* paradigm widely applied in studies researching non-viral retinal delivery after IVT injection has created a vicious circle with as adverse outcomes misinformation and inefficiency. In this paradigm, a novel NP is designed, usually based on the available literature on 'successful' nanomedicines. Then, the NP is further optimized *in vitro* to obtain high expression levels with limited toxicity. This optimized NP is next tested *in vivo* in mice which usually results in limited though encouraging results that are then published. However, the bulk of these projects cease here since the following drug delivery studies in larger animals fail, presumably due to the more realistic physiological barriers present in these species. Regrettably, these unfavorable results are not reported on which overall results in a collection of publications describing highly promiseful non-viral carriers that, in the end, do not deliver (i.e. misinformation). While this biased representation of the delivery potential of specific NPs misleads other researchers aiming to design an effective NP, we are furthermore

convinced that studying unrealistic drug delivery barriers prior to representative ones is rather inefficient. We therefore suggest to shift the large animal phase to an earlier stage in NP development, though applying an *ex vivo* approach rather than an *in vivo* one.

This problematic workflow and associated concerns can be traced back to one fundamental issue, i.e. the lack of accessible representative models that imitate the complexity of clinical reality. This matter was also brought forward by Hare *et al*. in their critical perspective where they stated that the application and **development of relevant animal models** is one of the key areas to focus on in order to get clinical translation of nanomedicines.[30] Using these models we could tune NP properties in function of their interaction with biological barriers rather than empirically testing various NPs.[30] *In vivo* experiments in non-human primates or large animals are the most ideal pre-clinical models, however, these studies require the approval of ethical committees and are very costly. Hence, they are only available for later stages of NP development and evaluation and will therefore not break the vicious circle explained above. However, as discussed in detail in **Chapter 2** we are strongly convinced that some *ex vivo* experimental models can be at least as valuable as *in vivo* ones while having the advantage of being more readily available to researchers.[46] In line with this view we have presented a novel large animal *ex vivo* model ourselves in **Chapter 3**. In addition, while research focusing on therapeutic applications is perhaps more challenging and obtains funding more easily, genuine **fundamental research remains pivotal** for the field to advance. It is sometimes necessary to take a few steps back in order to move forward in an effective way. In case of retinal gene therapy it would for example be valuable to characterize the barrier properties in commonly applied laboratory animals (see further). Finally, it goes without saying that **multidisciplinary collaborations**, where expertise in NP formulation and drug delivery models of all sorts can be combined, could speed up the quest for the ideal NP that is able of reaching the retina after IVT injection.

3. RETINAL GENE DELIVERY BY NANOMEDICINES AFTER INTRAVITREAL INJECTION: HOW DO WE GET THERE?

Design of successful nanoparticles

Due to the challenges described above only a few nanomedicines have shown true pre-clinical potential for the treatment of retinal diseases. Based on the reflections made throughout this chapter we therefore propose a general research strategy that might support the community to advance in the design of an effective non-viral carrier able of overcoming the different barriers present in the eye (**Figure 7.5**).

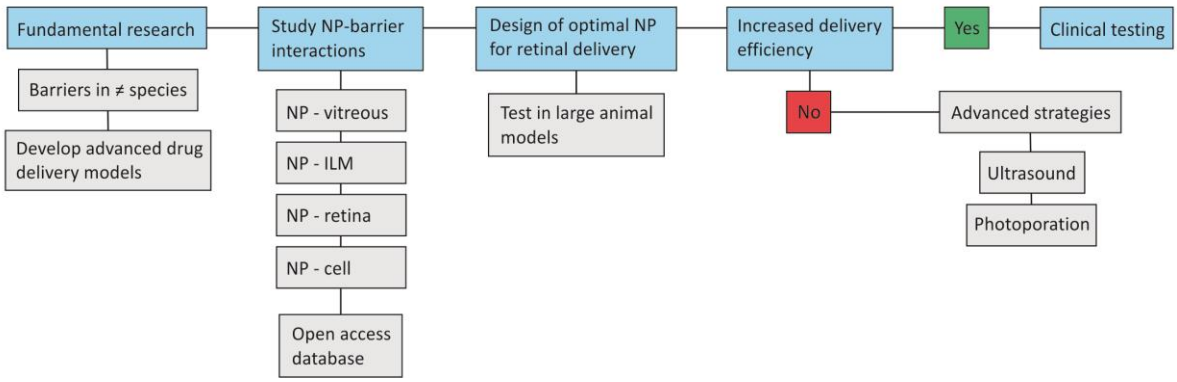

Figure 7.5 | Proposed workflow for research in retinal delivery of nanoparticles.

As a first step in this workflow, we feel it might be necessary to go back to the basics and put significant effort into **fundamental research**. This effort should be primarily focused on detailed characterization of the biological barriers present in the eye. As an example, it would be valuable to map the thickness, composition and morphology of the ILM in multiple species like pig and cow and compare this to the human state. Similar basic studies have been performed before on e.g. the vitreous composition of different species, yet these studies all date from the 80's. While it is obvious that human tissue is preferred, the demand greatly exceeds its availability. By accurately defining the properties and especially the potential differences among species, the correct animal model for each drug delivery barrier could be decided on. Furthermore, this could aid us in the development of **representative drug delivery models** that can be applied to **study NP-barrier interactions**. Our research group has already attempted to contribute to this concept by the development of two drug delivery models, one to check the interaction of NPs with the vitreous,[47] and the other one to examine the behavior of NPs in the vitreoretinal interface (cfr. **Chapter 3**). Applying models ranging from *in vitro* to *in vivo*, **systematic studies** into the interaction of diverse NP types with varying physicochemistry with the distinct extracellular and intracellular barriers could be performed. The observations made in these studies could then be collected in a structured **database** which is available to all researchers. A leading example of such a database is the Cancer Nanomedicine Repository,[48] which was created in response to a critical publication highlighting the current challenges in cancer nanomedicine.[28] By implementing the knowledge derived from a similarly structured database, optimal NPs for retinal delivery could be designed which next should be tested in *in vivo* models e.g. Non-human primates. If the results are beneficial, i.e. increased delivery efficiency is observed, these NPs could proceed further into clinical trials. However, if the optimal NP systems as designed based on our proposed workflow would not be adequately successful, we could look into advanced strategies to enhance the delivery of NPs into the retina.

Advanced strategies to enhance retinal delivery

Since the ILM represents the primary extracellular barrier to overcome for non-viral and viral particles after IVT injection (cfr. **Chapter 3**), the strategies discussed here focus on physical approaches to aid particles in overcoming this hurdle. A first strategy which is under investigation at the moment is the use of **ultrasound**. Ultrasound, routinely applied for diagnostic imaging, has gained a lot of attention in the drug delivery field over the last decade. In the ocular field it has been researched to enhance delivery across multiple barriers including the cornea,[49,50] the sclera[51] and the retina[52]. Generally, ultrasound-enhanced delivery across the VR interface could be achieved by two concepts: 1) physical destruction of the ILM elicited by the burst of ultrasound-responsive microbubbles,[53,54] and 2) use of the acoustic force that accompanies ultrasound to physically 'push' particles in the direction of the retina.[55,56] The concept of both strategies in context of IVT injection has been validated by proof-of-concept studies. IVT injection of a mixture of microbubbles with AAV vectors indeed elicited enhanced transgene expression upon ultrasound treatment in rats.[53] On the other hand, human serum albumin NPs showed higher diffusivity and permeation in a bovine retinal explant when exposed to ultrasound. [55] These observations indicate there is potential for ultrasound in retinal therapy, yet apart from these proof-of-concept studies the concept remains largely unexplored. Further fine-tuning of the method and future research into its safety and its therapeutic power in large *in vivo* models is crucial to define the true potential of this approach.

A currently unexplored approach in the eye is the concept of applying **photoporation** to puncture the ILM locally, in this way creating passageways for NPs to enter the retina. This could be achieved by applying gold nanoparticles (AuNPs) at the surface of the ILM, followed by irradiation with a short pulse of laser light. Upon absorption of the laser pulse the AuNPs heat up, resulting in evaporation of the water surrounding the AuNP surface, thus creating explosive vapour nanobubbles (VNB) that disrupt the ILM (**Figure 7.6**). Due to the extremely short lifetime of VNBs and the insulating effect of vapor, diffusion of heat from the AuNPs to the environment is negligible. Instead, the laser energy used to irradiate the AuNPs is completely converted into mechanical energy of the expanding and collapsing VNB.[57] Therefore, VNBs and the resulting high-pressure shock waves are ideally suited to cause local disruptions of their surroundings, without causing thermal damage to cells or tissues in the retina. Conveniently, the size of the VNB (and thus the extent of local damage) can be tuned (~0.1-10 µm) by adjusting the AuNP (size, shape) as well as the laser parameters (energy, illumination time). A particular benefit is that AuNPs have an extremely large light absorption cross-section, so that strong focusing of the laser beam is not needed. The combination of a broad laser beam (hundreds of micrometers)

with the fact that only one laser pulse is needed to generate VNB, a large area can be treated in a short amount of time.

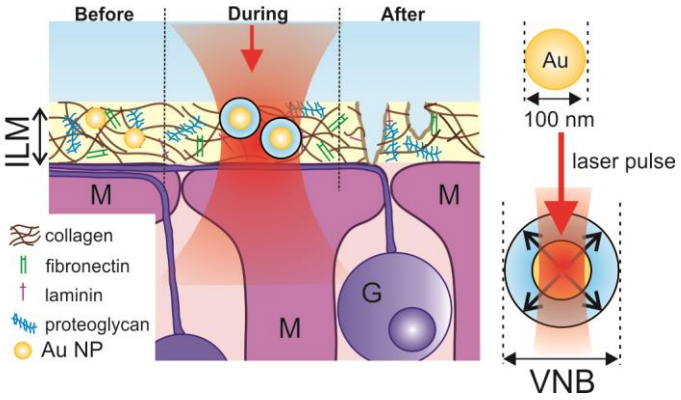

Figure 7.6 | Schematic drawing the photoporation approach to disrupt the ILM. AuNPs are delivered to the ILM after which they are illuminated with a short but powerful laser pulse. By absorption of the laserlight vapour nanobubbles (VNBs) form around the AuNP surface after which the VNBs collapse. This mechanical effect results in disruption of the ILM. M: Müller cell; G: ganglion cell.

Photoporation has already been investigated *in vitro* to enhance intracellular delivery of macromolecules as well as *in vivo* to eradicate microtumours.[57–59] In the retina, on the other hand, photoporation has not yet been investigated. It is obvious that while this is theoretically an innovative and attractive approach to overcome the ILM, the concept raises a lot of questions that need to be addressed, including the fate of the AuNPs following treatment, the toxicity of AuNPs in the eye and overall feasibility of the concept.

4. CONCLUSIONS

Many innovative therapeutic concepts invented to restore or preserve vision could be regarded as science-fiction 20 years ago, yet have now been at least proven to work preclinically (e.g. optogenetics or photovoltaic prostheses). Surely, the field of vision research is advancing fast, with the first retinal gene therapy treatment approved by the FDA only very recently. On the other hand, despite the immense worldwide interest in applying nanoparticles as drug delivery vehicles, the progress in this area is slightly disappointing. To rectify this, the community will have to rethink their current methodologies and set modest intermediate goals. As repeatedly emphasized throughout this thesis, we trust that the combination of systematic fundamental studies together with the development of more representative models will be essential to accomplish this reorganization and above all, to turn nano into a success story.

5. REFERENCES

1. Audo, I. *et al.* Development and application of a next-generation-sequencing (NGS) approach to detect known and novel gene defects underlying retinal diseases. *Orphanet J. Rare Dis.* **7,** 8 (2012).

2. Carrigan, M. *et al.* Panel-Based population next-generation sequencing for inherited retinal degenerations. *Sci. Rep.* **6,** 1–9 (2016).

3. Bennett, J. Taking Stock of Retinal Gene Therapy: Looking Back and Moving Forward. *Mol. Ther.* **25,** 1076–1094 (2017).

4. Veleri, S. *et al.* Biology and therapy of inherited retinal degenerative disease: insights from mouse models. *Dis. Model. Mech.* **8,** 109–129 (2015).

5. RetNet. at <https://sph.uth.edu/retnet/>

6. Day, T. P., Byrne, L. C., Schaffer, D. V. & Flannery, J. G. in *Advances in experimental medicine and biology* **801,** 687–693 (2014).

7. FDA Advisory Committee Unanimously Recommends Approval of Investigational LUXTURNA™ (voretigene neparvovec) for Patients with Biallelic RPE65-mediated Inherited Retinal Disease. *Spark Therapeutics press release* (2017). at <http://ir.sparktx.com/news-releases/news-release-details/fda-advisory-committee-unanimously-recommends-approval>

8. Gupta, P. R. & Huckfeldt, R. M. Gene therapy for inherited retinal degenerations: Initial successes and future challenges. *J. Neural Eng.* **14,** (2017).

9. Rajala, A. *et al.* Nanoparticle-Assisted Targeted Delivery of Eye-Speci fic Genes to Eyes Signi ficantly Improves the Vision of Blind Mice In Vivo. *Nano Lett.* **14,** 5257–5263 (2014).

10. Apaolaza, P. S. *et al.* Structural recovery of the retina in a retinoschisin-deficient mouse after gene replacement therapy by solid lipid nanoparticles. *Biomaterials* **90,** 40–49 (2016).

11. Farjo, R., Skaggs, J., Quiambao, A. B., Cooper, M. J. & Naash, M. I. Efficient non-viral ocular gene transfer with compacted DNA nanoparticles. *PLoS One* **1,** 1–8 (2006).

12. Han, Z. *et al.* Genomic DNA nanoparticles rescue rhodopsin-associated retinitis pigmentosa phenotype. *FASEB J.* **29,** 2535–2544 (2015).

13. Han, Z., Koirala, A., Makkia, R., Cooper, M. J. & Naash, M. I. Direct gene transfer with compacted DNA nanoparticles in retinal pigment epithelial cells: expression, repeat delivery and lack of toxicity. *Nanomedicine* **7,** 521–539 (2012).

14. Koirala, A., Conley, S. M. & Naash, M. I. A review of therapeutic prospects of non-viral gene therapy in the retinal pigment epithelium. *Biomaterials* **34,** 7158–7167 (2013).

15. Sahel, J. A., Marazova, K. & Audo, I. Clinical characteristics and current therapies for inherited retinal degenerations. *Cold Spring Harb. Perspect. Med.* **5,** 1–26 (2015).

16. Wu, W., Tang, L., D'Amore, P. A. & Lei, H. Application of CRISPR-Cas9 in eye disease. *Exp. Eye Res.* **161,** 116–123 (2017).

17. Bakondi, B. *et al.* In Vivo CRISPR/Cas9 Gene Editing Corrects Retinal Dystrophy in the S334ter-3 Rat Model of Autosomal Dominant Retinitis Pigmentosa. *Mol. Ther.* **24,** 556–

563 (2016).

18. Cho, S. W. *et al.* Analysis of off-target effects of CRISPR Cas-derived RNA-guided endonucleases and nickases. *Genome Res.* **24,** 132–141 (2014).

18a. RetroSense Therapeutics Completes Low Dose Cohort in Clinical Trial of Novel Gene Therapy Application of Optogenetics | Business Wire. *Press release* (2016). at <https://www.businesswire.com/news/home/20160810005731/en>

19. Kleinlogel, S. *et al.* Ultra light-sensitive and fast neuronal activation with the Ca2+-permeable channelrhodopsin CatCh. *Nat. Neurosci.* **14,** 513–518 (2011).

20. Chaffiol, A. *et al.* A New Promoter Allows Optogenetic Vision Restoration with Enhanced Sensitivity in Macaque Retina. *Mol. Ther.* **25,** 2546–2560 (2017).

21. Dalkara, D. *et al.* In vivo-directed evolution of a new adeno-associated virus for therapeutic outer retinal gene delivery from the vitreous. *Sci. Transl. Med.* **5,** 189ra76 (2013).

22. Gonenc, B., Chae, J., Gehlbach, P., Taylor, R. H. & Iordachita, I. Towards robot-assisted retinal vein cannulation: A motorized force-sensing microneedle integrated with a handheld micromanipulator. *Sensors* **17,** 1–25 (2017).

23. MacLaren, R. E., Bennett, J. & Schwartz, S. D. Gene Therapy and Stem Cell Transplantation in Retinal Disease: The New Frontier. *Ophthalmology* **123,** S98–S106 (2016).

24. Schwartz, S. D. *et al.* Human embryonic stem cell-derived retinal pigment epithelium in patients with age-related macular degeneration and Stargardt's macular dystrophy: Follow-up of two open-label phase 1/2 studies. *Lancet* **385,** 509–516 (2015).

25. Finn, A. P., Tripp, F., Whitaker, D. & Vajzovic, L. Synergistic Visual Gains Attained using Argus II Retinal Prosthesis with OrCam MyEye. *Ophthalmol. Retin.* in press (2017). doi:10.1016/j.oret.2017.08.008

26. Lorach, H. *et al.* Photovoltaic restoration of sight with high visual acuity. *Nat. Med.* **21,** 476–482 (2015).

27. Lorach, H. & Palanker, D. in *Artificial Vision: A Clinical Guide* (ed. Gabel, V. P.) 115–124 (Springer International Publishing, 2017). doi:10.1007/978-3-319-41876-6_9

28. Wilhelm, S. *et al.* Analysis of nanoparticle delivery to tumours. *Nat. Rev. Mater.* **1,** 16014 (2016).

29. Wicki, A., Witzigmann, D., Balasubramanian, V. & Huwyler, J. Nanomedicine in cancer therapy: Challenges, opportunities, and clinical applications. *J. Control. Release* **200,** 138–157 (2015).

30. Hare, J. I. *et al.* Challenges and strategies in anti-cancer nanomedicine development: An industry perspective. *Adv. Drug Deliv. Rev.* **108,** 25–38 (2017).

31. Caster, J. M., Patel, A. N., Zhang, T. & Wang, A. Investigational nanomedicines in 2016: a review of nanotherapeutics currently undergoing clinical trials. *Wiley Interdiscip. Rev. Nanomedicine Nanobiotechnology* **9,** (2017).

32. Hussain, S. M. *et al.* At the crossroads of nanotoxicology in vitro: Past achievements and current challenges. *Toxicol. Sci.* **147,** 5–16 (2015).

33. Kokkinopoulou, M., Simon, J., Landfester, K., Mailänder, V. & Lieberwirth, I. Visualization of the protein corona: towards a biomolecular understanding of nanoparticle-cell-interactions. *Nanoscale* **9,** 8858–8870 (2017).

34. Soenen, S. J. *et al.* Cytotoxic Effects of Gold Nanoparticles: A Multiparametric Study. *ACS Nano* **6,** 5767–5783 (2012).

35. Manshian, B. B. *et al.* High-Content Imaging and Gene Expression Approaches To Unravel the Effect of Surface Functionality on Cellular Interactions of Silver Nanoparticles. *ACS Nano* **9,** 10431–10444 (2015).

36. Nano-Measurement Protocols | NIST. at <https://www.nist.gov/mml/nano-measurement-protocols>

37. Roebben, G., Hackley, V. A. & Emons, H. in *Metrology and Standardization of Nanotechnology* 307–322 (Wiley-VCH Verlag GmbH & Co. KGaA, 2017). doi:10.1002/9783527800308.ch19

38. Teeguarden, J. G., Hinderliter, P. M., Orr, G., Thrall, B. D. & Pounds, J. G. Particokinetics in vitro: Dosimetry considerations for in vitro nanoparticle toxicity assessments. *Toxicol. Sci.* **95,** 300–312 (2007).

39. Zhu, M., Perrett, S. & Nie, G. Understanding the particokinetics of engineered nanomaterials for safe and effective therapeutic applications. *Small* **9,** 1619–34 (2013).

40. Martens, T. F. *et al.* Coating nanocarriers with hyaluronic acid facilitates intravitreal drug delivery for retinal gene therapy. *J. Control. Release* **202,** 83–92 (2015).

41. Martens, T. F. *et al.* Effect of hyaluronic acid-binding to lipoplexes on intravitreal drug delivery for retinal gene therapy. *Eur. J. Pharm. Sci.* **103,** 27–35 (2017).

42. Jeliazkova, N. *et al.* The eNanoMapper database for nanomaterial safety information. *Beilstein J. Nanotechnol.* **6,** 1609–1634 (2015).

43. Klionsky DJ, Abdelmohsen K, Abe A, Abedin MJ, Abeliovich H, Acevedo Arozena A, Adachi H, Adams CM, Adams PD, Adeli K, Adhihetty PJ, Adler SG, Agam G, Agarwal R, Aghi MK, Agnello M, Agostinis P, Aguilar PV, Aguirre-Ghiso J, Airoldi EM, Ait-Si-Ali S, Akemat, Z. S. Guidelines for use and interpretation of assays for monitoring autophagy (3rd edition). *Autophagy* **12,** 1–222 (2016).

44. Ye, L. *et al.* A pilot study in non-human primates shows no adverse response to intravenous injection of quantum dots. *Nat. Nanotechnol.* **7,** 453–8 (2012).

45. Joris, F. *et al.* Assessing nanoparticle toxicity in cell-based assays: influence of cell culture parameters and optimized models for bridging the in vitro–in vivo gap. *Chem. Soc. Rev.* **42,** 8339–8359 (2013).

46. Peynshaert, K., Devoldere, J., De Smedt, S. C. & Remaut, K. In vitro and ex vivo models to study drug delivery barriers in the posterior segment of the eye. *Adv. Drug Deliv. Rev.* (2017). doi:10.1016/j.addr.2017.09.007

47. Martens, T. F. *et al.* Measuring the intravitreal mobility of nanomedicines with single-particle tracking microscopy. *Nanomedicine (Lond)* **8,** 1955–1968 (2013).

48. Cancer Nanomedicine Repository. at <http://inbs.med.utoronto.ca/cgi-bin/Repository.cgi>

49. Sonoda, S. *et al.* Gene Transfer to Corneal Epithelium and Keratocytes Mediated by Ultrasound with Microbubbles. *Investig. Opthalmology Vis. Sci.* **47,** 558–564 (2006).

50. Zderic, V., Clark, J. I., Martin, R. W. & Vaezy, S. Ultrasound-Enhanced Transcorneal Drug Delivery. *Cornea* **23,** 804–811 (2004).

51. Murugappan, S. K. & Zhou, Y. Transsclera Drug Delivery by Pulsed High-Intensity Focused Ultrasound (HIFU): An *Ex Vivo* Study. *Curr. Eye Res.* **3683,** 1–9 (2014).

52. Peeters, L. *et al.* Can ultrasound solve the transport barrier of the neural retina? *Pharm. Res.* **25,** 2657–65 (2008).

53. Xie, W. *et al.* Ultrasound microbubbles enhance recombinant adeno-associated virus vector delivery to retinal ganglion cells in vivo. *Acad. Radiol.* **17,** 1242–1248 (2010).

54. Li, H. L. *et al.* Ultrasound-targeted microbubble destruction enhances AAV-mediated gene transfection in human RPE cells in vitro and rat retina in vivo. *Gene Ther.* **16,** 1146–1153 (2009).

55. Huang, D., Chen, Y. S., Thakur, S. S. & Rupenthal, I. D. Ultrasound-mediated nanoparticle delivery across ex vivo bovine retina after intravitreal injection. *Eur. J. Pharm. Biopharm.* **119,** 125–136 (2017).

56. Thakur, S. S., Barnett, N. L., Donaldson, M. J. & Parekh, H. S. Intravitreal drug delivery in retinal disease: are we out of our depth? *Expert Opin. Drug Deliv.* **11,** 1575–90 (2014).

57. Xiong, R. *et al.* Comparison of Gold Nanoparticle Mediated Photoporation: Vapor Nanobubbles Outperform Direct Heating for Delivering Macromolecules in Live Cells. *ACS Nano* **8,** 6288–6296 (2014).

58. Lukianova-Hleb, E. Y. *et al.* Intraoperative diagnostics and elimination of residual microtumours with plasmonic nanobubbles. *Nat. Nanotechnol.* **11,** 525–532 (2016).

59. Xiong, R. *et al.* Laser-induced vapor nanobubbles for efficient delivery of macromolecules in live cells. in *Progress in Biomedical Optics and Imaging - Proceedings of SPIE* **9338,** (2015)

Summary and conclusions

Thanks to worldwide research nanotechnology is one of the key drivers of the current scientific advancements in the 21st century. The field has expanded astonishingly over the last decade, where it is estimated that nearly 10 % of all publications indexed in Web of Science in 2016 involved nanotechnology. Nonetheless, despite this extensive research the translation of these widely investigated nanoparticles (NPs) toward the clinic is rather limited. For organic particles such as liposomes and polymeric particles this is mainly owing to their lack of efficacy evoked by the many intra-and extracellular barriers they encounter. The translation of inorganic particles is primarily restricted by safety concerns, since many of them, including Quantum Dots (QDs), are made up of heavy metals that are known to be toxic. As confirmed in this thesis, it is established that the physicochemical features define how the cell 'sees' the particle and thus dictates the NP's efficacy and toxicity – what you see is what you get!

While this perception is fully acknowledged by the nanotechnology community it remains challenging to connect certain physicochemical properties to specific biological effects, making it hard to predict the therapeutic power or potential toxicity of a NP. This is primarily due to faulty project design, the lack of representative models and the inherent complexities associated to working in the nano-range. The difficulty to link NP physicochemistry to desired or unwanted effects is an issue that affects nearly every research field that aims to take advantage of the unique and powerful properties of NPs, yet in this thesis we aimed to aid in overcoming this issue in context of retinal gene delivery (Part I, Chapter 1-4) and autophagy (Part II, Chapter 5 and 6).

In **Chapter 1** we provided an overview of the most prevalent acquired diseases and most well-documented inherited retinal diseases that could be treated with retinal gene therapy. We furthermore described the morphology and functions of the Müller cell, the target cell type for our non-viral approach.

Based on the overview of publications linking physicochemical properties of therapeutics and their carriers presented in **Chapter 2**, we concluded that the ideal physiochemical characteristics of a therapeutic (carrier) highly depends on the barrier it needs to overcome and therefore also on the preferred administration route. We further found that nearly each barrier undergoes changes in function of age and disease, an important notion when evaluating the potential of carriers to cross delivery barriers. We found many useful *in vitro* and *ex vivo* approaches to study

drug delivery barriers in the posterior segment of the eye, though argue that there is still a great need for more straightforward and representative models.

Convinced of the latter argument, we presented the so-called 'vitreoretinal explant' in **Chapter 3**, an novel *ex vivo* model especially developed to look into the interaction of nanomedicines with the vitreoretinal (VR) interface. This interface comprises the vitreous and the inner limiting membrane (ILM), both well-recognized drug delivery barriers. We confirmed the viability of this explant model and validated its value by means of polystyrene beads. Since 40 nm beads more efficiently crossed the VR interface than 100 or 200 nm particles we concluded that the entry of NPs into the retina is size-dependent. Moreover, we found that removing the vitreous, as commonly done for culture of conventional explants, led to an overestimation of NP uptake, and concluded that the principal barrier to overcome for retinal entry is unquestionably the ILM. This VR explant is currently the most representative *ex vivo* model available that is alive for a sufficiently long time to study NP uptake in the retina.

In **Chapter 4** we applied an elementary set-up to examine if Müller cells, which we regard as an ideal target for neuroprotective strategies, are able of efficiently processing lipoplexes and expressing their pDNA or mRNA cargo. Here, we found that mRNA lipoplexes outperformed the DNA lipoplexes in transfection of healthy Müller cells since both the number of transfected cells as well as the level of GFP expression was higher for mRNA lipoplexes. In Müller cells that were exposed to hyperglycemia, oxidative stress or hypoxia no changes in mRNA-induced expression was observed when compared to healthy Müller cells. On the other hand, we did find that Müller cells treated with oxidative stress or hypoxia were more sensitive to lipoplex-induced toxicity while hyperglycemia had a protective effect. Although preliminary, this study indicates that, despite a stressful environment, Müller cells are capable of taking up lipoplexes and expressing their nucleic acid cargo.

Chapter 5 presented an overview of the most relevant reports on NP-mediated autophagy alterations and intended to investigate the interplay between NP physicochemistry and autophagic changes. Hence, several NP properties were put forth as probable influencing factors of NP-induced autophagy disruption or upregulation such as size, charge and chemical composition. However, owing to the shortcomings of some studies and the contradicting claims made in literature it was virtually impossible to draw general conclusions. We thus judged that systematic studies which include sufficient characterization data could greatly support us to truly elucidate the impact of NP physicochemistry on NP-associated autophagy changes.

In view of this understanding we performed a study in **Chapter 6** with as goal to carefully define the influence of QD coating on lysosomal health and autophagy. Our study showed that the cellular effects induced by QDS on HeLa cells were strongly dictated by the surface coat (i.e. MPA or PEG) of the otherwise identical particles. MPA-coated QDs proved to be highly compatible as a result of lysosomal activation and ROS reduction, two cellular responses that help the cell to cope with NP-induced stress. In contrast, PEG-coated QDs were substantially more toxic owing to a rise in ROS production and lysosomal impairment. This impairment next resulted in autophagy dysfunction which likely added to their toxic effects. Taken together, our study showed that coating QDs with MPA is a better strategy than PEGylation for imaging applications.

In **Chapter 7**, we summarized the advances in retinal gene therapy and nanotoxicology and discussed potential challenges that hinder NPs to advance further into clinical stages. We brought forward several guidelines that we believe could aid the nano field to progress and reconstructed them into a general approach that could aid researchers in overcoming the NP delivery barriers after intravitreal injection.

Samenvatting en conclusies

Nanotechnologie is dankzij wereldwijd onderzoek geëvolueerd tot één van de belangrijkste drijfkrachten van de huidige wetenschappelijke vooruitgangen in de 21ste eeuw. Het veld is verbazingwekkend uitgebreid in het afgelopen decennium, waarbij naar schatting bijna 10% van alle publicaties die in Web of Science zijn geïndexeerd in 2016 nanotechnologie betrof. Niettegenstaande dit diepgaand onderzoek is de vertaling van nanopartikels (NP's) naar de kliniek eerder beperkt. In het geval van organische NPs zoals liposomen en polymere partikels komt dit voornamelijk door hun gebrek aan efficaciteit wat veroorzaakt wordt door de vele intra- en extracellulaire barrières die ze tegenkomen. De translatie van anorganische deeltjes wordt voornamelijk beperkt door veiligheidsbelangen gezien veel van deze partikels, waaronder Quantum Dots (QD's) zijn samengesteld uit zware metalen waarvan geweten is dat ze toxisch zijn. Zoals bevestigd in deze thesis, is reeds vastgesteld dat het de fysicochemische kenmerken zijn die bepalen hoe een cel een NP 'ziet' en dus zo de werkzaamheid en toxiciteit van het NP dicteert – what you see is what you get!

Hoewel deze perceptie volledig wordt erkend door de nanotechnologie gemeenschap, blijft het een uitdaging om specifieke fysicochemische eigenschappen te koppelen aan bepaalde biologische effecten. Hierdoor wordt het dan ook moeilijk om het therapeutisch vermogen of potentiële toxiciteit van een NP te voorspellen. Dit is voornamelijk te wijten aan gebrekkig project design, het ontbreken van representatieve modellen en de inherente complexiteiten die samengaan met het werken met NPs. De moeilijkheid om NP fysicochemie te koppelen aan gewenste of ongewenste effecten is een probleem dat bijna elk onderzoeksveld beïnvloedt dat als doel heeft voordeel te halen uit de unieke en krachtige eigenschappen van NPs. In deze thesis hebben we ons echter gefocust op het helpen oplossen van deze problemen in context van retinale genaflevering (Deel I, hoofdstuk 1-4) en autofagie (Deel II, hoofdstuk 5 en 6).

In **Hoofdstuk 1** hebben we een overzicht gegeven van de meest voorkomende verworven ziekten alsook de best gedocumenteerde erfelijke retinale aandoeningen die kunnen worden behandeld met retinale gentherapie. We beschreven verder de morfologie en de vele functies van de Müller cel, het doelceltype voor onze niet-virale aflevering van genen.

In **hoofdstuk 2** gaven we een overzicht van publicaties die de fysicochemische eigenschappen van therapeutica en hun dragers bespreken. Hieruit concludeerden we dat de ideale fysiochemische kenmerken van een therapeutische (drager) sterk afhangen van de barrière die het NP moet overwinnen en dus ook van de gewenste toedieningsroute. We ontdekten verder

dat bijna elke barrière veranderingen ondergaat in functie van leeftijd en ziekte, wat een belangrijke invloed kan hebben op het evalueren van het potentieel van dragers om deze barrières te overbruggen. We hebben veel nuttige *in vitro* en *ex vivo* methodes en modellen gevonden om barrières voor medicijnafgifte in het achterste segment van het oog te bestuderen, hoewel er volgens ons nog steeds veel behoefte is aan meer eenvoudige en representatieve modellen.

Overtuigd van dit laatste argument presenteerden we in **hoofdstuk 3** de zogenaamde 'vitreoretinale explant', een nieuw *ex vivo* model dat speciaal is ontwikkeld om de interactie van nanogeneesmiddelen met de vitreoretinale (VR) interface te onderzoeken. Deze interface omvat het vitreum en de inner limiting membrane (ILM), beide erkende hindernissen voor de aflevering van geneesmiddelen. We bevestigden de levensvatbaarheid van dit nieuw model en valideerden de waarde ervan met behulp van polystyrene partikels. Gezien 40 nm partikels efficiënter de VR interface doorkruisten dan 100 of 200 nm NPs, konden we concluderen dat de afgifte van NPs in de retina afhankelijk is van de grootte van NPs. We ontdekten bovendien dat het verwijderen van het vitreum, zoals vaak wordt gedaan voor de kweek van conventionele explants, leidde tot een overschatting van de NP-opname en concludeerden verder dat de voornaamste barrière die overwonnen moet worden voor om de retina te bereiken onbetwistbaar het ILM is. Deze VR explant is momenteel het meest representatieve *ex vivo* model op de markt dat voldoende lang in leven kan gehouden worden om de opname van NPs in de retina te bestuderen.

In **hoofdstuk 4** hebben we een elementaire set-up toegepast om te onderzoeken of Müller cellen, die we beschouwen als een ideaal doelwit voor neuroprotectieve strategieën, in staat zijn om lipoplexen efficiënt te verwerken en hun pDNA- of mRNA-lading tot expressie te brengen. We ondervonden dat mRNA-lipoplexen beter presteerden dan de DNA-lipoplexen bij transfectie van gezonde Müller-cellen, omdat zowel het aantal getransfecteerde cellen als het niveau van GFP-expressie hoger was voor mRNA-lipoplexen. In Müller cellen die werden blootgesteld aan hyperglycemie, oxidatieve stress of hypoxie werden geen veranderingen in mRNA-geïnduceerde expressie waargenomen in vergelijking met gezonde Müller cellen. Aan de andere kant vonden we dat Müller cellen behandeld met oxidatieve stress of hypoxie gevoeliger waren voor de door lipoplexen geïnduceerde toxiciteit, dit terwijl hyperglycemie een beschermend effect had. Hoewel ongetwijfeld meer onderzoek nodig is, geeft deze studie aan dat, ondanks een stressvolle omgeving, Müller cellen in staat zijn om lipoplexen op te nemen en hun nucleïnezuurlading tot expressie te brengen.

Hoofdstuk 5 gaf een overzicht van de meest relevante publicaties handelend over NP-gemedieerde veranderingen in autofagie dit met het oog op het onderzoeken van de interacties

tussen NP fysicochemie en veranderingen in autofagie. We hebben inderdaad verschillende NP-eigenschappen naar voren kunnen brengen die hoogstwaarschijnlijk de mate of manier van NP geïnduceerde verstoring van autofagie beïnvloeden, waaronder grootte, lading en chemische samenstelling. Vanwege de tekortkomingen van sommige studies en de tegenstrijdige beweringen in de literatuur was het echter vrijwel onmogelijk om algemene conclusies te trekken. We hebben daarom geoordeeld dat systematische studies die voldoende karakteriseringsgegevens bevatten ons enorm zouden kunnen ondersteunen om de impact van NP fysicochemie op NP-geassocieerde autofagiewijzigingen te verduidelijken.

Op basis van deze argumentatie hebben we in **hoofdstuk 6** een onderzoek uitgevoerd met als doel de invloed van QD coating op lysosomale integriteit en autofagie zorgvuldig the definiëren. Onze studie toonde aan dat de cellulaire effecten geïnduceerd door QDs op HeLa cellen sterk werden gedicteerd door de coating (zijnde MPA of PEG) van de overigens identieke deeltjes. MPA-gecoate QDs bleken zeer compatibel te zijn als gevolg van lysosomale activering en reductie van ROS, twee cellulaire responsen die de cel helpen om te gaan met NP-geïnduceerde stress. Daarentegen waren PEG-gecoate QDs aanzienlijk meer toxisch als gevolg van een toename in ROS productie en lysosomale stoornissen. Deze stoornissen resulteerden vervolgens in afwijkingen in autofagie die hoogstwaarschijnlijk bijdroegen aan de geobserveerde toxische effecten. Samengevat heeft ons onderzoek aangetoond dat voor biomedische toepassingen het coaten van QDs met MPA een betere strategie is dan met PEG.

In **Hoofdstuk 7** hebben we de vooruitgang in retinale gentherapie en nanotoxicologie samengevat en mogelijke uitdagingen besproken die NPs verhinderen om verder in de klinische stadia te geraken. We hebben verschillende richtlijnen naar voren gebracht waarvan we denken dat ze het nano-veld kunnen helpen om vooruitgang te boeken, en hebben deze tot een algemene benadering omgevormd die onderzoekers zou kunnen helpen bij het overwinnen van de NP-barrières na intravitreale injectie.

CURRICULUM VITAE

PERSONALIA

Name	Peynshaert
First Names	Karen Lucienne Emiel
Nationality	Belgian
Place of birth	Ghent
Date of birth	08/01/1989
Marital status	Married
Private address	Uitvangstraat 103 9032 Wondelgem
Telephone	+32 (0)472 755 761
Professional address	Laboratory for General Biochemistry and Physical Pharmacy Faculty of Pharmaceutical Sciences, Ghent University Ottergemsesteenweg 460 9000 Ghent Belgium
Email	Karen.Peynshaert@UGent.be
Website	https://www.biofys.ugent.be

DEGREES

June 2012	Ghent University, Ghent, Belgium Master in Drug Development – Pharmaceutical Sciences with distinction Master thesis: “Studies into the role of the actin cytoskeleton in regulating fluid phase endocytosis”, under supervision of Prof. dr. Arwyn T. Jones of Welsh School of Pharmacy of Cardiff University (U.K.) and Prof. dr. Kevin Braeckmans of Laboratory of General Biochemistry and Physical Pharmacy of Ghent University, Belgium.
June 2010	Ghent University, Ghent, Belgium Bachelor in Pharmaceutical Sciences

LANGUAGES

Dutch	Native language
English	Full professional proficiency
French	Limited working proficiency
German	Elementary proficiency
Arabic	Elementary proficiency

INTERNATIONAL PEER-REVIEWED A1 PUBLICATIONS

Al Soraj, M.; He, L.; Peynshaert, K.; Cousaert, J.; Vercauteren, D.; Braeckmans, K.; De Smedt, S. C.; Jones, A. T. "siRNA and pharmacological inhibition of endocytic pathways to characterize the differential role of macropinocytosis and the actin cytoskeleton on cellular uptake of dextran and cationic cell penetrating peptides octaarginine (R8) and HIV-Tat". *Journal of Controlled Release* 2012, *161*(1), 132-141

Joris, F.; Manshian, B. B.; Peynshaert, K.; De Smedt, S. C.; Braeckmans, K.; Soenen, S. J. "Assessing nanoparticle toxicity in cell-based assays: influence of cell culture parameters and optimized models for bridging the in vitro-in vivo gap." *Chemical Society Reviews* 2013, *42* (21), 8339-8359

Peynshaert, K.; Manshian, B. B.; Joris, F.; Braeckmans, K.; De Smedt, S. C.; Demeester, J.; Soenen, S. J. "Exploiting Intrinsic Nanoparticle Toxicity: The Pros and Cons of Nanoparticle-Induced Autophagy in Biomedical Research." *Chemical Reviews* 2014, *114* (15), 7581-7609.

Xiong, R.; Raemdonck, K.; Peynshaert, K.; Lentacker, I.; De Cock, I.; Demeester, J.; De Smedt, S. C.; Skirtach, A. G.; Braeckmans, K. "Comparison of Gold Nanoparticle Mediated Photoporation: Vapor Nanobubbles Outperform Direct Heating for Delivering Macromolecules in Live Cells." *ACS Nano* 2014, *8* (6), 6288-6296.

K. Peynshaert, S.J. Soenen, B.B. Manshian, S.H. Doak, K. Braeckmans, S.C. De Smedt, K. Remaut. "Coating of Quantum Dots strongly defines their effect on lysosomal health and autophagy". *Acta Biomaterialia* 2017, *48*, 195–205.

K. Peynshaert, J. Devoldere, V. Forster, S. Picaud, S.C. De Smedt, K. Remaut. "Toward smart design of retinal drug carriers: a novel bovine explant model to study the barrier role of the vitreoretinal interface." *Drug Delivery* 2017, *24*(1), 1384-1394

K. Peynshaert, J. Devoldere, S.C. De Smedt, K. Remaut. "In vitro and ex vivo models to study drug delivery barriers in the posterior segment of the eye." *Advanced Drug Delivery Reviews* (2017) in press.

NATIONAL AND INTERNATIONAL CONFERENCES WITH ORAL PRESENTATION

2017	Dutch Ophthalmology PhD Students Conference (DOPS), Nijmegen, Netherlands *Toward rational design of gene carriers: a novel ex vivo model to study the vitreoretinal interface as a barrier*
2016	European Association for Vision and Eye Research conference (EVER), Nice, France *Toward rational design of gene carriers: a novel ex vivo model to study the vitreoretinal interface as a barrier*

European Association for Vision and Eye Research conference (EVER), Nice, France
Exploring strategies to overcome the inner limiting membrane as a barrier for non)viral retinal gene therapy after intravitreal injection

2015 European Association for Vision and Eye Research conference (EVER), Nice, France
An in vitro and ex vivo study into the role of Müller cells in nanoparticle-based gene therapy after intravitreal injection

The 12th International Symposium on Ocular Pharmacolocy and Therapeutics (ISOPT), Berlin, Germany
A novel ex vivo assay to evaluate the role of Müller Cells in retinal drug delivery

NATIONAL AND INTERNATIONAL CONFERENCES WITH POSTER PRESENTATION

2017 Ophthalmologica Belgica, Brussels, Belgium
Exploring strategies to overcome the inner limiting membrane as a barrier for non)viral retinal gene therapy after intravitreal injection

2016 Ophthalmologica Belgica, Brussels, Belgium
An in vitro and ex vivo study into the role of Müller cells in nanoparticle-based gene therapy after intravitreal injection

Association for Research in Vision and Ophthalmology Annual Meeting (ARVO), Seattle, United States.
Study into the role of Müller cells in nanoparticle-based retinal gene therapy after
intravitreal injection

2015 Biopharmacy day, Leuven, Belgium
A novel ex vivo model to evaluate the role of Müller cells in retinal drug delivery

42nd Annual Meeting of the Controlled Release Society (CRS), Edinburgh, Scotland.
A novel ex vivo assay to evaluate the role of Müller Cells in retinal drug delivery

Pro-Retina Meeting, Potsdam, Germany
A novel ex vivo model to evaluate the role of Müller cells in retinal drug delivery

2014 Biopharmacy Day, Vlaardingen, Netherlands
Impact of Quantum Dot coating on cellular interactions

Knowledge for Growth, Ghent, Belgium
PEGylated Quantum Dots suppress autophagy by blocking lysosome-autophagosome fusion

NANOTOX2014, 7th international nanotoxicology congress, Antalya, Turkey

Impact of Quantum Dot – mediated autophagy alteration

Gordon Research Conference: autophagy in stress, development & disease, Lucca, Italy
PEGylated Quantum Dots suppress autophagy by blocking lysosome-autophagosome fusion

Biopharmacy Day, Ghent, Belgium
Nanoparticle-mediated autophagy: unraveling the impact of nanoparticle toxicity on therapeutic efficacy

AWARDS AND PRIZES

2017 Prize for best oral presentation at DOPS meeting in Nijmegen, Netherlands

2016 Award of 5000 € from Funds for Research in Ophthalmology for the research project: *Exploring strategies to overcome the inner limiting membrane as a barrier for non)viral retinal gene therapy after intravitreal injection*

2015 Award of 17.500 euro (2nd best prize) from Funds for Research in Ophthalmology for the research project: *An in vitro and ex vivo study into the role of Müller cells in nanoparticle-based gene therapy after intravitreal injection*

2012-2017 2 FWO and 3 Faculty travel grants for attending international conferences

INTERNATIONAL RESEARCH EXPERIENCE

December 2015	1 week of *ex* vivo experiments at 'Institute de la vision', Paris, Department of Visual Information Processing, research group of Prof. Serge Picaud.
June-august 2013	10-week stay abroad to work on a nanotoxicological project at DNA Damage Research Group (Prof. Shareen Doak), School of Medicine, Swansea University, Swansea, U.K.
February-May 2011	Masterthesis project: 'Studies into the role of the actin cytoskeleton in regulating fluid phase endocytosis' under supervision of Prof. Arwyn T. Jones, Endocytosis and Cellular Delivery Laboratory, Welsh School of Pharmacy, Cardiff, U.K.

TEACHING ACTIVITIES

2014-2017 Supervision of 5 students during their Master's research project.
2014-2016 Assistant in practical courses of 'Physicochemistry'
2014-2017 Communication coach for the practical sessions of the Doctoral Schools course of 'Effective Scientific Communication' given by Jean-Luc Doumont.

COURSES

TRANSFERABLE SKILLS: Effective Scientific Communication, Communication skills, Effective graphical displays, Creative Thinking.

SPECIALIST COURSES: Laboratory Animal Science I & II (by Prof. Katleen Hermans), FLAMES Summer School on Statistics.